CUTANEOUS LEISHMANIASIS: EXPLORING PATHOGENESIS AND IMMUNOMODULATORY APPROACHES

EDITED BY: Izabel Galhardo Demarchi, Wander Pavanelli, Iván D. Vélez and Lynn Soong

PUBLISHED IN: Frontiers in Cellular and Infection Microbiology

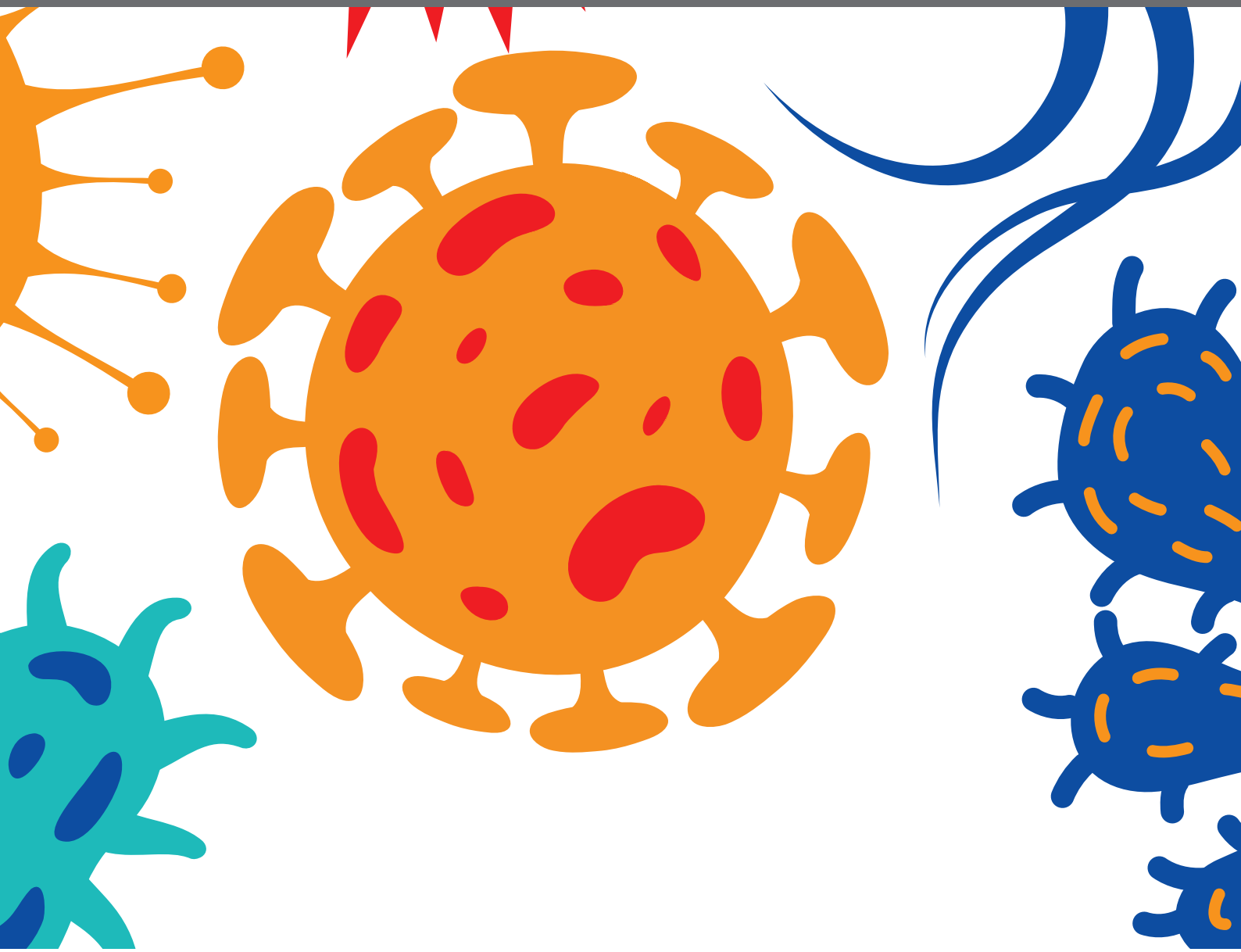

frontiers Research Topics

frontiers

ISSN 1664-8714
ISBN 978-2-88974-469-5
DOI 10.3389/978-2-88974-469-5

About Frontiers

Frontiers is more than just an open-access publisher of scholarly articles: it is a pioneering approach to the world of academia, radically improving the way scholarly research is managed. The grand vision of Frontiers is a world where all people have an equal opportunity to seek, share and generate knowledge. Frontiers provides immediate and permanent online open access to all its publications, but this alone is not enough to realize our grand goals.

Frontiers Journal Series

The Frontiers Journal Series is a multi-tier and interdisciplinary set of open-access, online journals, promising a paradigm shift from the current review, selection and dissemination processes in academic publishing. All Frontiers journals are driven by researchers for researchers; therefore, they constitute a service to the scholarly community. At the same time, the Frontiers Journal Series operates on a revolutionary invention, the tiered publishing system, initially addressing specific communities of scholars, and gradually climbing up to broader public understanding, thus serving the interests of the lay society, too.

Dedication to Quality

Each Frontiers article is a landmark of the highest quality, thanks to genuinely collaborative interactions between authors and review editors, who include some of the world's best academicians. Research must be certified by peers before entering a stream of knowledge that may eventually reach the public - and shape society; therefore, Frontiers only applies the most rigorous and unbiased reviews.
Frontiers revolutionizes research publishing by freely delivering the most outstanding research, evaluated with no bias from both the academic and social point of view. By applying the most advanced information technologies, Frontiers is catapulting scholarly publishing into a new generation.

What are Frontiers Research Topics?

Frontiers Research Topics are very popular trademarks of the Frontiers Journals Series: they are collections of at least ten articles, all centered on a particular subject. With their unique mix of varied contributions from Original Research to Review Articles, Frontiers Research Topics unify the most influential researchers, the latest key findings and historical advances in a hot research area! Find out more on how to host your own Frontiers Research Topic or contribute to one as an author by contacting the Frontiers Editorial Office: frontiersin.org/about/contact

CUTANEOUS LEISHMANIASIS: EXPLORING PATHOGENESIS AND IMMUNOMODULATORY APPROACHES

Topic Editors:
Izabel Galhardo Demarchi, Federal University of Santa Catarina, Brazil
Wander Pavanelli, State University of Londrina, Brazil
Iván D. Vélez, Universidad de Antioquia, Colombia
Lynn Soong, University of Texas Medical Branch at Galveston, United States

Citation: Demarchi, I. G., Pavanelli, W., Vélez, I. D., Soong, L., eds. (2022). Cutaneous Leishmaniasis: Exploring Pathogenesis and Immunomodulatory Approaches. Lausanne: Frontiers Media SA. doi: 10.3389/978-2-88974-469-5

Table of Contents

frontiers in Cellular and Infection Microbiology

EDITORIAL
published: 18 January 2022
doi: 10.3389/fcimb.2021.839851

Editorial: Cutaneous Leishmaniasis: Exploring Pathogenesis and Immunomodulatory Approaches

Wander Rogério Pavanelli[1] *and Izabel Galhardo Demarchi*[2*]

[1] *Departamento de Ciências Patológicas, Centro de Ciências da Saúde. Universidade Estadual de Londrina, Londrina, Brazil,*
[2] *Departamento de Análises Clínicas, Centro de Ciências da Saúde. Universidade Federal de Santa Catarina, Florianópolis, Brazil*

Keywords: ***Leishmania*, parasite, antiprotozoal agents, immunomodulatory agent, immunomodulation effect, tegumentary leishmaniasis**

Editorial on the Research Topic

Cutaneous Leishmaniasis: Exploring Pathogenesis and Immunomodulatory Approaches

Leishmaniases comprises a class of diseases that are caused by *Leishmania* protozoa. They are considered ancient enemies that emerged as successful parasites that invade both invertebrate and vertebrate hosts millions of years ago. Cutaneous leishmaniasis (CL) has affected ~1 million people worldwide, manifesting as different clinical forms (World Health Organization, 2021a; World Health Organization, 2021b). This form of trypanosomiasis is considered a neglected tropical disease, but it has also been reported in economically privileged countries (e.g., the United States; World Health Organization, 2021c). The complex and various life cycles of *Leishmania* and their ability to inhabit a wide range of hosts and diverse ecological niches have been associated with their persistence and expansion. In mammals, its pathogenesis consists of complex interactions between the parasite and the host's immune system, resulting in persistence of the parasite with different clinical manifestations and mechanisms of elimination (Kaye and Scott, 2011). Considering the variability of *Leishmania* species and hosts, the mammals' immune response orchestrates the success or failure of killing the pathogen (Kaye et al., 2020). Drug treatment is clearly essential, but the usual anti-leishmaniasis drugs can have severe adverse effects and toxicity, resulting in therapeutic failure or patient dropout from therapy. Thus, new immunomodulatory therapies need to be developed to successfully treat CL. The scientific community, global agencies, and governments have made efforts to develop strategies to eliminate leishmaniasis. Such research has provided critical insights into the mechanisms that influence the full spectrum of leishmaniasis, including its pathogenesis, diagnosis, and treatment.

Volpedo et al. reviewed the immunopathogenesis of CL and post-Kala-azar dermal leishmaniasis. They synthesized on balance between Th1 and Th2 responses for infection control. The exaggerated polarization of Th cells appears to be responsible for severe disease pathology. Gomez et al. explored early leukocyte responses in ex vivo models of healing and non-healing human *Leishmania (Viannia) panamensis* infections. The elucidation of immunological mechanisms will undoubtedly contribute to strategies to develop the next generation of therapeutics and vaccines for CL.

Pentavalent antimonials remain the first-choice therapy for CL because no effective human vaccines are currently available. Meglumine antimoniate is the most common drug that is used for CL treatment. In a recent systematic review by Pinar et al. (2020), moderate evidence was found for

Edited and reviewed by:
Jeroen P. J. Saeij,
University of California, Davis,
United States

***Correspondence:**
Izabel Galhardo Demarchi
i.g.demarchi@ufsc.br

Specialty section:
This article was submitted to Parasite and Host, a section of the journal Frontiers in Cellular and Infection Microbiology

Received: *20 December 2021*
Accepted: *31 December 2021*
Published: *18 January 2022*

Citation:
Pavanelli WR and Demarchi IG (2022) Editorial: Cutaneous Leishmaniasis: Exploring Pathogenesis and Immunomodulatory Approaches. Front. Cell. Infect. Microbiol. 11:839851. doi: 10.3389/fcimb.2021.839851

cure rates and adverse effects when intramuscular meglumine antimoniate was used for American CL. Thus, drug combinations have been proposed as alternative therapies to treat TL (Berbert et al., 2018). In a brief research report, a pilot randomized clinical trial was conducted using oral miltefosine and pentavalent antimonials that were combined with pentoxifylline to treat American TL.The authors observed similar cure rates and a lower risk of adverse effects (Martins et al.). Exploring new approaches on leishmaniasis drugs, Craig et al. explored new approaches to develop anti-leishmaniasis drugs and found that thermoresponsive copolymer nanoparticles improve the bioavailability of retrograde inhibitors *in vitro*. Compound encapsulation in copolymer was a viable strategy to dramatically increase the bioavailability and efficacy of anti-*Leishmania* compounds.

Although some studies have reported promising results, problems and limitations with various treatments remain. To explain therapeutic failures, resistance, and susceptibility, Fernández et al. showed human neutrophil activation ex vivo that influenced tolerance to meglumine antimoniate and the susceptibility of clinical strains of *L. (V.) panamensis*. They found lower reactive oxygen species production and higher CD62L and CD66b expression on cells that were infected with tolerant/resistant *L. (V.) panamensis* compared with cells that were infected with drug-sensitive strains.

Among tegumentary leishmaniasis, *Leishmania (Viannia) braziliensis* is the most prevalent parasite that is identified in infected mammals. This species is responsible for mucocutaneous leishmaniasis in Latin America (World Health Organization, 2021b). Souza et al. investigated the role of miR-548d-3p in *L. (V.) braziliensis* infection. The parasite appears to interfere with chemokine production by modulating miRNAs, consequently affecting inflammatory processes that are essential for lesion resolution. They suggested that miR-548d-3p may be a prognostic marker for TL and a host-directed therapeutic target. dos Santos et al. explored the intestines as a new target organ of chronic *L. (V.) braziliensis* infection in hamsters, highlighting a possible target for future studies to understand susceptibility and resistance. Animal models are frequently used to understand the pathogenesis of leishmaniasis and develop new therapeutic strategies (Cabral et al., 2021). Tomiotto-Pellissier et al. reported that arginase-1 and macrophages at lesion sites influence susceptibility to *Leishmania amazonensis* in mice. Their findings on protective immunity against *L. amazonensis* suggest new approaches to treat and prevent this disease.

A brief research report by de Lima et al. arelates high anti-Leishmania IgG antibody levels with the severity of mucosal leishmaniasis in humans. The reduction of antibody production could indicate treatment success in most patients. The authors suggested that these tests can be applied to assess therapeutic response.

Although no vaccine is currently available for CL and considering that vaccines are effective primary strategies to prevent infectious diseases, the in silico screening and rational selection of potential candidates on a large scale have been used as research tools prior to *in vitro* and *in vivo* evaluations (Flórez et al.). In the field of pharmaceutical sciences, these authors described Leishmania spp. epitopes in humans that were naturally resistant to leishmaniasis, working toward a synthetic vaccine.

The reports on cutaneous leishmaniasis in this Research Topic highlight areas that demand further investigation. Cutaneous leishmaniasis remains a global problem, requiring effective diagnostic measures and treatments. Considering the global health situation post-COVID-19 and neglected tropical diseases (Tilli et al., 2021), we strongly recommend further support for leishmaniasis research, based on promising results that have been generated to date.

AUTHOR CONTRIBUTIONS

All authors listed have made a substantial, direct, and intellectual contribution to the work and approved it for publication.

ACKNOWLEDGMENTS

Thanks to all researchers who participated in this Research Topic. And especially to the editors Dr Lynn Soong and Dr Ivan Velez.

REFERENCES

Berbert, T. R. N., de Mello, T. F. P., Nassif, P. W., Mota, C. A., Silveira, A. V., Duarte, G. C., et al. (2018). Pentavalent Antimonials Combined With Other Therapeutic Alternatives for the Treatment of Cutaneous and Mucocutaneous Leishmaniasis: A Systematic Review. *Dermatol. Res. Pract.* 2018, 9014726. doi: 10.1155/2018/9014726

Cabral, F. V., Souza, T. H. D. S., Sellera, F. P., Fontes, A., and Ribeiro, M. S. (2021). Towards Effective Cutaneous Leishmaniasis Treatment With Light-Based Technologies. A Systematic Review and Meta-Analysis of Preclinical Studies. *J. Photochem. Photobiol. B.* 221, 112236. doi: 10.1016/j.jphotobiol.2021.112236

Kaye, P. M., Cruz, I., Picado, A., Van Bocxlaer, K., and Croft, S. L. (2020). Leishmaniasis Immunopathology-Impact on Design and Use of Vaccines, Diagnostics and Drugs. *Semin. Immunopathol.* 42 (3), 247–264. doi: 10.1007/s00281-020-00788-y

Kaye, P., and Scott, P. (2011). Leishmaniasis: Complexity at the Host-Pathogen Interface. *Nat. Rev. Microbiol.* 9 (8), 604–615. doi: 10.1038/nrmicro2608

Pinart, M., Rueda, J. R., Romero, G. A., Pinzón-Flórez, C. E., Osorio-Arango, K., Maia-Elkhoury, A. N. S., et al. (2020). Interventions for American Cutaneous and Mucocutaneous Leishmaniasis. *Cochrane Database Syst. Rev.* 8 (8), CD004834. doi: 10.1002/14651858.CD004834.pub3

Tilli, M., Olliaro, P., Gobbi, F., Bisoffi, Z., Bartoloni, A., and Zammarchi, L. (2021). Neglected Tropical Diseases in non-Endemic Countries in the Era of COVID-19 Pandemic: The Great Forgotten. *J. Travel Med.* 28 (1), taaa179. doi: 10.1093/jtm/taaa179

World Health Organization, WHO. (2021a). *Cutaneous Leishmaniasis*. Available at: https://www.who.int/leishmaniasis/cutaneous_leishmaniasis/en/#:~:text=Cutaneous%20leishmaniasis%20is%20the%20most,the%20face%2C%20arms%20and%20legs.&text=When%20the%20ulcers%20heal%2C%20they,cause%20of%20serious%20social%20prejudice.

World Health Organization, WHO. (2021b). *Mucocutaneous Leishmaniasis*. Available at: https://www.who.int/leishmaniasis/mucocutaneous_leishmaniasis/en/#:~:text=In%20mucocutaneous%20leishmaniasis%2C%20the%20lesions,being%20rejected%20by%20the%20community.

World Health Organization, WHO. (2021c). *Control of Neglected Tropical Diseases*. Available at: https://www.who.int/teams/control-of-neglected-tropical-diseases/neglected-zoonotic-diseases.

Conflict of Interest: The authors declare that the research was conducted in the absence of any commercial or financial relationships that could be construed as a potential conflict of interest.

Publisher's Note: All claims expressed in this article are solely those of the authors and do not necessarily represent those of their affiliated organizations, or those of the publisher, the editors and the reviewers. Any product that may be evaluated in this article, or claim that may be made by its manufacturer, is not guaranteed or endorsed by the publisher.

frontiers in Cellular and Infection Microbiology

BRIEF RESEARCH REPORT
published: 09 April 2021
doi: 10.3389/fcimb.2021.652956

High Anti-*Leishmania* IgG Antibody Levels Are Associated With Severity of Mucosal Leishmaniasis

Clara Mônica F. de Lima[1,2], *Andrea S. Magalhães*[1], *Rúbia Costa*[1], *Carolina C. Barreto*[1], *Paulo R. L. Machado*[1,2,3], *Edgar M. Carvalho*[1,2,3,4], *Marcus M. Lessa*[1,2] *and Lucas P. Carvalho*[1,2,3,4]*

[1] Serviço de Imunologia, Hospital Universitário Prof. Edgard Santos, Universidade Federal da Bahia, Salvador, Brazil, [2] School of Medicine, Programa de Pós-graduação em Ciências da Saúde - Universidade Federal da Bahia, Salvador, Brazil, [3] Ministry of Sciences and Technology, Instituto Nacional de Ciência e Tecnologia em Doenças Tropicais, INCT-DT, Salvador, Brazil, [4] Laboratório de Pesquisas Clínicas (LAPEC), Instituto Gonçalo Moniz (IGM), Fiocruz, Salvador, Brazil

OPEN ACCESS

Edited by:
Izabel Galhardo Demarchi, Federal University of Santa Catarina, Brazil

Reviewed by:
Diego Luis Costa, University of São Paulo, Brazil
Paulo Marcos Matta Guedes, Federal University of Rio Grande do Norte, Brazil

***Correspondence:**
Lucas P. Carvalho
carvalholp76@gmail.com

Specialty section:
This article was submitted to Parasite and Host, a section of the journal Frontiers in Cellular and Infection Microbiology

Received: 13 January 2021
Accepted: 16 March 2021
Published: 09 April 2021

Citation:
de Lima CMF, Magalhães AS, Costa R, Barreto CC, Machado PRL, Carvalho EM, Lessa MM and Carvalho LP (2021) High Anti-Leishmania IgG Antibody Levels Are Associated With Severity of Mucosal Leishmaniasis. Front. Cell. Infect. Microbiol. 11:652956. doi: 10.3389/fcimb.2021.652956

Background: Mucosal leishmaniasis (ML), the most inflammatory form of tegumentary leishmaniasis, is predominantly caused by *Leishmania braziliensis*. The disease is characterized by the development of lesions, mainly in the nasal mucosa. An exacerbated inflammatory response has been associated with the presence of destructive and disfiguring lesions, with stages of severity ranging from small nodulations to the complete destruction of the nasal pyramid architecture. As *Leishmania* is an intracellular parasite, most immunological studies have emphasized the cell-mediated immune response, while relatively few studies aimed to investigate the role antibodies in protection against, or the pathology of ML.

Methods: Patients with a confirmed diagnosis of ML were classified according to clinical staging criteria. Serum levels of *Leishmania*-specific IgG, IgG1 and IgG2 antibodies were determined by ELISA before and after treatment with antimony or antimony plus pentoxifylline.

Results: Patients in stages IV and V produced higher concentrations of IgG and IgG1 antibodies when compared to those in stage I and II. Significant reductions were seen in the concentrations of IgG and IgG2 antibodies in most patients who responded well to treatment.

Conclusions: Our data demonstrate an association between IgG antibody titers and the severity of mucosal disease. The observed reduction in antibody production after successful treatment in most patients preliminarily indicates that these tests can be used to aid in the assessment of therapeutic response.

Keywords: mucosal leishmaniasis, antibodies, IgG subclasses, *Leishmania braziliensis*, therapeutic failure

INTRODUCTION

American tegumentary leishmaniasis (ATL) is widely distributed around the world, and often presents high morbidity due to the possibility of developing destructive lesions that can disfigure and disable individuals, significantly impacting their quality of life (World Health Organization - Control of Leishmaniasis, 2010). In endemic areas of *Leishmania braziliensis* transmission, mucosal leishmaniasis (ML), a disease also known as mucocutaneous leishmaniasis, occurs in 3% of patients concomitantly or following the cure of cutaneous leishmaniasis (CL). ML can also be caused by other *Leishmania* species, such as *Leishmania amazonensis* and *Leishmania guaianensis* (Grimaldi et al., 1987). In about 15% of cases, no previous history or scarring due to CL is documented (Boaventura et al., 2006; Miranda Lessa et al., 2007). Moreover, up to 40% of patients with an emergent disease termed disseminated cutaneous leishmaniasis (DL) have mucosal involvement (Carvalho et al., 1994). While ML primarily affects the nasal mucosa (90% of cases), the second most affected site is the pharyngeal mucosa, followed by the laryngeal mucosal and oral cavity (Marsden, 1994; Miranda Lessa et al., 2007). Importantly, the involvement of these latter areas is an indicator of disease severity (Marsden, 1994; Miranda Lessa et al., 2007). Our group proposed staging criteria (I to V) for patients who only have nasal mucosal involvement. Stage I is characterized by nodulation in the absence of ulceration in the mucosa of the nasal septum; stage II: superficial ulceration; stage III: deep ulceration; stage IV: nasal septum perforation; stage V: destruction of the nasal pyramid architecture (Lessa et al., 2012).

As *Leishmania* is an intracellular parasite, the role of the innate and T cell responses in the pathogenesis of disease has been widely studied. Lymphocytes from ML patients were found to be more proliferative than those from CL patients when stimulated with *Leishmania* antigens (Carvalho et al., 2007), and the production of cytokines/chemokines by macrophages and T cells, such as TNF, IFN-γ and CXCL9, was observed to be higher in ML compared to CL (Bacellar et al., 2002; Junqueira Pedras et al., 2003). The impairment in regulatory mechanisms that may attenuate the immune response also play an important role in the exaggerated inflammatory response observed in ML, as Cells from ML patients produce less IL-10 and its receptor than those from CL. The role of antibodies in *Leishmania* has not been completely elucidated. High levels of antibodies are produced in all clinical forms of leishmaniasis, and high levels of IgG and IgE antibodies are found in ML (Junqueira Pedras et al., 2003).

In the present study, we observed that antibodies against *Leishmania* antigens were associated with ML severity, and the data suggest that therapeutic success may be associated with decreases in antibody levels.

MATERIALS AND METHODS

Study Design

A longitudinal study was performed to investigate the association between IgG titers and disease severity, as well as response to therapy in ML patients. Clinical stages were determined upon ENT examination and classified from stages I to V according to the criteria established by Lessa et al. (2012). The production of anti-*Leishmania* antigens antibodies was determined before and after therapy. Treatment was considered successful upon the complete re-epithelization of nasal cavity lesions (clinical cure).

Study Area and Patients

This study received approval (CAAE: 01229212.0.0000.0049) from the Institutional Review Board of the Professor Edgard Santos University Hospital (HUPES-UFBA), Salvador, Bahia-Brazil. This study was carried in an area endemic for CL, Corte de Pedra, located in southeastern Bahia, Brazil. This region is home to a municipal clinic that houses a reference center for tegumentary leishmaniasis diagnosis and treatment. Diagnosis was based on the presence of nodules and ulcers in the nasal mucosa, and by the presence of *Leishmania* DNA as confirmed by PCR (Weirather et al., 2011). Twenty-seven ML patients were enrolled in this study, six of whom received pentavalent antimony alone (20 mg/Kg/day for 30 days), while 21 patients were treated with a combined regimen consisting of pentavalent antimony with pentoxifylline (1200 mg/day orally for 30 days). To evaluate serological test specificity using a soluble antigen of *Leishmania brazilliensis* (SLA) in patients with ML, serum from 25 patients with cutaneous leishmaniasis (CL) were used as controls. Clinical and serological evaluations were performed in ML patients prior to and 90 days following the onset of therapy.

Soluble *Leishmania* Antigen

A *L. braziliensis* strain (MHOM/BR/2001), isolated from a patient with ML, was used to prepare soluble *Leishmania* antigen by sonication and centrifugation, as previously described (Reed et al., 1986). SLA was used at a concentration of 5μg/mL, after testing negative for endotoxins using the Limulus amebocyte lysate test.

Detection of Anti-Leishmanial IgG Antibodies by ELISA

Peripheral blood from ML patients was added to a dry tube for serum separation and stored at -20°C. Polystyrene plates were sensitized with 5 μg/well of soluble *Leishmania* antigen in carbonate/bicarbonate buffer and incubated overnight at 4°C. To block unspecific antibody binding, 1% bovine albumin (BSA) in PBS was added for 1 hour at 37°C. Sera (1:50 dilution) from patients and healthy controls were added and incubated for 1 hour at 37°C. Peroxidase-conjugated monoclonal anti-human IgG (Sigma-Aldrich, St. Louis, MO, USA), or monoclonal anti-human IgG1 and IgG2 (Sigma-Aldrich, St. Louis, MO, USA) were then added. After each step described above, 4-7 washes were performed with phosphate buffered saline containing 0.05% Tween 20. Finally, the enzyme substrate Tetramethylbenzidine (TMB) was added, and after 15 minutes the reaction was quenched with 2N H_2SO_4. Readings were performed on a microplate reader at a wavelength of 450 nm, and results were expressed as optical density (OD). The cut off values (total IgG is

0.395; IgG1 0.042; IgG2 0.159) were established by taking into account the mean + 3 standard deviations of absorbance readings from healthy subjects.

Detection of Cytokines in Serum

Serum was obtained from peripheral blood from 15 ML patients. Determination of IFN-γ and TNF concentrations were performed by ELISA (BD biosciences) according to the manufactures instructions. The results are expressed in pg/ml.

Statistical Analysis

Non-parametric testing involved the Kruskal-Wallis and Wilcoxon signed-rank tests, for comparisons of continuous variables using GraphPad Prism version 5.0 (GraphPad Software, San Diego, CA, USA). Statistical differences were considered when p values were less than 0.05.

RESULTS

Twenty-seven patients with ML and 25 with CL were enrolled in this study. Due to the small number of patients classified as stage I or V, patients were divided into three groups: Stages I and II (40.7%), stage III (25.9%) and stages IV and V (33.4%). Regarding sex, males were predominant in most groups, although no statistical significant difference was found between groups. We also found no difference in the frequency of individuals that reached cure within 90 days after therapy initiation, between groups. Ninety-six percent of patients with ML had previous CL lesion whereas no CL patients had history of leishmaniasis.

Titers of IgG antibodies are known to increase in active CL and visceral leishmaniasis, and decrease after cure (Fagundes-Silva et al., 2012). Since ML is the most inflammatory form of tegumentary leishmaniasis, we first wanted to investigate whether there were differences among IgG titers between ML and CL patients and found no differences in total IgG, IgG1 and IgG2 titers between these groups (**Figure 1**). We also examined antibodies levels among ML patients in different stages of disease. Interestingly, patients on stages IV and V presented high titers of total IgG and IgG2 when compared to those in stages I and II (**Figure 2**).

To determine whether reduced antibody production was associated with a successful therapeutic response, the titers of *Leishmania*-specific IgG, IgG1 and IgG2 were determined before and 90 days following the onset of therapy in 18 ML patients. Reductions were observed in the absorbance of total IgG, in 73% of patients, and IgG2, in 89% of patients who successfully responded to antimonial treatment (**Figure 3**). Interestingly, increase in the levels of IgG, IgG1 and IgG2 was observed in the three individuals that failed therapy.

We have previously documented that mononuclear cells from ML patients produce high levels of IFN-γ and inflammatory cytokines in response to *Leishmania* antigens (Bacellar et al., 2002). It is known that IFN-γ induces IgG2 production and IgG induces TNF in monocytes through Fcγ III (Kawano and Noma, 1996; Chouchakova et al., 2001; Chakraborty et al., 2021). Here we found that serum levels of IFN-γ and TNF in ML patients are increased during disease and decreases after treatment, and a positive correlation between pre-treatment TNF and pre-treatment IgG1 serum levels was observed (**Figure 4**).

DISCUSSION

Although ML, which predominantly affects the nasal mucosa, only occurs in less than 5% of individuals with American tegumentary leishmaniasis, its importance is recognized by the potential to develop destructive nasal lesions, which could then spread to the face. Also, high rates of treatment failure have been documented, not only using pentavalent antimony, but also in response to other leishmanicidal drugs, such as amphotericin B and miltefosine (Soto et al., 2005; Machado et al., 2010). We previously showed that the combination of pentoxifylline with

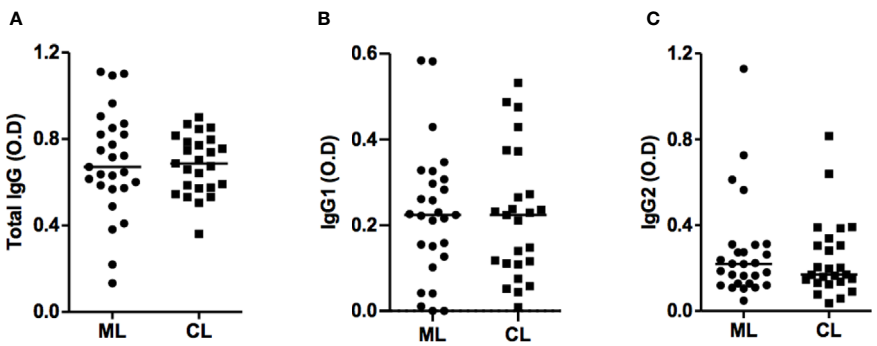

FIGURE 1 | ML and CL patients produce IgG antibodies against *Leishmania braziliensis* antigens. Anti-SLA total IgG **(A)**, IgG1 **(B)** and IgG2 **(C)** titers from ML (n=27) and CL (n=25) patients, performed by ELISA technique. Statistical analysis was performed by the Mann-Whitney U test. Results are expressed in optical density (OD).

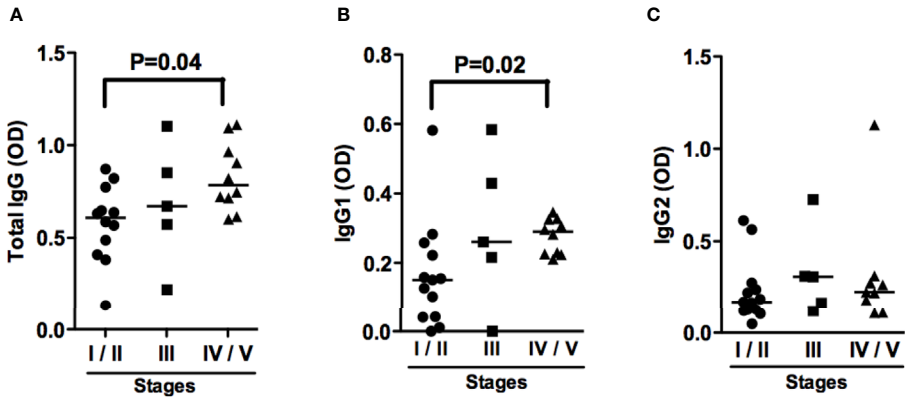

FIGURE 2 | ML patients with severe disease present increased Total IgG and IgG1 antibodies titers. Anti-SLA total IgG **(A)**, IgG1 **(B)** and IgG2 **(C)** titers from ML patients in different stage of the disease, performed by ELISA technique. Statistical analysis was performed by the Kruskal-Wallis test. Results are expressed in optical density (OD). ML stage I/II (n=12); ML stage III (n=5); ML stage IV/V (n=10).

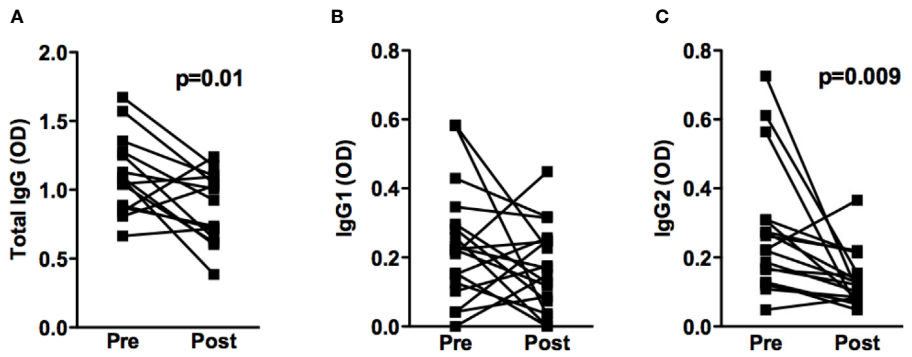

FIGURE 3 | IgG and IgG subclasses titers before and after treatment of ML patients. Anti-SLA total IgG (n=15) **(A)**, IgG1 (n=18) **(B)** and IgG2 (n=18) **(C)** titers from ML patients, performed by ELISA technique. Statistical analysis was performed by the Wilcoxon signed-rank test. Results are expressed in optical density (OD).

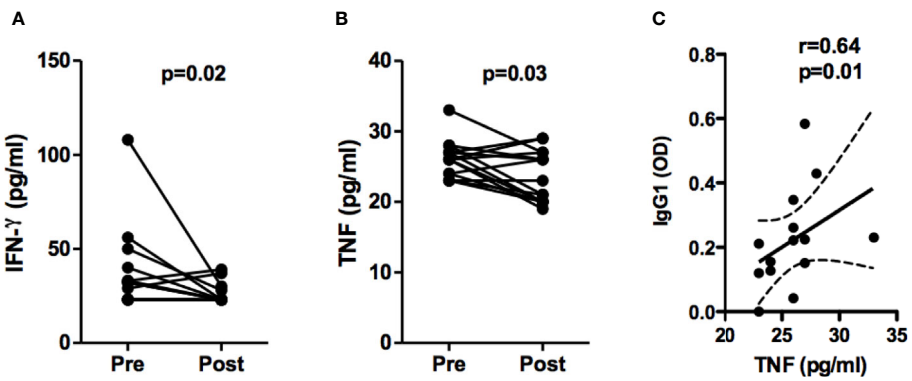

FIGURE 4 | Serum levels of IFN-γ and TNF from ML patients. Serum concentration of IFN-γ **(A)** and TNF **(B)** from ML patients (n=15) were assessed before and 90 days after pentavalent antimony therapy, by ELISA technique. Statistical analysis was performed by the Wilcoxon signed-rank test. Results are expressed in pg/ml. **(C)** Spearman correlation between TNF and IgG1 serum concentration, before treatment.

antimony increases ML cure rates and cures patients refractory to antimony. The high rate of cure observed herein stands in agreement with a previous study in which pentavalent antimony in association with pentoxifylline resulted in 100% of included ML patients evolving to cure (Machado et al., 2007).

Most immunological studies in patients with tegumentary leishmaniasis place emphasis on the cell-mediated response, while few investigations have focused on the role of immunoglobulins in protection against or severity of disease. The majority of studies involving the latter area, are concerned with the use of antibodies in serological testing leishmaniasis diagnostic purposes. To investigate associations between the severity of mucosal disease and elevated levels of antibodies against soluble *Leishmania braziliensis* antigen, we compared titers of IgG, IgG1 and IgG2 in the sera of patients with CL and ML prior to and following the onset of treatment, but found no differences between these clinical forms.

Interestingly, we documented an association between high levels of anti-leishmania IgG and IgG1 subclass antibodies with more advanced stages of ML, which suggests either the participation of antibodies in disease severity, or that the antibody absorbance represents a marker of severity. Antibodies may participate in the pathology of leishmaniasis by way of two mechanisms: 1- Opsonization, which increases parasite uptake by macrophages and, consequently, increases parasite burden within these cells; 2- Through increased antibody-mediated cytotoxicity, i.e. higher rates of infected macrophage killing lead to the release of *Leishmania* antigens (Barral-Netto et al., 1995). Both mechanisms can result in increases in inflammatory response and tissue damage. IFN-γ is known to induce IgG2 production, and IgG induces TNF through Fcγ III (CD16). We previously documented increase in the frequency of CD16+ circulating monocytes in CL patients and found that CD16+ monocytes are the main source of TNF and IL-1β in CL patients (Passos et al., 2015; Santos et al., 2018). In the present work we found a positive correlation between systemic concentrations of TNF and IgG1 antibodies, suggesting a contribution of IgG1 to the deleterious inflammatory response and immunopathology observed in ML.

The lack of markers of response to treatment in cutaneous leishmaniasis continues to present challenges to successful therapeutic intervention. Here we documented a drop in the levels of IgG and IgG2 in most ML patients between 60 and 90 days after treatment initiation. Reduced IgG antibody production after cure has also been observed in patients with CL (Schubach et al., 1998; Mendonca et al., 2004). To further investigate the potential applicability of antibodies as markers of therapeutic response in ML, new studies must be conducted involving higher numbers of patients with more extensive timepoint antibody measurements.

One limitation of the present study was the small number of patients evaluated after therapy. However, we were able to clearly demonstrate higher levels of IgG and IgG1 anti-*Leishmania* antibodies in more advanced stages of mucosal nasal disease, in which patients have already developed deep ulcers or septal perforation. Moreover, as the levels of these immunoglobulins drop in most patients after the onset of therapy, antibody measurements may serve as a biomarker of ML prognosis, as well as be a tool capable of supporting the decision to interrupt follow-up in outpatient settings.

Although current serological diagnostic capabilities cannot differentiate between patients with ML and those with CL, the presently established association between antibody absorbance and clinical disease staging suggests that antibodies do indeed participate in the pathogenesis of ML. In addition, the observed reductions in antibody production after treatment and cure provides a preliminary indication that these tests may prove useful in assessing therapeutic response.

DATA AVAILABILITY STATEMENT

The datasets presented in this study can be found in online repositories. The names of the repository/repositories and accession number(s) can be found below: https://doi.org/10.6084/m9.figshare.13415183.v1.

ETHICS STATEMENT

The studies involving human participants were reviewed and approved by Professor Edgard Santos University Hospital (HUPES-UFBA), Salvador, Bahia-Brazil. The patients/participants provided their written informed consent to participate in this study.

AUTHOR CONTRIBUTIONS

CL, LC, ML, RC, CC, and EC conceived and designed the study. CL, LC, AM, and RC analyzed the data. CL, LC, AM, and EC interpreted the data. CL, LC, AM, RC, and CC drafted the manuscript. CL, LC, ML, AM, RC, and EC critically revised the manuscript for intellectual content. EC is guarantor of the manuscript. All authors contributed to the article and approved the submitted version.

FUNDING

This study was supported by the US National Institutes of Health grant AI-136032.

ACKNOWLEDGMENTS

We acknowledge Ednaldo Lago for providing assistance with the patient selection. The authors also thank Andris K. Walter for English language manuscript revision and copyediting services.

REFERENCES

Bacellar, O., Lessa, H., Schriefer, A., Machado, P., Ribeiro de Jesus, A., Dutra, W. O., et al. (2002). Up-regulation of Th1-type responses in mucosal leishmaniasis patients. *Infect. Immun.* 70 (12), 6734–6740. doi: 10.1128/iai.70.12.6734-6740.2002

Barral-Netto, M., Barral, A., Brodskyn, C., Carvalho, E. M., and Reed, S. G. (1995). Cytotoxicity in human mucosal and cutaneous leishmaniasis. *Parasite Immunol.* 17 (1), 21–28. doi: 10.1111/j.1365-3024.1995.tb00962.x

Boaventura, V. S., Cafe, V., Costa, J., Oliveira, F., Bafica, A., Rosato, A., et al. (2006). Concomitant early mucosal and cutaneous leishmaniasis in Brazil. *Am. J. Trop. Med. Hyg.* 75 (2), 267–269. doi: 10.4269/ajtmh.2006.75.267

Carvalho, E. M., Barral, A., Costa, J. M., Bittencourt, A., and Marsden, P. (1994). Clinical and immunopathological aspects of disseminated cutaneous leishmaniasis. *Acta Trop.* 56 (4), 315–325. doi: 10.1016/0001-706x(94)90103-1

Carvalho, L. P., Passos, S., Bacellar, O., Lessa, M., Almeida, R. P., Magalhaes, A., et al. (2007). Differential immune regulation of activated T cells between cutaneous and mucosal leishmaniasis as a model for pathogenesis. *Parasite Immunol.* 29 (5), 251–258. doi: 10.1111/j.1365-3024.2007.00940.x

Chakraborty, S., Gonzalez, J., Edwards, K., Mallajosyula, V., Buzzanco, A. S., Sherwood, R., et al. (2021). Proinflammatory IgG Fc structures in patients with severe COVID-19. *Nat. Immunol.* 22 (1), 67–73. doi: 10.1038/s41590-020-00828-7

Chouchakova, N., Skokowa, J., Baumann, U., Tschernig, T., Philippens, K. M., Nieswandt, B., et al. (2001). Fc gamma RIII-mediated production of TNF-alpha induces immune complex alveolitis independently of CXC chemokine generation. *J. Immunol.* 166 (8), 5193–5200. doi: 10.4049/jimmunol.166.8.5193

Fagundes-Silva, G. A., Vieira-Goncalves, R., Nepomuceno, M. P., de Souza, M. A., Favoreto, S.Jr., Oliveira-Neto, M. P., et al. (2012). Decrease in anti-Leishmania IgG3 and IgG1 after cutaneous leishmaniasis lesion healing is correlated with the time of clinical cure. *Parasite Immunol.* 34 (10), 486–491. doi: 10.1111/j.1365-3024.2012.01379.x

Grimaldi, G.Jr., David, J. R., and McMahon-Pratt, D. (1987). Identification and distribution of New World Leishmania species characterized by serodeme analysis using monoclonal antibodies. *Am. J. Trop. Med. Hyg.* 36 (2), 270–287. doi: 10.4269/ajtmh.1987.36.270

Junqueira Pedras, M., Orsini, M., Castro, M., Passos, V. M., and Rabello, A. (2003). Antibody subclass profile against Leishmania braziliensis and Leishmania amazonensis in the diagnosis and follow-up of mucosal leishmaniasis. *Diagn. Microbiol. Infect. Dis.* 47 (3), 477–485. doi: 10.1016/s0732-8893(03)00141-x

Kawano, Y., and Noma, T. (1996). Role of interleukin-2 and interferon-gamma in inducing production of IgG subclasses in lymphocytes of human newborns. *Immunology* 88 (1), 40–48. doi: 10.1046/j.1365-2567.1996.d01-634.x

Lessa, H. A., Lessa, M. M., Guimaraes, L. H., Lima, C. M., Arruda, S., Machado, P. R., et al. (2012). A proposed new clinical staging system for patients with mucosal leishmaniasis. *Trans. R. Soc. Trop. Med. Hyg.* 106 (6), 376–381. doi: 10.1016/j.trstmh.2012.03.007

Machado, P. R., Lessa, H., Lessa, M., Guimaraes, L. H., Bang, H., Ho, J. L., et al. (2007). Oral pentoxifylline combined with pentavalent antimony: a randomized trial for mucosal leishmaniasis. *Clin. Infect. Dis.* 44 (6), 788–793. doi: 10.1086/511643

Machado, P. R., Ampuero, J., Guimaraes, L. H., Villasboas, L., Rocha, A. T., Schriefer, A., et al. (2010). Miltefosine in the treatment of cutaneous leishmaniasis caused by Leishmania braziliensis in Brazil: a randomized and controlled trial. *PloS Negl. Trop. Dis.* 4 (12), e912. doi: 10.1371/journal.pntd.0000912

Marsden, P. D. (1994). Mucosal leishmaniasis due to Leishmania (Viannia) braziliensis L(V)b in Tres Bracos, Bahia-Brazil. *Rev. Soc. Bras. Med. Trop.* 27 (2), 93–101. doi: 10.1590/s0037-86821994000200007

Mendonca, M. G., de Brito, M. E., Rodrigues, E. H., Bandeira, V., Jardim, M. L., and Abath, F. G. (2004). Persistence of leishmania parasites in scars after clinical cure of American cutaneous leishmaniasis: is there a sterile cure? *J. Infect. Dis.* 189 (6), 1018–1023. doi: 10.1086/382135

Miranda Lessa, M., Andrade Lessa, H., Castro, T. W. N., Oliveira, A., Scherifer, A., Machado, P., et al. (2007). Mucosal leishmaniasis: epidemiological and clinical aspects. *Braz. J. Otorhinolaryngol.* 73 (6), 843–847. doi: 10.1016/S1808-8694(15)31181-2

Passos, S., Carvalho, L. P., Costa, R. S., Campos, T. M., Novais, F. O., Magalhães, A., et al. (2015). Intermediate monocytes contribute to pathologic immune response in Leishmania braziliensis infections. *J. Infect. Dis.* 211 (2), 274–282. doi: 10.1093/infdis/jiu439

Reed, S. G., Badaro, R., Masur, H., Carvalho, E. M., Lorenco, R., Lisboa, A., et al. (1986). Selection of a skin test antigen for American visceral leishmaniasis. *Am. J. Trop. Med. Hyg.* 35 (1), 79–85. doi: 10.4269/ajtmh.1986.35.79

Santos, D., Campos, T. M., Saldanha, M., Oliveira, S. C., Nascimento, M., Zamboni, D. S., et al. (2018). IL-1β Production by Intermediate Monocytes Is Associated with Immunopathology in Cutaneous Leishmaniasis. *J. Invest. Dermatol.* 138 (5), 1107–1115. doi: 10.1016/j.jid.2017.11.029

Schubach, A., Marzochi, M. C., Cuzzi-Maya, T., Oliveira, A. V., Araujo, M. L., Oliveira, A. L., et al. (1998). Cutaneous scars in American tegumentary leishmaniasis patients: a site of Leishmania (Viannia) braziliensis persistence and viability eleven years after antimonial therapy and clinical cure. *Am. J. Trop. Med. Hyg.* 58 (6), 824–827. doi: 10.4269/ajtmh.1998.58.824

Soto, J., Toledo, J., Vega, J., and Berman, J. (2005). Short report: efficacy of pentavalent antimony for treatment of colombian cutaneous leishmaniasis. *Am. J. Trop. Med. Hyg.* 72 (4), 421–422. doi: 10.4269/ajtmh.2005.72.421

Weirather, J. L., Jeronimo, S. M., Gautam, S., Sundar, S., Kang, M., Kurtz, M. A., et al. (2011). Serial quantitative PCR assay for detection, species discrimination, and quantification of Leishmania spp. in human samples. *J. Clin. Microbiol.* 49 (11), 3892–3904. doi: 10.1128/JCM.r00764-11

World Health Organization - Control of Leishmaniasis. (2010). *WHO Technical Report Series*. Iris - International repository for information sharing.

Conflict of Interest : The authors declare that the research was conducted in the absence of any commercial or financial relationships that could be construed as a potential conflict of interest.

frontiers in Cellular and Infection Microbiology

ORIGINAL RESEARCH
published: 07 June 2021
doi: 10.3389/fcimb.2021.631019

Leishmania spp Epitopes in Humans Naturally Resistant to the Disease: Working Toward a Synthetic Vaccine

*Magda Melissa Flórez[1], Rocío Rodríguez[2], José Antonio Cabrera[3], Sara M. Robledo[4] and Gabriela Delgado[1]**

[1] Grupo de Investigación en Inmunotoxicología, Departamento de Farmacia, Facultad de Ciencias, Universidad Nacional de Colombia, Bogotá D.C., Colombia, [2] Secretaría Municipal de Salud, Municipio de Rovira, Tolima, Colombia, [3] Hospital San Vicente, Municipio de Rovira, Tolima, Colombia, [4] Programa de Estudio y Control de Enfermedades Tropicales (PECET)-Facultad de Medicina, Universidad de Antioquia, Medellín, Colombia

OPEN ACCESS

Edited by:
Wander Pavanelli, State University of Londrina, Brazil

Reviewed by:
Chiranjib Pal, West Bengal State University, India
Giuseppe Palmisano, University of São Paulo, Brazil

***Correspondence:**
Gabriela Delgado
lgdelgadom@unal.edu.co

Specialty section:
This article was submitted to Parasite and Host, a section of the journal Frontiers in Cellular and Infection Microbiology

Received: *19 November 2020*
Accepted: *20 April 2021*
Published: *07 June 2021*

Citation:
Flórez MM, Rodríguez R, Cabrera JA, Robledo SM and Delgado G (2021) Leishmania spp Epitopes in Humans Naturally Resistant to the Disease: Working Toward a Synthetic Vaccine. Front. Cell. Infect. Microbiol. 11:631019. doi: 10.3389/fcimb.2021.631019

Vaccines are one of the most effective strategies to fight infectious diseases. Reverse vaccinology strategies provide tools to perform *in silico* screening and a rational selection of potential candidates on a large scale before reaching *in vitro* and *in vivo* evaluations. *Leishmania* infection in humans produces clinical symptoms in some individuals, while another part of the population is naturally resistant (asymptomatic course) to the disease, and therefore their immune response controls parasite replication. By the identification of epitopes directly in humans, especially in those resistant to the disease, the probabilities of designing an effective vaccine are higher. The aim of this work was the identification of *Leishmania* epitopes in resistant humans. To achieve that, 11 peptide sequences (from *Leishmania* antigenic proteins) were selected using epitope prediction tools, and then, peripheral blood mononuclear cells (PBMCs) were isolated from human volunteers who were previously divided into four clinical groups: susceptible, resistant, exposed and not exposed to the parasite. The induction of inflammatory cytokines and lymphoproliferation was assessed using monocyte-derived dendritic cells (moDCs) as antigen-presenting cells (APCs). The response was evaluated after exposing volunteers' cells to each peptide. As a result, we learned that STI41 and STI46 peptides induced IL-8 and IL-12 in moDCs and lymphoproliferation and low levels of IL-10 in lymphocytes differentially in resistant volunteers, similar behavior to that observed in those individuals to *L. panamensis* lysate antigens. We conclude that, *in silico* analysis allowed for the identification of natural *Leishmania* epitopes in humans, and also STI41 and STI46 peptides could be epitopes that lead to a cellular immune response directed at parasite control.

Keywords: synthetic peptides, reverse vaccinology, leishmaniasis, humans, naturally resistant, T epitopes

INTRODUCTION

Vaccines have decreased the incidence of several infectious diseases, especially those caused by bacteria and viruses because of either the generation of neutralizing antibodies or by the activation of memory T lymphocytes essential in pathogen elimination, and therefore allowing for the protection of the individual to reinfections (Sallusto et al., 2010).

One of the strategies available for vaccine development is reverse vaccinology that implies the use of pathogen and host OMICS to rationally design vaccine candidates. This approach has advanced significantly in vaccine research since the first full sequencing of a microorganism in 1995 (Fleischmann et al., 1995), up to the thousands of microbial genomes characterized so far. The above has allowed researchers to understand the polymorphisms between the pathogen species and the variability in human proteins involved in antigen presentation, therefore favoring a more accurate approach in the development of vaccines. These advances also allow bioinformatics tools to be more precise in their *in silico* screening performance, thus making research less time-consuming by reducing the possible candidates to be evaluated in *in vitro* and *in vivo* assays (Donati and Rappuoli, 2013; Grubaugh et al., 2013; Seyed et al., 2016).

T cell epitope prediction tools, based on human antigen presentation molecules, use algorithms that predict the binding of pathogen proteins to HLA molecules (Gfeller and Bassani-Sternberg, 2018).

Antigen searches made directly in humans increase the possibilities of success in candidate selection, although it is still a major challenge to reduce the gap between animal and human experimentation, as has happened in previous leishmaniasis vaccine attempts (Kedzierski, 2010). Depending on the endemic area and infecting specie, among other factors, between 20% and 91% of individuals exposed to the parasite rapidly resolve infection and the disease course becomes mild or even asymptomatic, these individuals are considered "naturally resistant" (evidenced by positive Leishmanin Skin Tests [LSTs], without any history of the disease) (Weigle et al., 1991; Das et al., 2014; Andrade-Narvaez et al., 2016; Best et al., 2018). Taking into account this information, T cell epitope screening in a naturally exposed population may open new possibilities to identify sequences linked to the natural resistance to the disease, which may be associated with the induction of protection toward the immunization of susceptible individuals.

Because *Leishmania* is an obligated intracellular parasite, T cell-mediated immune response plays an important role in the resolution of the disease. Although the immune response against the parasite has been described mainly in murine models, where there is a clear dichotomy between the protection mediated by Th1 response and susceptibility mediated by Th2 response (Belkaid et al., 1998; Belkaid et al., 2000), in humans such a dichotomy is not established. However, a predominant Th1 profile response, next to interleukin-12 (IL-12), interferon-gamma (IFN-ɣ), and tumor necrosis factor-alpha (TNF-α) production are essential to eliminate the parasite (Ajdary et al., 2000; Maspi et al., 2016). On the other hand, the IL-10 role is controversial because it has been identified as necessary to balance and avoid severe damage caused by an exacerbated immune response, but it has also been associated with the persistence of viable parasites after a clinical cure (Belkaid et al., 2002). The assessment of immune response in individuals "naturally resistant" to leishmaniasis would ease the comprehension of the immune response involved in resistance in humans, and therefore, it would guide the characterization of epitopes driving protection against the disease as potential vaccine candidates.

Therefore, in order to identify epitopes associated with leishmaniasis resistance: *(i)* we selected peptide sequences from *Leishmania* proteins, with a high probability to bind human HLA-DR haplotypes throughout *in silico* tools and *(ii)* we evaluated *ex vivo* antigenicity of those peptides in cells from individuals "naturally resistant" to the parasite, using monocyte-derived dendritic cells (moDCs) as antigen-presenting cells (APCs).

MATERIALS AND METHODS

In Silico Analysis for T Epitopes

Leishmania spp. proteins were selected for *in silico* analysis considering: *i)* expression in amastigote parasite form, *ii)* high homology between *Leishmania* species causing cutaneous leishmaniasis in both old and new world, and *iii)* proteins previously reported as immunogenic *in vitro* and *in vivo*, with the induction of a Th1 response and/or reported as inductor of disease resistance, in different models. The selected proteins were: *i)* kinetoplastid membrane protein-11 (KMP-11, NCBI accession number AAF32344.1), *ii) Leishmania*-activated protein kinase C receptor (LACK, NCBI accession number AAG31685), *iii)* tryparedoxin peroxidase (TSA, NCBI accession number XP_010697482.1), *iv)* stress-induced protein 1 (STI1, NCBI accession number XP_010704221.1), and *v) Leishmania* eukaryotic initiation factor 4a (LEIF accession number XP_010696717.1). The T epitopes prediction tools were IEDB Analysis Resource (http://tools.iedb.org/mhcii/) (Wang et al., 2008; Wang et al., 2010), NetMHCIIpan (http://www.cbs.dtu.dk/services/NetMHCIIpan/) (Jensen et al., 2018), and Tepitopepan (http://datamining-iip.fudan.edu.cn/service/TEPITOPEpan/TEPITOPEpan.html) (Sturniolo et al., 1999; Nielsen et al., 2008; Zhang et al., 2009; Bordner and Mittelmann, 2010; Nielsen et al., 2010). Some 15-mer peptide sequences were selected by the following criteria: i) sequences with %Rank≥2 (strong binders) for at least two out of three prediction tools for more than one HLA-DR allele evaluated; ii) identical or similar sequences (synonym substitutions) between *L. panamensis*, *L. braziliensis*, and *L. major* species; and iii) sequences different from their human homolog when applicable. HLA-DR alleles taken in these predictions were based on studies of the most frequent alleles in the Colombian population (Trachtenberg et al., 1996; Correa et al., 2002; Reyes et al., 2007; Arias-Murillo et al., 2010; Ávila-Portillo et al., 2010; Yunis et al., 2013).

Peptide Synthesis

Peptides were synthesized by the Chemistry Group belonging to Fundación Instituto de Inmunología de Colombia (FIDIC), based on Merriefield's solid phase peptide synthesis methodology (Merrifield, 2006; Vanegas Murcia, 2014), using

aminoacids T-BOC protected and purified by reverse-phase HPLC and mass spectrometry MALDI-TOF.

Human Volunteers

Individuals included in this study were from different endemic areas in Colombia: *i)* rural area (La Luisa) of Rovira/Tolima, *ii)* PECET-UDEA research center, Medellín/Antioquia, and *iii)* Bogotá D.C. (non-endemic area, volunteers used as negative control). Human experiments were carried out following the Declaration of Helsinki. All volunteers included here agreed to participate through informed consent after the nature and possible consequences of the studies had been fully explained (approved by the ethical committee, act number 12, submitted on August 3, 2015, Science Faculty, National University of Colombia).

Humans were injected with 0.1 mL of LST solution (*Leishmania panamensis* preparation) by the intradermal route in the forearm, and the response was measured 72 h later. An induration diameter ≥4 mm was considered positive. Considering the clinical history of leishmaniasis and the LST result of each individual, they were classified into four clinical groups: *i*) susceptible to the disease (S n=10), including those with active cutaneous leishmaniasis and those cured after treatment, all of them with positive LST, all of them with a confirmed parasitological diagnosis; *ii*) resistant to the disease (R, n=10), characterized by a positive LST response without a history of leishmaniasis (no lesions history, nor leishmaniasis scars); *iii*) people living in endemic areas with a negative LST result (identified as individuals living in the same houses as susceptible volunteers, it means that they have been exposed to the same environmental risk factors), named exposed (E, n=14); and *vi*) not exposed individuals (NE, n=11), volunteers living in non-endemic areas with a negative LST response. It is important to highlight that the study place is not a T. cruzi circulation area, therefore it is a Chagas disease-free zone.

Isolation and Differentiation of moDCs

Venous heparinized blood was collected, and PBMC´s (peripheral blood mononuclear cells) were isolated using density gradient reagent Lymphoprep™ (STEMCELL, Vancouver Canada). Cells were grown in RPMI 1640 medium (Invitrogen, USA), supplemented with inactivated fetal bovine serum (Hyclone, GE, Illinois, USA) 1% and incubated for 2 h at 37°C and 5% CO_2. Afterward, the non-adherent fraction was recovered and preserved for posterior use, while the adherent fraction was stimulated with 1 ng/ml of IL-4rh (Invitrogen, USA) and 2 ng/ml of GM-CSFrh (Invitrogen, USA) every other day (2 pulses) for 5 days, to obtain moDCs.

In Vitro Antigen Presentation

moDCs were pulsed with 10 μg/ml of each peptide or 10 μg/ml of *L. panamensis* lysate, or 25 ug/ml of PHA (Phytohaemagglutinin)–last two as controls–for 72 h; the supernatants were collected to assess inflammatory cytokines IL-8, IL-1β, IL-6, IL-10 TNFα, and IL-12p70 (CBA Becton Dickinson USA). After complete medium removal, moDCs were co-incubated for 7 days with the autologous non-adherent fraction (previously preserved) at a 1:10 ratio and stained with 5 μM of CFSE (Invitrogen, USA) in order to evaluate lymphoproliferation and the secretion of Th1-1h2-Treg cytokines IL-2, IL-4, IL-10, TNFα, and IFNɣ (CBA Becton Dickinson USA) in supernatants by flow cytometry (FACS Canto II BD).

Data Analysis

Each result was normalized for each individual according to the Reactivity Index (RI), calculated by dividing the results of stimulated cells with each antigen between autologous cells without stimulation. The lymphoproliferation was evaluated as the Proliferation Index (PI) or Division Index (DI) calculated using FCS Express software. Data were analyzed by the non-parametric Kruskal-Wallis method to compare differences in cytokines and proliferation between all clinical groups. Graphs and statistical analyses were made using Graphpad Prism 7.0 software.

RESULTS

In Silico Analysis

Under the *in silico* conditions described above, KMP-11, LACK, STI1, TSA, and LEIF proteins were pre-selected, and along the linear sequences, 1,483 overlapped 15-mer peptides were obtained overlapping 14 out of 15 amino acids in the next peptide. With each bioinformatic tool, a binding prediction for each peptide was run against 29 HLA-DR alleles (frequent in the Colombian population) resulting in 129,021 predictions, 43,007 for each tool. The results showed 73 sequences associated with high binding to any of the HLA-DR alleles evaluated. Finally, after considering the selection criteria previously described, 11 sequences met the established conditions (**Table 1**). None of the KMP-11 or TSA-derived sequences fulfilled the selection criteria, due to low binding prediction and high homology between parasite and human protein, respectively.

Table 1 shows that, although the same cut off was applied for all of the tools, IEDB was identified as a strong binder of a higher number of sequences compared with NetMHCIIpan and TepitopePan, which, in a few cases, were identified as strong binders to the HLA-DRs evaluated. The results indicated that it is necessary to employ more than one *in silico* platform to improve precision for epitope identification. After *in silico* sequence selection, the 11 peptides were synthesized, and their biological evaluation was performed *ex vivo* in humans naturally exposed to infection by the *Leishmania* parasite. When we compared the peptide sequences with *Trypanosoma cruzi* proteins, we found a range between 46.6% and 93.3% of identity (**Table 1**), however considering that the samples were taken in a Chagas disease-free area, plus the absence of IgG against *T. cruzi* in the serum of all of the samples collected (data not shown), we can tell that the response observed in these individuals is linked to *Leishmania spp* exposure.

Evaluation of Peptides Biological Response in Human Cells

Inflammatory Cytokine Production by moDCs

After the prediction of sequences (15-mer peptides) as probable T $CD4^+$ epitopes, their antigenicity was evaluated in human cells

TABLE 1 | *In silico* analysis of binding prediction to HLA-DR alleles.

Protein	Code	Sequence	Prediction tool			Identity between *Leishmania* species[§]	Homology (%) with human protein	Identity (%) with T. cruzi sequence**
			IEDB[‡]	NETMHCIIpan[‡]	TepitopePan[‡]			
LACK	LACK08	LEGHTGFVSCVSLAH	04:01, 04:04, 04:10, 11:01, 11:02, 13:05.	NB	04:01, 04:05, 04:07, 10:01.	100%	NO (33%)	60%
STI1	STI72	GRYVEAVNYFSKAIQ	11:02, 11:01, 13:01, 13:04.	NB	11:02, 13:04.	100%	NO (33%)	60%
	STI40	NWAKGYVRRGAALHG	01:02, 11:01, 13:04.	NB	08:02, 08:03.	100%	NO (53%)	80%
	STI41	KLSLLMLQPDYVKMV	01:02, 01:03, 03:01, 04:03, 04:04, 04:06, 04:11, 10:01, 15:01,	01:02, 04:03, 04:04, 04:06, 04:10, 04:11, 08:03, 12:01, 14:01, 15:01,	NB	100%	NO (20%)	73.3%
	STI42	ALTLMYLSGMKIPND	01:01, 01:02, 04:04, 11:01, 13:05, 15:01.	15:01.	01:02, 01:03.	100%	NO (27%)	46.6%
	STI43	TLYILNVSAVYFEQR	01:01, 01:02, 03:01, 04:10, 11:02, 12:01, 13:01, 13:02,	01:03, 04:07, 08:03, 13:02, 13:03, 14:02, 16:02.	NB	*93%	NO (53%)	53.3%
	STI44	YTIVAKLMTRHAFCL	08:03, 11:01, 11:02, 12:02, 13:03, 13:05, 14:01, 14:02, 16:02.	01:02, 04:04, 04:10, 04:11, 08:02, 11:01, 11:02, 12:01, 12:02, 13:01, 13:04, 13:05, 14:01.	NB	*80%	NO (33%)	73.3%
	STI46	SVKINKLISAGIIRF	01:03, 01:02, 03:01, 04:03, 04:04, 04:06, 04:11, 07:01, 08:02.10:01, 11:01, 11:02, 13:03, 14:01, 15:01.	01:01, 01:02, 01:03, 04:07, 07:01, 08:03, 11:02, 12:01, 13:01, 13:04, 14:01, 15:01.	NB	*93%	NO (40%)	80%
LEIF	LEIF73	FSIGLLQRLDFRHNL	13:05, 13:01, 11:01, 03:01, 13:04.	12:02.	12:02, 13:05.	100%	NO (47%)	93.3%
	LEIF50	YEIFRFLPKDIQVAL	01:02, 11:01, 11:02, 13:01, 13:04.	12:02.	13:03, 14:02.	100%	NO (47%)	86.6%
	LEIF52	QSVIFANTRRKVDWI	08:03, 11:01, 11:02, 13:03, 13:01, 14:01, 14:02,	11:01, 11:02, 13:01, 13:03, 13:04, 13:05.	NB	100%	NO (73%)	93.3%

‡*Alleles with predicted strong binding to the sequence.*
**Sequences with amino acids substitution for another with similar characteristics.*
[§]*L. panamensis, L. braziliensis, and L. major species.*
NB, Non-binders.
***Trypanosoma cruzi strain CL Brener.*

isolated from volunteers belonging to the four clinical groups (**Table 2**).

moDCs, obtained from each participant, were pulsed with either a single peptide or a control antigen, for 72 h, while cytokines IL-8, IL-1β, IL-6, IL-10, TNF-α, and IL-12p70 were measured in culture supernatant as an indirect measure of cell maturation. **Figure 1** shows the levels of cytokines produced by each clinical group in response to antigen stimulation. All antigens tested induced production of inflammatory cytokines by moDCs (**Figure 1**), without clear discrimination between the ones previously exposed to the parasite (LST+) and the ones who did not (LST-), however, the R group tended to produce higher IL-12 levels and to a lesser extend IL-6 when cells were stimulated with *L. panamensis* lysate (**Figure 1D**). When moDCs were exposed to each peptide, the R group secreted differential cytokines compared with the S group with the following stimulations: *i*) LACK08 induced higher levels of IL-6 (**Figure 1A**). *ii*) STI72, STI43 and STI44, LEIF50 induced higher

TABLE 2 | Classification of human volunteers.

Clinical group	Characteristics	n	Parasitological diagnosis	Leishmanin Skin Test (LST)	Gender*	Age in years old: mean (range)
Susceptible (S)	Affected by the disease	10	Confirmed	Positive	F:7M:3	44.1 (12-81)
Resistant (R)	No disease history	10	No lesions	Positive	F:6M:4	29.5 (18-55)
Exposed (E)	Living in endemic areas	14	No lesions	Negative	F:6M:8	47.6 (13-88)
Not exposed (NE)	Living in non-endemic areas	11	No lesions	Negative	F:7M:4	31.4 (23-57)
Total		45			F:26M:19	38.45 (12-88)

**F, female; M, male.*

secretion of IL-8 and IL-6; and *iii*) STI40 and STI42 promoted IL-6 and TNFα or IL-6 alone, respectively (**Figures 1B, C**).

The exposure of immature moDCs to the 15-mer peptides induces its apparent maturation, which is evident in its ability to secrete inflammatory cytokines into the culture supernatant in volunteers belonging to all clinal groups. It means that, as expected for the innate immune response, there was no preference depending on whether there was previous exposure to the pathogen or not. However, R group individuals produced significantly higher levels of proinflammatory cytokines against some peptides than those from the S group, behavior that could favor parasite control in the first ones. Although PHA has been reported as an inductor of proliferation and differentiation of lymphocytes (in this study we found that it modulates the immune response in immature moDCs) toward a predominant TNF-α response, followed by IL-6 and IL-8, and to a lesser

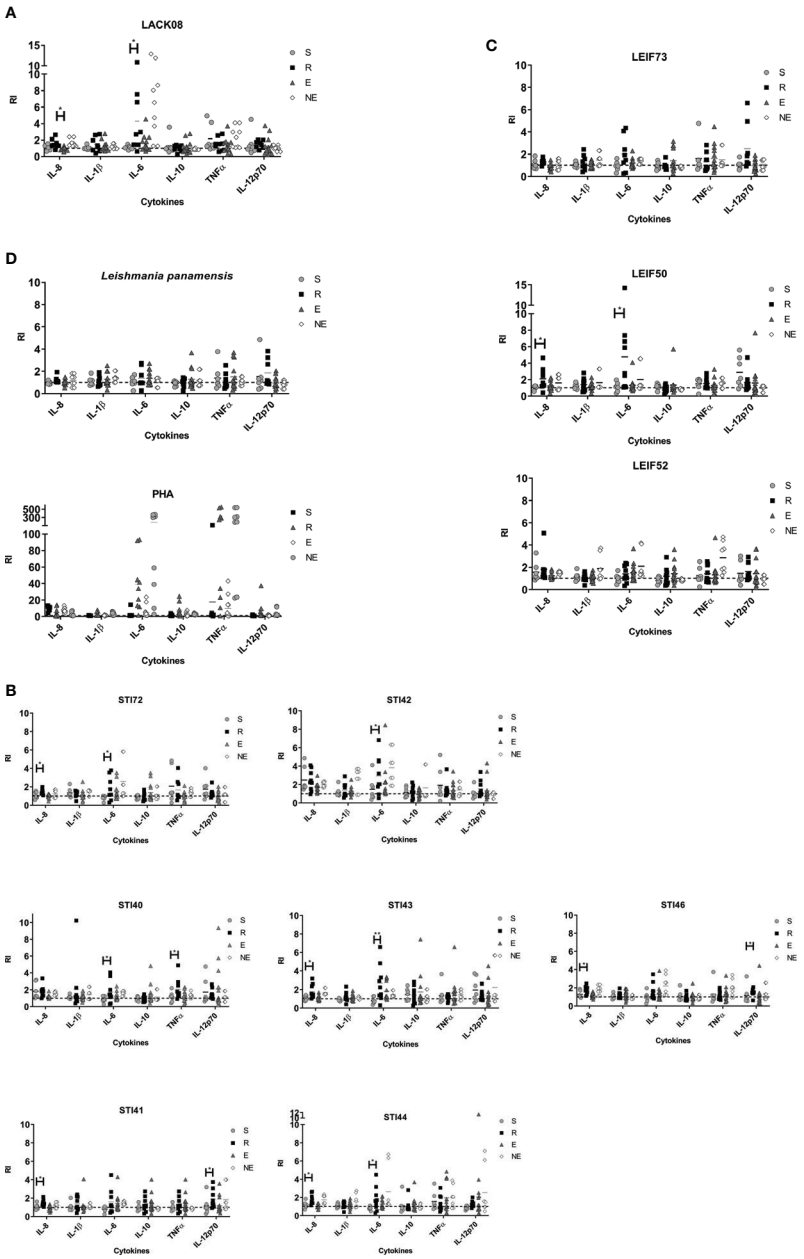

FIGURE 1 | Cytokines detected in human moDCs supernatants from S (susceptible), R (resistant), E (exposed), and NE (not exposed) groups. Cell pulsed with **(A)** peptides derived from LACK protein; **(B)** peptides derived from STI1 protein; **(C)** peptides derived from LEIF, and **(D)** *L. panamensis* or PHA. P<0.05(*), P<0.01 (**). Dashed line: non-stimulated cell response.

extend IL-1β, IL-10, and IL-12, being mediated by PHA is a unique stimulus (**Figure 1D**).

Lymphoproliferation

After moDCs were stimulated with each antigen for 72 h, the cells were co-cultured with autologous lymphocytes for 7 days. PI represents the average number of cells that an initial cell became (ability to proliferate considering the overall population), and DI means the average number of cells that a dividing cell became (ability to proliferate of responding cells). Lymphocyte proliferation is generated as the result of specific recognition of its cognate antigen and preferentially observed in memory cells.

Proliferation observed with PHA stimulus showed that cells isolated from all the volunteers had the ability to respond (**Figure 2D**). Cells exposed to *L. panamensis* lysate showed that PI and DI were significantly higher in the R group than LST- participants. These results indicate that the difference between humans naturally resistant compared with those who present disease symptoms reflects a higher proliferative function of the lymphocytes that recognize parasite antigens (**Figures 2D** and **3D**). When proliferation was assessed with peptides stimulation, R and S groups responded in different levels of PI to each antigen, especially the R group which showed significantly higher PI with LACK08, STI42, STI46, and LEIF73 than the NE group ($p<0,05$); however, the E group also showed a predominant response against STI40, STI41, STI43, and STI44 (**Figures 2A–C**). These results could be due to an unspecific response, not restricted to a volunteer previously exposed to Leishmania (LST+), however, when DI was evaluated, the proliferation response was more specific in S and R groups, especially against STI41, STI46, LEIF73, LEIF50, and LEIF52, where DI was higher in the R group (behavior similar to *L. panamensis* lysate) (**Figures 3A–C**). Lymphoproliferation triggered by the APC-peptide complex indicates that these individuals have the capability to recognize that sequence as an epitope. The hypothesis is reinforced by the result in the NE group, which did not respond to most of the sequences derived from *Leishmania*. Also, some individuals from the E group showed proliferation (PI but not DI) against some antigens. Although LST in the E group was negative, such a response could be due to cross-reactions with phylogenetically related pathogens, circulating in the same geographical area, and therefore, the volunteers recognize homologous proteins. It is worth noting that there were no reports of Chagas disease in the zone where volunteers were included (PortalSivigila, 2019 Estadísticas de Vigilancia Rutinaria), so, cross-reaction with *Trypanosoma cruzi* is unlikely.

T Helper Profile Cytokine Production

At the end of proliferation assay, supernatants were collected and Th1-Th2-Treg profile cytokines (IL-2, IL-4, IL-10, TNFα, and IFN-γ) were quantified. In general, PHA stimulation induced high levels of TNFα and IFN-γ, while peptide stimulation generated slight cytokine secretion (**Figure 4**). Considering that this work focused on the identification of epitopes related to disease resistance in humans, peptides that showed high PI or DI in the R group compared with NE were selected, therefore lymphocyte cytokines are described for STI41, STI42, STI46, LEIF73, LEIF50, and LEIF52 peptides (**Figure 4**).

Cells from group S individuals exposed to *L. panamensis* lysate produced small amounts of TNF-α and IFN-γ, while the R group produced IFN-γ and IL-2, predominantly. Focusing on the differences between the S group and R group, it is important to highlight that IL-2 was higher which correlated with proliferation in the latter group (**Figure 4B**). Additionally, there was a higher production (non-significantly) of IL-10 in the S group. With the previous information, we support the idea that the ability of an individual to produce IL-2 is related to a higher proliferative capability in lymphocytes, next to the secretion of Th-1 profile cytokines (especially IFN-γ) and low levels of IL-10, and could be generating a favorable activity against the parasite, promoting disease control.

Peptides STI41, STI42, and LEIF50, although they induced higher DI in the R group, IL-2 levels were lower than the S group (**Figure 4A**). STI41 and STI46 peptides did not produce detectable IL-10 levels in the R group, while the S and E groups did, showing similar behavior to cells exposed to *L. panamensis* lysate. Finally, cells exposed to LEIF73 and LEIF52 did not show important cytokine production or differences between clinical groups (**Figure 4A**).

Together all results obtained in this work, we could identify the STI46 peptide as a possible epitope associated with leishmaniasis resistance in human volunteers, because the R group mainly induced IL-8 and IL-12 at the time of antigen presentation, plus higher PI and lower IL-10 by lymphocytes than the S group. Cellular response activation associated with a pro-inflammatory profile that promotes intracellular parasite effective elimination such as *Leishmania* leads us to think that STI46 represents a prominent vaccine candidate that could be included in further *in vivo* studies and directed to evaluate its protective ability against leishmaniasis. The STI41 peptide induced IL-12 and IL-8 in moDCs from the R group, and IFN-γ and next to low IL-10 levels in lymphocytes. Although IL-2 is not detectable in supernatants—regardless of proliferation evidence—it could be evaluated in further assays to probe its usefulness as a vaccine candidate.

DISCUSSION

Reverse vaccinology strategies such as prediction by bioinformatic tools allow for the refining of a rational search for candidates to control infectious diseases. In order to increase probabilities to identify epitopes, it is necessary to apply more than one tool, each one with different algorithms—as we did in our study—thus favoring the discovery of natural epitopes in leishmaniasis or another infectious disease.

So far, leishmaniasis vaccines have been limited by a lack of correlation between animal models and humans, which is associated with the fact that most of the prototypes fail in clinical trial phases. For that reason, the identification of effective immune response directly in humans, and especially in those naturally resistant to the disease will provide more information about features that confer protection against leishmaniasis. In this study, LST+ individuals, although reflecting L*eishmania* cellular memory and *in vitro* lymphocytes proliferative capacity to whole parasite antigens, was lower in susceptible than naturally resistant

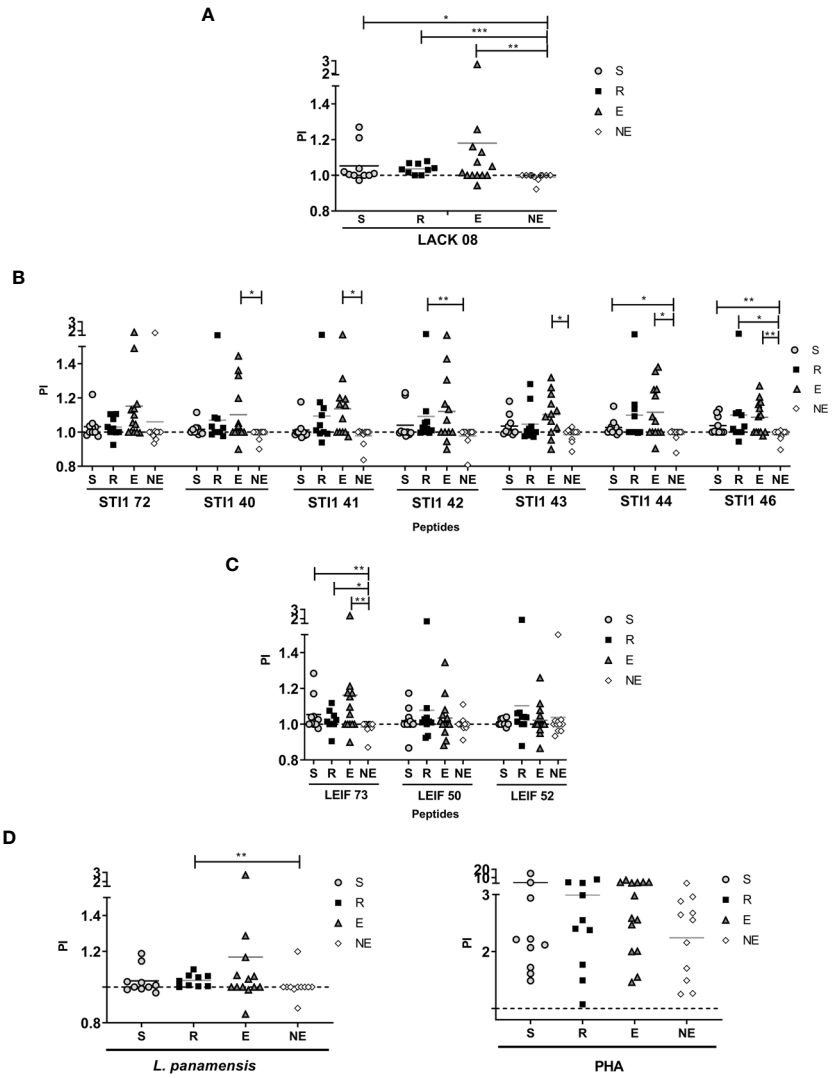

FIGURE 2 | Proliferation Index (PI) evaluated in S (susceptible), R (resistant), E (exposed), and NE (not exposed) groups. Cells response to **(A)** peptides derived from LACK protein; **(B)** peptides derived from STI1 protein; **(C)** peptides derived from LEIF, and **(D)** *L. panamensis* or PHA. p<0.05(*), P<0.01(**), P<0.001(***). Dashed line: non-stimulated cell response.

individuals, pointing out that it could be one of the reasons why in some individuals, the disease does not progress.

Consequently, Division Indexes generated in lymphocytes are related to the number of generations that each stimulus prompted. The final clone count is the outcome of the TCR affinity, exposition time to the antigen-MHC complex, co-stimulation signals, as well as the surrounding cytokines and chemokines (van Stipdonk et al., 2008; Heinzel et al., 2018). Expansion potential against any antigenic stimulus depends on the lymphocyte profile itself. For example, Veiga-Fernandes et al. (2000) showed that, under the same circumstances, memory cells expand more and faster than naïve cells in an experimental murine model expressing the same TCR, at the same time a higher percentage of memory cells expressed effector cytokines and showed multifunctionality (Veiga-Fernandes et al., 2000). Also, Rogers et al. (2000) proved that low antigen doses caused a higher number of generations in memory T cells and showed higher cytokine secretion kinetics than naïve cells (Rogers et al., 2000), while Whitmire et al. (2008) reported that both memory and naïve cells start proliferation at the same time, but memory cells rapidly overcome its counterpart in numbers (Whitmire et al., 2008). Gudmundsdottir et al. (1999) demonstrated that IFN-ɣ production in a murine model is strongly related with cellular division (Gudmundsdottir et al., 1999), as well as Keshavarz Valian et al. (2013) who described in humans infected with leishmaniasis that cells that had more division cycles expressed higher IFN-ɣ levels compared with low division ones (Keshavarz Valian et al., 2013).

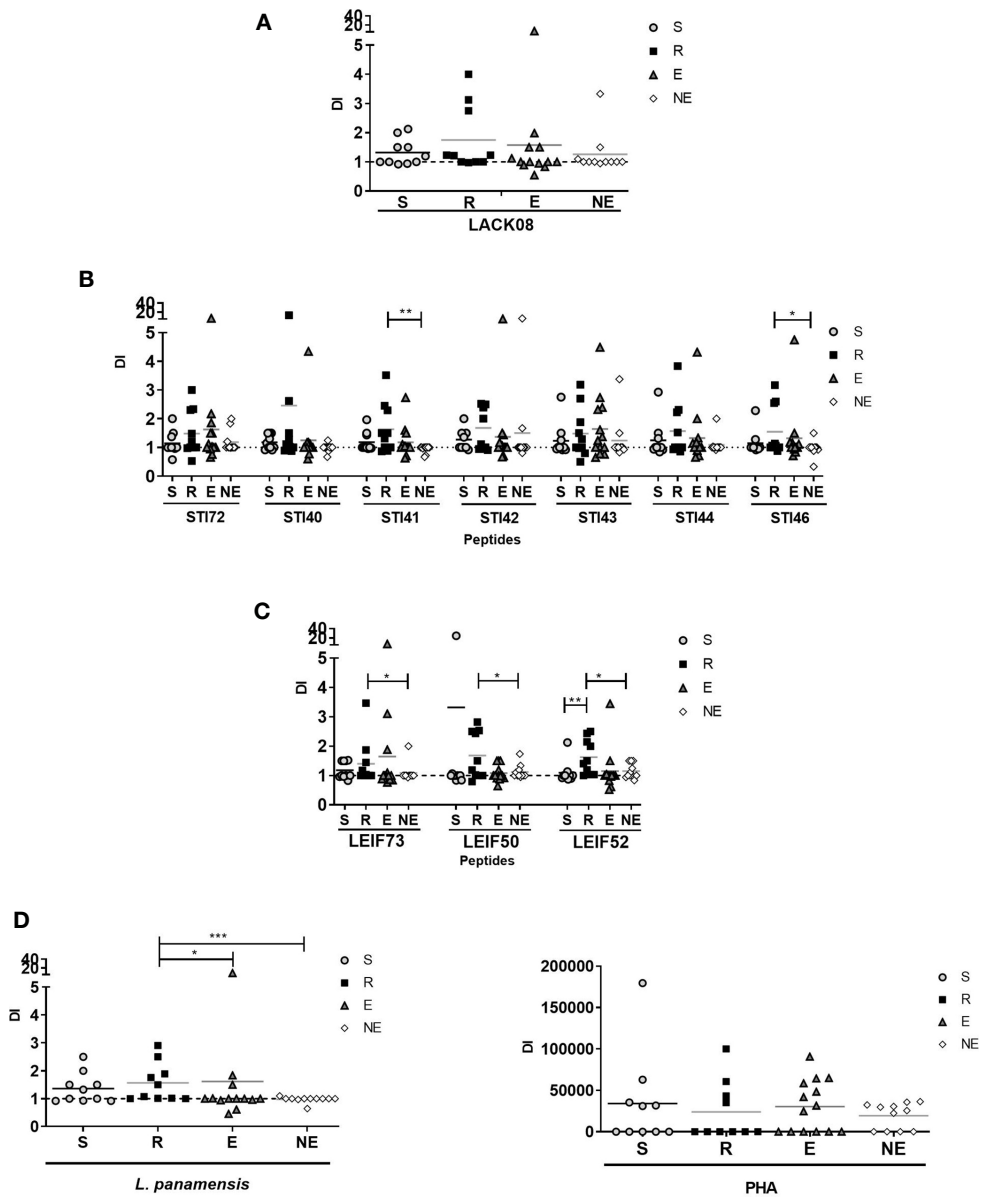

FIGURE 3 | Division Index (DI) evaluated in S (susceptible), R (resistant), E (exposed), and NE (not exposed) groups. Cells response to **(A)** peptides derived from LACK protein; **(B)** peptides derived from STI1 protein; **(C)** peptides derived from LEIF, and **(D)** *L. panamensis* or PHA. p<0.05(*), P<0.01(**), P<0.001(***). Dashed line: non-stimulated cell response.

Considering that high PI and DI in response to some stimuli could reflect those epitopes which induced memory in resistant individuals—and therefore are considered *Leishmania* natural epitopes in humans who effectively control the disease—we propose that PI and DI could be used as vaccine candidate selection criteria and also as possible indicators of protection in experimental *in vivo* models. Additionally, peptides that induce Th1 cytokines next to IL-2 could also be considered as promising, because they could be related to cellular proliferative ability and its potential to generate memory cells.

Previous reports show that IL-10 induction next to the production of IFN-γ allows for parasite elimination and lesion resolution (Belkaid et al., 2002), however other reports, as well as in our study, suggest that high levels of IL-10 could be related to susceptibility to the disease (Stober et al., 2005; Rodrigues et al., 2014; De Luca and Macedo, 2016), as reported by Stober et al. (2005) in which after BALB/c mice were immunized with vaccine antigens, they identified a correlation between levels of IL-10 and the failure of the protection against parasite challenge with *L. major*. Additionally, by blocking IL-10 receptor with antibodies in vaccinated animals, those showed better resistance

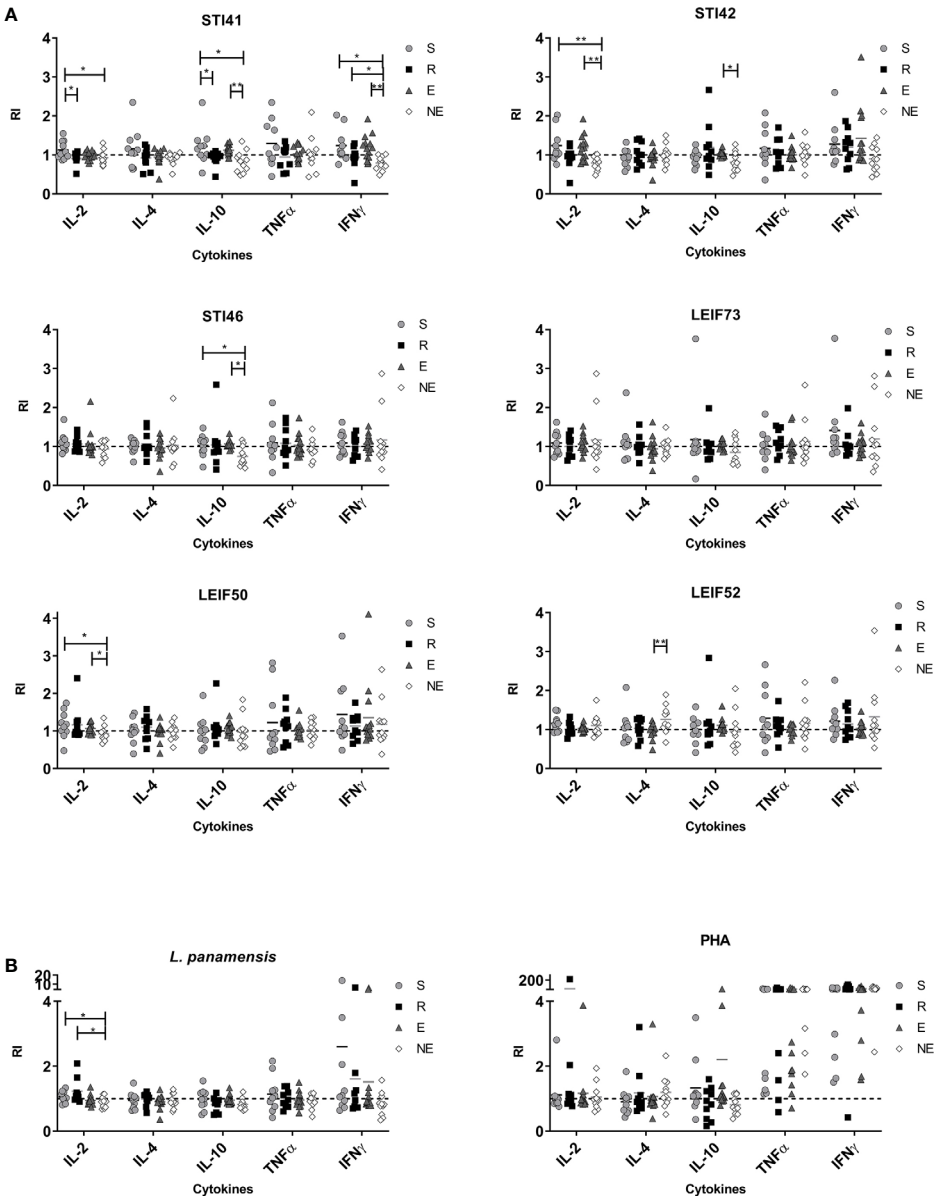

FIGURE 4 | Cytokines from lymphocytes detected in culture supernatants in S (susceptible), R (resistant), E (exposed), and NE (not exposed) groups. Cell exposed to **(A)** Pre-selected peptides and **(B)** *L. panamensis* or PHA. p<0.05(*), P<0.01(**). Dashed line: non-stimulated cells response.

to the disease, suggesting that the IFN-γ/IL-10 relationship could be an indicator of vaccine success (Stober et al., 2005). Different from our results, Bittar et al. (2007) described lower proliferation in asymptomatic individuals and higher IL-10 production compared with those cured of the disease in cells exposed *in vitro* to *L. braziliensis* (Bittar et al., 2007). On the other hand, Trujillo et al. (2002) found similar lymphoproliferation responses and IFN-γ, IL-12, and IL-10 secretion between cured and asymptomatic individuals, after exposing PBMCs *in vitro* to *L. panamensis* (Trujillo et al. (2002), while Bosque et al. (2000) observed higher lymphoproliferation in asymptomatic compared with cured humans in PBMCs exposed to *L. panamensis* amastigotes (Bosque et al., 2000), similar to our work.

CONCLUSION

In silico analysis, under established conditions, allowed for the identification of *Leishmania* natural epitopes in humans, a process that favors the wide screening of vaccine candidates for future studies and a reasonable selection of a lower number of those to be evaluated at the biological level. STI41 and STI46 peptides from Leishmania proteins were identified as promissory candidates to be

included in further research and toward its analysis as potential synthetic vaccines against cutaneous leishmaniasis.

DATA AVAILABILITY STATEMENT

The raw data supporting the conclusions of this article will be made available by the authors, without undue reservation.

ETHICS STATEMENT

The studies involving human participants were reviewed and approved by Approved by the ethical committee, act 12, august 3th 2015, National University of Colombia, Science Faculty. The patients/participants provided their written informed consent to participate in this study.

AUTHOR CONTRIBUTIONS

Project design: MF and GD. Development of laboratory methodology: MF. Approaching volunteers: RR, JC, and SR. Analysis and interpretation of data: MF and GD. Writing draft: MF. Review and editing: GD and SR. All authors contributed to the article and approved the submitted version.

FUNDING

This work was funded by the "National project call for Research, Creation and Innovation strength", Hermes code 37153 of Universidad Nacional de Colombia and also the principal author was financed by the Colombian Ministry of Science, Technology and Innovation, Colciencias-Colfuturo grant 6172-2014 for national Ph.D. students.

ACKNOWLEDGMENTS

We thank Silveria Bonilla for helping us to approach volunteers from rural Rovira areas. Also, Alex Rodriguez and Elaine Torres for their support in the methodology development and fieldwork. Additionally, special thanks to all volunteers included in this work for their generosity and confidence with the research team.

REFERENCES

Ajdary, S., Alimohammadian, M. H., Eslami, M. B., Kemp, K., and Kharazmi, A. (2000). Comparison of the Immune Profile of Nonhealing Cutaneous Leishmaniasis Patients With Those With Active Lesions and Those Who Have Recovered From Infection. *Infect. Immun.* 68, 1760–1764. doi: 10.1128/IAI.68.4.1760-1764.2000

Andrade-Narvaez, F. J., Loría-Cervera, E. N., Sosa-Bibiano, E. I., and Van Wynsberghe, N. R. (2016). Asymptomatic Infection With American Cutaneous Leishmaniasis: Epidemiological and Immunological Studies. *Mem. Inst. Oswaldo Cruz* 111, 599–604. doi: 10.1590/0074-02760160138

Arias-Murillo, Y. R, Castro-Jiménez, M. A, Ríos-Espinosa, M. F, López-Rivera, J. J, Echeverry-Coral, S. J, Martínez-Nieto, O, et al (2010). Analysis of HLA-A, HLA-B, HLA-DRB1 Allelic, Genotypic, and Haplotypic Frequencies in Colombian Population. *Colomb. Biomédica* 41.

Ávila-Portillo, L. M., Carmona, A., Franco, L., Briceño, I., Casas, M. C., and Gómez, A. (2010). Bajo Polimorfismo En El Sistema De Antígenos De Leucocitos Humanos En Población Mestiza Colombiana. *Univ. Médica* 51, 359–370. doi: 10.11144/javeriana.umed51-4.bpsa

Belkaid, Y., Kamhawi, S., Modi, G., Valenzuela, J., Noben-Trauth, N., Rowton, E., et al. (1998). Development of a Natural Model of Cutaneous Leishmaniasis: Powerful Effects of Vector Saliva and Saliva Preexposure on the Long-Term Outcome of Leishmania Major Infection in the Mouse Ear Dermis. *J. Exp. Med.* 188, 1941–1953. doi: 10.1084/jem.188.10.1941

Belkaid, Y., Mendez, S., Lira, R., Kadambi, N., Milon, G., and Sacks, D. (2000). A Natural Model of Leishmania Major Infection Reveals a Prolonged "Silent" Phase of Parasite Amplification in the Skin Before the Onset of Lesion Formation and Immunity. *J. Immunol.* 165, 969–977. doi: 10.4049/jimmunol.165.2.969

Belkaid, Y., Piccirillo, C. A., Mendez, S., Shevach, E. M., and Sacks, D. L. (2002). CD4+CD25+ Regulatory T Cells Control Leishmania Major Persistence and Immunity. *Nature* 420, 502–507. doi: 10.1038/nature01152

Best, I., Privat-Maldonado, A., Cruz, M., Zimic, M., Bras-Gonçalves, R., Lemesre, J. L., et al. (2018). IFN-γ Response is Associated to Time Exposure Among Asymptomatic Immune Responders That Visited American Tegumentary Leishmaniasis Endemic Areas in Peru. *Front. Cell. Infect. Microbiol.* 8, 289–296. doi: 10.3389/fcimb.2018.00289

Bittar, R. C., Nogueira, R. S., Vieira-Gonçalves, R., Pinho-Ribeiro, V., Mattos, M. S., Oliveira-Neto, M. P., et al. (2007). T-Cell Responses Associated With Resistance to Leishmania Infection in Individuals From Endemic Areas for Leishmania (Viannia) Braziliensis. *Mem. Inst. Oswaldo Cruz* 102, 625–630. doi: 10.1590/S0074-02762007005000069

Bordner, A. J., and Mittelmann, H. D. (2010). Multirta: A Simple Yet Reliable Method for Predicting Peptide Binding Affinities for Multiple Class II Mhc Allotypes. *BMC Bioinf.* 11, 482. doi: 10.1186/1471-2105-11-482

Bosque, F., Saravia, N. G., Valderrama, L., and Milon, G. (2000). Distinct Innate and Acquired Immune Responses to Leishmania in Putative Susceptible and Resistant Human Populations Endemically Exposed to L. (Viannia) Panamensis Infection. *Scand. J. Immunol.* 51, 533–541. doi: 10.1046/j.1365-3083.2000.00724.x

Correa, P. A., Whitworth, W. C., Kuffner, T., McNicholl, J., and Anaya, J. M. (2002). HLA-DR and DQB1 Gene Polymorphism in the North-western Colombian Population. *Tissue Antigens* 59, 436–439. doi: 10.1034/j.1399-0039.2002.590515.x

Das, S., Matlashewski,, G., Bhunia, G. S., Kesari, S., and Das, P. (2014). Asymptomatic Leishmania Infections in Northern India: A Threat for the Elimination Programme? *Trans. R. Soc. Trop. Med. Hyg* 108, 679–684. doi: 10.1093/trstmh/tru146

De Luca, P. M., and Macedo, A. B. B. (2016). Cutaneous Leishmaniasis Vaccination: A Matter of Quality. *Front. Immunol.* 7, 151. doi: 10.3389/fimmu.2016.00151

Donati, C., and Rappuoli, R. (2013). Reverse Vaccinology in the 21st Century: Improvements Over the Original Design. *Ann. N. Y. Acad. Sci.* 1285, 115–132. doi: 10.1111/nyas.12046

Fleischmann, R. D., Adams, M. D., White, O., Clayton, R. A., Kirkness, E. F., Kerlavage, A. R., et al. (1995). Whole-Genome Random Sequencing and Assembly of Haemophilus Influenzae Rd. *Science (80-.)* 269, 496–512. doi: 10.1126/science.7542800

Gfeller, D., and Bassani-Sternberg, M. (2018). Predicting Antigen Presentation-What Could We Learn From a Million Peptides? *Front. Immunol.* 9, 1716. doi: 10.3389/fimmu.2018.01716

Grubaugh, D., Flechtner, J. B., and Higgins, D. E. (2013). Proteins as T Cell Antigens: Methods for High-Throughput Identification. *Vaccine* 31, 3805–3810. doi: 10.1016/j.vaccine.2013.06.046

Gudmundsdottir, H., Wells, A. D., and Turka, L. A. (1999). Dynamics and Requirements of T Cell Clonal Expansion In Vivo at the Single-Cell Level: Effector Function is Linked to Proliferative Capacity - Pubmed. *J. Immunol.* 162, 5212–5223.

Heinzel, S., Marchingo, J. M., Horton, M. B., and Hodgkin, P. D. (2018). The Regulation of Lymphocyte Activation and Proliferation. *Curr. Opin. Immunol.* 51, 32–38. doi: 10.1016/j.coi.2018.01.002

Jensen, K. K., Andreatta, M., Marcatili, P., Buus, S., Greenbaum, J. A., Yan, Z., et al. (2018). Improved Methods for Predicting Peptide Binding Affinity to MHC Class II Molecules. *Immunology* 154, 394–406. doi: 10.1111/imm.12889

Kedzierski, L. (2010). Leishmaniasis Vaccine: Where are We Today? *J. Glob. Infect. Dis.* 2, 177. doi: 10.4103/0974-777x.62881

Keshavarz Valian, H., Nateghi Rostami, M., Tasbihi, M., Miramin Mohammadi, A., Eskandari, S. E., Sarrafnejad, A., et al. (2013). Ccr7+ Central and CCR7 Effector Memory Cd4+ T Cells in Human Cutaneous Leishmaniasis. *J. Clin. Immunol.* 33, 220–234. doi: 10.1007/s10875-012-9788-7

Maspi, N., Abdoli, A., and Ghaffarifar, F. (2016). Pro- and Anti-Inflammatory Cytokines in Cutaneous Leishmaniasis: A Review. *Pathog. Glob. Health* 110, 247–260. doi: 10.1080/20477724.2016.1232042

Merrifield, R. B. (2006). "Solid-Phase Peptide Synthesis," in *Advances in Enzymology and Related Areas of Molecular Biology. Adv. Enzymol. Relat. Areas Mol. Biol.* 32, 221–296. doi: 10.1002/9780470122778.ch6

Nielsen, M., Justesen, S., Lund, O., Lundegaard, C., and Buus, S. (2010). NetMHCIIpan-2.0 - Improved Pan-Specific HLA-DR Predictions Using a Novel Concurrent Alignment and Weight Optimization Training Procedure. *Immunome Res.* 6, 1–10. doi: 10.1186/1745-7580-6-9

Nielsen, M., Lundegaard, C., Blicher, T., Peters, B., Sette, A., Justesen, S., et al. (2008). Quantitative Predictions of Peptide Binding to Any Hla-Dr Molecule of Known Sequence: Netmhciipan. *PloS Comput. Biol.* 4, e1000107. doi: 10.1371/journal.pcbi.1000107

PortalSivigila 2019 Estadísticas De Vigilancia Rutinaria. Available at: http://portalsivigila.ins.gov.co/Paginas/Vigilancia-Rutinaria.aspx (Accessed October 20, 2020).

Reyes, H. O., Manrique, A., Quintanilla, S., and Peña, V. A. (2007). Polimorfismos Del Sistema HLA (loci A*, B* Y DRB1*) En Población. *Nova* 5 (7), 25. doi: 10.22490/24629448.369

Rodrigues, F. M. D., Coelho Neto, G. T., Menezes, J. G. P. B., Gama, M. E. A., Gonçalves, E. G., Silva, A. R., et al. (2014). Expression of Foxp3, TGF-β and IL-10 in American Cutaneous Leishmaniasis Lesions. *Arch. Dermatol. Res.* 306, 163–171. doi: 10.1007/s00403-013-1396-8

Rogers, P. R., Dubey, C., and Swain, S. L. (2000). Qualitative Changes Accompany Memory T Cell Generation: Faster, More Effective Responses at Lower Doses of Antigen. *J. Immunol.* 164, 2338–2346. doi: 10.4049/jimmunol.164.5.2338

Sallusto, F., Lanzavecchia, A., Araki, K., and Ahmed, R. (2010). From Vaccines to Memory and Back. *Immunity* 33, 451–463. doi: 10.1016/j.immuni.2010.10.008

Seyed, N., Taheri, T., and Rafati, S. (2016). Post-Genomics and Vaccine Improvement for Leishmania. *Front. Microbiol.* 7, 467. doi: 10.3389/fmicb.2016.00467

Stober, C. B., Lange, U. G., Roberts, M. T. M., Alcami, A., and Blackwell, J. M. (2005). Il-10 From Regulatory T Cells Determines Vaccine Efficacy in Murine Leishmania Major Infection. *J. Immunol.* 175, 2517–2524. doi: 10.4049/jimmunol.175.4.2517

Sturniolo, T., Bono, E., Ding, J., Raddrizzani, L., Tuereci, O., Sahin, U., et al. (1999). Generation of Tissue-Specific and Promiscuous Hla Ligand Databases Using DNA Microarrays and Virtual Hla Class II Matrices. *Nat. Biotechnol.* 17, 555–561. doi: 10.1038/9858

Trachtenberg, E. A., Keyeux, G., Bernal, J. E., Rhodas, M. C., and Erlich, H. A. (1996). Results of Expedicion Humana I. Analysis of HLA Class II (DRB1-DQA1-DQB1-DPB1) Alleles and DR-DQ Haplotypes in Nine Amerindian Populations From Columbia. *Tissue Antigens* 48, 174–181. doi: 10.1111/j.1399-0039.1996.tb02625.x

Trujillo, C. M., Robledo, S. M., Franco, J. L., Velez, I. D., Erb, K. J., and Patiño, P. J. (2002). Endemically Exposed Asymptomatic Individuals Show No Increase in the Specific Leishmania (Viannia) Panamensis-Th1 Immune Response in Comparison to Patients With Localized Cutaneous Leishmaniasis. *Parasite Immunol* 24 (9–10), 455–462. doi: 10.1046/j.1365-3024.2002.00488.x

Vanegas Murcia, M. (2014) *Síntesis De Constructos De Multicopias Peptídicas De Secuencias Derivadas De La Proteína Apical Sushi Protein (asp) De Plasmodium Falciparum: Caracterización Fisicoquímica Y Estudios De Inmunogenicidad*. Available at: http://bdigital.unal.edu.co/43373/ (Accessed October 20, 2020).

van Stipdonk, M. J. B., Sluijter, M., Han, W. G. H., and Offringa, R. (2008). Development of CTL Memory Despite Arrested Clonal Expansion. *Eur. J. Immunol.* 38, 1839–1846. doi: 10.1002/eji.200737974

Veiga-Fernandes, H., Walter, U., Bourgeois, C., McLean, A., and Rocha, B. (2000). Response of Naïve and Memory CD8+ T Cells to Antigen Stimulation In Vivo. *Nat. Immunol.* 1, 47–53. doi: 10.1038/76907

Wang, P., Sidney, J., Dow, C., Mothé, B., Sette, A., and Peters, B. (2008). A Systematic Assessment of MHC Class II Peptide Binding Predictions and Evaluation of a Consensus Approach. *PloS Comput. Biol.* 4, e1000048. doi: 10.1371/journal.pcbi.1000048

Wang, P., Sidney, J., Kim, Y., Sette, A., Lund, O., Nielsen, M., et al. (2010). Peptide Binding Predictions for HLA Dr, DP and DQ Molecules. *BMC Bioinf.* 11, 568. doi: 10.1186/1471-2105-11-568

Weigle, K. A., Valderrama, L., Arias, A. L., Santrich, C., and Saravia, N. G. (1991). Leishmanin Skin Test Standardization and Evaluation of Safety, Dose, Storage, Longevity of Reaction and Sensitization. *Am. J. Trop. Med. Hyg.* 44, 260–271. doi: 10.4269/ajtmh.1991.44.260

Whitmire, J. K., Eam, B., and Whitton, J. L. (2008). Tentative T Cells: Memory Cells Are Quick to Respond, But Slow to Divide. *PloS Pathog.* 4, e1000041. doi: 10.1371/journal.ppat.1000041

Yunis, J. J., Yunis, E. J., and Yunis, E. (2013). Mhc Class Ii Haplotypes of Colombian Amerindian Tribes. *Genet. Mol. Biol.* 36, 158–166. doi: 10.1590/S1415-47572013005000014

Zhang, H., Lund, O., and Nielsen, M. (2009). The PickPocket Method for Predicting Binding Specificities for Receptors Based on Receptor Pocket Similarities: Application to MHC-Peptide Binding. *Bioinformatics* 25, 1293–1299. doi: 10.1093/bioinformatics/btp137

Conflict of Interest: The authors declare that the research was conducted in the absence of any commercial or financial relationships that could be construed as a potential conflict of interest.

frontiers in Cellular and Infection Microbiology

REVIEW
published: 08 June 2021
doi: 10.3389/fcimb.2021.685296

Mechanisms of Immunopathogenesis in Cutaneous Leishmaniasis And Post Kala-azar Dermal Leishmaniasis (PKDL)

Greta Volpedo[1,2†], Thalia Pacheco-Fernandez[1†], Erin A. Holcomb[1†], Natalie Cipriano[1†], Blake Cox[1†] and Abhay R. Satoskar[1,2]*

[1] Department of Pathology, The Ohio State University Wexner Medical Center, Columbus, OH, United States, [2] Department of Microbiology, College of Arts and Sciences, The Ohio State University, Columbus, OH, United States

OPEN ACCESS

Edited by:
Izabel Galhardo Demarchi, Federal University of Santa Catarina, Brazil

Reviewed by:
Chiranjib Pal, West Bengal State University, India
Jindřich Chmelař, University of South Bohemia in České Budějovice, Czechia

***Correspondence:**
Abhay R. Satoskar
Abhay.Satoskar@osumc.edu

[†]These authors have contributed equally to this work

Specialty section:
This article was submitted to Parasite and Host, a section of the journal Frontiers in Cellular and Infection Microbiology

Received: 24 March 2021
Accepted: 24 May 2021
Published: 08 June 2021

Citation:
Volpedo G, Pacheco-Fernandez T, Holcomb EA, Cipriano N, Cox B and Satoskar AR (2021) Mechanisms of Immunopathogenesis in Cutaneous Leishmaniasis And Post Kala-azar Dermal Leishmaniasis (PKDL). Front. Cell. Infect. Microbiol. 11:685296. doi: 10.3389/fcimb.2021.685296

Leishmaniasis is a neglected tropical disease that affects 12 million people worldwide. The disease has high morbidity and mortality rates and is prevalent in over 80 countries, leaving more than 300 million people at risk of infection. Of all of the manifestations of this disease, cutaneous leishmaniasis (CL) is the most common form and it presents as ulcerating skin lesions that can self-heal or become chronic, leading to disfiguring scars. This review focuses on the different pathologies and disease manifestations of CL, as well as their varying degrees of severity. In particular, this review will discuss self-healing localized cutaneous leishmaniasis (LCL), leishmaniasis recidivans (LR), mucocutaneous leishmaniasis (MCL), anergic diffuse cutaneous leishmaniasis (ADCL), disseminated leishmaniasis (DL), and Post Kala-azar Dermal Leishmaniasis (PKDL), which is a cutaneous manifestation observed in some visceral leishmaniasis (VL) patients after successful treatment. The different clinical manifestations of CL are determined by a variety of factors including the species of the parasites and the host's immune response. Specifically, the balance between the pro and anti-inflammatory mediators plays a vital role in the clinical presentation and outcome of the disease. Depending upon the immune response, *Leishmania* infection can also transition from one form of the disease to another. In this review, different forms of cutaneous *Leishmania* infections and their immunology are described.

Keywords: Th1/Th2, Cutaneous leishmaniasis, post Kala-azar dermal leishmaniasis, immunoregulation, immunopathology

INTRODUCTION

Leishmaniasis is one of the 17 Neglected Tropical Diseases (NTDs) as defined by the World Health Organization (WHO) (Centers for Disease Control and Prevention, 2020; World Health Organization 2021a). NTDs are endemic in tropical and sub-tropical countries with limited access to healthcare, and where a large portion of the population lives in close contact with disease vectors and reservoirs (Harhay et al., 2011; Millán et al., 2014). Leishmaniasis affects 12 million people worldwide, with over 300 million individuals at risk of contracting the infection

(Pavli and Maltezou, 2010). Despite the significant morbidity and mortality of leishmaniasis around the globe, there is currently no prophylactic vaccine and the available therapeutics present significant challenges, including toxicities, poor patience compliance, and the development of parasitic resistance (McGwire and Satoskar, 2014).

Leishmaniasis is caused by over 21 species of the genus *Leishmania*, a protozoan parasite transmitted by the sand fly vector (Pace, 2014). During a blood meal, flagellated promastigotes deposited into the dermis are engulfed by phagocytes such as neutrophils and macrophages, where they transform into amastigotes, a stage of the parasite better equipped to deal with the temperature and pH changes. Amastigotes replicate inside the phagocyte until they rupture the cell and infect other tissues (McGwire and Satoskar, 2014).

Leishmania parasites cause a wide range of diseases, such as cutaneous (CL), diffuse cutaneous (DCL), mucosal (MCL) and visceral (VL) leishmaniasis (Pace, 2014). Cutaneous leishmaniasis (CL) is the most common form, which is characterized by skin lesions that can ulcerate and leave disfiguring scars, a source of discrimination in the affected communities (Okwor and Uzonna, 2016a; World Health Organization 2021b). Although CL is not lethal, it can lead to disabilities that can affect an individual's ability to work and lead a normal life. The impact of this disease has significantly increased in the past few decades; in particular, the disability adjusted life years (DALYs) from CL rose 43.5% between 1990 and 2016 (Hotez, 2018).

Cutaneous *Leishmania* infections can manifest as self-healing localized cutaneous leishmaniasis (LCL), leishmaniasis recidivans (LR), mucocutaneous leishmaniasis (MCL), anergic diffuse cutaneous leishmaniasis (ADCL), and disseminated leishmaniasis (DL) (Scorza et al., 2017). Furthermore, Post Kala-azar Dermal Leishmaniasis (PKDL) is a dermatological complication of VL, which occurs in some VL patients in Africa and Asia within a year after completion of WHO recommended treatment (McGwire and Satoskar, 2014). Transmission of *Leishmania* spp. specific to each disease form is carried out by 98 species of phlebotomine sandflies coming from the genus *Phlebotomus* and *Lutzomyia*. In the Old World, 42 *Phlebotomus* species allow for the transmission of *L. infantum, L. donovani, L. major, L. tropica*, and *L. aethiopica*. In almost all cases, each species of *Phlebotomus* transmits only one species of *Leishmania*. In the New World, 56 *Lutzomyia* species transmit 15 species of *Leishmania*, including *L. infantum (= Leishmania chagasi), Leishmania guyanensis, Leishmania mexicana, Leishmania amazonensis, Leishmania braziliensis*, and *Leishmania panamensis*. Contrary to the genus *Phlebotomus*, *Lutzomyia* spp. have been shown to transmit more than one species of *Leishmania*. Maroli et al. provides an extensive review of the numerous sandfly species associated with *Leishmania* spp., which we encourage the reader to reference (Maroli et al., 2013).

This review describes in detail different clinical forms of cutaneous *Leishmania* infections and PKDL, with a special focus on the unique immunological signatures that are associated with these diseases. In particular, a balance between a Th1 and Th2 response is necessary for controlling the infection. An exaggerated polarization towards Th1 or Th2 leads to severe disease pathology (**Figure 1**). Understanding the immunological mechanisms that are responsible for resolution or pathogenesis of different clinical forms of CL and PKDL will allow development of the next generation of therapeutics and vaccines against leishmaniasis.

SELF-HEALING LOCALIZED CUTANEOUS LEISHMANIASIS (LCL)

Epidemiology

The most common clinical manifestation of leishmaniasis is Localized Cutaneous Leishmaniasis (LCL). More than 70% of LCL cases worldwide are reported in ten countries: Afghanistan, Algeria, Brazil, Colombia, Costa Rica, Ethiopia, Iran, Syria, North Sudan, and Peru (Alvar et al., 2012). LCL is commonly caused by *L. major*, *L. tropica*, and *L. aethiopica* in the Old World, but it can also be due to *L. infantum* (Steverding, 2017). Interestingly, in Sri Lanka LCL can also be caused by a local *L. donovani* strain, which is genetically different from other *L. donovani* strains (Kariyawasam et al., 2017; Siriwardana et al., 2018). In the New World, LCL is caused by *L. amazonensis, L. mexicana*, *L. venezuelensis*, and *L. braziliensis* (Steverding, 2017) (**Table 1**).

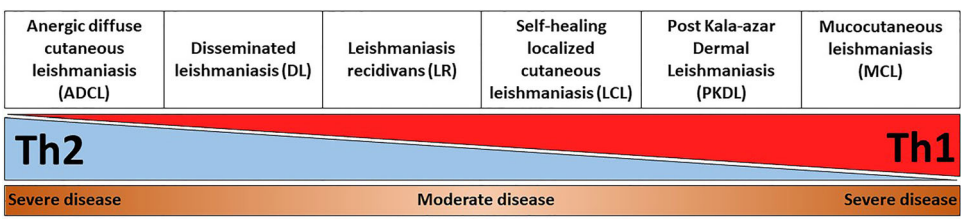

FIGURE 1 | Representation of disease severity and Th1-Th2 balance across different CL and PKDL forms. An exaggerated Th1, or alternatively Th2, response is equally detrimental for leishmaniasis patients as it results in enhanced disease severity. For instance, an uncontrolled Th2 response in anergic diffuse cutaneous leishmaniasis (ADCL) can lead to cell anergy and increased disease pathology. On the other hand, an unrestrained Th1 response in mucocutaneous leishmaniasis (MCL) can cause sustained inflammation and tissue damage.

TABLE 1 | Geographical distribution and causative species of different CL and PKDL forms.

CL/PKDL form	*Leishmania* causative species	Geographical location
Self-healing localized cutaneous leishmaniasis (LCL)	**OLD WORLD:** *L. major* *L. tropica* *L. aethiopica* *L. donovani* *L. infantum* **NEW WORLD:** *L. amazonensis* *L. mexicana* *L. venezuelensis* *L. braziliensis*	**OLD WORLD:** Afghanistan, Algeria, Ethiopia, Iran, North Sudan, Syria, Sri Lanka **NEW WORLD:** Brazil, Colombia, Costa Rica, Peru
Leishmaniasis recidivans (LR)	**OLD WORLD:** *L. major* *L. tropica* **NEW WORLD:** *L. braziliensis* *L. amazonensis* *L. panamensis* *L. guyanensis*	**OLD WORLD:** Ethiopia, India, Pakistan **NEW WORLD:** Brazil
Mucocutaneous leishmaniasis (MCL)	**OLD WORLD:** *L. major* *L. tropica* *L. aethiopica* *L. donovani* *L. infantum* **NEW WORLD:** *L. braziliensis* *L. amazonensis* *L. panamensis* *L. guyanensis*	**OLD WORLD:** Ethiopia, Iran, Sudan **NEW WORLD:** Bolivia, Brazil, Peru
Anergic diffuse cutaneous leishmaniasis (ADCL)	**OLD WORLD:** *L. aethiopica* **NEW WORLD:** *L. mexicana* *L. amazonensis*	**OLD WORLD:** Ethiopia and Kenya, Namibia, Tanzania **NEW WORLD:** Brazil, Bolivia, Colombia, Dominican Republic, Ecuador, Honduras, Mexico, Nicaragua, Peru, U.S.A. (Texas), and Venezuela
Disseminated leishmaniasis (DL)	**NEW WORLD:** *L. braziliensis* *L. panamensis* *L. guyanensis* *L. amazoniensis*	**NEW WORLD:** North-east Brazil, Colombia
Post Kala-azar Dermal Leishmaniasis (PKDL)	**OLD WORLD:** *L. donovani*	**OLD WORLD:** East Africa: Ethiopia, Kenya, Sudan, Uganda South East Asia: Bangladesh, India, Nepal

LCL is characterized by the formation of slow healing skin lesions at or near the site of the bite of the infected sand fly. Lesions begin as small red papules and develop into painless nodules, which normally ulcerate to form circumscribed ulcers (Dowlati, 1996). These lesions can get secondarily infected with bacteria or fungi, most commonly with Staphylococcal species (Ziaei et al., 2008), and can be mistaken for skin lesions caused by other infectious and non-infectious skin ailments (Alfahaad, 2020). The onset of clinical symptoms and lesion development in the host occurs after an asymptomatic incubation period ranging from a few days to 3 years, but typically lasting 2-8 weeks (Scorza et al., 2017). The parasites remain localized to the infection site during this time, so that each lesion represents an independent sand fly bite. These infection sites are usually found on exposed sites of the body such as the arms, legs, and face (Maurer et al., 2009).

LCL lesions self-heal without treatment (Scorza et al., 2017) in 0% to over 70% of patients (Morizot et al., 2013), depending on the immune response and the species of *Leishmania* (Scott and Novais, 2016). The first-line treatment for LCL is most commonly intralesional antimonials and amphotericin B (McGwire and Satoskar, 2014). However, intravenous (IV) and intramuscular (IM) treatments are often recommended due to having cure rates greater than 90% (Alfahaad, 2020). Other non-pharmacological treatments include cryotherapy or heat therapy (McGwire and Satoskar, 2014). Despite self-healing and clinical cure, parasites and parasitic DNA can persist in the scars of healed lesions for many years (Schubach et al., 1998). This phenomenon can lead to resistance against re-infection or to the development of mucosal lesions and severe disease (Schubach et al., 1998).

Immunology

Whether or not LCL lesions self-heal or become chronic depends primarily on the initial immune response (Scott and Novais, 2016). The main characteristics of an immune response to LCL are summarized in **Figure 2**. Immediately after infection, *Leishmania* parasites are phagocytosed by immune cells recruited to the site of the infection, such as neutrophils, dendritic cells (DCs), and monocytes (Ribeiro-Gomes et al., 2012; Scott and Novais, 2016; Rossi and Fasel, 2018). Neutrophils play divergent roles during infection, as they can be leishmanicidal, but also function as Trojan horses for the parasites (Scott and Novais, 2016). For instance, neutrophil extracellular traps (NET)s have been shown to kill *L. amazonensis* promastigotes (Guimarães-Costa et al., 2009). On the other hand, phagocytosis of *L. major*-infected apoptotic neutrophils hinders the activation of macrophages and DCs, resulting in the persistence of the parasites (van Zandbergen et al., 2004). Although neutrophils have been canonically described as the first cells to be recruited after *Leishmania* infection, new evidence suggests that a population of Ly6C+ inflammatory monocytes migrate to inflamed tissues first. Some studies indicate that these monocytes can control *L. major* parasites through a quick release of reactive oxygen species (ROS) during phagocytosis, known as a respiratory burst (Goncalves et al., 2011; Ponath and Kaina, 2017). However, others have shown that Ly6C monocytes contribute to the pathogenesis of infection by serving as a reservoir for parasite proliferation and cell-to-cell transmission (Romano et al., 2017; Heyde et al., 2018). In the later stages of the infection, macrophages become the canonical host for *Leishmania* parasites (Scott and Novais, 2016).

While innate immunity plays an important role in the initial response against LCL, activation of the adaptive cell-mediated immune response is critical for disease resolution and development of long term immunity. Although a mixed T helper (Th) 1 and Th2 response has been observed during active infection, a robust Th1 immune profile is mainly responsible for clinical cure (Schriefer et al., 2008; Castellano et al., 2009). Interleukin (IL)-12 is pivotal to controlling *Leishmania* infection, as it promotes the Th1 response and induces the production of Interferon gamma (IFN-γ) (Okwor and Uzonna, 2016b). Peripheral blood mononuclear cells (PBMC)s from patients with an acquired immunity to LCL stimulated with *L. major* antigen showed an increase in IFN-γ and tumor necrosis factor (TNF)-α (Kemp et al., 1999). Both IFN-γ and TNF-α activate macrophages and promote ROS production to mediate *Leishmania* clearance (Rossi and Fasel, 2018). LCL caused by the Sri Lanka *L. donovani* strain is also characterized by significantly higher levels of IFN-γ and TNF-α in the cutaneous lesions, which are involved in both parasitic killing and tissue damage (Manamperi et al., 2017; Kariyawasam et al., 2018). This strong Th1 response led to resolution of the infection in Sri Lankan LCL, while an increase in the Th2 cytokine IL-4 was observed in lesions with a poor response to treatment (Manamperi et al., 2017).

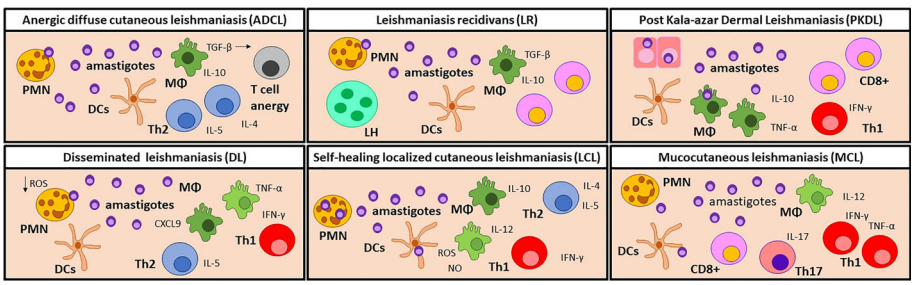

FIGURE 2 | Immune cell profiles in the skin lesion of CL and PKDL patients. Anergic diffuse cutaneous leishmaniasis (ADCL) lesions are developed due to a lack of a Th1 response. Parasites can interact directly with macrophages which, even when abundant, are polarized towards an M2 profile and produce high levels of TGF-β. Consequently, T cells are activated towards IL-4, IL-5, and IL-10-producer Th2 cells. In this environment, T cells become anergic, leading to chronic disease. It is noteworthy that this manifestation is particularly common in immunosuppressed patients. Disseminated leishmaniasis (DL) patients show a temporary impairment of the early T cell response, which allows for dissemination of the parasite. Later, CXCL9 attracts T-cells to the lesion site, causing a lack of systemic Th1 response. In the lesion, IL-10, iNOS, TNF-α, and IFN-γ are found in similar levels as LCL lesions. In self-healing localized cutaneous leishmaniasis (LCL), phagocytes are the first responders against infection by producing ROS and NO to destroy the parasites, but can also become permissive hosts for amastigotes. A Th1 response, characterized by IL-12 and IFN-γ, is necessary for the control of the disease while the Th2 immune response promotes tissue repair, leading to the self-healing of the lesion. In rare occasions, LCL can relapse as Leishmaniasis recidivans (LR), but the trigger stimulus is still unknown. LR is characterized by TGF-β and IL-10 production, as well as an increased ratio of CD8+ vs. CD4+ T cells. LR lesions also show a granulomatous infiltrate containing lymphohistiocytic and multinucleated giant cells. Post Kala-azar Dermal Leishmaniasis (PKDL) develops when the cellular response is reactivated after drug treatment. The remaining parasites in the skin elicit an increased inflammatory response and the development of dermal lesions. An increased proportion of CD8+ T cells over CD4+T cells is often observed, but the role of CD8 T cells is still unclear. Mucocutaneous Leishmaniasis (MCL) lesions are characterized by a chronic and hyperactive inflammatory immune response. IFN-γ and TNF-α producing Th1 cells and cytotoxic CD8+ cells are predominant leading to tissue destruction. The high numbers of Th17 and polymorphonuclear neutrophils (PMN) contribute to exacerbated inflammation, while the low levels of IL-10 detected are related to the poor control of inflammation. Manifestations with a mixed immune profile lead to a moderate pathology, while a hyperpolarized response results in a severe disease. MΦ, Macrophages; DCs, dendritic cells; PMN, Neutrophils; Th, T helper cells; LH, lymphohistiocytic and multinucleated giant cells; PKDL, Post Kala-azar Dermal Leishmaniasis.

Nitric oxide (NO) and ROS act as the two main microbicidal mediators involved in controlling *Leishmania* infection. Phagocytic cells can mediate anti-parasitic activity quickly during the initial phases of infection, even in the absence of activation, by producing ROS (Novais et al., 2014). These molecules play an especially important role in *L. braziliensis* infection, as *L. braziliensis* amastigotes are known to be susceptible to ROS and they survive and replicate particularly well in the absence of ROS (Novais et al., 2014). Inducible NO synthase (iNOS) induces production of NO in macrophages following activation by IFN-γ and TNF-α, and ultimately mediates killing of *Leishmania* parasites (Castellano et al., 2009; Scott and Novais, 2016). Studies have demonstrated that mice lacking iNOS fail to control *L. major* infection, despite mounting a greater Th1 response than wild-type mice. NO, along with O2-, are the predominant molecules released by macrophages in the respiratory burst to kill *Leishmania* parasites in both mice and humans (Wei et al., 1995; Carneiro et al., 2016).

The induction of both a Th1 and Th2 response in LCL is supported by a study showing high levels of IFN-γ, TNF-α, IL-12, IL-10, and IL-4 in PBMCs culture supernatants from patients with active lesions (Castellano et al., 2009). An early Th2 response allows for the persistence of the parasitic infection through the production of its characteristic cytokines: IL-4, IL-10, and IL-13 (Rossi and Fasel, 2018). Studies show a decrease in both IL-10 and IL-4 after clinical cure of LCL lesions, suggesting these cytokines are involved in exacerbation of the disease and promotion of parasite proliferation (Schriefer et al., 2008; Castellano et al., 2009). IL-4 inhibits the production of IFN-γ and the differentiation of Th1 cells, while IL-10 inhibits IFN-γ-induced activation and leishmanicidal activity of macrophages (Schriefer et al., 2008; Castellano et al., 2009). Low levels of IFN-γ and high levels of IL-10 in the blood have been observed during the early stages of *L. braziliensis* infection. However, as the infection progresses, IL-10 levels decrease and IFN-γ concentrations increase in every clinical form caused by this *Leishmania* species (Schriefer et al., 2008; Oliveira et al., 2014). These findings indicate that the balance between anti-inflammatory and pro-inflammatory cytokines is the key to the full resolution of LCL lesions. For instance, studies demonstrate that as the levels of IL-10 increased in the PBMC of patients with LCL, TNF-α also increases, maintaining a balance between the two responses, which is not only necessary for controlling infection but also for preventing immunopatholgy (Gaze et al., 2006).

While a Th1 response is crucial to control the infection, Th2 cytokines promote tissue regeneration and reduce the severity of inflammation during lesion healing (Maspi et al., 2016). Increased levels of IL-10 can suppress the effects of IFN-γ, as high levels of IFN-γ can lead to tissue damage (Rocha et al., 1999). Furthermore, IL-4 and IL-13 can induce arginase-1 (Arg-1), a Th2 enzyme involved in tissue repair (El Kasmi et al., 2008). The activity of Arg-1 results in the generation of ornithine, which is converted to polyamine and proline resulting in collagen formation and tissue regeneration (Morris, 2007). Taken together, these observations suggest that both Th1 and Th2 responses are crucial to the self-healing of LCL lesions, as a Th1 immune response is critical for eradication of the parasites, while a Th2 immune response aids in tissue repair and preventing immunopathology.

Patients with LCL also show increased production of IL-17 by PBMCs, compared to healthy controls (Oliveira et al., 2014). IL-17 is a pro-inflammatory cytokine that promotes neutrophil recruitment and is involved in immunity to intracellular pathogens. Expression of IL-17 is observed in the lesions of LCL patients, suggesting its role in immunity, but also in promoting tissue damage and lesion formation. In *L. braziliensis* infection, IL-17 and TNF-α production is reduced by IL-10 and transforming growth factor (TGF)-β, which can inhibit inflammation and tissue destruction (Oliveira et al., 2014).

The persistence of a small number of *Leishmania* parasites in the dermis after healing of the lesion is due to the IL-10 mediated suppression of acquired immunity by a population of IL-10/IFN-γ dual producers CD4+CD25- Foxp3- Th1 cells (Trinchieri, 2001; Belkaid et al., 2002; Anderson et al., 2007). The continued presence of these parasites maintains a population of *Leishmania*-specific memory T cells (Peters et al., 2014). Interestingly, the Th1 response to *Leishmania* can also result in the production of effector memory T cells that provide immunity even in the absence of any remaining parasites (Colpitts et al., 2009). Previous research suggests that CD8+ T cells are important for the immune response to re-infection with *Leishmania*, however, others have reported that CD8+ T cells have a limited role in the secondary immune response (Okwor et al., 2014; Scott and Novais, 2016). Secondary immunity was found to be dominated by CD4+ T cells in LCL (Okwor et al., 2014).

It is important to mention that although self-healing is common in LCL, evasion of the immune system by parasites can lead to more severe manifestations of CL, as described below.

LEISHMANIASIS RECIDIVANS (LR)

Epidemiology

Leishmaniasis recidivans (LR) is a rare chronic form of CL occurring in only about 3-10% of patients. It is characterized by the formation of relapsing papules around or within a scar from a previously healed acute lesion (Faccini-Martínez and Falqueto, 2016). These papules or nodules generally appear within months to years after healing of the primary lesion and do not progress to ulcers (Bittencourt et al., 1993; Goto and Lindoso, 2010). However, recurrence of LR following LCL has occurred even after 43 years following initial LCL infection (Marovich et al., 2001). In the Old World, namely Ethiopia, India, and Pakistan, LR is primarily caused by *L. tropica*, and rarely by *L. major* (Marovich et al., 2001; Stefanidou et al., 2008; Sharifi et al., 2010). In the New World, namely Brazil, however, LR cases are less frequent and have been due *to L. braziliensis,*

L. amazonensis, L. panamensis, and *L. guyanensis* (Calvopina et al., 2006; Gangneux et al., 2007) (**Table 1**). Unlike acute lesions, diagnosis of LR can be difficult due to absence of parasites in lesion biopsies. Therefore, PCR must be used to identify the causative *Leishmania* species (Oliveira-Neto et al., 1998).

Immunology

The main characteristics of an immune response to LR are summarized in **Figure 2**. Patients with LR display a strong hypersensitivity response to *Leishmania* antigen (Calvopina et al., 2006). Furthermore, LR lesions possess a granulomatous infiltrate containing lymphohistiocytic and multinucleated giant cells (Calvopina et al., 2006; Stefanidou et al., 2008; Ekiz et al., 2015). Since new LR lesions occur proximally to the location of the cured acute lesion, it is likely that the parasites persist at the site of initial infection and are reactivated by an unknown stimulus. One study found that, during *L. braziliensis* infection, *Leishmania* DNA located in the nasal mucosa resulted in an increased occurrence of LR (36.4% of positive patients) (Canário et al., 2019). It has also been hypothesized that local trauma or treatment with corticosteroids can contribute to LR relapse, possibly due to the induction of the wound-healing immune response, which provides a favorable anti-inflammatory environment for the parasite (Wortmann et al., 2000; Gangneux et al., 2007).

Since resistance to *Leishmania* is linked to a strong Th1 inflammatory immune response and subsequent macrophage activation to clear the intracellular parasites, it has been proposed that LR occurs due to putative defects in the cellular immunity of the host (Dassoni et al., 2017). For instance, anti-inflammatory cytokines IL-10 and TGFβ have been shown to mediate persistence of chronic infection in C57BL/6 mice after resolution of initial infection with *L. tropica*, the species most responsible for recurring LR (Anderson et al., 2008). However, this correlation has not yet been documented in human LR. Nonetheless, these experimental findings suggest that *Leishmania* parasites are never completely eliminated from the host, and they continue to persist and maintain immunity. One study reported a decreased ratio of CD4+ to CD8+ T lymphocytes in the peripheral blood during LR (Jaroskova et al., 1986). Conversely, resolution of LR after combination therapy is associated with an increase in CD4+ T lymphocyte proliferation, as well as IFN-γ production. Interestingly, this trend was enhanced when CD8+ cells were depleted in PBMCs, suggesting that CD8+ cells may also play a suppressive role in LR (Marovich et al., 2001).

MUCOCUTANEOUS LEISHMANIASIS

Epidemiology

Mucocutaneous leishmaniasis (MCL) is a rare clinical manifestation caused by the progression of CL into a more severe disease (David and Craft, 2009). In the New World, *Leishmania* parasites of the *Viannia* subgenus, such as *L. braziliensis*, *L. panamanensis*, *L. guyanensis*, and *L. amazoniensis*, can metastasize and cause MCL lesions (Sabzevari et al., 2020). Of these species, *L. braziliensis* accounts for most of the cases of MCL in South America (Amato et al., 2008). MCL endemic areas in the New World include Bolivia, Peru and Brazil (World Health Organization 2021c). MCL is less common in the Old World, but has been reported in Iran and certain areas of East Africa, especially Ethiopia and Sudan, and is caused by *L. major*, *L. tropica*, *L. aethiopica*, *L.donovani* and *L. infantum* (Strazzulla et al., 2013; Sunyoto et al., 2018; Sabzevari et al., 2020) (**Table 1**).

MCL metastatic lesions can appear simultaneously with CL lesions, or develop months to years after the resolution of primary lesions, ultimately leading to a progressive destruction of the mucosal tissue of the nose, mouth, and throat (Handler et al., 2015). Tissue necrosis results in facial disfiguration, which attracts stigma and marginalization in affected communities. Destruction of the mucosal membranes can also progress into life threatening disabilities that can prevent the patient from working and earning a living (World Health Organization 2021c).

Development of MCL occurs in up to 20% of all CL patients, and can depend on the size and number of cutaneous lesions, the parasite species and virulence, the host's immune response, and the patient's sex, age, and nutritional status (Machado-Coelho et al., 2005; David and Craft, 2009). Furthermore, there is evidence suggesting that RNA viruses that infect *Leishmania* can favor development of MCL and predict failure of treatment. These viruses have been abundantly found in human MCL lesions, but were infrequent in CL lesions (Zangger et al., 2013). In particular, *Leishmania* RNA Virus 1 (LRV1), harbored by *L. guyanensis* and *L. braziliensis*, has been shown to promote autophagy in the host and leads to disease exacerbation and ultimately to the development of MCL (Olivier and Zamboni, 2020).

MCL lesions can develop upon the direct bite of a sand fly on the mouth or nose, or as a consequence of proximal facial skin lesions, as seen during *L. major* infection. They can also arise at later time points from different parts of the body, as with parasites of the *L. braziliensis* complex. In this instance, new or latent parasites are likely to spread from one location to another *via* the blood or lymphatic system (Strazzulla et al., 2013). The *Leishmania* species capable of causing MCL have to overcome a crucial challenge: adapting to survive and persist in the mucosal membranes. It has been hypothesized that some species, such as *L. infantum*, can acquire the temperature resistance needed to survive in the mucosa, and travel through the blood stream to reach a distal mucosal membrane and establish a new infection (Aliaga et al., 2003; Faucher et al., 2011; Cocuzza et al., 2013).

Immunology

The key feature of MCL, which distinguishes it from other forms of leishmaniasis, is chronic and elevated inflammation and hypersensitivity (**Figure 2**). In contrast to LCL, a Th1 and CD8+ T cell-polarized response in MCL can become detrimental, as it can lead to cytotoxicity and tissue destruction. While severe disease in many forms of CL is driven by high parasitic burdens and a limited Th1 response, exacerbation of MCL is mediated by immunopathology and an exaggerated cellular response (Scott and Novais, 2016).

PBMCs from MCL patients show elevated IFN-γ and TNF-α production and lower IL-10 levels after antigen stimulation, compared to patients without mucosal involvement (Bacellar et al., 2002; Nylén and Eidsmo, 2012). This strong Th1-polarization is characterized by a delayed-type hypersensitivity response, and low numbers of parasites in the lesions (Scott and Novais, 2016). Another study demonstrated an increase in lymphocyte activation in MCL patients, presented by higher frequencies of CD4+ CD62L–, CD4+ CD69+, CD8+ CD69+, and CD4+ CD28– T cells compared to patients with other forms of CL (Gaze et al., 2006). In particular, CD4+ CD28– T cells form a population of chronically activated lymphocytes, implicated in promiscuous cytotoxicity and co-stimulation (Gaze et al., 2006). Furthermore, MCL patients display a higher percentage of IFN-γ and TNF-α-expressing CD4+ T cells in their blood, and lower levels of IL-10-producing regulatory monocytes compared to patients without mucosal involvement (Gaze et al., 2006). MCL lesions also show high levels of Th17 cells and neutrophils, as well as increased expression of IL-17 (Boaventura et al., 2010; Borges et al., 2018).

PBMCs from MCL patients exhibit increased cytolytic properties compared to those from patients with other forms of CL and healthy controls (Brodskyn et al., 1997). For instance, as disease severity progresses in *L. braziliensis* patients, the percentage of CD8+ over CD4+ T cells increases. These CD8+ have cytotoxic activity characterized by granzyme A expression (Faria et al., 2009). Cytotoxicity is the key feature in *L. braziliensis* lesions, as highlighted by a transcriptional profiling study, and it occurs concurrently with skin destruction in humans (Novais et al., 2015). Along with CD4+ and CD8+ cells, MCL lesions display increased number of CD68+ macrophages, and elevated levels of IFN-γ (Dutra et al., 2011). Another possible mechanism for apoptosis in the skin is mediated by Foxp3+ T reg cell, positively correlated with an upregulation of FasL and active caspase-3 in MCL lesions (Carneiro et al., 2009). Finally, antibody responses are also higher in MCL, compared to patients without mucosal involvement, due to an accumulation of B and plasma cells in the lesions. These cells have also been implicated in contributing to tissue damage (Nylén and Eidsmo, 2012).

Interestingly, *Leishmania* virus LRV1 can also induce pro-inflammatory cytokines and chemokines that contribute to tissue destruction and disease exacerbation (Rossi and Fasel, 2018). LRV1 activates the TLR3/TRIF signaling pathway in macrophages, leading to the production of Type I IFNs and mediating autophagy, a process known to inhibit inflammosome activation, important for parasitic clearance. MCL lesions show lower levels of inflammosome products, such as IL-1β and cleaved caspase-1, compared to lesions of patients with other forms of CL (Olivier and Zamboni, 2020).

A balance between Th1 and Th2 responses is crucial to maintain homeostasis and promote wound healing and tissue regeneration. With a hyperactive Th1 response, PBMCs from MCL patients display a limited response to IL-10 stimulation, possibly mediated by lower expression of the IL-10 receptor in the lesions, compared to LCL patients (Bacellar et al., 2002; Faria et al., 2005).

ANERGIC DIFFUSE CUTANEOUS LEISHMANIASIS (ADCL)

Epidemiology

Another less common manifestation of CL is Anergic Diffuse Cutaneous Leishmania (ADCL), which is caused by *L. aethiopica* in the highlands of Ethiopia and Kenya, but also reported in Namibia and Tanzania (Walton and Velasco, 1989); and by *L. amazonesis* and *L. mexicana* throughout the Americas in countries such as Ecuador, Venezuela, Brazil, Dominican republic, Mexico, Honduras, Nicaragua, Peru, Bolivia, Colombia and the United States of America (southern Texas) (Walton and Velasco, 1989; Pearson and Sousa, 1996; Silveira et al., 2004; Reithinger et al., 2007; Hashiguchi et al., 2016) (**Table 1**). ADCL is particularly prevalent in immunocompromised patients, such as those infected with HIV (Amato et al., 2004).

ADCL starts as a papule, usually on the extremities or the face, and without the development of ulcers. The spread of ADCL is slow but can persist for decades, leading to the development of further papules and tubercules (Pearson and Sousa, 1996). Unlike other forms of *Leishmania* infection, parasites disseminate through the peripheral lymphohaematogenic route in ADCL (Silveira, 2019), promoting a chronic disease refractory to standard treatments (Amato et al., 2004). Interestingly, the Delayed-type Hypersensitive (DTH) skin test is negative in the majority of ADCL patients, indicating a suppression of the Th1 response (Silveira et al., 2004).

Immunology

The main features of an immune response to ADCL are summarized in **Figure 2**. The nodules contain a large number of macrophages infected with *Leishmania* amastigotes, but there is a noticeable lack of T cells (Silveira et al., 2004). Immunologically, ADCL is characterized by T cell anergy, which is the key feature that distinguishes ADCL from other forms of CL (Reithinger et al., 2007). One proposed mechanism behind T cell anergy is an excessive release of TGF-β by macrophages. TGF-β is an immunosuppressive and pro-apoptotic cytokine, and high TGF-β levels suppress CD4+ T cells responses during *L. amazonesis* infection (Pinheiro et al., 2004). Macrophages are not the only source of TGF-β and other cells may be concurrently involved in the apoptosis observed in ADCL (Pinheiro et al., 2004).

Individuals with ADCL also show high levels of Th2 cytokines, such as IL-4, IL-5, and IL-10, but low levels of Th1 cytokines, such as IFN-γ, in lesion biopsies (Silveira et al., 2004). These observations indicated that despite T cell anergy, ADCL patients display enhancement of a Th2 response, which polarizes macrophages towards a *Leishmania*-permissive M2 anti-inflammatory phenotype (Pinheiro et al., 2004). Increased Th2 cytokine production is also associated with decreased IFN-γ levels, which consequently impairs macrophage activation and leads to clinical progression of ADCL (Silveira et al., 2004).

Surface antigens on *Leishmania* parasites also contribute to this unbalanced cell mediated response (Nogueira et al., 2016). A specific *Leishmania* antigen important for ADCL is LPG, which

interacts with TLR4 on antigen presenting cells, altering their phenotype to promote differentiation of Th2 CD4+ T cells (Silveira, 2019). This is mediated by a reduction of NO and pro-inflammatory cytokines, such as IFN-γ (Nogueira et al., 2016). *Leishmania* species such as *L. amazonesis* also inhibit activation of macrophages by interacting with TLR9 (Silveira et al., 2004). TLR9 activation increases the expression of CD200, an immunosuppressive glycoprotein that downregulates NO production in the few macrophages still activated during the ADCL immune response. This likely contributes to the strong Th2 response observed in patients, ineffective against *Leishmania* parasites (Sauter et al., 2019).

DISSEMINATED LEISHMANIASIS (DL)

Epidemiology

Disseminated leishmaniasis (DL) is characterized by the presence of multiple lesions in two or more non-contiguous body regions. These lesions may be a mixture of acneiform, papular, nodular, and ulcerative types with involvement of the nasal mucosa in up to 44% of DL patients (Turetz et al., 2002; Machado et al., 2011). An increase in epidermal hyperplasia and the presence of a follicular pattern in the acneiform type lesion has been observed, unlike classical LCL (Carvalho et al., 1994). Parasites from the original infection location spread quickly to distal sites and produce DL lesions within days to weeks of infection (Turetz et al., 2002). It should be noted that DL is distinct from ADCL, as DL patients exhibit a strongly positive Leishman skin test, present few parasites at the lesion site, and develop lesions that often ulcerate, unlike ADCL, as described above (Hashiguchi et al., 2016).

DL is mainly endemic in the New World, almost exclusively in northern and northeastern Brazil, and is caused primarily by *L. braziliensis* (Costa et al., 1986; Galvão et al., 1993; Membrive et al., 2017). However, *L. amazonensis* and *L. panamensis/guyanensis* have also been reported as the causative agents of DL in Brazil and Colombia (Carvalho et al., 1994; Hashiguchi et al., 2016; Cataño and Pinzón, 2019; Ovalle-Bracho et al., 2019) (**Table 1**). DL has been identified as an emerging disease in northeastern Brazil and constitutes 1.9% of all CL cases, compared to 0.2% in the past decades (Jones et al., 1987; Turetz et al., 2002). Increases in DL incidence precede a similar upsurge in American Tegumentary Leishmaniasis (ATL) cases by about 2 years. Thus, it is hypothesized that the factors affecting DL transmission respond more quickly to environmental changes than CL and ML (Schriefer et al., 2009). Those with the highest risk of developing DL, compared to LCL, are males above 19 years of age in agricultural occupations (Turetz et al., 2002).

Immunology

The ability of the parasite to disseminate rapidly to other locations of the skin and mucosa, the absence of lymph node enlargement, and prodromal symptoms such as fever and malaise, suggest that *Leishmania* is disseminated through the bloodstream during DL (Turetz et al., 2002). Furthermore, it has been proposed that proliferation of blood vessels mediates inflammation during DL and enhances growth and survival of the parasite (Mendes et al., 2013). Both host and parasite factors are hypothesized to play roles in promoting parasite dissemination in DL. The main immunological features of DL are summarized in **Figure 2**.

Similar to LCL, lesions from patients with DL are characterized by mononuclear cell infiltration as well as granuloma formation (Carvalho et al., 1994). In particular, inflammatory infiltrates in the non-ulcerative DL lesion biopsies were primarily comprised of macrophages, plasmacytes, T cells, and B cells (Mendes et al., 2013). However, DL biopsies contained lower numbers of B cells compared to those of LCL (Vieira et al., 2002). This decreased number of B cells may explain the presence of non-ulcerative lesions in DL, since B cells have been linked to tissue damage during *Leishmania* infection (Nylén and Eidsmo, 2012). On the other hand, DL patients exhibit higher antibody titers to *Leishmania* antigen than LCL, with increased antibody levels correlating to higher mucosal involvement (Carvalho et al., 1994).

Neutrophils are another important cell type in this form of leishmaniasis, since they are the first responders to infection with *Leishmania* and have been linked to pathogenesis of infection (Peters et al., 2008). It has been shown that *L. braziliensis* isolates from DL patients infect neutrophils at a lower frequency than *L. braziliensis* isolates from LCL patients. Furthermore, these DL-infected neutrophils contain lower intracellular amastigote numbers than those of LCL. However, neutrophils from *L. braziliensis* DL isolates also display decreased activation markers and oxidative burst compared to neutrophils infected with isolates from LCL patients. This data suggests that increased production of reactive oxidants by neutrophils is not responsible for control of the parasite in DL (Conceição et al., 2016; Cardoso et al., 2019).

Previous data suggests that parasite dissemination in DL is due to a lack of peripheral Th1 immune response. Following *Leishmania* antigen stimulation, PBMCs from *L. braziliensis* DL patients produce less IFN-γ and TNF-α but similar levels of IL-5 and IL-10 compared to PBMCs from CL patients. This observation is intriguing since antigen produced from *L. braziliensis* parasites isolated from DL patients stimulated higher production of IFN-γ and TNF-α in PBMCs from both CL and DL patients, than *L. braziliensis* antigen from LCL patients (Turetz et al., 2002; Leopoldo et al., 2006). Although DL patients produce less TNF-α than LCL and MCL patients, DL patients with mucosal lesions exhibited increased TNF-α production by PBMCs compared to those without mucosal involvement (Machado et al., 2011). Similar to PBMCs from DL patients (Leopoldo et al., 2006), biopsies from DL patients have also showed lower expression of IFN-γ compared to individuals with LCL. However, the frequency of TNF-α and iNOS producing cells as well as CD68+ macrophages remained the same between these DL and LCL biopsies (Vieira et al., 2002).

A study by Machado et al., investigating the *in situ* and systemic response to *L. braziliensis*–caused DL provided more clarity behind this immune response by evaluating cytokine and

chemokine production. They found that peripheral production of IFN-γ and TNF-α was reduced in PBMCs as reported previously (Leopoldo et al., 2006; Machado et al., 2011). Yet, *in situ* production of IFN-γ, TNF-α, and IL-10 in papular and ulcerated lesions of DL and classical American cutaneous leishmaniasis (ACL) patients was comparable. Moreover, serum levels of CXCL9, a T cell chemoattractant, was higher in DL than ACL patients, suggesting that *Leishmania*-reactive T cells migrate to the lesion site (Machado et al., 2011). This migration is likely to reduce T cells in the peripheral blood, possibly explaining why PBMCs from *L. braziliensis* DL patients produce less IFN-γ and TNF-α, while maintaining a positive T cell response against *Leishmania* antigen in the tissue. In contrast to *L. braziliensis*-caused DL infection, one study found that DL patients infected with *L. amazonensis* exhibited decreased CD4+ cells and a lack of T cell response to *Leishmania* antigen, yet these abnormalities were restored after successful treatment (Carvalho et al., 1994).

Collectively, these observations suggest that a temporary impairment of the early T cell response, as well as peripheral Th1 response, allows for dissemination of the parasite, but a later immune response in the tissue is able to control the infection. This may be the reason for the low parasite numbers observed in DL lesions, as well as presentation of ulcers similar LCL due to a delayed inflammatory response at the lesion site (Machado et al., 2011). Although pro-inflammatory cytokines allow for defense against the parasite, they also contribute to the formation of ulcers (Machado et al., 2002). However, the development of DL is not linked to immune suppression of the host, since it has been also observed in young and immunocompetent individuals (Jirmanus et al., 2012).

Although the exact mechanism by which *L. braziliensis* generates different clinical forms is unknown, genetic variability between *L. braziliensis* strains is thought to play a role in the different disease outcomes in *L. braziliensis* infection. Randomly amplified polymorphic genetic markers was used to distinguish parasite isolates and define five separate clades of *L. braziliensis* in Corte de Pedra. DL patient isolates were enriched in two of these distinct clades based on RAPD profile, designated clades A and D, in comparison to LCL and mucosal isolates (Schriefer et al., 2004; Schriefer et al., 2009). A further study revealed an association between single-nucleotide polymorphisms, insertions-deletions, and certain haplotypes of *L. braziliensis* with increased risk of developing DL (Queiroz et al., 2012). Moreover, geographic distribution of DL in this area correlated with the *L. braziliensis* genotype clades associated with DL. This observation further supports the notion that certain parasite strains account for active DL foci (Schriefer et al., 2009).

POST KALA-AZAR DERMAL LEISHMANIASIS

Epidemiology

Post Kala-azar dermal leishmaniasis (PKDL) is a dermatological complication of VL observed in some patients years after completion of WHO recommended therapy, especially in two specific regions (**Table 1**) with different manifestations of the disease (**Table 2**) (McGwire and Satoskar, 2014). In South Asia, PKDL manifests as papulonodular lesions (polymorphic), while in East Africa it causes hypomelanotic (macular) lesions (Ramesh et al., 2015; Chatterjee et al., 2020). Although PKDL is not life threating, it negatively affects the quality of life of the patients (Pal et al., 2017), and it represents a socioeconomic burden in the endemic regions (Mukhopadhyay et al., 2014).

In the South Asian region (India, Nepal, Bangladesh), 5-10% of the patients with supposedly cured VL develop PKDL 2-3 years after treatment (Burza et al., 2018; Rijal et al., 2019). Whereas, in East Africa (primarily in Sudan, but also Ethiopia, Kenya and Uganda) the incidence is 50-60% and the clinical manifestations appear either after VL remission or even during the treatment (Zijlstra and el-Hassan, 2001; Zijlstra and Alvar, 2012; Zijlstra et al., 2020). In both regions, the relapse time depends on the treatment regimen (Zijlstra and el-Hassan, 2001; Rijal et al., 2019; Goyal et al., 2020; Zijlstra et al., 2020). The immune responses to PKDL in Asia and Africa are different. Approximately 85% of cases in Africa show self-healing lesions, but lesions rarely resolve in the Asian PKDL (Burza et al., 2018). However, it is noteworthy that *L. donovani* parasites are genetically varied depending on the geographical regions (Zemanová et al., 2004; Lukes et al., 2007).

Environmental and host related factors can favor the transition to PKDL, such as the exposure to UV light, genetic polymorphisms and even genetic changes of the parasite itself. It is been hypothesized that UV light might contribute to the development of PKDL (Mukhopadhyay et al., 2014). UV can induce inflammation and damage in skin cells affecting the function of antigen presenting cells, particularly Langerhans cells, leading to the generation of suppressor T cells and altered

TABLE 2 | Comparison between PKDL in the two main endemic regions in the Old World.

Geographic region	East Africa	South Asia
Countries affected	Mostly Sudan, but also Ethiopia, Kenya and Uganda	India, Nepal and Bangladesh
Most common dermal manifestations	Macular	Polymorphic and macular
Incidence within VL patients	50-60%	5-10%
Time of appearance after VL	1 year after treatment or concomitant	2-3 years after treatment
Self-healing lesions	Yes (within 1 year)	No
Parasitic burden in lesions	Lower	Higher
Cell infiltrate	Scarce and patchy	Dense and diffuse

PKDL, Post Kala-azar Dermal Leishmaniasis; VL, Visceral Leishmaniasis.

cytokine production, hence disrupting cellular immunity resulting in replication of parasites in the dermis (Clydesdale et al., 2001; Seité et al., 2003). Nevertheless, this hypothesis implies that the sun-exposed areas of the body would be the ones affected by UV light, which does not match the all-over the body distribution observed in macular cases by Sengupta et al., 2019b.

A polymorphism in the IFN-γ receptor gene (*IFNGR1*) is associated with an increased risk of developing PKDL. Interestingly, it does not increase susceptibility to VL, which is linked to a polymorphism in *IL-4* gene (Mohamed et al., 2003; Salih et al., 2007). Genetic changes in *L. donovani* have also been identified and likely contribute to development of PKDL. Parasites isolated from VL and PKDL patients are consistently identical among groups, but it is possible that parasites have gained genetic modifications defined by the stage of the disease (PKDL vs. VL) and geographical region (Sreenivas et al., 2004; Dey and Singh, 2007). Genetic factors from the host and the parasite might play a role in susceptibility and development of PKDL after VL.

Even though PKDL is not lethal, it increases the spread of VL (Le Rutte et al., 2019). Patients' skin lesions serve as reservoirs for *L. donovani* by making the parasites accessible to the sandflies during blood meals (Molina et al., 2017; Mondal et al., 2019). In fact, Chapman et al estimated that PKDL could have contributed up to 25% of VL cases in a Bangladesh population (Chapman et al., 2020).

General Immune Response

In general, the development time of PKDL after VL remission induces different immune profiles. The main characteristics of this immune response are summarized in **Figure 2**. Asian PKDL is more likely to become chronic and is associated with CD8+ T cell infiltration into the cutaneous lesions, while Sudanese PKDL appears sooner after remission of VL and is characterized by the reactivation of the immune response (Mukhopadhyay et al., 2014).

In PKDL, the Th1 response increases as a direct result of treatment, but it can also occur spontaneously in some instances, and is believed to contribute to disease pathogenesis (Zijlstra and Alvar, 2012). The successful treatment of VL reactivates the cellular immune response (Gasim et al., 2000), characterized by a decrease in regulatory T cells, TGF-β and IL-10 levels, and an increase in IFN-γ, TNF-α, and IL-12 (Mondal et al., 2010; Katara et al., 2011). *L. donovani* persisting in the skin is detected by re-activated immune cells, which infiltrate into the cutaneous tissue causing dermal inflammation. *Leishmania*-reactive T cells from peripheral blood also migrate to the skin and produce IFN-γ, exacerbating the inflammatory response and giving rise to the dermal manifestations characteristic of PKDL (Ismail et al., 1999; Gasim et al., 2000).

Immunology of South Asian PKDL

Patients can be categorized into two different subgroups: polymorphic and monomorphic PKDL, depending on the characteristics of the lesions. In polymorphic PKDL is characterized by the development of papules and/or nodules, as well as hypopigmented macules. In monomorphic PKDL, patients develop only one type of lesion, mostly papulonodes (Zijlstra and Alvar, 2012; Kaushal et al., 2016). Even though polymorphic PKDL has been previously recognized as the most common manifestation (Zijlstra and Alvar, 2012), a recent surveillance study in Bengal indicates that the proportion might be equal for both manifestations (Sengupta et al., 2019a).

Histologically, the polymorphic lesions are characterized by the presence of dense and diffuse dermis cell infiltrate comprised of elevated numbers of macrophages and B cells, but fewer DCs and Langerhans cells (Mukherjee et al., 2015; Mukherjee et al., 2019; Sengupta et al., 2019b). The increase in macrophages is associated with an enhanced expression of IL-10, IL-12p40 (Mukherjee et al., 2015), M2-macrophage markers, and a reduction of TLR2/4 expression as well as ROS, and NO production (Mukhopadhyay et al., 2015), which constitutes a favorable milieu for parasite replication. In the lesions of monomorphic PKDL, the cell infiltrate is patchy and less abundant. In contrast with the polymorphic manifestation, monomorphic PKDL is characterized by a reduction of *Leishmania*-Donovan bodies (reflecting a lower parasitic load), DCs, CD4+ T-cells, and macrophage infiltrates (Sengupta et al., 2019b).

Polymorphic PKDL lesions show a higher parasitic burden, as well as higher levels of IFN-γ and TNF-α, compared to monomorphic lesions (Kaushal et al., 2016; Sengupta et al., 2019b). In terms of cellular infiltration in the lesion, polymorphic patients show an increase of CD3+ T cells and NK cells compared to the naïve group, whereas the monomorphic group is comparable to the naïve. The higher lymphoproliferation in the polymorphic PKDL patients can be explained by the higher number of circulating parasites, which also correlates with increased IFN-γ and TNF-α levels (Kaushal et al., 2016). A higher proportion of CD8+ cells over CD4+ T cells in dermal lesions is often reported in both variants, but is more elevated in the polymorphic one (Mukherjee et al., 2019; Sengupta et al., 2019b). In particular, high numbers of CD8+ CCR4+ cells are attracted to the dermal lesion site by the chemokines CCL17 and CCL22 expressed in the lesions (Mukherjee et al., 2019). Although the role of CD8+ cells in PKDL pathogenesis has yet to be clarified, one study reported increased levels of granzyme B, associated with cytotoxic lymphocyte responses, and a higher percentage of CD8+ CD64+ and CD4+ CD64+ T cells in the blood compared to naïve patients (Kaushal et al., 2016). In contrast, another study showed a reduction in the cytotoxic response, characterized by a decrease in Granzyme B, perforin, Zap70, and PD1 expression during PKDL, which reflects the exhaustion of CD8+ cytotoxic cells associated with disease progression. It is noteworthy that the suppressive profile was reverted after treatment with sodium antimony gluconate and miltefosine (Mukherjee et al., 2019).

The Th17 response is also increased during PKDL. In particular, *Il-17*, *Il-23* and *RORγt* mRNA levels were increased in the lesions during infection, and were restored to control levels after treatment (Katara et al., 2012). High levels of IL-17 lead to increased production of NO and TNF-α in PBMCs from the same patients, promoting a sustained inflammatory response (Katara et al., 2012).

Circulating levels of CXCL13, a B-cell recruiting chemokine, were also elevated in PKDL lesions, compared to healthy

samples. This resulted in B cell numbers being increased 6.5-fold in polymorphic and 4-fold in monomorphic PKDL lesions (Sengupta et al., 2019b). Antibody production by B cells has been hypothesized to promote an immunosuppressive environment in PKDL (Sengupta et al., 2019b), as *Leishmania* parasites can directly ligate to IgG FC gamma receptors on infected macrophages to induce the production of IL-10 (Sutterwala et al., 1998; Kane and Mosser, 2001). Nevertheless, no conclusive data has been published to this date regarding this particular role for B-cells.

Immunology of African PKDL

In East Africa, specifically Sudan, but also Ethiopia, Kenya and Uganda, the most common manifestation of PKDL is the macular form (Zijlstra and Alvar, 2012). Less information is available regarding Sudanese PKDL compared to the Asian disease, nevertheless, some differences have been documented. The Sudanese population displayed a high *Leishmania*-specific cellular response, which is observable only until the patients start developing PKDL. This response is characterized by an increase of PBMC proliferation and IFN-γ production (Gasim et al., 2000). Development of PKDL depends on the reactivation of the immune system and IFN-γ production against skin parasites. IFN-γ appears to be the main cytokine involved in PKDL development, as levels of IL-4, IL-5 and IL-10 were not different between patients who developed the cutaneous manifestation after VL and those who did not (Gasim et al., 2000).

CONCLUSION AND FINAL REMARKS

Infection with *Leishmania* results in a broad spectrum of clinical manifestations, from the development of self-healing cutaneous lesions to more destructive infections. Together with the causative *Leishmania* strain, the immune response is the cornerstone that defines the pathology of the disease. Clearly, an exaggerated immune polarization, either towards a Th1 or Th2, leads to the development of a more severe disease, which is the case for MCL and ADCL, respectively. On the other hand, the balance between inflammatory and anti-inflammatory responses results in a more moderate disease, as in DL, and especially in LCL, where lesions are commonly self-healing (**Figure 1**).

First line treatments, such as pentavalent antimonials, amphotericin B, paromomycin, and miltefosine have demonstrated their effectiveness in parasite killing. However, numerous side effects such as cardiotoxicity, pancreatitis, nephrotoxicity, renal failure, teratogenicity, and impaired liver function in addition to the rise in parasitic resistance to these chemotherapies are associated with current therapies (Amato et al., 2007; Amato et al., 2008; Roatt et al., 2014). Hence, host directed therapies, which directly modulate the immune response against parasites could be novel treatments for different forms of CL. Efficacy of immunomodulators in the treatment of CL has not only been demonstrated in experimental animal studies (Buates and Matlashewski, 1999), but also in patients (Chouhan et al., 2014; Dos Santos et al., 2018; Caridha et al., 2019; Nahidi et al., 2021). Immunotherapy can also be a suitable option for patients with clinical resistance to recommended drugs; for example, patients from Peru with resistance to antimony showed a faster resolution of CL lesions after the use of the TLR7 agonist imiquimod (Miranda-Verástegui et al., 2005). Also, in MCL patients infected with *L. braziliensis*, the administration of a TNF-α inhibitor together with pentavalent antimony reduced the healing time of antimony alone, as well as reducing exposure to chemotherapy (Lessa et al., 2001; Machado et al., 2007).

It is worth mentioning that the major risk factors in developing all types of leishmaniasis are related to social conditions. Poverty leads to malnutrition, which could compromise immunity and lead to the development of a full-blown disease. Climate change, occupational exposure, and poor sanitary conditions expose people to a closer contact with the parasites in forested areas and migration of non-immune people to endemic areas favors the transmission cycles (Centers for Disease Control and Prevention, 2020).

Taken all together, these observations show that expanding the knowledge about the interplay between the parasite and the immune system is crucial for developing a comprehensive strategy to combat the disease, as it has provided a broad range of potential therapies to improve the treatment of leishmaniasis.

AUTHOR CONTRIBUTIONS

GV, TP-F, EH, NC, and BC wrote the paper. AS conceptualize and wrote the paper. All authors contributed to the article and approved the submitted version.

FUNDING

Research in ARS lab is supported by funding from NIAID, Global Health Innovation Technology Fund and Wellcome Trust.

REFERENCES

Alfahaad H. A. (2020). Combined Intralesional and Intramuscular Sodium Stibogluconate Appears More Effective in the Treatment of Localized Cutaneous Leishmaniasis Lesions, An Experimental Study. *J. Pakistan Assoc. Dermatol.* 30, 396–401. doi: 10.1111/j.1468-3083.2009.03417

Aliaga L., Cobo F., Mediavilla J. D., Bravo J., Osuna A., Amador J. M., et al. (2003). Localized Mucosal Leishmaniasis Due to Leishmania (Leishmania) Infantum: Clinical and Microbiologic Findings in 31 Patients. *Med. (Baltimore)* 82 (3), 147–158. doi: 10.1097/01.md.0000076009.64510.b8

Alvar J., Vélez I. D., Bern C., Herrero M., Desjeux P., Cano J., et al. (2012). Leishmaniasis Worldwide and Global Estimates of Its Incidence. *PloS One* 7 (5), e35671. doi: 10.1371/journal.pone.0035671

Amato V. S., Rabello A., Rotondo-Silva A., Kono A., Maldonado T. P., Alves I. C., et al. (2004). Successful Treatment of Cutaneous Leishmaniasis With Lipid Formulations of Amphotericin B in Two Immunocompromised Patients. *Acta Trop.* 92 (2), 127–132. doi: 10.1016/j.actatropica.2004.06.006

Amato V. S., Tuon F. F., Bacha H. A., Neto V. A., and Nicodemo A. C. (2008). Mucosal Leishmaniasis . Current Scenario and Prospects for Treatment. *Acta Trop.* 105 (1), 1–9. doi: 10.1016/j.actatropica.2007.08.003

Amato V. S., Tuon F. F., Siqueira A. M., Nicodemo A. C., and Neto V. A. (2007). Treatment of Mucosal Leishmaniasis in Latin America: Systematic Review. *Am. J. Trop. Med. Hyg.* 77 (2), 266–274. doi: 10.4269/ajtmh.2007.77.266

Anderson C. F., Lira R., Kamhawi S., Belkaid Y., Wynn T. A., and Sacks D. (2008). Il-10 and TGF-Beta Control the Establishment of Persistent and Transmissible Infections Produced by Leishmania Tropica in C57BL/6 Mice. *J. Immunol.* 180 (6), 4090–4097. doi: 10.4049/jimmunol.180.6.4090

Anderson C. F., Oukka M., Kuchroo V. J., and Sacks D. (2007). Cd4(+)Cd25(-) Foxp3(-) Th1 Cells are the Source of IL-10-Mediated Immune Suppression in Chronic Cutaneous Leishmaniasis. *J. Exp. Med.* 204 (2), 285–297. doi: 10.1084/jem.20061886

Bacellar O., Lessa H., Schriefer A., Machado P., Ribeiro de Jesus A., Dutra W. O., et al. (2002). Up-Regulation of Th1-Type Responses in Mucosal Leishmaniasis Patients. *Infect. Immun.* 70 (12), 6734–6740. doi: 10.1128/iai.70.12.6734-6740.2002

Belkaid Y., Piccirillo C. A., Mendez S., Shevach E. M., and Sacks D. L. (2002). CD4 +CD25+ Regulatory T Cells Control Leishmania Major Persistence and Immunity. *Nature* 420 (6915), 502–507. doi: 10.1038/nature01152

Bittencourt A. L., Costa J. M., Carvalho E. M., and Barral A. (1993). Leishmaniasis Recidiva Cutis in American Cutaneous Leishmaniasis. *Int. J. Dermatol.* 32 (11), 802–805. doi: 10.1111/j.1365-4362.1993.tb02767.x

Boaventura V. S., Santos C. S., Cardoso C. R., de Andrade J., Dos Santos W. L., Clarêncio J., et al. (2010). Human Mucosal Leishmaniasis: Neutrophils Infiltrate Areas of Tissue Damage That Express High Levels of Th17-Related Cytokines. *Eur. J. Immunol.* 40 (10), 2830–2836. doi: 10.1002/eji.200940115

Borges A. F., Gomes R. S., and Ribeiro-Dias F. (2018). Leishmania (Viannia) Guyanensis in Tegumentary Leishmaniasis. *Pathog. Dis.* 76 (4). doi: 10.1093/femspd/fty025

Brodskyn C. I., Barral A., Boaventura V., Carvalho E., and Barral-Netto M. (1997). Parasite-Driven In Vitro Human Lymphocyte Cytotoxicity Against Autologous Infected Macrophages From Mucosal Leishmaniasis. *J. Immunol.* 159 (9), 4467–4473.

Buates S., and Matlashewski G. (1999). Treatment of Experimental Leishmaniasis With the Immunomodulators Imiquimod and S-28463: Efficacy and Mode of Action. *J. Infect. Dis.* 179 (6), 1485–1494. doi: 10.1086/314782

Burza S., Croft S. L., and Boelaert M. (2018). Leishmaniasis. *Lancet* 392 (10151), 951–970. doi: 10.1016/S0140-6736(18)31204-2

Calvopina M., Uezato H., Gomez E. A., Korenaga M., Nonaka S., and Hashiguchi Y. (2006). Leishmaniasis Recidiva Cutis Due to Leishmania (Viannia) Panamensis in Subtropical Ecuador: Isoenzymatic Characterization. *Int. J. Dermatol.* 45 (2), 116–120. doi: 10.1111/j.1365-4632.2004.02518.x

Canário A., Queiroz M., Cunha G., Cavalcante T., Riesz V., Sharma R., et al. (2019). Presence of Parasite DNA in Clinically Unaffected Nasal Mucosa During Cutaneous Leishmaniasis Caused by Leishmania (Viannia) Braziliensis. *Clin. Microbiol. Infect.* 25 (4), 515.e5–515.e7. doi: 10.1016/j.cmi.2018.12.027

Cardoso T., Bezerra C., Medina L. S., Ramasawmy R., Scheriefer A., Bacellar O., et al. (2019). Leishmania Braziliensis Isolated From Disseminated Leishmaniasis Patients Downmodulate Neutrophil Function. *Parasit. Immunol.* 41 (5), e12620. doi: 10.1111/pim.12620

Caridha D., Vesely B., van Bocxlaer K., Arana B., Mowbray C. E., Rafati S., et al. (2019). Route Map for the Discovery and Pre-Clinical Development of New Drugs and Treatments for Cutaneous Leishmaniasis. *Int. J. Parasitol. Drugs Drug Resist.* 11, 106–117. doi: 10.1016/j.ijpddr.2019.06.003

Carneiro P. P., Conceição J., Macedo M., Magalhães V., Carvalho E. M., and Bacellar O. (2016). The Role of Nitric Oxide and Reactive Oxygen Species in the Killing of Leishmania Braziliensis by Monocytes From Patients With Cutaneous Leishmaniasis. *PloS One* 11 (2), e0148084. doi: 10.1371/journal.pone.0148084

Carneiro F. P., De Magalhães A. V., De Jesus Abreu Almeida Couto M., Bocca A. L., Muniz-Junqueira M. I., and Ribeiro Sampaio R. N. (2009). Foxp3 Expression in Lesions of the Different Clinical Forms of American Tegumentary Leishmaniasis. *Parasit. Immunol.* 31 (10), 646–651. doi: 10.1111/j.1365-3024.2009.01148.x

Carvalho E. M., Barral A., Costa J. M., Bittencourt A., and Marsden P. (1994). Clinical and Immunopathological Aspects of Disseminated Cutaneous Leishmaniasis. *Acta Trop.* 56 (4), 315–325. doi: 10.1016/0001-706x(94)90103-1

Castellano L. R., Filho D. C., Argiro L., Dessein H., Prata A., Dessein A., et al. (2009). Th1/Th2 Immune Responses Are Associated With Active Cutaneous Leishmaniasis and Clinical Cure Is Associated With Strong Interferon-Gamma Production. *Hum. Immunol.* 70 (6), 383–390. doi: 10.1016/j.humimm.2009.01.007

Cataño J. C., and Pinzón M. A. (2019). Disseminated Cutaneous Leishmaniasis in a Patient Infected by. *Am. J. Trop. Med. Hyg.* 100 (3), 489–490. doi: 10.4269/ajtmh.18-0843

Centers for Disease Control and Prevention, CDC. (2020). *Neglected Tropical Diseases*. Available at: https://www.cdc.gov/globalhealth/ntd/diseases/index.html.

Chapman L. A. C., Spencer S. E. F., Pollington T. M., Jewell C. P., Mondal D., Alvar J., et al. (2020). Inferring Transmission Trees to Guide Targeting of Interventions Against Visceral Leishmaniasis and Post-Kala-Azar Dermal Leishmaniasis. *Proc. Natl. Acad. Sci. U. S. A.* 117 (41), 25742–25750. doi: 10.1073/pnas.2002731117

Chatterjee M., Sengupta R., Mukhopadhyay D., Mukherjee S., Dighal A., Moulik S., et al. (2020). Immune Responses in Post Kala-Azar Dermal Leishmaniasis. *Indian J. Dermatol.* 65 (6), 452–460. doi: 10.4103/ijd.IJD_258_20

Chouhan G., Islamuddin M., Sahal D., and Afrin F. (2014). Exploring the Role of Medicinal Plant-Based Immunomodulators for Effective Therapy of Leishmaniasis. *Front. Immunol.* 5, 193. doi: 10.3389/fimmu.2014.00193

Clydesdale G. J., Dandie G. W., and Muller H. K. (2001). Ultraviolet Light Induced Injury: Immunological and Inflammatory Effects. *Immunol. Cell Biol.* 79 (6), 547–568. doi: 10.1046/j.1440-1711.2001.01047.x

Cocuzza S., Strazzulla A., Pinzone M. R., Cosentino S., Serra A., Caltabiano R., et al. (2013). Isolated Laryngeal Leishmaniasis in Immunocompetent Patients: An Underdiagnosed Disease. *Case Rep. Infect. Dis.* 2013, 165409. doi: 10.1155/2013/165409

Colpitts S. L., Dalton N. M., and Scott P. (2009). IL-7 Receptor Expression Provides the Potential for Long-Term Survival of Both CD62Lhigh Central Memory T Cells and Th1 Effector Cells During Leishmania Major Infection. *J. Immunol.* 182 (9), 5702–5711. doi: 10.4049/jimmunol.0803450

Conceição J., Davis R., Carneiro P. P., Giudice A., Muniz A. C., Wilson M. E., et al. (2016). Characterization of Neutrophil Function in Human Cutaneous Leishmaniasis Caused by Leishmania Braziliensis. *PloS Negl. Trop. Dis.* 10 (5), e0004715. doi: 10.1371/journal.pntd.0004715

Costa J. M., Marsden P. D., Llanos-Cuentas E. A., Netto E. M., Carvalho E. M., Barral A., et al. (1986). Disseminated Cutaneous Leishmaniasis in a Field Clinic in Bahia, Brazil: A Report of Eight Cases. *J. Trop. Med. Hyg.* 89 (6), 319–323.

Dassoni F., Daba F., Naafs B., and Morrone A. (2017). Leishmaniasis Recidivans in Ethiopia: Cutaneous and Mucocutaneous Features. *J. Infect. Dev. Ctries* 11 (1), 106–110. doi: 10.3855/jidc.8516

David C. V., and Craft N. (2009). Cutaneous and Mucocutaneous Leishmaniasis. *Dermatol. Ther.* 22 (6), 491–502. doi: 10.1111/j.1529-8019.2009.01272.x

Dey A., and Singh S. (2007). Genetic Heterogeneity Among Visceral and Post-Kala-Azar Dermal Leishmaniasis Strains From Eastern India. *Infect. Genet. Evol.* 7 (2), 219–222. doi: 10.1016/j.meegid.2006.09.001

Dos Santos I. B., da Silva D. A. M., Paz F. A. C. R., Garcia D. M., Carmona A. K., Teixeira D., et al. (2018). Leishmanicidal and Immunomodulatory Activities of the Palladacycle Complex DPPE 1.1, A Potential Candidate for Treatment of Cutaneous Leishmaniasis. *Front. Microbiol.* 9, 1427. doi: 10.3389/fmicb.2018.01427

Dowlati Y. (1996). Cutaneous Leishmaniasis: Clinical Aspect. *Clin. Dermatol.* 14 (5), 425–431. doi: 10.1016/0738-081x(96)00058-2

Dutra W. O., de Faria D. R., Lima Machado P. R., Guimarães L. H., Schriefer A., Carvalho E., et al. (2011). Immunoregulatory and Effector Activities in Human Cutaneous and Mucosal Leishmaniasis: Understanding Mechanisms of Pathology. *Drug Dev. Res.* 72 (6), 430–436. doi: 10.1002/ddr.20449

Ekiz Ö, Rifaioğlu E. N., Şen B. B., Çulha G., Özgür T., and Doğramaci A. (2015). Leishmaniasis Recidiva Cutis of the Lips Mimicking Granulomatous Cheilitis. *Indian J. Dermatol.* 60 (2), 216. doi: 10.4103/0019-5154.152576

El Kasmi K. C., Qualls J. E., Pesce J. T., Smith A. M., Thompson R. W., Henao-Tamayo M., et al. (2008). Toll-Like Receptor-Induced Arginase 1 in Macrophages Thwarts Effective Immunity Against Intracellular Pathogens. *Nat. Immunol.* 9 (12), 1399–1406. doi: 10.1038/ni.1671

Faccini-Martínez ÁA, and Falqueto A. (2016). Leishmaniasis Recidiva Cutis. *Am. J. Trop. Med. Hyg.* 95 (6), 1221–1222. doi: 10.4269/ajtmh.16-0459

Faria D. R., Gollob K. J., Barbosa J., Schriefer A., Machado P. R., Lessa H., et al. (2005). Decreased In Situ Expression of Interleukin-10 Receptor Is Correlated With the Exacerbated Inflammatory and Cytotoxic Responses Observed in Mucosal Leishmaniasis. *Infect. Immun.* 73 (12), 7853–7859. doi: 10.1128/IAI.73.12.7853-7859.2005

Faria D. R., Souza P. E., Durães F. V., Carvalho E. M., Gollob K. J., Machado P. R., et al. (2009). Recruitment of CD8(+) T Cells Expressing Granzyme A Is Associated With Lesion Progression in Human Cutaneous Leishmaniasis. *Parasit. Immunol.* 31 (8), 432–439. doi: 10.1111/j.1365-3024.2009.01125.x

Faucher B., Pomares C., Fourcade S., Benyamine A., Marty P., Pratlong L., et al. (2011). Mucosal Leishmania Infantum Leishmaniasis: Specific Pattern in a Multicentre Survey and Historical Cases. *J. Infect.* 63 (1), 76–82. doi: 10.1016/j.jinf.2011.03.012

Galvão C. E., Silva A. C., Saldanha A. C., Silva C. M., Costa M., and Costa J. M. (1993). Disseminated Cutaneous Leishmaniasis Due to Leishmania Viannia Braziliensis in the State of Maranhão, Brazil. *Rev. Soc. Bras. Med. Trop.* 26 (2), 121–123. doi: 10.1590/s0037-86821993000200008

Gangneux J. P., Sauzet S., Donnard S., Meyer N., Cornillet A., Pratlong F., et al. (2007). Recurrent American Cutaneous Leishmaniasis. *Emerg. Infect. Dis.* 13 (9), 1436–1438. doi: 10.3201/eid1309.061446

Gasim S., Elhassan A. M., Kharazmi A., Khalil E. A., Ismail A., and Theander T. G. (2000). The Development of Post-Kala-Azar Dermal Leishmaniasis (PKDL) Is Associated With Acquisition of Leishmania Reactivity by Peripheral Blood Mononuclear Cells (PBMC). *Clin. Exp. Immunol.* 119 (3), 523–529. doi: 10.1046/j.1365-2249.2000.01163.x

Gaze S. T., Dutra W. O., Lessa M., Lessa H., Guimarães L. H., Jesus A. R., et al. (2006). Mucosal Leishmaniasis Patients Display an Activated Inflammatory T-Cell Phenotype Associated With a Nonbalanced Monocyte Population. *Scand. J. Immunol.* 63 (1), 70–78. doi: 10.1111/j.1365-3083.2005.01707.x

Goncalves R., Zhang X., Cohen H., Debrabant A., and Mosser D. M. (2011). Platelet Activation Attracts a Subpopulation of Effector Monocytes to Sites of Leishmania Major Infection. *J. Exp. Med.* 208 (6), 1253–1265. doi: 10.1084/jem.20101751

Goto H., and Lindoso J. A. (2010). Current Diagnosis and Treatment of Cutaneous and Mucocutaneous Leishmaniasis. *Expert Rev. Anti Infect. Ther.* 8 (4), 419–433. doi: 10.1586/eri.10.19

Goyal V., Das V. N. R., Singh S. N., Singh R. S., Pandey K., Verma N., et al. (2020). Long-Term Incidence of Relapse and Post-Kala-Azar Dermal Leishmaniasis After Three Different Visceral Leishmaniasis Treatment Regimens in Bihar, India. *PloS Negl. Trop. Dis.* 14 (7), e0008429. doi: 10.1371/journal.pntd.0008429

Guimarães-Costa A. B., Nascimento M. T., Froment G. S., Soares R. P., Morgado F. N., Conceição-Silva F., et al. (2009). Leishmania Amazonensis Promastigotes Induce and Are Killed by Neutrophil Extracellular Traps. *Proc. Natl. Acad. Sci. U. S. A.* 106 (16), 6748–6753. doi: 10.1073/pnas.0900226106

Handler M. Z., Patel P. A., Kapila R., Al-Qubati Y., and Schwartz R. A. (2015). Cutaneous and Mucocutaneous Leishmaniasis: Clinical Perspectives. *J. Am. Acad. Dermatol.* 73 (6), 897–908; quiz 909-10. doi: 10.1016/j.jaad.2014.08.051

Harhay M. O., Olliaro P. L., Costa D. L., and Costa C. H. (2011). Urban Parasitology: Visceral Leishmaniasis in Brazil. *Trends Parasitol.* 27 (9), 403–409. doi: 10.1016/j.pt.2011.04.001

Hashiguchi Y., Gomez E. L., Kato H., Martini L. R., Velez L. N., and Uezato H. (2016). Diffuse and Disseminated Cutaneous Leishmaniasis: Clinical Cases Experienced in Ecuador and a Brief Review. *Trop. Med. Health* 44, 2. doi: 10.1186/s41182-016-0002-0

Heyde S., Philipsen L., Formaglio P., Fu Y., Baars I., Höbbel G., et al. (2018). CD11c-Expressing Ly6C+CCR2+ Monocytes Constitute a Reservoir for Efficient Leishmania Proliferation and Cell-to-Cell Transmission. *PloS Pathog.* 14 (10), e1007374. doi: 10.1371/journal.ppat.1007374

Hotez P. J. (2018). The Rise of Leishmaniasis in the Twenty-First Century. *Trans. R Soc. Trop. Med. Hyg.* 112 (9), 421–422. doi: 10.1093/trstmh/try075

Ismail A., El Hassan A. M., Kemp K., Gasim S., Kadaru A. E., Moller T., et al. (1999). Immunopathology of Post Kala-Azar Dermal Leishmaniasis (PKDL): T-Cell Phenotypes and Cytokine Profile. *J. Pathol.* 189 (4), 615–622. doi: 10.1002/(SICI)1096-9896(199912)189:4<615::AID-PATH466>3.0.CO;2-Z

Jaroskova L., Selim M. M., Vlasin Z., and Al-Taqui M. (1986). Study of T Cell Subsets in Patients With Cutaneous Leishmaniasis. *Parasit. Immunol.* 8 (4), 381–389. doi: 10.1111/j.1365-3024.1986.tb00854.x

Jirmanus L., Glesby M. J., Guimarães L. H., Lago E., Rosa M. E., Machado P. R., et al. (2012). Epidemiological and Clinical Changes in American Tegumentary Leishmaniasis in an Area of Leishmania (Viannia) Braziliensis Transmission Over a 20-Year Period. *Am. J. Trop. Med. Hyg.* 86 (3), 426–433. doi: 10.4269/ajtmh.2012.11-0378

Jones T. C., Johnson W. D., Barretto A. C., Lago E., Badaro R., Cerf B., et al. (1987). Epidemiology of American Cutaneous Leishmaniasis Due to Leishmania Braziliensis Braziliensis. *J. Infect. Dis.* 156 (1), 73–83. doi: 10.1093/infdis/156.1.73

Kane M. M., and Mosser D. M. (2001). The Role of IL-10 in Promoting Disease Progression in Leishmaniasis. *J. Immunol.* 166 (2), 1141–1147. doi: 10.4049/jimmunol.166.2.1141

Kariyawasam U. L., Selvapandiyan A., Rai K., Wani T. H., Ahuja K., Beg M. A., et al. (2017). Genetic Diversity of Leishmania Donovani That Causes Cutaneous Leishmaniasis in Sri Lanka: A Cross Sectional Study With Regional Comparisons. *BMC Infect. Dis.* 17 (1), 791. doi: 10.1186/s12879-017-2883-x

Kariyawasam K. K. G.DUL, Selvapandiyan A., Siriwardana H. V. Y. D., Dube A., Karunanayake P., Senanayake S. A. S. C., et al. (2018). Dermotropic Leishmania Donovani in Sri Lanka: Visceralizing Potential in Clinical and Preclinical Studies. *Parasitology* 145 (4), 443–452. doi: 10.1017/S003118201700169X

Katara G. K., Ansari N. A., Singh A., Ramesh V., and Salotra P. (2012). Evidence for Involvement of Th17 Type Responses in Post Kala Azar Dermal Leishmaniasis (PKDL). *PloS Negl. Trop. Dis.* 6 (6), e1703. doi: 10.1371/journal.pntd.0001703

Katara G. K., Ansari N. A., Verma S., Ramesh V., and Salotra P. (2011). Foxp3 and IL-10 Expression Correlates With Parasite Burden in Lesional Tissues of Post Kala Azar Dermal Leishmaniasis (PKDL) Patients. *PloS Negl. Trop. Dis.* 5 (5), e1171. doi: 10.1371/journal.pntd.0001171

Kaushal H., Bras-Gonçalves R., Avishek K., Kumar Deep D., Petitdidier E., Lemesre J. L., et al. (2016). Evaluation of Cellular Immunological Responses in Mono- and Polymorphic Clinical Forms of Post-Kala-Azar Dermal Leishmaniasis in India. *Clin. Exp. Immunol.* 185 (1), 50–60. doi: 10.1111/cei.12787

Kemp K., Theander T. G., Hviid L., Garfar A., Kharazmi A., and Kemp M. (1999). Interferon-Gamma- and Tumour Necrosis Factor-Alpha-Producing Cells in Humans Who are Immune to Cutaneous Leishmaniasis. *Scand. J. Immunol.* 49 (6), 655–659. doi: 10.1046/j.1365-3083.1999.00554.x

Leopoldo P. T., Machado P. R., Almeida R. P., Schriefer A., Giudice A., de Jesus A. R., et al. (2006). Differential Effects of Antigens From L. Braziliensis Isolates From Disseminated and Cutaneous Leishmaniasis on In Vitro Cytokine Production. *BMC Infect. Dis.* 6:75. doi: 10.1186/1471-2334-6-75

Le Rutte E. A., Zijlstra E. E., and de Vlas S. J. (2019). Post-Kala-Azar Dermal Leishmaniasis as a Reservoir for Visceral Leishmaniasis Transmission. *Trends Parasitol.* 35 (8), 590–592. doi: 10.1016/j.pt.2019.06.007

Lessa H. A., Machado P., Lima F., Cruz A. A., Bacellar O., Guerreiro J., et al. (2001). Successful Treatment of Refractory Mucosal Leishmaniasis With Pentoxifylline Plus Antimony. *Am. J. Trop. Med. Hyg.* 65 (2), 87–89. doi: 10.4269/ajtmh.2001.65.87

Lukes J., Mauricio I. L., Schönian G., Dujardin J. C., Soteriadou K., Dedet J. P., et al. (2007). Evolutionary and Geographical History of the Leishmania Donovani Complex With a Revision of Current Taxonomy. *Proc. Natl. Acad. Sci. U. S. A.* 104 (22), 9375–9380. doi: 10.1073/pnas.0703678104

Machado P., Araújo C., Da Silva A. T., Almeida R. P., D'Oliveira A.Jr., Bittencourt A., et al. (2002). Failure of Early Treatment of Cutaneous Leishmaniasis in Preventing the Development of an Ulcer. *Clin. Infect. Dis.* 34 (12), E69–E73. doi: 10.1086/340526

Machado-Coelho G. L., Caiaffa W. T., Genaro O., Magalhães P. A., and Mayrink W. (2005). Risk Factors for Mucosal Manifestation of American Cutaneous Leishmaniasis. *Trans. R Soc. Trop. Med. Hyg.* 99 (1), 55–61. doi: 10.1016/j.trstmh.2003.08.001

Machado P. R., Lessa H., Lessa M., Guimarães L. H., Bang H., Ho J. L., et al. (2007). Oral Pentoxifylline Combined With Pentavalent Antimony: A Randomized Trial for Mucosal Leishmaniasis. *Clin. Infect. Dis.* 44 (6), 788–793. doi: 10.1086/511643

Machado P. R., Rosa M. E., Costa D., Mignac M., Silva J. S., Schriefer A., et al. (2011). Reappraisal of the Immunopathogenesis of Disseminated

Leishmaniasis: in Situ and Systemic Immune Response. *Trans. R Soc. Trop. Med. Hyg.* 105 (8), 438–444. doi: 10.1016/j.trstmh.2011.05.002

Manamperi N. H., Oghumu S., Pathirana N., de Silva M. V., Abeyewickreme W., Satoskar A. R., et al. (2017). In Situ Immunopathological Changes in Cutaneous Leishmaniasis Due to Leishmania Donovani. *Parasit. Immunol.* 39 (3), 438–444. doi: 10.1111/pim.12413

Maroli M., Feliciangeli M. D., Bichaud L., Charrel R. N., and Gradoni L. (2013). Phlebotomine Sandflies and the Spreading of Leishmaniases and Other Diseases of Public Health Concern. *Med. Vet. Entomol.* 27 (2), 123–147. doi: 10.1111/j.1365-2915.2012.01034.x

Marovich M. A., Lira R., Shepard M., Fuchs G. H., Kruetzer R., Nutman T. B., et al. (2001). Leishmaniasis Recidivans Recurrence After 43 Years: A Clinical and Immunologic Report After Successful Treatment. *Clin. Infect. Dis.* 33 (7), 1076–1079. doi: 10.1086/322643

Maspi N., Abdoli A., and Ghaffarifar F. (2016). Pro- and Anti-Inflammatory Cytokines in Cutaneous Leishmaniasis: A Review. *Pathog. Glob. Health* 110 (6), 247–260. doi: 10.1080/20477724.2016.1232042

Maurer M., Dondji B., and von Stebut E. (2009). What Determines the Success or Failure of Intracellular Cutaneous Parasites? Lessons Learned From Leishmaniasis. *Med. Microbiol. Immunol.* 198 (3), 137–146. doi: 10.1007/s00430-009-0114-9

McGwire B. S., and Satoskar A. R. (2014). Leishmaniasis: Clinical Syndromes and Treatment. *QJM* 107 (1), 7–14. doi: 10.1093/qjmed/hct116

Membrive N. A., Kazuma F. J., Silveira T. G. V., Teixeira J. J. V., Reinhold-Castro K. R., and Teodoro U. (2017). Disseminated Cutaneous Leishmaniasis Caused by Leishmania Braziliensis in Southern Brazil. *Rev. Inst. Med. Trop. Sao Paulo* 59, e37. doi: 10.1590/S1678-9946201759037

Mendes D. S., Dantas M. L., Gomes J. M., Santos W. L., Silva A. Q., Guimarães L. H., et al. (2013). Inflammation in Disseminated Lesions: An Analysis of CD4+, Cd20+, CD68+, CD31+ and vW+ Cells in Non-Ulcerated Lesions of Disseminated Leishmaniasis. *Mem Inst. Oswaldo Cruz* 108 (1), 18–22. doi: 10.1590/s0074-02762013000100003

Millán J., Ferroglio E., and Solano-Gallego L. (2014). Role of Wildlife in the Epidemiology of Leishmania Infantum Infection in Europe. *Parasitol. Res.* 113 (6), 2005–2014. doi: 10.1007/s00436-014-3929-2

Miranda-Verástegui C., Llanos-Cuentas A., Arévalo I., Ward B. J., and Matlashewski G. (2005). Randomized, Double-Blind Clinical Trial of Topical Imiquimod 5% With Parenteral Meglumine Antimoniate in the Treatment of Cutaneous Leishmaniasis in Peru. *Clin. Infect. Dis.* 40 (10), 1395–1403. doi: 10.1086/429238

Mohamed H. S., Ibrahim M. E., Miller E. N., Peacock C. S., Khalil E. A., Cordell H. J., et al. (2003). Genetic Susceptibility to Visceral Leishmaniasis in The Sudan: Linkage and Association With IL4 and IFNGR1. *Genes Immun.* 4 (5), 351–355. doi: 10.1038/sj.gene.6363977

Molina R., Ghosh D., Carrillo E., Monnerat S., Bern C., Mondal D., et al. (2017). Infectivity of Post-Kala-azar Dermal Leishmaniasis Patients to Sand Flies: Revisiting a Proof of Concept in the Context of the Kala-azar Elimination Program in the Indian Subcontinent. *Clin. Infect. Dis.* 65 (1), 150–153. doi: 10.1093/cid/cix245

Mondal D., Bern C., Ghosh D., Rashid M., Molina R., Chowdhury R., et al. (2019). Quantifying the Infectiousness of Post-Kala-Azar Dermal Leishmaniasis Toward Sand Flies. *Clin. Infect. Dis.* 69 (2), 251–258. doi: 10.1093/cid/ciy891

Mondal S., Bhattacharya P., Rahaman M., Ali N., and Goswami R. P. (2010). A Curative Immune Profile One Week After Treatment of Indian Kala-Azar Patients Predicts Success With a Short-Course Liposomal Amphotericin B Therapy. *PloS Negl. Trop. Dis.* 4 (7), e764. doi: 10.1371/journal.pntd.0000764

Morizot G., Kendjo E., Mouri O., Thellier M., Pérignon A., Foulet F., et al. (2013). Travelers With Cutaneous Leishmaniasis Cured Without Systemic Therapy. *Clin. Infect. Dis.* 57 (3), 370–380. doi: 10.1093/cid/cit269

Morris S. M. (2007). Arginine Metabolism: Boundaries of Our Knowledge. *J. Nutr.* 137 (6 Suppl 2), 1602S–1609S. doi: 10.1093/jn/137.6.1602S

Mukherjee S., Mukhopadhyay D., Braun C., Barbhuiya J. N., Das N. K., Chatterjee U., et al. (2015). Decreased Presence of Langerhans Cells is a Critical Determinant for Indian Post Kala-Azar Dermal Leishmaniasis. *Exp. Dermatol.* 24 (3), 232–234. doi: 10.1111/exd.12635

Mukherjee S., Sengupta R., Mukhopadhyay D., Braun C., Mitra S., Roy S., et al. (2019). Impaired Activation of Lesional CD8+ T-Cells is Associated With Enhanced Expression of Programmed Death-1 in Indian Post Kala-azar Dermal Leishmaniasis. *Sci. Rep.* 9 (1), 762. doi: 10.1038/s41598-018-37144-y

Mukhopadhyay D., Dalton J. E., Kaye P. M., and Chatterjee M. (2014). Post Kala-Azar Dermal Leishmaniasis: An Unresolved Mystery. *Trends Parasitol.* 30 (2), 65–74. doi: 10.1016/j.pt.2013.12.004

Mukhopadhyay D., Mukherjee S., Roy S., Dalton J. E., Kundu S., Sarkar A., et al. (2015). M2 Polarization of Monocytes-Macrophages is a Hallmark of Indian Post Kala-Azar Dermal Leishmaniasis. *PloS Negl. Trop. Dis.* 9 (10), e0004145. doi: 10.1371/journal.pntd.0004145

Nahidi Y., Mashayekhi Goyonlo V., Layegh P., Taghavi F., and Najaf Najafi M. (2021). Immunomodulatory Effects of Topical Diphencyprone for the Treatment of Acute Urban Cutaneous Leishmaniasis. *J. Dermatol. Treat* 32 (2), 220–226. doi: 10.1080/09546634.2019.1642997

Nogueira P. M., Assis R. R., Torrecilhas A. C., Saraiva E. M., Pessoa N. L., Campos M. A., et al. (2016). Lipophosphoglycans From Leishmania Amazonensis Strains Display Immunomodulatory Properties Via TLR4 and Do Not Affect Sand Fly Infection. *PloS Negl. Trop. Dis.* 10 (8), e0004848. doi: 10.1371/journal.pntd.0004848

Novais F. O., Carvalho L. P., Passos S., Roos D. S., Carvalho E. M., Scott P., et al. (2015). Genomic Profiling of Human Leishmania Braziliensis Lesions Identifies Transcriptional Modules Associated With Cutaneous Immunopathology. *J. Invest. Dermatol.* 135 (1), 94–101. doi: 10.1038/jid.2014.305

Novais F. O., Nguyen B. T., Beiting D. P., Carvalho L. P., Glennie N. D., Passos S., et al. (2014). Human Classical Monocytes Control the Intracellular Stage of Leishmania Braziliensis by Reactive Oxygen Species. *J. Infect. Dis.* 209 (8), 1288–1296. doi: 10.1093/infdis/jiu013

Nylén S., and Eidsmo L. (2012). Tissue Damage and Immunity in Cutaneous Leishmaniasis. *Parasit. Immunol.* 34 (12), 551–561. doi: 10.1111/pim.12007

Okwor I. B., Jia P., Mou Z., Onyilagha C., and Uzonna J. E. (2014). Cd8+ T Cells are Preferentially Activated During Primary Low Dose Leishmania Major Infection But are Completely Dispensable During Secondary anti-Leishmania Immunity. *PloS Negl. Trop. Dis.* 8 (11), e3300. doi: 10.1371/journal.pntd.0003300

Okwor I., and Uzonna J. (2016a). Social and Economic Burden of Human Leishmaniasis. *Am. J. Trop. Med. Hyg.* 94 (3), 489–493. doi: 10.4269/ajtmh.15-0408

Okwor I., and Uzonna J. E. (2016b). Pathways Leading to interleukin-12 Production and Protective Immunity in Cutaneous Leishmaniasis. *Cell Immunol.* 309, 32–36. doi: 10.1016/j.cellimm.2016.06.004

Oliveira-Neto M. P., Mattos M., Souza C. S., Fernandes O., and Pirmez C. (1998). Leishmaniasis Recidiva Cutis in New World Cutaneous Leishmaniasis. *Int. J. Dermatol.* 37 (11), 846–849. doi: 10.1046/j.1365-4362.1998.00478.x

Oliveira W. N., Ribeiro L. E., Schrieffer A., Machado P., Carvalho E. M., and Bacellar O. (2014). The Role of Inflammatory and Anti-Inflammatory Cytokines in the Pathogenesis of Human Tegumentary Leishmaniasis. *Cytokine* 66 (2), 127–132. doi: 10.1016/j.cyto.2013.12.016

Olivier M., and Zamboni D. S. (2020). Leishmania Viannia Guyanensis, LRV1 Virus and Extracellular Vesicles: A Dangerous Trio Influencing the Faith of Immune Response During Muco-Cutaneous Leishmaniasis. *Curr. Opin. Immunol.* 66, 108–113. doi: 10.1016/j.coi.2020.08.004

Ovalle-Bracho C., Londoño-Barbosa D., Salgado-Almario J., and González C. (2019). Evaluating the Spatial Distribution of Leishmania Parasites in Colombia From Clinical Samples and Human Isolateto 2016). *PloS One* 14 (3), e0214124. doi: 10.1371/journal.pone.0214124

Pace D. (2014). Leishmaniasis. *J. Infect.* 69 (Suppl 1), S10–S18. doi: 10.1016/j.jinf.2014.07.016

Pal B., Murti K., Siddiqui N. A., Das P., Lal C. S., Babu R., et al. (2017). Assessment of Quality of Life in Patients With Post Kalaazar Dermal Leishmaniasis. *Health Qual. Life Outcomes* 15 (1), 148. doi: 10.1186/s12955-017-0720-y

Pavli A., and Maltezou H. C. (2010). Leishmaniasis, an Emerging Infection in Travelers. *Int. J. Infect. Dis.* 14 (12), e1032–e1039. doi: 10.1016/j.ijid.2010.06.019

Pearson R. D., and Sousa A. Q. (1996). Clinical Spectrum of Leishmaniasis. *Clin. Infect. Dis.* 22 (1), 1–13. doi: 10.1093/clinids/22.1.1

Peters N. C., Egen J. G., Secundino N., Debrabant A., Kimblin N., Kamhawi S., et al. (2008). In Vivo Imaging Reveals an Essential Role for Neutrophils in Leishmaniasis Transmitted by Sand Flies. *Science* 321 (5891), 970–974. doi: 10.1126/science.1159194

Peters N. C., Pagán A. J., Lawyer P. G., Hand T. W., Roma E. H., Stamper L. W., et al. (2014). Chronic Parasitic Infection Maintains High Frequencies of

Short-Lived Ly6C+ CD4+ Effector T Cells That Are Required for Protection Against Re-Infection. *PloS Pathog.* 10 (12), e1004538. doi: 10.1371/journal.ppat.1004538

Pinheiro R. O., Pinto E. F., Benedito A. B., Lopes U. G., and Rossi-Bergmann B. (2004). The T-Cell Anergy Induced by Leishmania Amazonensis Antigens Is Related With Defective Antigen Presentation and Apoptosis. *Acad. Bras. Cienc.* 76 (3), 519–527. doi: 10.1590/s0001-37652004000300006

Ponath V., and Kaina B. (2017). Death of Monocytes Through Oxidative Burst of Macrophages and Neutrophils: Killing in Trans. *PloS One* 12 (1), e0170347. doi: 10.1371/journal.pone.0170347

Queiroz A., Sousa R., Heine C., Cardoso M., Guimarães L. H., Machado P. R., et al. (2012). Association Between an Emerging Disseminated Form of Leishmaniasis and Leishmania (Viannia) Braziliensis Strain Polymorphisms. *J. Clin. Microbiol.* 50 (12), 4028–4034. doi: 10.1128/JCM.02064-12

Ramesh V., Kaushal H., Mishra A. K., Singh R., and Salotra P. (2015). Clinico-Epidemiological Analysis of Post Kala-Azar Dermal Leishmaniasis (PKDL) Cases in India Over Last Two Decades: A Hospital Based Retrospective Study. *BMC Public Health* 15, 1092. doi: 10.1186/s12889-015-2424-8

Reithinger R., Dujardin J. C., Louzir H., Pirmez C., Alexander B., and Brooker S. (2007). Cutaneous Leishmaniasis. *Lancet Infect. Dis.* 7 (9), 581–596. doi: 10.1016/S1473-3099(07)70209-8

Ribeiro-Gomes F. L., Peters N. C., Debrabant A., and Sacks D. L. (2012). Efficient Capture of Infected Neutrophils by Dendritic Cells in the Skin Inhibits the Early Anti-Leishmania Response. *PloS Pathog.* 8 (2), e1002536. doi: 10.1371/journal.ppat.1002536

Rijal S., Sundar S., Mondal D., Das P., Alvar J., and Boelaert M. (2019). Eliminating Visceral Leishmaniasis in South Asia: The Road Ahead. *BMJ* 364, k5224. doi: 10.1136/bmj.k5224

Roatt B. M., Aguiar-Soares R. D., Coura-Vital W., Ker H. G., Moreira N., Vitoriano-Souza J., et al. (2014). Immunotherapy and Immunochemotherapy in Visceral Leishmaniasis: Promising Treatments for This Neglected Disease. *Front. Immunol.* 5, 272. doi: 10.3389/fimmu.2014.00272

Rocha P. N., Almeida R. P., Bacellar O., de Jesus A. R., Filho D. C., Filho A. C., et al. (1999). Down-Regulation of Th1 Type of Response in Early Human American Cutaneous Leishmaniasis. *J. Infect. Dis.* 180 (5), 1731–1734. doi: 10.1086/315071

Romano A., Carneiro M. B. H., Doria N. A., Roma E. H., Ribeiro-Gomes F. L., Inbar E., et al. (2017). Divergent Roles for Ly6C+CCR2+CX3CR1+ Inflammatory Monocytes During Primary or Secondary Infection of the Skin With the Intra-Phagosomal Pathogen Leishmania Major. *PloS Pathog.* 13 (6), e1006479. doi: 10.1371/journal.ppat.1006479

Rossi M., and Fasel N. (2018). How to Master the Host Immune System? Leishmania Parasites Have the Solutions!". *Int. Immunol.* 30 (3), 103–111. doi: 10.1093/intimm/dxx075

Sabzevari S., Mohebali M., and Hashemi S. A. (2020). Mucosal and Mucocutaneous Leishmaniasis in Iran From 1968 to 2018: A Narrative Review of Clinical Features, Treatments, and Outcomes. *Int. J. Dermatol.* 59 (5), 606–612. doi: 10.1111/ijd.14762

Salih M. A., Ibrahim M. E., Blackwell J. M., Miller E. N., Khalil E. A., ElHassan A. M., et al. (2007). IFNG and IFNGR1 Gene Polymorphisms and Susceptibility to Post-Kala-Azar Dermal Leishmaniasis in Sudan. *Genes Immun.* 8 (1), 75–78. doi: 10.1038/sj.gene.6364353

Sauter I. P., Madrid K. G., de Assis J. B., Sá-Nunes A., Torrecilhas A. C., Staquicini D. I., et al. (2019). Tlr9/MyD88/TRIF Signaling Activates Host Immune Inhibitory CD200 in Leishmania Infection. *JCI Insight* 4 (10). doi: 10.1172/jci.insight.126207

Schriefer A., Guimarães L. H., Machado P. R., Lessa M., Lessa H. A., Lago E., et al. (2009). Geographic Clustering of Leishmaniasis in Northeastern Brazil. *Emerg. Infect. Dis.* 15 (6), 871–876. doi: 10.3201/eid1506.080406

Schriefer A., Schriefer A. L., Góes-Neto A., Guimarães L. H., Carvalho L. P., Almeida R. P., et al. (2004). Multiclonal Leishmania Braziliensis Population Structure and its Clinical Implication in a Region of Endemicity for American Tegumentary Leishmaniasis. *Infect. Immun.* 72 (1), 508–514. doi: 10.1128/iai.72.1.508-514.2004

Schriefer A., Wilson M. E., and Carvalho E. M. (2008). Recent Developments Leading Toward a Paradigm Switch in the Diagnostic and Therapeutic Approach to Human Leishmaniasis. *Curr. Opin. Infect. Dis.* 21 (5), 483–488. doi: 10.1097/QCO.0b013e32830d0ee8

Schubach A., Haddad F., Oliveira-Neto M. P., Degrave W., Pirmez C., Grimaldi G., et al. (1998). Detection of Leishmania DNA by Polymerase Chain Reaction in Scars of Treated Human Patients. *J. Infect. Dis.* 178 (3), 911–914. doi: 10.1086/515355

Scorza B. M., Carvalho E. M., and Wilson M. E. (2017). Cutaneous Manifestations of Human and Murine Leishmaniasis. *Int. J. Mol. Sci.* 18 (6). doi: 10.3390/ijms18061296

Scott P., and Novais F. O. (2016). Cutaneous Leishmaniasis: Immune Responses in Protection and Pathogenesis. *Nat. Rev. Immunol.* 16 (9), 581–592. doi: 10.1038/nri.2016.72

Seité S., Zucchi H., Moyal D., Tison S., Compan D., Christiaens F., et al. (2003). Alterations in Human Epidermal Langerhans Cells by Ultraviolet Radiation: Quantitative and Morphological Study. *Br. J. Dermatol.* 148 (2), 291–299. doi: 10.1046/j.1365-2133.2003.05112.x

Sengupta R., Chaudhuri S. J., Moulik S., Ghosh M. K., Saha B., Das N. K., et al. (2019a). Active Surveillance Identified a Neglected Burden of Macular Cases of Post Kala-Azar Dermal Leishmaniasis in West Bengal. *PloS Negl. Trop. Dis.* 13 (3), e0007249. doi: 10.1371/journal.pntd.0007249

Sengupta R., Mukherjee S., Moulik S., Mitra S., Chaudhuri S. J., Das N. K., et al. (2019b). In-Situ Immune Profile of Polymorphic vs. Macular Indian Post Kala-Azar Dermal Leishmaniasis. *Int. J. Parasitol. Drugs Drug Resist.* 11, 166–176. doi: 10.1016/j.ijpddr.2019.08.005

Sharifi I., Fekri A. R., Aflatoonian M. R., Khamesipour A., Mahboudi F., Dowlati Y., et al. (2010). Leishmaniasis Recidivans Among School Children in Bam, South-East Ira-2006. *Int. J. Dermatol.* 49 (5), 557–561. doi: 10.1111/j.1365-4632.2010.04419.x

Silveira F. T. (2019). What Makes Mucosal and Anergic Diffuse Cutaneous Leishmaniases So Clinically and Immunopathogically Different? A Review in Brazil. *Trans. R Soc. Trop. Med. Hyg.* 113 (9), 505–516. doi: 10.1093/trstmh/trz037

Silveira F. T., Lainson R., and Corbett C. E. (2004). Clinical and Immunopathological Spectrum of American Cutaneous Leishmaniasis With Special Reference to the Disease in Amazonian Brazil: A Review. *Mem Inst. Oswaldo Cruz* 99 (3), 239–251. doi: 10.1590/s0074-02762004000300001

Siriwardana Y. D., Deepachandi B., Ranasinghe S., Soysa P., and Karunaweera N. (2018). Evidence for Seroprevalence in Human Localized Cutaneous Leishmaniasis Caused by. *BioMed. Res. Int.* 2018:9320367. doi: 10.1155/2018/9320367

Sreenivas G., Raju B. V., Singh R., Selvapandiyan A., Duncan R., Sarkar D., et al. (2004). DNA Polymorphism Assay Distinguishes Isolates of Leishmania Donovani That Cause Kala-Azar From Those That Cause Post-Kala-Azar Dermal Leishmaniasis in Humans. *J. Clin. Microbiol.* 42 (4), 1739–1741. doi: 10.1128/jcm.42.4.1739-1741.2004

Stefanidou M. P., Antoniou M., Koutsopoulos A. V., Neofytou Y. T., Krasagakis K., Krüger-Krasagakis S., et al. (2008). A Rare Case of Leishmaniasis Recidiva Cutis Evolving for 31 Years Caused by Leishmania Tropica. *Int. J. Dermatol.* 47 (6), 588–589. doi: 10.1111/j.1365-4632.2008.03240.x

Steverding D. (2017). The History of Leishmaniasis. *Parasit. Vectors* 10 (1), 82. doi: 10.1186/s13071-017-2028-5

Strazzulla A., Cocuzza S., Pinzone M. R., Postorino M. C., Cosentino S., Serra A., et al. (2013). Mucosal Leishmaniasis: An Underestimated Presentation of a Neglected Disease. *BioMed. Res. Int.* 2013, 805108. doi: 10.1155/2013/805108

Sunyoto T., Verdonck K., El Safi S., Potet J., Picado A., and Boelaert M. (2018). Uncharted Territory of the Epidemiological Burden of Cutaneous Leishmaniasis in Sub-Saharan Africa-A Systematic Review. *PloS Negl. Trop. Dis.* 12 (10), e0006914. doi: 10.1371/journal.pntd.0006914

Sutterwala F. S., Noel G. J., Salgame P., and Mosser D. M. (1998). Reversal of Proinflammatory Responses by Ligating the Macrophage Fcgamma Receptor Type I. *J. Exp. Med.* 188 (1), 217–222. doi: 10.1084/jem.188.1.217

Trinchieri G. (2001). Regulatory Role of T Cells Producing Both Interferon Gamma and Interleukin 10 in Persistent Infection. *J. Exp. Med.* 194 (10), F53–F57. doi: 10.1084/jem.194.10.f53

Turetz M. L., Machado P. R., Ko A. I., Alves F., Bittencourt A., Almeida R. P., et al. (2002). Disseminated Leishmaniasis: A New and Emerging Form of Leishmaniasis Observed in Northeastern Brazil. *J. Infect. Dis.* 186 (12), 1829–1834. doi: 10.1086/345772

van Zandbergen G., Klinger M., Mueller A., Dannenberg S., Gebert A., Solbach W., et al. (2004). Cutting Edge: Neutrophil Granulocyte Serves as a Vector for Leishmania Entry Into Macrophages. *J. Immunol.* 173 (11), 6521–6525. doi: 10.4049/jimmunol.173.11.6521

Vieira M. G., Oliveira F., Arruda S., Bittencourt A. L., Barbosa A. A., Barral-Netto M., et al. (2002). B-Cell Infiltration and Frequency of Cytokine Producing Cells Differ Between Localized and Disseminated Human Cutaneous Leishmaniases. *Mem Inst. Oswaldo Cruz* 97 (7), 979–983. doi: 10.1590/s0074-02762002000700009

Walton B. C., and Velasco O. (1989). "The Distribution and Aetiology of Diffuse Cutaneous Leishmaniasis in the New World", in: *Leishmaniasis. NATO Asi Series (Series A: Life Sciences)*. Ed. D. T. Hart (Boston, MA: Springer).

Wei X. Q., Charles I. G., Smith A., Ure J., Feng G. J., Huang F. P., et al. (1995). Altered Immune Responses in Mice Lacking Inducible Nitric Oxide Synthase. *Nature* 375 (6530), 408–411. doi: 10.1038/375408a0

World Health Organization, WHO. (2021a). *Control of Neglected Tropical Diseases*. Available at: https://www.who.int/teams/control-of-neglected-tropical-diseases/neglected-zoonotic-diseases.

World Health Organization, WHO. (2021b). *Cutaneous Leishmaniasis*. Available at: https://www.who.int/leishmaniasis/cutaneous_leishmaniasis/en/#:~:text=Cutaneous%20leishmaniasis%20is%20the%20most,the%20face%2C%20arms%20and%20legs.&text=When%20the%20ulcers%20heal%2C%20they,cause%20of%20serious%20social%20prejudice.

World Health Organization, WHO. (2021c). *Mucocutaneous Leishmaniasis*. Available at: https://www.who.int/leishmaniasis/mucocutaneous_leishmaniasis/en/#:~:text=In%20mucocutaneous%20leishmaniasis%2C%20the%20lesions,being%20rejected%20by%20the%20community.

Wortmann G. W., Aronson N. E., Miller R. S., Blazes D., and Oster C. N. (2000). Cutaneous Leishmaniasis Following Local Trauma: A Clinical Pearl. *Clin. Infect. Dis.* 31 (1), 199–201. doi: 10.1086/313924

Zangger H., Ronet C., Desponds C., Kuhlmann F. M., Robinson J., Hartley M. A., et al. (2013). Detection of Leishmania RNA Virus in Leishmania Parasites. *PloS Negl. Trop. Dis.* 7 (1), e2006. doi: 10.1371/journal.pntd.0002006

Zemanová E., Jirků M., Mauricio I. L., Miles M. A., and Lukes J. (2004). Genetic Polymorphism Within the Leishmania Donovani Complex: Correlation With Geographic Origin. *Am. J. Trop. Med. Hyg.* 70 (6), 613–617. doi: 10.4269/ajtmh.2004.70.613

Ziaei H., Sadeghian G., and Hejazi S. H. (2008). Distribution Frequency of Pathogenic Bacteria Isolated From Cutaneus Leishmaniasis Lesions. *Korean J. Parasitol.* 46 (3), 191–193. doi: 10.3347/kjp.2008.46.3.191

Zijlstra E. E., and Alvar J. (2012). *The Post Kala-Azar Dermal Leishmaniasis (PKDL) Atlas A Manual for Health Workers* (Spain: World Health Organization, WHO).

Zijlstra E. E., and el-Hassan A. M. (2001). Leishmaniasis in Sudan. Post Kala-Azar Dermal Leishmaniasis. *Trans. R Soc. Trop. Med. Hyg.* 95 (Suppl;1), S59–S76. doi: 10.1016/s0035-9203(01)90219-6

Zijlstra E. E., Kumar A., Sharma A., Rijal S., Mondal D., and Routray S. (2020). Report of the Fifth Post-Kala-Azar Dermal Leishmaniasis Consortium Meeting, Colombo, Sri Lanka, 14-16 May 2018. *Parasit. Vectors* 13 (1), 159. doi: 10.1186/s13071-020-04011-7

Conflict of Interest: The authors declare that the research was conducted in the absence of any commercial or financial relationships that could be construed as a potential conflict of interest.

frontiers in Cellular and Infection Microbiology

ORIGINAL RESEARCH
published: 10 June 2021
doi: 10.3389/fcimb.2021.687647

miR-548d-3p Alters Parasite Growth and Inflammation in *Leishmania (Viannia) braziliensis* Infection

*Marina de Assis Souza[1], Eduardo Milton Ramos-Sanchez[1,2], Sandra Márcia Muxel[3], Dimitris Lagos[4], Luiza Campos Reis[1], Valéria Rêgo Alves Pereira[5], Maria Edileuza Felinto Brito[5], Ricardo Andrade Zampieri[3], Paul Martin Kaye[4], Lucile Maria Floeter-Winter[3] and Hiro Goto[1,6]**

[1] Instituto de Medicina Tropical, Faculdade de Medicina, Universidade de São Paulo (IMTSP/USP), São Paulo, Brazil, [2] Departamento de Salud Publica, Facultad de Ciencias de La Salud, Universidad Nacional Toribio Rodriguez de Mendoza de Amazonas, Chachapoyas, Peru, [3] Instituto de Biociências, Universidade de São Paulo, São Paulo, Brazil, [4] York Biomedical Research Institute, Hull York Medical School, University of York, York, United Kingdom, [5] Instituto Aggeu Magalhães, Fundação Oswaldo Cruz (IAM/FIOCRUZ), Recife, Brazil, [6] Departamento de Medicina Preventiva, Faculdade de Medicina, Universidade de São Paulo, São Paulo, Brazil

OPEN ACCESS

Edited by:
Izabel Galhardo Demarchi,
Federal University of Santa Catarina, Brazil

Reviewed by:
Alireza Badirzadeh,
Iran University of Medical Sciences, Iran
Walderez Ornelas Dutra,
Federal University of Minas Gerais, Brazil

***Correspondence:**
Hiro Goto
hgoto@usp.br

Specialty section:
This article was submitted to Parasite and Host, a section of the journal Frontiers in Cellular and Infection Microbiology

Received: 29 March 2021
Accepted: 24 May 2021
Published: 10 June 2021

Citation:
Souza MdA, Ramos-Sanchez EM, Muxel SM, Lagos D, Reis LC, Pereira VRA, Brito MEFD, Zampieri RA, Kaye PM, Floeter-Winter LM and Goto H (2021) miR-548d-3p Alters Parasite Growth and Inflammation in Leishmania (Viannia) braziliensis Infection. Front. Cell. Infect. Microbiol. 11:687647. doi: 10.3389/fcimb.2021.687647

American Tegumentary Leishmaniasis (ATL) is an endemic disease in Latin America, mainly caused in Brazil by *Leishmania (Viannia) braziliensis*. Clinical manifestations vary from mild, localized cutaneous leishmaniasis (CL) to aggressive mucosal disease. The host immune response strongly determines the outcome of infection and pattern of disease. However, the pathogenesis of ATL is not well understood, and host microRNAs (miRNAs) may have a role in this context. In the present study, miRNAs were quantified using qPCR arrays in human monocytic THP-1 cells infected *in vitro* with *L. (V.) braziliensis* promastigotes and in plasma from patients with ATL, focusing on inflammatory response-specific miRNAs. Patients with active or self-healed cutaneous leishmaniasis patients, with confirmed parasitological or immunological diagnosis, were compared with healthy controls. Computational target prediction of significantly-altered miRNAs from *in vitro L. (V.) braziliensis*-infected THP-1 cells revealed predicted targets involved in diverse pathways, including chemokine signaling, inflammatory, cellular proliferation, and tissue repair processes. In plasma, we observed distinct miRNA expression in patients with self-healed and active lesions compared with healthy controls. Some miRNAs dysregulated during THP-1 *in vitro* infection were also found in plasma from self-healed patients, including miR-548d-3p, which was upregulated in infected THP-1 cells and in plasma from self-healed patients. As miR-548d-3p was predicted to target the chemokine pathway and inflammation is a central to the pathogenesis of ATL, we evaluated the effect of transient transfection of a miR-548d-3p inhibitor on *L. (V.) braziliensis* infected-THP-1 cells. Inhibition of miR-548d-3p reduced parasite growth early after infection and increased production of MCP1/CCL2, RANTES/CCL5, and IP10/CXCL10. In plasma of self-healed patients, MCP1/CCL2, RANTES/CCL5, and IL-8/CXCL8 concentrations were significantly decreased and MIG/CXCL9 and IP-10/CXCL10 increased compared to patients with active disease. These data suggest that by modulating miRNAs,

L. (V.) braziliensis may interfere with chemokine production and hence the inflammatory processes underpinning lesion resolution. Our data suggest miR-548d-3p could be further evaluated as a prognostic marker for ATL and/or as a host-directed therapeutic target.

Keywords: *Leishmania braziliensis*, microRNA, pathogenesis, active cutaneous leishmaniasis, self-healed cutaneous leishmaniasis, THP-1 cells

INTRODUCTION

The leishmaniases are vector-borne diseases caused by protozoan parasites of the genus *Leishmania.* Transmitted by *Phlebotomine* sandflies, the leishmaniases are endemic in tropical and subtropical areas, with one million cases/year in 98 countries (Burza et al., 2018). During its life cycle, *Leishmania* exists as promastigotes (elongated forms with an external flagellum) in the sandfly gut and as amastigotes (round or ovoid forms without an external flagellum) within mononuclear phagocytes of the vertebrate host. After promastigote inoculation in the skin by the vector, the parasites interact primarily with tissue humoral and cellular elements and the infection may progress to overt disease. Depending on the *Leishmania* species and host characteristics, the disease may manifest as visceral leishmaniasis, affecting organs, such as the liver and spleen, or tegumentary form, causing lesions in the skin and mucosa. More than 15 species may cause cutaneous leishmaniasis, with *Leishmania (Viannia) braziliensis* the most prevalent species in Brazil, where disease presents as either localized cutaneous leishmaniasis (CL), disseminated cutaneous leishmaniasis, or disfiguring mucosal leishmaniases (Turetz et al., 2002; Machado et al., 2011; Goto and Lauletta Lindoso, 2012). Once diagnosed, most patients are treated with anti-*Leishmania* drugs but rarely the patients heal without any specific treatment. Comparing active cutaneous and self-healed leishmaniasis patients constitutes a unique opportunity to explore pathogenic mechanisms of lesion development and control that are not fully elucidated.

In human CL, lesion development is not directly related to parasite growth, and few parasites are seen in the skin (Sotto et al., 1989). Instead, Th-1-type immune responses essential for infection control also drive inflammation and lesion development and cause tissue damage if uncontrolled (Vieira et al., 2002). In CL lesions characterized by chronic inflammation, activated $CD69^+$ T cells (Diaz et al., 2002) and regulatory $CD4^+CD25^+FOXP3^+$ IL-10–producing T cells, granzyme A $CD8^+$ cytotoxic T cells, or even pro-inflammatory $CD4^+$ IFN-γ–producing T cells (Bourreau et al., 2009; Faria et al., 2009) have all been observed. In a recent transcriptomic study of skin samples of cutaneous leishmaniasis patients, delayed or absence of cure was correlated with higher expression of gene sets related to the cytolytic pathway, including mRNAs for granzyme (*GZMB*), perforin (*PRF1*), and granulysin (*GNLY*) (Amorim et al., 2019).

microRNAs (miRNAs), endogenous small non-coding RNAs of ~22 nucleotides, have a fundamental role in shaping the host transcriptome (Baltimore et al., 2008) and act as key regulators in gene expression networks, including those regulating cell cycle, mitosis, apoptosis, differentiation, and immune functions. MicroRNAs mediate gene silencing post-transcriptionally by base-pairing to the 3′-untranslated regions (3'UTR) of their respective target genes. Up/down-regulation of miRNA expression impacts various cellular processes during homeostasis but may also result in dysfunction of cellular activities (Bartel, 2004; Bartel, 2009) and participate in pathological processes including infection and inflammation (O'Connell et al., 2012). In the human immune system, miRNA-clusters have been shown to exert essential roles in the regulation of related gene expression, impacting innate and adaptive immune responses (Hirschberger et al., 2018). Furthermore, as most miRNAs are considered stable in biological fluids and resistant to environmental conditions (Sohel, 2016), miRNAs are suitable for evaluation in plasma samples and represent attractive candidates as biomarkers of disease or therapeutic response.

MicroRNAs can be modulated by different pathogens, such as viruses, bacteria, and protozoan parasites (Chandan et al., 2019; Acuna et al., 2020). Differential expression of diverse miRNA has been identified in *Leishmania*-host interaction *in vitro* and experimental *in vivo* systems with visceral and cutaneous strains of *Leishmania* (Acuna et al., 2020) as well as human leishmaniasis (Paul et al., 2020). Specifically, in cutaneous leishmaniasis caused by *L. braziliensis* miR-361-3p, a regulator of GZMB and tumor necrosis factor (TNF) was down-regulated and related to treatment failure (Lago et al., 2018). In contrast, expression of miR-193b and miR-67, involved in regulating expression of triggering receptor expressed on myeloid cells-1 (TREM-1) was positively related to good treatment outcome (Nunes et al., 2018).

In the present study, we searched for differentially expressed microRNA in plasma of patients with active *L. (V.) braziliensis* infection and self-healed CL patients. In addition, we studied *in vitro L. (V.) braziliensis* infected-human monocyte-derived THP-1 cells to provide more direct insights into miRNA function. We focused on miRNA related to immune-inflammatory processes given the role of such processes in CL lesion development and resolution. miRNA expression was found to be markedly different between patients with self-healed leishmaniasis compared to healthy controls and cases with active CL. Among various differentially expressed miRNAs in patient plasma and *L. braziliensis*-infected THP-1 cells, we selected miR-548d-3p that was upregulated in both settings for further validation.

MiR-548d-3p inhibition in THP-1 cells reduced early parasite growth and increased MCP1/CCL2, RANTES/CCL5, and IP-10/CXCL10, whereas in self-healed patients, MCP1/CCL2, RANTES/CXCL5, and IL-8/CXCL8 were decreased, and MIG/CXCL9 and

IP-10/CXCL10 were increased compared with active cases. Collectively, these data suggest that *L. (V.) braziliensis* exploits miRNAs to modulate the production of discrete sets of pro-inflammatory cytokines that are involved in lesion resolution.

MATERIALS AND METHODS

Ethics Statement

The experimental protocols were approved by the ethics committee of the Faculdade de Medicina, Universidade de São Paulo (CAAE 35670314.0.1001.0065) and are in the accordance with the World Medical Association Declaration of Helsinki on Ethical Principles for Medical Research lnvolving Human Subjects of 1964 with latest amendment of 2013. All individuals agreed to participate by signing the Informed Consent Form.

Patients

Individuals of both gender and age from 15 to 60 years old were selected from endemic areas in Pernambuco state, Northeastern Brazil where *L. (V.) braziliensis* is the predominant species causing CL. Five patients with active disease were chosen based on the presence of up to five cutaneous lesions, confirmed diagnosis of leishmaniasis and absence of local concomitant bacterial infections, comorbidities such as HIV/aids, diabetes mellitus, dermatitis, peripheral vascular diseases, and previous chemotherapy. The diagnosis of active cases was confirmed by submitting sample to direct microscopic parasitological exam of lesion scrapings, by culture, by inoculation into hamsters for parasitological recovery or by polymerase chain reaction specific for *Viannia* subgenus (Brito et al., 2009).

Five self-healed patients with a history of previous cutaneous leishmaniasis were also recruited, showing characteristic scars, confirmed diagnosis, and absence of abovementioned comorbidities, co-infections, and previous chemotherapy. Another five healthy individuals represented the control group, being recruited from non-endemic areas and without previous leishmaniasis, abovementioned comorbidities, or co-infections.

The patients with active or self-healed leishmaniases were from the municipalities of Paudalho, Moreno, Jaboatão, and Bezerros, localities close by preserved remnants of Atlantic forest, in the State of Pernambuco, Northeast Brazil, where intertwine rural and urban environments where they live and work (**Figure 1**).

After confirmed diagnosis, four milliliters of whole blood were collected in EDTA from each individual, and plasma stored at −80°C until use.

Parasites

Leishmania parasites were previously isolated from a patient with mucosal leishmaniasis at Corte de Pedra, Bahia, Brazil, and characterized as *L. (V.) braziliensis* by the *Leishmania* Collection at Fundação Oswaldo Cruz—CLIOC/FIOCRUZ. To preserve the infectivity, the parasites were inoculated *via* intraperitoneal route and maintained through regular passages in hamster (*Mesocricetus auratus*). Amastigotes were then purified from the spleen of hamster and expanded in axenic culture with Schneider's insect medium (Sigma-Aldrich, USA) containing 100 UI/ml penicilin and 100 µg/ml streptomycin and supplemented with 10% heat-inactivated fetal calf serum (FCS) (Cultilab, Brazil) at 26°C. The amastigote-derived promastigotes were cryopreserved in aliquots and thawed for use in specific experiments. Promastigotes were cultured in Schneider's insect medium (Sigma-Aldrich, USA) containing 100 UI/ml penicilin and 100 µg/ml streptomycin and supplemented with 10% heat-inactivated fetal calf serum (FCS) (Cultilab, Brazil) at 26°C. The parasites used in the experiments were at the stationary phase of growth and with no more than four passages in culture.

Infection of Macrophages With *L. (V.) braziliensis*

THP-1 monocytic cell line (ATCC) was maintained in RPMI 1640 medium (Sigma-Aldrich, USA) supplemented with 2 mM L-glutamine, 1 mM sodium piruvate, 0.2% sodium bicarbonate, and 5% FCS (complete medium). Then 10^6 cells in 1 ml of RPMI 1640 medium were plated onto 24-well plates (Costar, USA) and incubated in the presence of 20 ng/ml phorbol myristate acetate (PMA; Sigma-Aldrich, USA) for 48 h at 37°C in a humid atmosphere with 5% CO_2 to allow differentiation into macrophages (Tsuchiya et al., 1982). In experiments for parasite load analysis, round coverslips were placed in the well. Non-adherent cells were then removed and *L. (V.) braziliensis*

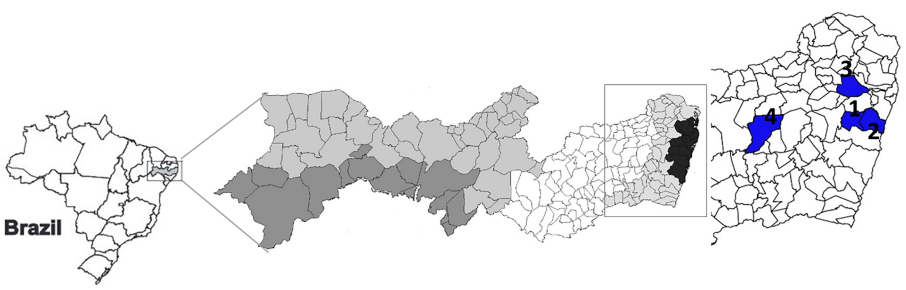

FIGURE 1 | Cartographical representation of the State of Pernambuco, Northeastern Brazil. Regions in blue indicate Moreno (1), Jaboatão (2), Paudalho (3), and Bezerros (4) municipalities.

promastigotes were added to the wells in triplicates (parasite:cell ratio = 5:1) and incubated for 4 h at 33°C in humid atmosphere with 5% CO_2 to allow infection of macrophages. Non-infected cells were maintained only with culture medium, being the negative control of the experiment. After washing out the non-internalized parasites, complete RPMI medium was added to the wells, beginning the experimental period (0 h). The plates were then maintained for 6 or 24 h at 37°C in a humid atmosphere with 5% CO_2.

Evaluation of Parasite Load in Macrophages

Glass coverslips were removed from the wells and stained with panoptic dyes (Instant Newprov, Brazil) and mounted on glass slides for evaluation of parasitism. A total of 900 cells were counted for each experimental condition, 300 cells/coverslip, under light microscope (Carl Zeiss, Germany), and the number of parasites per 100 cells calculated as [(number of parasites/number of infected cells) × (number of infected cells/total number of cells) × 100].

RNA Extraction, Reverse Transcription, and Pre-Amplification

Total RNA extraction from adherent THP-1 cells was performed using the miRVana PARIS isolation kit (Thermo Fisher, USA), according to the manufacturer's instructions, and RNA integrity was determined in spectrophotometer as an OD260/280 absorption ratio between 1.8 and 2.1. The total RNA purification in plasma samples was performed using the miRNeasy Serum/Plasma kit (Qiagen, USA), with the addition of a spike-in control (*Caenorhabditis elegans* cel-miR-39) to ensure the quality of the procedure and to allow qPCR normalization, according to the manufacturer's instructions. Complementary DNA (cDNA) to template RNA purified from THP-1 cells and plasma samples was synthesized with miScript II RT kit (Qiagen, USA). Briefly, 250 ng of total RNA from THP-1 cells were added to 2 µl of 5× miScript HiSpec Buffer, 1 µl of 10× Nucleics Mix, and 1 µl of miScript Reverse Transcriptase Mix. RNase-free water was added to a final volume of 10 µl. The RNA was incubated for 60 min at 37°C to insert poly-A tail downstream of the miRNA sequence and anneal a T-tail tag for the cDNA elongation. The enzyme was inactivated at 95°C for 5 min. The reaction was performed in the Mastercycler Gradient thermal cycler (Eppendorf, Germany), and the product was stored at −20°C until use. The reverse transcription reaction for plasma samples followed the same protocol, with the manufacturer's instructions to add 4.5 µl of the purified total RNA. Then, 40 µl of DEPC water was added into each 10 µl RT-PCR product and submitted to a pre-amplification reaction (preAmp), using the miScript PreAmp PCR Kit (Qiagen, USA) according to the manufacturer's instructions. Then the samples were diluted 10× and stored at −20°C.

Quantitative Real-Time PCR for miRNA

miRNA expression was evaluated with the miScript microRNA PCR array (Qiagen, USA), focusing on inflammation, and auto-immunity pathway-related molecules (MIHS-105Z). Ready-to-use qPCR plates containing a set of 84 specific primers for miRNAs and 12 internal controls were filled in with the previously prepared master mix containing PCR Buffer, SYBR Green, and the 10-fold diluted cDNA for *in vitro* infected THP-1 macrophages or preAmp samples of plasma samples. Quantitative PCR conditions were 40 cycles of 94°C for 15 s, 55°C for 30 s, and 70°C for 30 s. Normalization of miRNA expression in THP-1-derived macrophages was performed using SNORD95 and RNU6-6p as reference genes amplified in the qPCR plate. The relative expression levels were calculated using the Comparative Ct method, with non-infected cells being considered as the calibrator group.

For plasma samples, miRNA expression was also evaluated by relative quantification after previous normalization described by Marabita et al. (2016). The cel-miR-39 spike-in control was considered as a technical reference. Simultaneously, a geometric mean of all expressed miRNAs was used as a normalization factor to calculate relative expression to a calibrator group, which varied depending on the analysis.

In Silico miRNA Target Prediction

Target prediction strategy was performed in two different platforms, considering the miRNAs differentially expressed in the *in vitro* experiment. For an initial screening in human leishmaniasis pathway, we used DIANA-miRpath 3.0 server in the reverse search module (Vlachos et al., 2015), with Targetscan (Agarwal et al., 2015) as the chosen algorithm. To discover potential interactions with other biological pathways related to human leishmaniasis pathogenesis, we performed a second analysis using MiEAA (MiRNA Enrichment Analysis and Annotation), which integrates data from different databases such as miRBase, miRWalk, and miRTarBase (Backes et al., 2016).

In Vitro miRNA Inhibition

The inhibition of miR-548d-3p in THP-1-derived macrophages was performed in an *in vitro* infection experiment through a transient transfection protocol. Assays with three different concentrations (3, 10, and 30 nM) of the mirVana® miR-548d3p inhibitor (Ambion, USA) or mirVana® miRNA Mimic, scramble Negative Control (Ambion, USA) were performed, and 10 nM concentration was chosen for further use (**Figure S1**). At the end of the experiment, the cell viability was evaluated by Trypan blue exclusion test when viability higher than 95% was seen in all conditions. Before the addition of *L. (V.) braziliensis* promastigotes, a solution containing the miR-548d-3p inhibitor or the negative control together with 3 µl of FUGENE transfection reagent (Promega, USA) diluted in 500 µl of RPMI medium previously incubated for 20 min at room temperature was added into each well, and maintained for 24 h. Simultaneously, non-transfected cells received only complete RPMI medium. The experiment continued with promastigote infection for evaluation of parasitism, and chemokine levels in supernatants collected and stored at −80°C until use.

Evaluation of Chemokine Production

Chemokine quantification in culture supernatants was performed using CBA – Human Chemokine Kit (BD Biosciences, USA) in accordance with manufacturer's instructions. Briefly, 50 µl of capture beads for MCP1/CCL2, RANTES/CCL5, IL-8/CXCL8, MIG/CXCL9, and IP10/CXCL10, 50 µl of Detection Reagent, and 50 µl of the studied sample or standard were added consecutively to each sample tube and incubated for 3 h at room temperature, in the dark. Next, the samples were washed with 1 ml of Wash buffer, and centrifuged. After discarding the supernatant, the pellet was resuspended in 300 µl buffer and analyzed in a FACS LSR Fortessa flow cytometer (BD Biosciences, USA). Raw data was then analyzed using FCAP Array software (BD Biosciences, USA). The detection limits of each chemokine were as follows: 2.7 pg/ml for MCP1/CCL2, 1.0 pg/ml for RANTES/CCL5, 0.2 pg/ml for IL-8/CXCL8, 2.5 pg/ml for MIG/CXCL9, and 2.8 pg/ml for IP10/CXCL10.

Statistical Analysis

Regarding *in vitro* miRNA expression, statistical analyses were performed with Qiagen miScript miRNA PCR Array Data Analysis online software, where data were submitted to an integrated Student's t test under the manufacturer's recommendation that was applied in the previous similar work (Muxel et al., 2017). *Ex vivo* data were also submitted to Student's t test, with Bonferroni's correction, using Microsoft Excel 365. Parasite load data were analyzed by ANOVA with Tukey's post-test, and data from chemokine quantification by Kruskal-Wallis test with Bonferroni's correction. The differences were considered significant when $P < 0.05$.

RESULTS

miRNA Expression in *L. (V.) braziliensis* Promastigote-Infected THP-1 Cells

We evaluated miRNA expression at 6 and 24 h post infection with *L. (V.) braziliensis* promastigotes, considering non-infected THP-1 cells as the calibrator group. 19 out of 84 miRNAs presented significant alteration in expression ($P < 0.05$). At 6 h p.i., seven miRNAs were upregulated while five were down-regulated (**Figure 2A**). In contrast, eight miRNAs were up regulated in 24 h (**Figure 2B**). From these results, we observed that these miRNAs expression was modulated through time and classified them into four groups. MiR-106b-5p, miR-29b-3p, and miR-29c-3p were the down-regulated molecules at both 6 and 24 h, while miR-195-5p, miR-30a-5p, and miR-340-5p were up-regulated at 6 h and down-regulated at 24 h. There were also down-regulated miRNAs at 6 h and upregulated at 24 h, such as miR-130a-3p, miR-211-5p, miR-520d-3p, and miR-545-3p, whereas let7i-5p, miR-30e-5p, miR-302a-3p, miR-302b-3p,

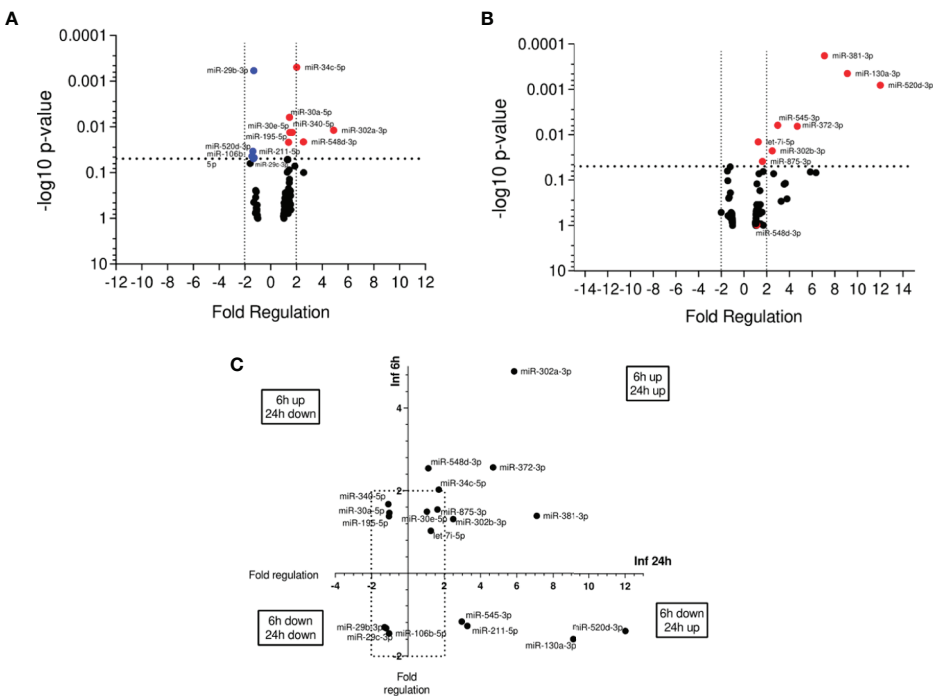

FIGURE 2 | miRNA profiles of *L. braziliensis* infected THP-1-macrophages. Volcano plot of differential expression of miRNA in *L. (V.) braziliensis* promastigote-infected THP-1 macrophages in relation to non-infected cells at 6 h **(A)** and 24 h **(B)** post-infection compared to uninfected-macrophages. Each dot represents one miRNA. Red dots indicate the up-regulated miRNAs, and the blue dots represent the down-regulated miRNAs ($P < 0.05$). Black dotted line corresponds to $p = 0.05$, log 10. The relative up- and down-regulation of miRNAs, expressed as boundaries of 2 or -2 of Fold Regulation, respectively. P-value was determined based on two-tailed Student's t test. Significantly expressed miRNAs in different times distributed in four groups **(C)**. Experiments were repeated three times.

miR-34c-5p, miR-372-3p, miR-381-3p, miR-548d-3p, and miR-875-5p were upregulated at both time-points (**Figure 2C**).

miRNA Profiling of Serum From ATL Patients

The participants of this study were predominantly male and the active disease patients were younger (mean 20 and median 20 years old, minimum-maximum:18-22 ya) than self-healed patients (mean 26.2 and median 27 years old, minimum-maximum: 21-30 ya). The number of present or past lesions, and their localization were similar in both groups. The patients with active disease presented lesions characteristic of the localized form of CL (rounded, ulcerated, with well-defined and elevated edges and granulomatous bottom) on uncovered parts of the body, with evolution ranging from 15 to 28 days. The self-healed individuals presented typical scars without previous anti-*Leishmania* chemotherapy, with healing time ranging from three to nine months (**Table 1**).

The miRNA expression in plasma samples of patients with active disease was not significantly different compared to the control group (**Figure 3A**). In contrast, self-healed individuals presented 14 differentially expressed miRNAs, eight of them up-regulated (miR-15b-3p, miR-29b-3p, miR-181-5p, miR-202-3p, miR-211-5p, miR-302c-5p, miR-373-3p, miR-449-5p), and six down-regulated (miR-19b-3p, miR-21-5p, miR-29c-3p, miR-30e-5p, miR-656-3p, miR-93-5p) in relation to the control group (**Figure 3B**). When comparing self-healed patients with the active disease group, we found a total of 23 significantly altered miRNAs, with 14 of these up-regulated (miR-15b-5p, miR-20b-5p, miR-29b-3p, miR-181a-5p, miR-181d-3p, miR-202-3p, miR-211-5p, miR-300, 302c-5p, miR-410-3p, miR-548d-3p, miR-875-3p, miR-655-3p, miR-1324), and nine down-regulated (miR-16-5p, miR-17-5p, miR-19b-3p, miR-21-5p, miR-29c-3p, miR-30e-5p, miR-93-5p, miR-454-3p, miR-656-3p) (**Figure 3C**). Our data suggest distinct miRNA profiles in plasma samples of active and self-healed ATL patients.

Concomitant Altered Expression of miRNAs in *In Vitro* and *Ex Vivo* Experiments

To focus on understanding the miRNA modulation and function during infection, we searched for correlations between up- and down-regulated miRNAs. We found some miRNAs differentially expressed in infected THP-1 cells and plasma samples of ATL patients (**Table 2**). The miR-548d-3p and miR-875 were upregulated in self-healed patients and *in vitro* at 6 and 24 h of incubation post-infection. Despite that, miR-211-5p and miR-29b-3p were upregulated in self-healed patients, but down-regulated at 6 h of incubation post-infection *in vitro*. Down-regulated expression was observed for miR-29c-3p *ex vivo*, showing similar modulation in the *in vitro* experiment at both time points. Finally, miR-30e-5p was upregulated *in vitro* at 6 and 24 h of incubation post-infection and down-regulated in plasma samples (**Figures 2C** and **3C**).

miRNA Predicted Targets and Interactions With Biological Pathways Related to ATL Pathogenesis

We used Diana MiRPath 3.0 with TargetScan2 as the chosen algorithm to predict miRNA/mRNA interactions, focusing on miRNAs modulated in infected THP-1 cells. Among the interactions predicted in the initial analysis using the Diana

TABLE 1 | Demographic and clinical data of active disease and self-healed patients.

	Code	Gender/Age (years old)	Occupation	Locality	Clinical form	Lesions (n)	Size (cm)	Evolution	Lesion site	Parasite search	PCR	Isolation Parasite	IDRM
Active disease patients	0001	M/19	Military	Paudalho/PE	Ulcerated	01	1.0 × 2.0	15 days	Left leg	+	+	ND	+
	0002	M/21	Military	Paudalho/PE	Ulcerated	01	0.5 × 0.5	15 days	Right flank	+	+	–	+
	0003	M/22	Military	Paudalho/PE	Ulcerated	01	0.5 × 0.5	15 days	Right hand	+	–	+	+
	0004	M/20	Military	Paudalho/PE	Ulcerated	01	0.6 × 0.6	1 month	Right hand	+	–	–	+
	0005	M/18	Student	Moreno/PE	Ulcerated	01	1.5 × 1.5	15 days	Left Leg	+	+	+	+
	Code	**Gender/Age**	**Occupation**	**Provenance**	**Reported clinical form**	**Scars (n)**	**Size (cm)**	**Healing time**	**Scar sites**	**Parasite search**	**PCR**	**Parasite Isolation**	**IDRM**
Self-healed patients	0006	M/27	Farmer	Moreno/PE	Ulcerated	02	2.0 × 3.0; 1.0 × 1.0	4 months	Right foot	+	–	–	ND
	0007	M/29	Machine operator	Jaboatão/PE	Ulcerated	01	4.0 × 3.0	9 months	Left leg	–	+	–	ND
	0008	M/30	Engineer	Bezerros/PE	Ulcerated	02	2.0 × 2.0	6 months	Left leg	–	+	–	ND
	0009	F/24	Housewife	Moreno/PE	Ulcerated	01	1.5 × 1.5	4 months	Right leg	+	+	–	ND
	0010	M/21	Farmer	Moreno/PE	Ulcerated	01	2.0 × 2.0	3 months	Right thigh	–	+	+	ND

M, male; F, female; L, left; R, right; PCR, polymerase chain reaction; IDRM, Montenegro skin test; ND, not done.

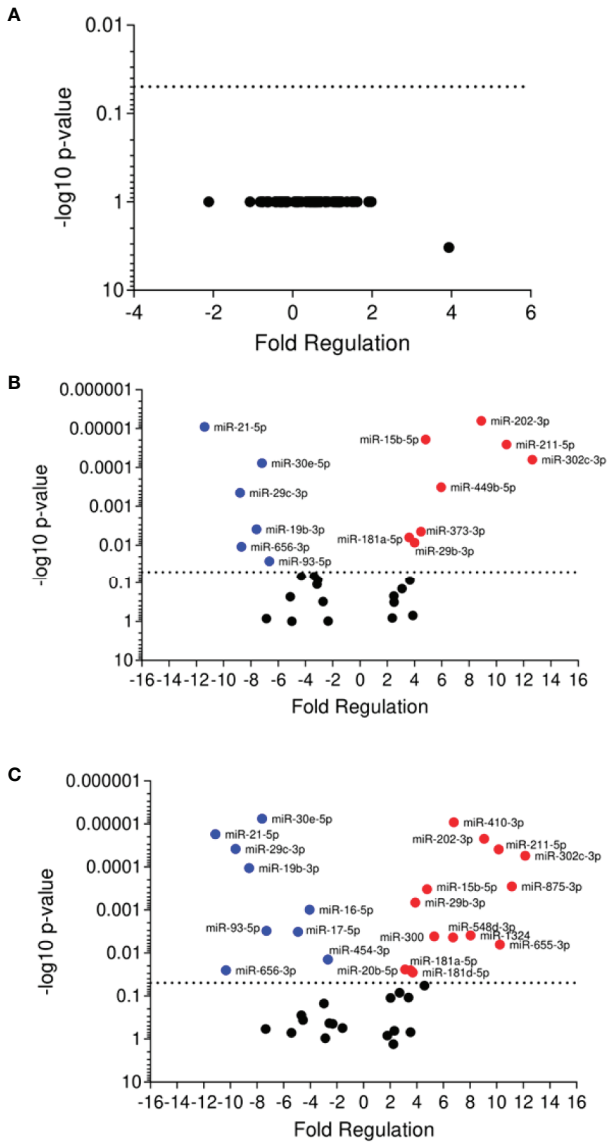

FIGURE 3 | Volcano plot of differential expression of miRNA in plasma of cutaneous leishmaniasis patients. Volcano plot of differential expression of miRNA in plasma samples of active disease patients **(A)** and self-healed **(B)** compared to healthy individuals, and self-healed **(C)** compared to active disease patients. Each dot represents one miRNA. Red dots indicate the up-regulated miRNAs, and the blue dots represent the down-regulated miRNAs ($P < 0.05$). Black dotted line corresponds to p=0.05, log 10. The relative up- and down-regulation of miRNAs, expressed as boundaries of 2 or -2 of Fold Regulation, respectively. P-value was determined based on two-tailed Student's t test. $P < 0.05$ (Student *t* test and Bonferroni correction).

platform, there were cytokines encoded by the *TGFB2* and *IL10* genes, MHC class II proteins (HLA-DPA1, HLA-DRB5, and HLA-DOA) and genes related to signaling pathways (e.g. MAPK1, MAP3K7, IRAK4) (**Figure 4**).

Further predictions made in MiEAA platform showed, in more than one classification system (PANTHERDB, WikiPathways, and KEGG), some pathways known to be important in the parasite-host interaction that can be regulated by the expressed microRNAs in *L. braziliensis*-infected THP-1 cells (**Figure 5A**) and in self-cured patients plasma compared with active patient sample (**Figure 5B**). Cytokine signaling pathways, such as IFN-γ, TNF-α, and TGF-β, are known to be involved in the immune response against *Leishmania*. Also, signal transduction pathways such as JAK-STAT and PI3K were putative targets of differentially expressed miRNAs, as well as the VEGF, Wnt, and HIF-1 pathways. There is also a potential interference of miRNAs expressed in the oxidative stress pathway. Finally, the signaling cascade activated by IGF receptors may be influenced by the differentially expressed microRNAs. Searching predicted pathways targeted by the circulating microRNAs present in plasma, we observed the inflammation mediated by chemokines and cytokines and the chemokine signaling pathways. Besides, important pathways involved in B cell development like B cell activation and mTOR signaling pathways were predicted. Pathways involved in Th17 and Th2 differentiation and T cell proliferation such as T cell activation, IL-4, IL-6, and IL-2 signaling were evidenced.

Among various differentially expressed miRNAs, we selected miR-548d-3p that was upregulated in patient plasma and *L. braziliensis*-infected THP-1 cells and targets only two pathways for further validation.

Effect of miR-548d-3p Inhibition on Parasite Load in THP-1 Infection With *L. (V.) braziliensis*

The function of miR548d-3p during *L. braziliensis* infection was evaluated using 10 nM specific inhibitor or scrambled miRNA. At both 6 and 24 h post-infection, a significant decrease was observed in parasite load when miR-548d-3p was inhibited ($P < 0.05$), compared to transfection with scrambled RNA, negative control (**Figure 6A**).

miR-548d-3p Inhibition on Chemokine Production in *L. (V.) braziliensis*–Infected THP-1 Cells

Inhibition of miR-548d-3p did not affect the production of CCL2 by infected THP-1 cells at 6 h p.i. but led to a >2-fold increase in secretion of CCL2 at 24 h p/i/compared to both untreated infected cells and cells treated with the scrambled RNA-negative control (**Figure 6B**). In contrast, CCL5 production appeared more susceptible to modulation by transfection of the scrambled control RNA and use of the inhibitor tended to normalize the production to that seen in untransfected cells (**Figure 6C**). The production of CXCL8 and CXCL10 were not significantly affected by the miR-548d-3p inhibitor in comparison to untransfected cells but a small but significant increase in CXCL10 was observed compared to the scrambled inhibitor at 24 h p.i. (**Figures 6D, E**).

Chemokine Levels in Plasma of ATL Patients

CCL2 was found at significantly higher concentration in plasma samples of patients with active disease compared to self-healed and control groups (**Figure 7A**), whereas CXCL5 and CXCL8

TABLE 2 | Set of miRNAs significantly expressed both in *in vitro* and *ex vivo* contexts.

Up regulated	Down regulated
miR-410-3p	**miR-30e-5p**
miR-202-3p	miR-21-5p
miR-211-5p	**miR-29c-3p**
miR-302c-3p	miR-19b-3p
miR-15b-5p	miR-16-5p
miR-875-3p	miR-17-5p
miR-29b-3p	miR-93-5p
miR-548d-3p	miR-454-3p
miR-300	miR-656-3p
miR-1324	
miR-655-3p	
miR-181a-5p	
miR-181d-5p	
miR-20b-5p	

miRNAs in bold, molecules modulated in similar ways in both experiments.

were decreased in self-healed cases compared to active cases (**Figures 7B, C**). Significantly higher concentrations of CXCL9 (**Figure 7D**) and IP-10 (**Figure 7E**) were seen in self-healed patients in relation to healthy individuals and patients with active disease ($P < 0.05$).

DISCUSSION

Macrophages exert a dual role in the pathogenesis of CL, being both host cell and also the main effector cell for parasite clearance (Tomiotto-Pellissier et al., 2018). The disease outcome depends on the interplay between *Leishmania* and the host immune responses which govern these opposing macrophage functions. *Leishmania* employ strategies to evade the host immune response, including altering the miRNAs expression (Lemaire et al., 2013; Muxel et al., 2017; Muxel et al., 2018; Nunes et al., 2018; Fernandes et al., 2019; Paul et al., 2020). In this context, having access to *L. braziliensis*-infected active and self-healed CL patients, we searched for differentially expressed miRNAs in plasma and in parallel conducted an *in vitro* study using *L. (V.) braziliensis* infected-human monocyte-derived THP-1 cells. With this approach, we sought to attribute altered miRNA profiles to mechanisms of disease pathogenesis.

Alterations of miRNA expression were seen in self-healed patient samples compared with active cutaneous leishmaniasis cases and healthy controls, the latter being indistinguishable by miRNA profile. Thus, these data suggest that host cells from individuals that cure without treatment are more active in altering miRNA expression upon *L. (V.) braziliensis* infection, although we cannot rule out at this preliminary stage in our investigation whether this is confounded by other factors unrelated to infection e.g., environmental exposure or host genetics. Concerning environment, the patients were from endemic areas, from nearby cities with similar climate and environmental characteristics. Differentially expressed miRNAs have been related to inflammatory chemokine levels, and this may contribute to the self-healing nature of these patients. An additional weakness of the study is that parasites from these patients were not genotyped or functionally evaluated. This may

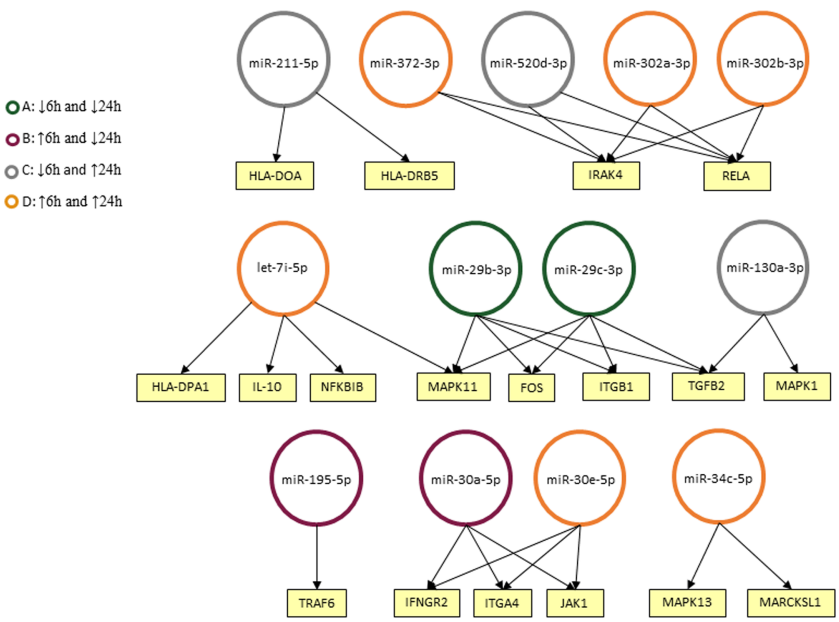

FIGURE 4 | Predicted interactions between the set of differentially expressed microRNAs in THP-1 cells after 6 and 24 h post infection. The genes on which they are suggested to act in the Leishmaniasis pathway in humans are shown as seen in KEGG. miRNAs were classified into four groups according to their modulation through time: down-regulated in 6 and 24 h **(A)**, up-regulated on 6 h and down-regulated in 24 h **(B)**, down-regulated in 6 h and up-regulated in 24 h **(C)** and up-regulated in both timepoints **(D)**.

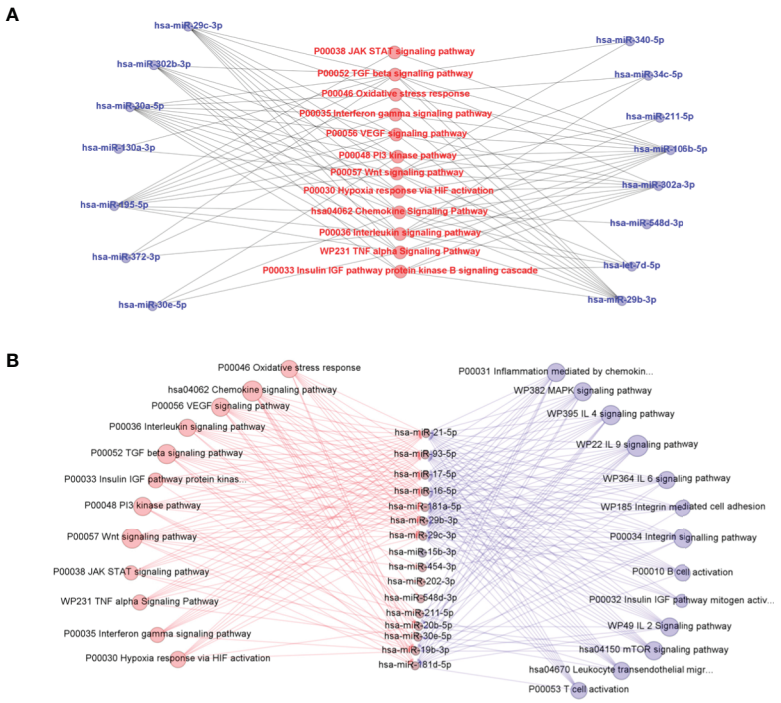

FIGURE 5 | Predicted interactions between the set of differentially expressed microRNAs in THP-1 cells after 6 and 24 h post infection with *L. braziliensis* **(A)** and in plasma samples from self-healed patients compared to active disease individuals **(B)** and the biological pathways related to inflammatory response on which they are suggested to act according to MiEAA algorithms. In **(B)**, pathways in red were predictably targeted by *in vitro* and *ex vivo* miRNA sets, while the others in blue were evidenced only in miRNAs significantly quantified in plasma.

be important given that some strains of *L. braziliensis* are more susceptible to oxidative stress than others, and induce lesions with a higher tendency to spontaneous healing (Souza et al., 2010; Sarkar et al., 2012). In addition, we have to consider a proper balance between regulatory and pro-inflammatory mediators, especially IFN-γ and IL-10, that may differ depending on the hosts background, important for the lesion to heal (Gomes-Silva et al., 2007; de Assis Souza et al., 2013).

Evaluation of altered miRNA expression *in vitro L. (V.) braziliensis* infected-human monocyte-derived THP-1 cells showed a set of miRNAs also found altered in plasma of leishmaniasis patients. In silico prediction of THP-1 expressed miRNA targets and interactions with biological pathways suggested a link between the differentially expressed miRNAs and altered expression targeted cytokine, chemokine, and signaling pathways, signal transduction pathways, and others.

A total of 19 out of 84 miRNAs exhibited an altered *in vitro* expression compared with non-infected THP-1 cells either at 6 or 24 h of incubation after infection, showing that *Leishmania* can modulate these molecules in a temporally distinct manner during the early stages of *in vitro* infection as seen by others (Guerfali et al., 2008; Bazzoni et al., 2009; Lemaire et al., 2013). In the in-silico predictions using DIANA miRPath 3.0, considering *Leishmania* infection pathway, upregulated miR-195-5p at 6 h may target tumor-necrosis factor receptor-associated factor 6 (TRAF6), an important player in signal transduction of both the TNF receptor (TNFR) superfamily and the interleukin-1 receptor (IL-1R). These are crucial to ultimately activate transcription factors, such as nuclear factor kappa B (NF-κB) and interferon-regulatory factor (IRF), to induce immune and inflammatory responses (Ye et al., 2002; Wang et al., 2010). In addition, two isoforms of miR-30 family, miR-30a-5p, and miR-30e-5p, were suggested to target Interferon gamma receptor 2 (IFNGR2), Janus kinase 1 (JAK1), Integrin subunit alpha 4 (ITGA4) genes throughout time. These predicted interactions suggest participation in parasite control mechanism and inflammatory process. Other important events of the immune response such as Toll-like receptor signaling and antigen presentation were also predicted to be compromised by the influence of let-7i-5p, miR-130a-3p, miR-520d-3p, and two isoforms of miR-302.

Other relevant pathways that are known to play a role in the adaptive immune response in cutaneous leishmaniasis were targeted by miRNAs identified exclusively in plasma samples from self-healed patients compared with active disease subjects. Pathways related to T and B cell activation including mTOR pathway that can modulate B cell development (Limon and Fruman, 2012; Iwata et al., 2017) were predicted. Cytokine related pathways such as IL-2, IL-4, IL-6, and IL-9 were also evidenced. These different pathways potentially targeted by circulating microRNAs might reflect the diversity of cells participating in the immune response in humans, in contrast to exclusively monocyte/macrophage *in vitro* experiment.

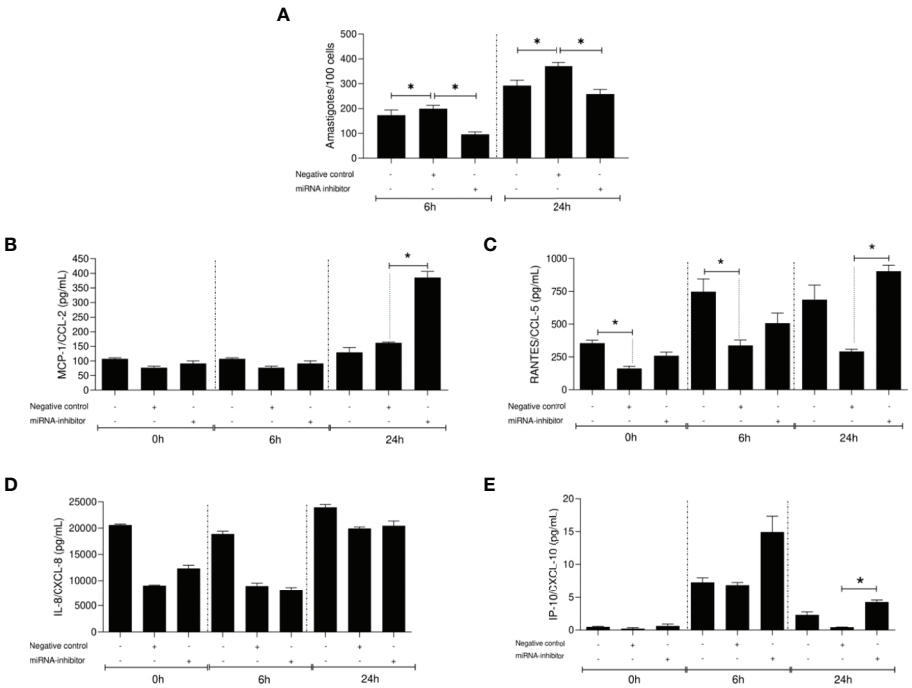

FIGURE 6 | Parasite load (number of amastigotes/100 cells) **(A)** and chemokine levels (pg/ml) **(B–E)** in *L. (V.) braziliensis* promastigote-infected THP-1 cells transiently transfected with miR-548d-3p inhibitor at 6 and 24 h post-infection. One experiment was carried out by adding the miR-548d-3p inhibitor (10 nM) or negative control (scrambled miRNA; 10 nM) with the transfection reagent diluted in RPMI medium or only RPMI medium (non-transfected cells) to wells containing 10^6 THP-1 adherent cells and maintained for 24 h at 37°C (5% CO2) then infected with *L. (V.) braziliensis* promastigotes. **(A)** * = $P < 0.05$ (one way ANOVA and Student *t* test). MCP1/CCL2 **(B)**, RANTES/CXCL5 **(C)**, IL-8/CXCL8 **(D)**, and IP-10/CXCL10 **(E)** concentrations were measured by flow-cytometry using the CBA kit. **(B–E)** * = $p < 0.05$ (Kruskal-Wallis and Bonferroni tests).

Among altered miRNAs in the present study, other miRNAs belonging to the same family were previously analyzed in *Leishmania* infection. The modulation of miR-29b, miR-29c, and miR-30e were observed in *L. amazonensis*-infected murine macrophages (Muxel et al., 2017; Muxel et al., 2018; Fernandes et al., 2019). Upregulation of miR-29b was observed in *L. major*-infected human monocyte-derived macrophages, whereas this miRNA was down-regulated in *L. donovani* infection (Geraci et al., 2015). Stimulation of the nucleotide-binding oligomerization domain containing 2 (NOD2) induces miR-29 family upregulation, resulting in downregulation of IL-12p40 without alteration to IL-6, TGF-β or IL-10 production (Yu et al., 2002; Guo et al., 2012; Reveneau et al., 2012). However, NOD2-stimulation increases the levels of IL-1β, IL-6, and IL-23 cytokines, Nitric Oxide Synthase 2 (NOS2) expression and nitric oxide (NO) production during *Leishmania* infection (Lima-Junior et al., 2013).

We also searched for other biological pathways that could be affected during *Leishmania* infection, and our predictions using the MiEAA platform pointed to some involved in inflammation and wound healing as follows. Also, our predictions highlighted TNF, IFN-γ, and TGF-β signaling pathways, cytokines with respective proinflammatory and regulatory roles in *Leishmania* infection (Souza et al., 2012; de Assis Souza et al., 2013; Souza et al., 2016). The oxidative stress response pathway was also revealed once reactive oxygen and nitrogen species (ROS and RNS) produced during an inflammatory response are an important part of host-defense strategies of organisms to kill the parasite (Kocyigit et al., 2005).

Many characteristics of leishmanial lesions such as microcirculation impairment, metabolic demand for leukocytes, parasite proliferation, and secondary bacterial infection are indicators of a hypoxic event in those lesions (Fraga et al., 2012). Related to this condition, changes in miRNAs that regulate Hypoxia-inducible factor 1 *(*HIF-1) activation in response to hypoxia were also identified in silico. Other possible consequence of a hypoxic, inflammatory microenvironment is the induction of vascular remodeling *via* Vascular endothelial growth factor A/Vascular endothelial growth factor receptor (VEGF-A/VEGFR) expression by HIF-1 influence, which are elevated in the skin of humans and mice infected with *Leishmania* parasites (Fraga et al., 2012; Araujo and Giorgio, 2015). Differentially expressed miRNA affecting VEGF were also observed in our data. Our in-silico predictions also showed that some of the altered miRNAs targets the IGF-I signaling pathway. The role of this hormone in *Leishmania* infection has been long studied with pleiotropic effect in innate and adaptive immune response and pathogenesis in leishmaniases (Reis et al., 2021).

Cutaneous lesions are characterized by chronic inflammation where concur activated $CD69^+$ T cells (Diaz et al., 2002), regulatory $CD4^+CD25^+FOXP3^+$ IL-10–producing T cells,

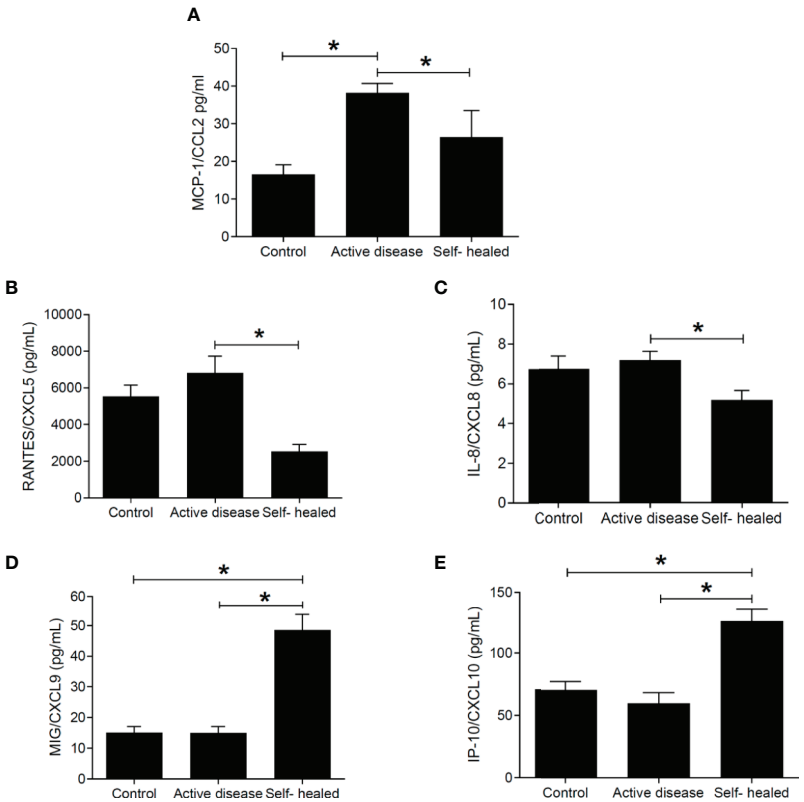

FIGURE 7 | Chemokine concentration (pg/ml) in plasma of cutaneous leishmaniasis patients and controls. MCP1/CCL2 **(A)**, RANTES/CXCL5 **(B)**, IL-8/CXCL8 **(C)**, MIG/CXCL9 **(D)**, and IP-10/CXCL10 **(E)** concentrations were measured by flow-cytometry using the CBA kit. * = $p < 0.05$ (Kruskal-Wallis and Bonferroni tests). N =5 patients and controls per group.

granzyme A $CD8^+$ cytotoxic T cells, $CD4^+$ IFN-γ–producing T cells (Bourreau et al., 2009; Faria et al., 2009) and where higher expression of gene sets related to the cytolytic pathway is observed (Amorim et al., 2019). The influx of cells into the lesion reflects the role of chemokines and one of miRNA seen altered *in vitro* and patients' plasma in the present study was miR-548d-3p. miR-548d-3p and others from the same family were reported related to wound healing and inflammation in rheumatoid arthritis and *Leishmania donovani* infection (Wang et al., 2018; Huang et al., 2020) thus we proceeded with functional validation of the miR-548d-3p in *L. braziliensis* infected-THP-1 cells. The miR-548 family is a larger and poorly conserved, encompassing 69 human miR-548 genes located in almost all human chromosomes (Liang et al., 2012). Previous studies showed that miR-548d are processed from the same encoded hairpin cluster of miR-548aa1 (GenBank ID 100500863) and that miR-548d-3p belongs to the cluster family of hsa-miR-548-d1 (miRbase ID MI0003668) (Cummins et al., 2006; Landgraf et al., 2007) transcribed from negative strand of intronic region of ATPase family AAA domain containing 2 (ATAD2, gene ID NM_014109.4) gene located into chromosome 8 (search in miRIAD toll) (Cummins et al., 2006). The transcription of miR-548d1 is related to transcription of the ATAD2 gene, as observed upon glucocorticoid stimulation (Rainer et al., 2009). This information showed the complex changes in miRNA/miRtron expression regulation upon distinct stimuli. ATAD2 has a ATP-binding site and ATPase activity, regulating the assembly of protein complexes (Morozumi et al., 2016), as CREB-binding promoter region or regulating histone hyperacetylation (Koo et al., 2016; Lazarchuk et al., 2020), suggesting the ATAD2/miR-548d can alter gene transcription during infection. ATAD2 inhibits the expression of vascular endothelial growth factor A (VEGFA) by altering miR-520a levels (Hong et al., 2018), linking miR-548d expression to modulation of other miRNAs. Also, ATAD2 can be a target of miRNAs, including miRNAs modulated during *Leishmania* infection including molecules described in our study such as miR-302, miR-373, and miR-93 (Bragato et al., 2018; Fernandes et al., 2019; Kumar et al., 2020).

miR-548d-3p was shown to enhance cell proliferation and inhibit apoptosis in breast cancer cells (Song et al., 2016), suggesting a possible role in inhibition of apoptosis seen in *L. donovani*-infected macrophages (Moore and Matlashewski, 1994). The miR-548 family can regulate expression of High mobility group box1 (HMBG1) a non-histone nuclear protein, a potent stimulator of tissue damage and inflammation through expression of pro-inflammatory cytokines (Martinotti et al., 2015; Son et al., 2019). The miR-548d-3p was seen previously

in healing and inflammatory processes. In post-burn wound healing, the vascular endothelial growth factor-A (VEGFA) a key factor involved in the wound healing process was shown to likely be targeted by miR-548d-3p (Huang et al., 2020). In rheumatoid arthritis, an autoimmune inflammatory disease, another member of the miR-548 family, miR-548a-3p, was significantly down-regulated in serum samples targeting Toll-like receptor 4/nuclear factor kappa B (TLR4/NF-kappaB) signaling pathway (Wang et al., 2018). In THP-1 cells infected with promastigotes isolates from post-kala-azar dermal leishmaniasis, other members of the 548-miRNA family, miR-548at-5p, miR-548t-3p, were upregulated when compared to THP-1 cells infected with promastigotes isolated from visceral leishmaniasis patients (Kumar et al., 2020).

Importantly, miR-548d-3p was induced in both self-healed leishmaniasis patient samples and *in vitro L. braziliensis*-infected THP-1 cells. Because the miR-548-3p was found in patients' plasma, it is likely that it is secreted by *L. braziliensis*-infected THP-1 cells, an aspect deserving further studies. It is known that THP-1 cell line can actively secrete microvesicles and exosomes that may contain miRNAs, such as miR-150 (Zhang et al., 2010) and miR-103-3p (Chen et al., 2020). Further, the content of microvesicles and exosomes may be modified by inflammatory conditions, infections including *Leishmania*, apoptosis, etc (Silverman et al., 2010; Baxter et al., 2019; Yao et al., 2019).

Inhibiting miR-548d-3p in THP-1 cells we observed a decrease in parasite load, and an increase in the production of MCP1/CCL2, RANTES/CCL5, and IP-10/CXCL10. In parallel, in plasma of self-healed patients, MCP1/CCL2, RANTES/CCL5, and IL-8/CXCL8 were decreased but increased MIG/CXCL9 and IP-10/CXCL10. We should be cautious to relate the *in vitro* experimental data to the evaluation in plasma. However, we observe a dichotomy impact of miR-548d, when upregulated in the early stage of *in vitro* infection of THP-1 derived monocytes by *L. braziliensis* (6–24 h) that is apparently reducing MCP-1 and RANTES at the infection site, contributing to the control of local inflammatory response, but at the same time, it is enabling parasite growth subverting the inflammatory response and lesion wound healing. These findings, considering the possibility of secretion of miR548d-3p by macrophages, are in line with the upregulated miR548d-3p found in the self-healed plasma patients that may reduce the MCP-1 and RANTES at systemic levels, contributing positively to wound healing modulating the inflammation. High IP-10 and MIG secretion in self-healed patients suggests that the miR-548-3p is not able to control the secretion of these cytokines. Previously, we observed higher levels of IP-10 and MIG, IFN-γ, and TNF in active and self-healed cutaneous leishmaniasis regulating parasite growth control (Souza et al., 2012; de Assis Souza et al., 2013).

Other studies have reported the role of these chemokines in cutaneous leishmaniasis. RANTES/CCL5, together with KC/CXCL1 and MIP-2/CXCL2 (Ohmori and Hamilton, 1994; Lebovic et al., 2001) participate in neutrophil, monocyte, and lymphocyte recruitment to inflammatory focus and interfere in the persistence of cutaneous leishmaniasis lesions (Teixeira et al., 2005; Costa-Silva et al., 2014). In experimental cutaneous leishmaniasis, the upregulation of miR-294 regulated *Ccl2*/*Mcp*-1 mRNA levels and infectivity in *L. amazonensis* infected BALB/c bone marrow-derived macrophages (Fernandes et al., 2019). Similarly, the downregulation of chemokines CCL2, CCL5, CXCL10, CXCL11, and CXCL12 was seen with upregulation of let-7a, miR-25, miR-26a, miR-132, miR-140, miR-146a, and miR-155 in *L. major*-infected human macrophages (Guerfali et al., 2008).

miRNAs are promising tools for diagnosis, treatment, and prognostic markers. Product for diagnosis is a reality mainly for cancers. No miRNA-based therapeutic formulations like miRNA mimics and antagomirs have reached the pharmaceutical breakthrough, but some are currently in clinical trials. In CL caused by *L. braziliensis*, miR-361-3p was appointed as a prognostic marker related to therapeutic failure. The miR-548d-3p evaluated in the present study was shown to exert tumor-suppressive effects in osteosarcoma cells and proposed as a therapeutic tool for osteosarcoma (Chen et al., 2019). Based on our findings, further studies are warranted to more clearly establish a role for miR-548d-3p as a prognostic marker and therapeutic target in cutaneous leishmaniasis.

DATA AVAILABILITY STATEMENT

The original contributions presented in the study are included in the article/**Supplementary Material**. Further inquiries can be directed to the corresponding author.

ETHICS STATEMENT

The studies involving human participants were reviewed and approved by Comite de Etica e Pesquisa da Faculdade de Medicina da Universidade de São Paulo. The patients/participants provided their written informed consent to participate in this study.

AUTHOR CONTRIBUTIONS

HG: Conceptualization, study design, project and researcher supervision, manuscript preparation. MS, and ER-S: Conceptualization, study design, experimental work, data analysis, manuscript preparation. LF-W: study design, researcher supervision, manuscript preparation. SM: study design, experimental work, data analysis, manuscript preparation. LR: experimental work, manuscript preparation. RZ: experimental work. VP and MB: coordination of sample and data collection in endemic area, data interpretation. DL and PK: data analysis, manuscript preparation. All authors contributed to the article and approved the submitted version.

FUNDING

This work was supported by the Fundação de Amparo à Pesquisa do Estado de São Paulo (grants 2018/23512-0, 2018/14398-0, and

2018/24693-9, fellowship 2014/14756-2 to MS and 2019/25393-1 to LR), Medical Research Council (grants MR/P024661/1 and MR/S019472), the Conselho Nacional de Pesquisa (research fellowship to HG), the Coordenação de Aperfeiçoamento de Pessoal de Nível Superior (CAPES; fellowship to MS) and LIM 38 (Hospital das Clínicas, Faculdade de Medicina, Universidade de São Paulo).

ACKNOWLEDGMENTS

We acknowledge Alexis Germán Murillo Carrasco for providing technical assistance with the bioinformatics approach.

REFERENCES

Acuna S. M., Floeter-Winter L. M., and Muxel S. M. (2020). MicroRNAs: Biological Regulators in Pathogen-Host Interactions. *Cells* 9 (1), 113. doi: 10.3390/cells9010113

Agarwal V., Bell G. W., Nam J. W., and Bartel D. P. (2015). Predicting Effective microRNA Target Sites in Mammalian mRNAs. *Elife* 4, e05005. doi: 10.7554/eLife.05005

Amorim C. F., Novais F. O., Nguyen B. T., Misic A. M., Carvalho L. P., Carvalho E. M., et al. (2019). Variable Gene Expression and Parasite Load Predict Treatment Outcome in Cutaneous Leishmaniasis. *Sci. Transl. Med.* 11 (519), eaax4204. doi: 10.1126/scitranslmed.aax4204

Araujo A. P., and Giorgio S. (2015). Immunohistochemical Evidence of Stress and Inflammatory Markers in Mouse Models of Cutaneous Leishmaniosis. *Arch. Dermatol. Res.* 307 (8), 671–682. doi: 10.1007/s00403-015-1564-0

Backes C., Khaleeq Q. T., Meese E., and Keller A. (2016). miEAA: microRNA Enrichment Analysis and Annotation. *Nucleic Acids Res.* 44 (W1), W110–W116. doi: 10.1093/nar/gkw345

Baltimore D., Boldin M. P., O'Connell R. M., Rao D. S., and Taganov K. D. (2008). MicroRNAs: New Regulators of Immune Cell Development and Function. *Nat. Immunol.* 9 (8), 839–845. doi: 10.1038/ni.f.209

Bartel D. P. (2004). MicroRNAs: Genomics, Biogenesis, Mechanism, and Function. *Cell* 116 (2), 281–297. doi: 10.1016/s0092-8674(04)00045-5

Bartel D. P. (2009). MicroRNAs: Target Recognition and Regulatory Functions. *Cell* 136 (2), 215–233. doi: 10.1016/j.cell.2009.01.002

Baxter A. A., Phan T. K., Hanssen E., Liem M., Hulett M. D., Mathivanan S., et al. (2019). Analysis of Extracellular Vesicles Generated From Monocytes Under Conditions of Lytic Cell Death. *Sci. Rep.* 9 (1), 7538. doi: 10.1038/s41598-019-44021-9

Bazzoni F., Rossato M., Fabbri M., Gaudiosi D., Mirolo M., Mori L., et al. (2009). Induction and Regulatory Function of miR-9 in Human Monocytes and Neutrophils Exposed to Proinflammatory Signals. *Proc. Natl. Acad. Sci. U. S. A.* 106 (13), 5282–5287. doi: 10.1073/pnas.0810909106

Bourreau E., Ronet C., Darsissac E., Lise M. C., Marie D. S., Clity E., et al. (2009). In Leishmaniasis Due to Leishmania Guyanensis Infection, Distinct Intralesional Interleukin-10 and Foxp3 mRNA Expression Are Associated With Unresponsiveness to Treatment. *J. Infect. Dis.* 199 (4), 576–579. doi: 10.1086/596508

Bragato J. P., Melo L. M., Venturin G. L., Rebech G. T., Garcia L. E., Lopes F. L., et al. (2018). Relationship of Peripheral Blood Mononuclear Cells miRNA Expression and Parasitic Load in Canine Visceral Leishmaniasis. *PloS One* 13 (12), e0206876. doi: 10.1371/journal.pone.0206876

Brito M. E., Andrade M. S., Mendonca M. G., Silva C. J., Almeida E. L., Lima B. S., et al. (2009). Species Diversity of Leishmania (Viannia) Parasites Circulating in an Endemic Area for Cutaneous Leishmaniasis Located in the Atlantic Rainforest Region of Northeastern Brazil. *Trop. Med. Int. Health* 14 (10), 1278–1286. doi: 10.1111/j.1365-3156.2009.02361.x

Burza S., Croft S. L., and Boelaert M. (2018). Leishmaniasis. *Lancet* 392 (10151), 951–970. doi: 10.1016/S0140-6736(18)31204-2

Chandan K., Gupta M., and Sarwat M. (2019). Role of Host and Pathogen-Derived MicroRNAs in Immune Regulation During Infectious and Inflammatory Diseases. *Front. Immunol.* 10, 3081. doi: 10.3389/fimmu.2019.03081

SUPPLEMENTARY MATERIAL

The Supplementary Material for this article can be found online at: https://www.frontiersin.org/articles/10.3389/fcimb.2021.687647/full#supplementary-material

Supplementary Figure 1 | Effect of different concentrations of miR-548d-3p inhibitor or negative control (scrambled miRNA) transiently transfected on parasite load (number of amastigotes/100 cells) in *L. (V.) braziliensis* promastigote-infected THP-1 cells at 6 h **(A)** and 24 h **(B)** post-infection. The experiment was carried out by adding the synthetic molecules at 3nM, 10nM or 30nM with the transfection reagent diluted in RPMI medium or only RPMI medium (non-transfected cells) to wells containing 10^6 THP-1 adherent cells and maintained for 24 h at 37°C (5% CO_2) then infected with *L. (V.) braziliensis* promastigotes. **(A)** * = $P < 0.05$ (one way ANOVA and student t test).

Chen J., Yan C., Yu H., Zhen S., and Yuan Q. (2019). miR-548d-3p Inhibits Osteosarcoma by Downregulating KRAS. *Aging (Albany N. Y.)* 11 (14), 5058–5069. doi: 10.18632/aging.102097

Chen L., Yao X., Yao H., Ji Q., Ding G., and Liu X. (2020). Exosomal miR-103-3p From LPS-Activated THP-1 Macrophage Contributes to the Activation of Hepatic Stellate Cells. *FASEB J.* 34 (4), 5178–5192. doi: 10.1096/fj.201902307RRR

Costa-Silva M. F., Gomes L. I., Martins-Filho O. A., Rodrigues-Silva R., Freire Jde M., Quaresma P. F., et al. (2014). Gene Expression Profile of Cytokines and Chemokines in Skin Lesions From Brazilian Indians With Localized Cutaneous Leishmaniasis. *Mol. Immunol.* 57 (2), 74–85. doi: 10.1016/j.molimm.2013.08.008

Cummins J. M., He Y., Leary R. J., Pagliarini R., Diaz L. A. Jr, Sjoblom T., et al. (2006). The Colorectal microRNAome. *Proc. Natl. Acad. Sci. U. S. A.* 103 (10), 3687–3692. doi: 10.1073/pnas.0511155103

de Assis Souza M., de Castro M. C., de Oliveira A. P., de Almeida A. F., de Almeida T. M., Reis L. C., et al. (2013). Cytokines and NO in American Tegumentary Leishmaniasis Patients: Profiles in Active Disease, After Therapy and in Self-Healed Individuals. *Microb. Pathog.* 57, 27–32. doi: 10.1016/j.micpath.2013.02.004

Diaz N. L., Zerpa O., Ponce L. V., Convit J., Rondon A. J., and Tapia F. J. (2002). Intermediate or Chronic Cutaneous Leishmaniasis: Leukocyte Immunophenotypes and Cytokine Characterisation of the Lesion. *Exp. Dermatol.* 11 (1), 34–41. doi: 10.1034/j.1600-0625.2002.110104.x

Faria D. R., Souza P. E., Duraes F. V., Carvalho E. M., Gollob K. J., Machado P. R., et al. (2009). Recruitment of CD8(+) T Cells Expressing Granzyme A Is Associated With Lesion Progression in Human Cutaneous Leishmaniasis. *Parasite Immunol.* 31 (8), 432–439. doi: 10.1111/j.1365-3024.2009.01125.x

Fernandes J. C. R., Aoki J. I., Maia Acuna S., Zampieri R. A., Markus R. P., Floeter-Winter L. M., et al. (2019). Melatonin and Leishmania Amazonensis Infection Altered miR-294, miR-30e, and Mir-302d Impacting on Tnf, Mcp-1, and Nos2 Expression. *Front. Cell Infect. Microbiol.* 9:60. doi: 10.3389/fcimb.2019.00060

Fraga C. A., Oliveira M. V., Alves L. R., Viana A. G., Sousa A. A., Carvalho S. F., et al. (2012). Immunohistochemical Profile of HIF-1alpha, Vegf-a, VEGFR2 and MMP9 Proteins in Tegumentary Leishmaniasis. *Bras. Dermatol.* 87 (5), 709–713. doi: 10.1590/s0365-05962012000500006

Geraci N. S., Tan J. C., and McDowell M. A. (2015). Characterization of microRNA Expression Profiles in Leishmania-Infected Human Phagocytes. *Parasite Immunol.* 37 (1), 43–51. doi: 10.1111/pim.12156

Gomes-Silva A., de Cassia Bittar R., Dos Santos Nogueira R., Amato V. S., da Silva Mattos M., Oliveira-Neto M. P., et al. (2007). Can Interferon-Gamma and Interleukin-10 Balance Be Associated With Severity of Human Leishmania (Viannia) Braziliensis Infection? *Clin. Exp. Immunol.* 149 (3), 440–444. doi: 10.1111/j.1365-2249.2007.03436.x

Goto H., and Lauletta Lindoso J. A. (2012). Cutaneous and Mucocutaneous Leishmaniasis. *Infect. Dis. Clin. North Am.* 26 (2), 293–307. doi: 10.1016/j.idc.2012.03.001

Guerfali F. Z., Laouini D., Guizani-Tabbane L., Ottones F., Ben-Aissa K., Benkahla A., et al. (2008). Simultaneous Gene Expression Profiling in Human Macrophages Infected With Leishmania Major Parasites Using SAGE. *BMC Genomics* 9, 238. doi: 10.1186/1471-2164-9-238

Guo Z., Shao L., Zheng L., Du Q., Li P., John B., et al. (2012). miRNA-939 Regulates Human Inducible Nitric Oxide Synthase Posttranscriptional Gene Expression in Human Hepatocytes. *Proc. Natl. Acad. Sci. U. S. A.* 109 (15), 5826–5831. doi: 10.1073/pnas.1118118109

Hirschberger S., Hinske L. C., and Kreth S. (2018). MiRNAs: Dynamic Regulators of Immune Cell Functions in Inflammation and Cancer. *Cancer Lett.* 431, 11–21. doi: 10.1016/j.canlet.2018.05.020

Hong S., Chen S., Wang X., Sun D., Yan Z., Tai J., et al. (2018). ATAD2 Silencing Decreases VEGFA Secretion Through Targeting has-miR-520a to Inhibit Angiogenesis in Colorectal Cancer. *Biochem. Cell Biol.* 96 (6), 761–768. doi: 10.1139/bcb-2018-0081

Huang M., Huang X., Jiang B., Zhang P., Guo L., Cui X., et al. (2020). Linc00174-EZH2-ZNF24/Runx1-VEGFA Regulatory Mechanism Modulates Post-Burn Wound Healing. *Mol. Ther. Nucleic Acids* 21, 824–836. doi: 10.1016/j.omtn.2020.07.010

Iwata T. N., Ramirez-Komo J. A., Park H., and Iritani B. M. (2017). Control of B Lymphocyte Development and Functions by the mTOR Signaling Pathways. *Cytokine Growth Factor Rev.* 35, 47–62. doi: 10.1016/j.cytogfr.2017.04.005

Kocyigit A., Keles H., Selek S., Guzel S., Celik H., and Erel O. (2005). Increased DNA Damage and Oxidative Stress in Patients With Cutaneous Leishmaniasis. *Mutat. Res.* 585 (1-2), 71–78. doi: 10.1016/j.mrgentox.2005.04.012

Koo S. J., Fernandez-Montalvan A. E., Badock V., Ott C. J., Holton S. J., von Ahsen O., et al. (2016). ATAD2 Is an Epigenetic Reader of Newly Synthesized Histone Marks During DNA Replication. *Oncotarget* 7 (43), 70323–70335. doi: 10.18632/oncotarget.11855

Kumar A., Vijaykumar S., Dikhit M. R., Abhishek K., Mukherjee R., Sen A., et al. (2020). Differential Regulation of Mirna Profiles of Human Cells Experimentally Infected by Leishmania Donovani Isolated From Indian Visceral Leishmaniasis and Post-Kala-Azar Dermal Leishmaniasis. *Front. Microbiol.* 11, 1716. doi: 10.3389/fmicb.2020.01716

Lago T. S., Silva J. A., Lago E. L., Carvalho E. M., Zanette D. L., and Castellucci L. C. (2018). The miRNA 361-3p, a Regulator of GZMB and TNF Is Associated With Therapeutic Failure and Longer Time Healing of Cutaneous Leishmaniasis Caused by L. (Viannia) Braziliensis. *Front. Immunol.* 9, 2621. doi: 10.3389/fimmu.2018.02621

Landgraf P., Rusu M., Sheridan R., Sewer A., Iovino N., Aravin A., et al. (2007). A Mammalian microRNA Expression Atlas Based on Small RNA Library Sequencing. *Cell* 129 (7), 1401–1414. doi: 10.1016/j.cell.2007.04.040

Lazarchuk P., Hernandez-Villanueva J., Pavlova M. N., Federation A., MacCoss M., and Sidorova J. M. (2020). Mutual Balance of Histone Deacetylases 1 and 2 and the Acetyl Reader ATAD2 Regulates the Level of Acetylation of Histone H4 on Nascent Chromatin of Human Cells. *Mol. Cell Biol.* 40 (9), e00421–19. doi: 10.1128/MCB.00421-19

Lebovic D. I., Chao V. A., Martini J. F., and Taylor R. N. (2001). Il-1beta Induction of RANTES (Regulated Upon Activation, Normal T Cell Expressed and Secreted) Chemokine Gene Expression in Endometriotic Stromal Cells Depends on a Nuclear Factor-Kappab Site in the Proximal Promoter. *J. Clin. Endocrinol. Metab.* 86 (10), 4759–4764. doi: 10.1210/jcem.86.10.7890

Lemaire J., Mkannez G., Guerfali F. Z., Gustin C., Attia H., Sghaier R. M., et al. (2013). MicroRNA Expression Profile in Human Macrophages in Response to Leishmania Major Infection. *PloS Negl. Trop. Dis.* 7 (10), e2478. doi: 10.1371/journal.pntd.0002478

Liang T., Guo L., and Liu C. (2012). Genome-Wide Analysis of mir-548 Gene Family Reveals Evolutionary and Functional Implications. *J. BioMed. Biotechnol.* 2012, 679563. doi: 10.1155/2012/679563

Lima-Junior D. S., Costa D. L., Carregaro V., Cunha L. D., Silva A. L., Mineo T. W., et al. (2013). Inflammasome-Derived IL-1beta Production Induces Nitric Oxide-Mediated Resistance to Leishmania. *Nat. Med.* 19 (7), 909–915. doi: 10.1038/nm.3221

Limon J. J., and Fruman D. A. (2012). Akt and mTOR in B Cell Activation and Differentiation. *Front. Immunol.* 3, 228. doi: 10.3389/fimmu.2012.00228

Machado P. R., Rosa M. E., Costa D., Mignac M., Silva J. S., Schriefer A., et al. (2011). Reappraisal of the Immunopathogenesis of Disseminated Leishmaniasis: *In Situ* and Systemic Immune Response. *Trans. R. Soc. Trop. Med. Hyg.* 105 (8), 438–444. doi: 10.1016/j.trstmh.2011.05.002

Marabita F., de Candia P., Torri A., Tegner J., Abrignani S., and Rossi R. L. (2016). Normalization of Circulating MicroRNA Expression Data Obtained by Quantitative Real-Time RT-PCR. *Brief Bioinform.* 17 (2), 204–212. doi: 10.1093/bib/bbv056

Martinotti S., Patrone M., and Ranzato E. (2015). Emerging Roles for HMGB1 Protein in Immunity, Inflammation, and Cancer. *Immunotarg. Ther.* 4, 101–109. doi: 10.2147/ITT.S58064

Moore K. J., and Matlashewski G. (1994). Intracellular Infection by Leishmania Donovani Inhibits Macrophage Apoptosis. *J. Immunol.* 152 (6), 2930–2937.

Morozumi Y., Boussouar F., Tan M., Chaikuad A., Jamshidikia M., Colak G., et al. (2016). Atad2 is a Generalist Facilitator of Chromatin Dynamics in Embryonic Stem Cells. *J. Mol. Cell Biol.* 8 (4), 349–362. doi: 10.1093/jmcb/mjv060

Muxel S. M., Acuna S. M., Aoki J. I., Zampieri R. A., and Floeter-Winter L. M. (2018). Toll-Like Receptor and Mirna-Let-7e Expression Alter the Inflammatory Response in Leishmania amazonensis-Infected Macrophages. *Front. Immunol.* 9, 2792. doi: 10.3389/fimmu.2018.02792

Muxel S. M., Laranjeira-Silva M. F., Zampieri R. A., and Floeter-Winter L. M. (2017). Leishmania (Leishmania) Amazonensis Induces Macrophage miR-294 and miR-721 Expression and Modulates Infection by Targeting NOS2 and L-arginine Metabolism. *Sci. Rep.* 7, 44141. doi: 10.1038/srep44141

Nunes S., Silva I. B., Ampuero M. R., de Noronha A. L. L., de Souza L. C. L., Correia T. C., et al. (2018). Integrated Analysis Reveals That miR-193b, miR-671, and TREM-1 Correlate With a Good Response to Treatment of Human Localized Cutaneous Leishmaniasis Caused by Leishmania Braziliensis. *Front. Immunol.* 9, 640. doi: 10.3389/fimmu.2018.00640

O'Connell R. M., Rao D. S., and Baltimore D. (2012). microRNA Regulation of Inflammatory Responses. *Annu. Rev. Immunol.* 30, 295–312. doi: 10.1146/annurev-immunol-020711-075013

Ohmori Y., and Hamilton T. A. (1994). IFN-Gamma Selectively Inhibits Lipopolysaccharide-Inducible JE/monocyte Chemoattractant Protein-1 and KC/GRO/Melanoma Growth-Stimulating Activity Gene Expression in Mouse Peritoneal Macrophages. *J. Immunol.* 153 (5), 2204–2212.

Paul S., Ruiz-Manriquez L. M., Serrano-Cano F. I., Estrada-Meza C., Solorio-Diaz K. A., and Srivastava A. (2020). Human microRNAs in Host-Parasite Interaction: A Review. *3 Biotech.* 10 (12), 510. doi: 10.1007/s13205-020-02498-6

Rainer J., Ploner C., Jesacher S., Ploner A., Eduardoff M., Mansha M., et al. (2009). Glucocorticoid-Regulated microRNAs and Mirtrons in Acute Lymphoblastic Leukemia. *Leukemia* 23 (4), 746–752. doi: 10.1038/leu.2008.370

Reis L. C., Ramos-Sanchez E. M., Araujo F. N., Leal A. F., Ozaki C. Y., Sevillano O. R., et al. (2021). Pleiotropic Effect of Hormone Insulin-Like Growth Factor-I in Immune Response and Pathogenesis in Leishmaniases. *J. Immunol. Res*. 2021, 6614475. doi: 10.1155/2021/6614475

Reveneau S., Petrakis T. G., Goldring C. E., Chantome A., and Jeannin J. F. (2012). Oct-1 Cooperates With the TATA Binding Initiation Complex to Control Rapid Transcription of Human Inos. *Cell Mol. Life Sci.* 69 (15), 2609–2619. doi: 10.1007/s00018-012-0939-z

Sarkar A., Ghosh S., Pakrashi S., Roy D., Sen S., and Chatterjee M. (2012). Leishmania Strains Causing Self-Healing Cutaneous Leishmaniasis Have Greater Susceptibility Towards Oxidative Stress. *Free Radic. Res.* 46 (5), 665–673. doi: 10.3109/10715762.2012.668186

Silverman J. M., Clos J., de'Oliveira C. C., Shirvani O., Fang Y., Wang C., et al. (2010). An Exosome-Based Secretion Pathway Is Responsible for Protein Export From Leishmania and Communication With Macrophages. *J. Cell Sci.* 123 (Pt 6), 842–852. doi: 10.1242/jcs.056465

Sohel M. A. (2016). Extracellular/Circulating MicroRNAs: Release Mechanisms, Functions and Challenges. *Achievements Life Sci.* 10, 175–186. doi: 10.1016/j.als.2016.11.007

Song Q., Song J., Wang Q., Ma Y., Sun N., Ma J., et al. (2016). miR-548d-3p/TP53BP2 Axis Regulates the Proliferation and Apoptosis of Breast Cancer Cells. *Cancer Med.* 5 (2), 315–324. doi: 10.1002/cam4.567

Son G. H., Kim Y., Lee J. J., Lee K. Y., Ham H., Song J. E., et al. (2019). MicroRNA-548 Regulates High Mobility Group Box 1 Expression in Patients With Preterm Birth and Chorioamnionitis. *Sci. Rep.* 9 (1), 19746. doi: 10.1038/s41598-019-56327-9

Sotto M. N., Yamashiro-Kanashiro E. H., da Matta V. L., and de Brito T. (1989). Cutaneous Leishmaniasis of the New World: Diagnostic Immunopathology and Antigen Pathways in Skin and Mucosa. *Acta Trop.* 46 (2), 121–130. doi: 10.1016/0001-706x(89)90006-5

Souza M. A., Almeida T. M., Castro M. C., Oliveira-Mendes A. P., Almeida A. F., Oliveira B. C., et al. (2016). American Tegumentary Leishmaniasis: mRNA Expression for Th1 and Treg Mediators Are Predominant in Patients With

Recent Active Disease. *Immunobiology* 221 (2), 253–259. doi: 10.1016/j.imbio.2015.08.009

Souza M. A., Castro M. C., Oliveira A. P., Almeida A. F., Reis L. C., Silva C. J., et al. (2012). American Tegumentary Leishmaniasis: Cytokines and Nitric Oxide in Active Disease and After Clinical Cure, With or Without Chemotherapy. *Scand. J. Immunol.* 76 (2), 175–180. doi: 10.1111/j.1365-3083.2012.02717.x

Souza A. S., Giudice A., Pereira J. M., Guimaraes L. H., de Jesus A. R., de Moura T. R., et al. (2010). Resistance of Leishmania (Viannia) Braziliensis to Nitric Oxide: Correlation With Antimony Therapy and TNF-Alpha Production. *BMC Infect. Dis.* 10, 209. doi: 10.1186/1471-2334-10-209

Teixeira M. J., Fernandes J. D., Teixeira C. R., Andrade B. B., Pompeu M. L., Santana da Silva J., et al. (2005). Distinct Leishmania Braziliensis Isolates Induce Different Paces of Chemokine Expression Patterns. *Infect. Immun.* 73 (2), 1191–1195. doi: 10.1128/IAI.73.2.1191-1195.2005

Tomiotto-Pellissier F., Bortoleti B., Assolini J. P., Goncalves M. D., Carloto A. C. M., Miranda-Sapla M. M., et al. (2018). Macrophage Polarization in Leishmaniasis: Broadening Horizons. *Front. Immunol.* 9, 2529. doi: 10.3389/fimmu.2018.02529

Tsuchiya S., Kobayashi Y., Goto Y., Okumura H., Nakae S., Konno T., et al. (1982). Induction of Maturation in Cultured Human Monocytic Leukemia Cells by a Phorbol Diester. *Cancer Res.* 42 (4), 1530–1536.

Turetz M. L., Machado P. R., Ko A. I., Alves F., Bittencourt A., Almeida R. P., et al. (2002). Disseminated Leishmaniasis: A New and Emerging Form of Leishmaniasis Observed in Northeastern Brazil. *J. Infect. Dis.* 186 (12), 1829–1834. doi: 10.1086/345772

Vieira M. G., Oliveira F., Arruda S., Bittencourt A. L., Barbosa A. A.Jr., Barral-Netto M., et al. (2002). B-Cell Infiltration and Frequency of Cytokine Producing Cells Differ Between Localized and Disseminated Human Cutaneous Leishmaniases. *Mem Inst Oswaldo Cruz* 97 (7), 979–983. doi: 10.1590/s0074-02762002000700009

Vlachos I. S., Zagganas K., Paraskevopoulou M. D., Georgakilas G., Karagkouni D., Vergoulis T., et al. (2015). Diana-miRPath v3.0: Deciphering microRNA Function With Experimental Support. *Nucleic Acids Res.* 43 (W1), W460–W466. doi: 10.1093/nar/gkv403

Wang Y., Zhang P., Liu Y., and Cheng G. (2010). TRAF-Mediated Regulation of Immune and Inflammatory Responses. *Sci. China Life Sci.* 53 (2), 159–168. doi: 10.1007/s11427-010-0050-3

Wang Y., Zheng F., Gao G., Yan S., Zhang L., Wang L., et al. (2018). MiR-548a-3p Regulates Inflammatory Response *Via* TLR4/NF-kappaB Signaling Pathway in Rheumatoid Arthritis. *J. Cell Biochem.* 120 (2), 1133–1140 doi: 10.1002/jcb.26659

Yao Z., Jia X., Megger D. A., Chen J., Liu Y., Li J., et al. (2019). Label-Free Proteomic Analysis of Exosomes Secreted From THP-1-Derived Macrophages Treated With IFN-alpha Identifies Antiviral Proteins Enriched in Exosomes. *J. Proteome Res.* 18 (3), 855–864. doi: 10.1021/acs.jproteome.8b00514

Ye H., Arron J. R., Lamothe B., Cirilli M., Kobayashi T., Shevde N. K., et al. (2002). Distinct Molecular Mechanism for Initiating TRAF6 Signalling. *Nature* 418 (6896), 443–447. doi: 10.1038/nature00888

Yu Z., Zhang W., and Kone B. C. (2002). Signal Transducers and Activators of Transcription 3 (STAT3) Inhibits Transcription of the Inducible Nitric Oxide Synthase Gene by Interacting With Nuclear Factor Kappab. *Biochem. J.* 367 (Pt 1), 97–105. doi: 10.1042/BJ20020588

Zhang Y., Liu D., Chen X., Li J., Li L., Bian Z., et al. (2010). Secreted Monocytic miR-150 Enhances Targeted Endothelial Cell Migration. *Mol. Cell* 39 (1), 133–144. doi: 10.1016/j.molcel.2010.06.010

Conflict of Interest: The authors declare that the research was conducted in the absence of any commercial or financial relationships that could be construed as a potential conflict of interest.

frontiers in Cellular and Infection Microbiology

BRIEF RESEARCH REPORT
published: 01 July 2021
doi: 10.3389/fcimb.2021.700323

A Pilot Randomized Clinical Trial: Oral Miltefosine and Pentavalent Antimonials Associated With Pentoxifylline for the Treatment of American Tegumentary Leishmaniasis

Sofia Sales Martins[1,2*], *Daniel Holanda Barroso*[2,3,4], *Bruna Côrtes Rodrigues*[2,3], *Jorgeth de Oliveira Carneiro da Motta*[2], *Gustavo Subtil Magalhães Freire*[2], *Ledice Inácia de Araújo Pereira*[5], *Patrícia Shu Kurisky*[2,3], *Ciro Martins Gomes*[2,3,4] *and Raimunda Nonata Ribeiro Sampaio*[1,2,3,4]

[1] Pós-Graduação de Ciências da Saúde da Faculdade de Ciências Saúde, Universidade de Brasília, Brasília, Brazil, [2] Hospital Universitário de Brasília, Universidade de Brasília, Brasília, Brazil, [3] Pós-Graduação de Ciências Médicas da Faculdade de Medicina, Universidade de Brasília, Brasília, Brazil, [4] Laboratório de Dermatomicologia da Faculdade de Medicina, Universidade de Brasília, Brasília, Brazil, [5] Departamento de Doenças Infecciosas, Hospital de Doenças Tropicais Dr. Anuar Auad (HDT), Goiânia, Brazil

OPEN ACCESS

Edited by:
Izabel Galhardo Demarchi, Federal University of Santa Catarina, Brazil

Reviewed by:
Sara M. Robledo, University of Antioquia, Colombia
Patricia Quaresma, Federal University of Santa Catarina, Brazil

***Correspondence:**
Sofia Sales Martins
sofiasalesm@gmail.com

Specialty section:
This article was submitted to Parasite and Host, a section of the journal Frontiers in Cellular and Infection Microbiology

Received: 26 April 2021
Accepted: 14 June 2021
Published: 01 July 2021

Citation:
Martins SS, Barroso DH, Rodrigues BC, Motta JOC, Freire GSM, Pereira LIA, Kurisky PS, Gomes CM and Sampaio RNR (2021) A Pilot Randomized Clinical Trial: Oral Miltefosine and Pentavalent Antimonials Associated With Pentoxifylline for the Treatment of American Tegumentary Leishmaniasis. Front. Cell. Infect. Microbiol. 11:700323. doi: 10.3389/fcimb.2021.700323

Introduction: American tegumentary leishmaniasis (ATL), which can present as either cutaneous (CL) or mucosal leishmaniasis (ML), is endemic in South America, and first-line antimonial treatments are known for their wide range of adverse effects (AEs). Growing reports of drug resistance increase the urgency of the need for better treatment options. The objective of this pilot clinical trial was to assess the efficacy of and AEs associated with the oral combination of miltefosine and pentoxifylline based on a *post hoc* analysis.

Methods: A pilot, randomized, open-label clinical trial was performed. The experimental group (M+P) received 50 mg twice a day (BID) miltefosine and 400 mg three times a day (TID) pentoxifylline, and the control group (A+P) received 20 mg Sb+V/kg/day intravenously and 400 mg TID pentoxifylline. Patients with ML received treatment for 28 days, and patients with CL received treatment for 20 days.

Results: Forty-three patients were included: 25 with ML and 18 with CL caused by *L.(V.) braziliensis*. AEs were more frequent in the A+P group (p=0.322), and there was a need for treatment interruption due to severe AEs (p=0.027). Patients with CL had a higher chance of achieving a cure (p=0.042) and a higher risk of AEs (p=0.033). There was no difference in the chance of a cure based on the treatment (p=0.058).

Conclusion: In this pilot randomized clinical trial, M+P treatment and A+P treatment yielded similar cure rates, and the former was associated with a lower risk of AEs. Future studies with more patients and longer follow-up are recommended.

Keywords: pentavalent antimonial, randomized clinical trial, pentoxifylline, miltefosine, cutaneous leishmaniasis, mucosal leishmaniasis, American tegumentary leishmaniasis

INTRODUCTION

Between 2001 and 2017, there were 940.396 new cases of tegumentary leishmaniasis, including both the cutaneous (CL) and mucous (ML) forms, in the Americas, with an annual mean of 55.317 cases. These cases were reported by 17 of the 18 endemic countries on the continent, and 72.6% of the cases were in Brazil. The incidence of ML was 3.78% of all LTA cases in Brazil (Organização Pan-Americana da Saúde, 2019).

Active drug treatment is the main form of disease control, although it does not affect asymptomatic infected individuals. Many drugs have been used to treat leishmaniasis, but first-line therapy with pentavalent antimonials (PAs) has not changed for decades. PAs have been used in the Americas since the 1940s. PAs are known for their wide range of adverse effects (AEs), leading to treatment interruptions, hepatic and cardiac alterations and even death, and the rate of drug resistance is increasing. Other second-line therapies, such as amphotericin and pentamidine, are also injectable and are associated with significant AEs. Currently, cure rates vary from 70 to 90% in patients with CL and from 30% to 91% in those with ML (Chakravarty and Sundar, 2019).

A 40% rate of treatment failure has been reported in patients treated with intravenous PAs alone for infection with *Leishmania (V) braziliensis* (Ventin et al., 2018). Therapeutic failure is becoming increasingly common in Brazil, especially in patients with *L. (V) braziliensis* infections (Ponte-Sucre et al., 2017; Rugani et al., 2018). The underlying mechanisms are not yet clear but seem to be related to parasitological drug resistance and the lack of a host immune response. The current treatment recommended by the Brazilian Health Ministry for LC is 10 to 20 mg SbV/kg/day for 20 days and that for LM is 20 mg SbV/kg/day combined with 400 mg pentoxifylline three times per day for 30 days (Ministério da Saúde, 2017).

In this context, treatments involving a combination of oral drugs are interesting alternatives with the aim of increasing efficacy, reducing AEs and increasing treatment adherence in patients with leishmaniasis (Chakravarty and Sundar, 2019). Combining oral drugs is already a successful treatment strategy for other infectious diseases caused by intracellular microorganisms, such as tuberculosis and leprosy, and is known to reduce drug resistance.

Miltefosine is the first oral drug with efficacy against leishmaniasis, and it has been used since 2002 for the treatment of both visceral (Sundar et al., 2002) and mucocutaneous leishmaniasis. It affects the phospholipid membrane integrity and mitochondrial function of microorganisms (Sundar et al., 2002; Soto et al., 2004; Chrusciak-Talhari et al., 2011; Sampaio et al., 2019). It also has an indirect effect by acting as an immunomodulator against Leishmania, promoting the production of IFN-γ, TNF-α and IL-12 and stimulating phagocytosis and the Th1 pathway (Santarem et al., 2014).

Miltefosine is usually well tolerated, with mild gastric and hepatic AEs; however, it is known to be a teratogenic drug (Dorlo et al., 2012). Unfortunately, there are already reports of resistance to miltefosine when it is used alone for both visceral and tegumentary leishmaniasis. *In vitro*, *L. (V.) braziliensis* had a 68% rate of resistance to monotherapy with miltefosine (Fernández et al., 2014), and one treatment course was sufficient for the development of resistance (Berman, 2008).

Pentoxifylline is a methylxanthine with anti-inflammatory effects that suppresses TNF-α gene transcription, increases nitric oxide production and decreases leukocyte migration and adhesion. It is known to have an adjuvant immunologic effect when associated with pentavalent antimony for the treatment of mucocutaneous leishmaniasis (González et al., 2009; Santarem et al., 2014; Burza et al., 2018). It also has a nephroprotective effect when associated with PAs (Santarem et al., 2014). In C5BL/6 mice infected with *L. (L.) amazonensis*, pentoxifylline combined with antimonials was able to reduce macrophage vacuolization and induce more effective parasite destruction (Santarem et al., 2014).

Considering the urgent need for clinical trials of treatments for ATL (Ponte-Sucre et al., 2017; Pinart et al., 2020), especially neglected ML, the objective of this pilot clinical trial was to assess the efficacy and toxicity of the oral combination of miltefosine and pentoxifylline and the standard treatment, consisting of intravenous PAs and oral pentoxifylline, in an endemic region for *Leishmania (V.) braziliensis*, based on a *post hoc* analysis.

MATERIAL AND METHODS

Population and Case Definition

A pilot, open-label randomized clinical trial (RCT) was performed from August 2015 to August 2020 in two referral centers for leishmaniasis in the central region of Brazil located in the cities Brasília and Goiânia (Universidade de Brasília and Hospital Estadual de Doenças Tropicais Dr. Anuar Auad). The ATL case definition relied on the presence of cutaneous or mucosal symptoms observed on clinical examination and rhinoscopy (cutaneous ulcer, infiltrated cutaneous plaque or nodulus, progressive nasal congestion, rhinorrhea, epistaxis and destructive lesions of the nasal septum, lips and palate) associated with laboratory and epidemiological confirmation as described elsewhere (Gomes et al., 2014). TaqMan-based real-time PCR with specific *L (V.) braziliensis* probes was performed as described elsewhere (Gomes et al., 2017; Bergmann et al., 2019) as a method of diagnosis and species identification.

All eligible ATL patients were consecutively included and underwent video nasoendoscopy and cutaneous, nasal or laryngeal biopsy with histopathological evaluation. We excluded patients under 18 years of age and over 80 years of age, patients with more than 3 cutaneous lesions, patients who received any antileishmanial drugs 6 months prior to the diagnosis, and patients with severe hepatic, renal or cardiac disease, malignant neoplasia, HIV infection or Chagas disease. Due to the potential teratogenic effects of pentavalent antimonials and miltefosine, pregnant or breastfeeding women, women who were not using effective contraceptive methods were also excluded.

Randomization

Patients were automatically randomized in blocks of 4, 6 and 8 using the online randomization system Sealed Envelop™ (Sealed Envelope Ltd. 2011) at a ratio of 1:1 into two groups (M+P or A+P).

Interventions

The experimental group (M+P) received 50 mg twice a day (BID) miltefosine and 400 mg three times a day (TID) pentoxifylline for 28 days if they had confirmed mucosal lesions or for 20 days if they had no evidence of mucosal lesions and only had CL. Patients in the control group (A+P) received 20 mg Sb+V/kg/day up to 1215 mg/day intravenously and 400 mg TID pentoxifylline for 30 days if they had ML or for 20 days if they had CL, according to the treatment recommended by the Brazilian Ministry of Health.

Outcomes

The primary outcome was defined as the cure of leishmaniasis. The occurrence of AEs was considered a secondary outcome. Patients were considered cured if they had complete healing (reepithelization without infiltrations or erythema) of the lesions up to 90 days after the beginning of the treatment. An additional evaluation of the curative effect was performed 180 days after the beginning of the treatment.

Patient Follow-Up

Patients were monitored weekly to identify AEs, which were characterized as clinical, laboratory and electrocardiographic changes that occurred during treatment and had no possible causal relationship with external factors. AEs were classified as mild or severe.

The mild AEs were myalgia, arthralgia, headache, local inflammation, nausea, vomiting, dizziness, asthenia and stomachache. If they developed mild AEs, patients were monitored closely. Severe AEs were hepatic alterations with elevated transaminase levels [>2.5x upper limit of normal (ULN)], renal alterations (creatinine > 1.5x ULN), elevated levels of amylase (>1.5x ULN), anemia (hemoglobin <9.5 g/dL) and cardiac alterations with QTc interval enlargement (QTc>450 ms). In those cases, patients discontinued treatment, which was only reintroduced when the alterations were normalized.

If patients could not complete the proposed drug therapy 75 days after it was initiated due to severe or persistent AEs, they were treated with liposomal amphotericin B (LAB). Patients were followed-up at 30, 60, 90, and 180 days after the beginning of treatment and once a year thereafter.

Statistical Analysis

Bivariate and multivariate Cox regression were used to determine the significant predictors of achieving a cure and the occurrence of AEs, and the model and the associated 95% confidence interval were constructed. Hazzard ratios (HRs) and their respective 95% confidence intervals were calculated. Multicollinearity was evaluated between the independent variables. The cutoff value of the tolerance indicator for the detection of multicollinearity was 0.603. $P < 0.05$ was considered significant. The analyses were conducted using SAS® 9.4 software (SAS Institute Inc., Cary, North Carolina, USA).

This RCT was registered at clinicaltrials.gov under the number CT02530697 and in the Brazilian clinical trials registry under the number RBR-72dv9n. The Brazilian ethics committee approved it in May 2015 under the number CAAE: 40068714.1.1001.5558.

RESULTS

Of the 384 patients with suspected diagnoses of ATL in the pilot RCT period, 43 patients were included and randomized. Twenty-two were assigned to the M+P group and 21 to the A+P group (**Figure 1**). There were 348 patients with a confirmed diagnosis of LC, of whom 18 were included, and there were 43 patients with LM, of whom 25 were included.

Demographic Characteristics

The mean age of all included patients was 51.8 years (ranging from 19 to 79 years), and approximately 67% of the patients were male. The time between the beginning of symptoms and the diagnosis ranged from 1 to 180 months, with a mean of 28 months. Twenty-five patients had ML and 18 had CL. Three patients had received specific treatment for leishmaniasis more than 6 months before being included in this RCT (6.9%). The number of lesions ranged from 1 to 2, but the majority of the patients had only one lesion, with a mean of 1.18. The patients' weight ranged from 48.5 to 88 kg, with a mean of 68.7 kg. Forty-eight percent of all patients had one or more comorbidities, and the most frequent comorbidities were hypertension and diabetes mellitus. When we analyzed only the 25 patients with ML, the mean age was 58 years, and the mean time from symptom onset to diagnosis was 41 months.

There were no significant differences in the clinical and demographic characteristics (sex, weight, number of lesions, time from lesion detection to diagnosis, disease form (LC or LM), previous treatment and comorbidities) between the two groups.

Treatment Duration and Doses

In the intention-to-treat analysis, the treatment duration varied from zero to 54 days (**Table 1**). One of the patients in the M+P group could not start treatment because after randomization, his pharyngeal lesion worsened, and he was not able to swallow the drugs. This patient was then treated with LAB.

Patients in the M+P group had to discontinue treatment for a mean of 0.15 days, as most patients did not interrupt treatment, while in the A+P group, the mean number of days of treatment interruption was 10.86. When we considered the entire duration of the treatment, including interruptions, the mean duration in the M+P group was 22.63 days and that in the A+P group was 37.68 days ($p=0.014$) (**Table 1**). The proportions of patients who needed to discontinue treatment due to AEs were 13.63% in the M+P group and 57.14% in the A+P group ($p = 0.027$) (**Table 1**).

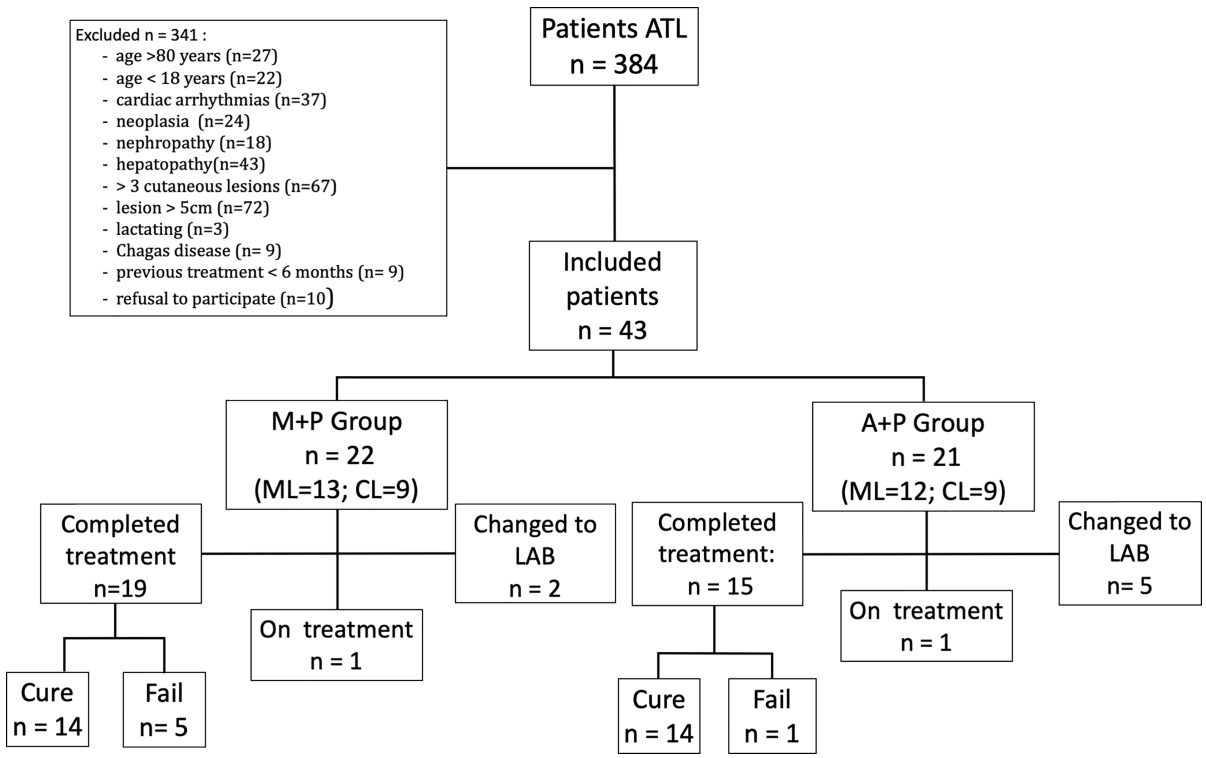

FIGURE 1 | Flow diagram showing eligible patients, randomized patients and cure outcomes.

TABLE 1 | Univariate analysis of treatment outcomes.

	Group		p-value
	M+P (n = 22) Mean (SD)	**A+P (n = 21) Mean (SD)**	
Treatment duration (days)	22.5 (7.35)	26.75(14.89)	0.241
Interruption duration (days)	0.15 (0.67)	10.86 (16.22)	0.258
Total treatment duration (days)	22.63 (7.33)	37.68 (26.42)	0.014
Dosage of Sb5+ (mg/kg/day)	–	17.19 (2.16)	-
Dosage of miltefosine (mg/kg/day)	1.36 (0.35)	–	-
	n (%)	**n (%)**	
Treatment interruption	3 (13.63)	12 (57.14)	0.027
Treatment changed to LAB	2 (9.09)	5 (23.08)	0.229
Complete healing 30 days from the beginning of treatment	6 (27.27)	8 (38.09)	0.452
Cure	14 (69.23)	14 (66.66)	0.196
Adverse effects	11 (50)	19 (90.47)	0.003

Legend M+P, treatment with miltefosine and pentoxifylline; A+ P, treatment with pentavalent antimonial and pentoxifylline; SD, standard deviation; n, number of patients; Sb5+, pentavalent antimonial; LAB, liposomal; B, amphotericin.
We compared treatment duration, dosing and outcomes in the M+P and A+P groups.

The PA dosage varied from 13.96 to 19.91 mg/kg/day, with a mean of 17.19 mg/kg/day. In the M+P group, the daily miltefosine dosage varied from 1.13 mg to 1.79 mg/kg/day, with a mean of 1.36 mg/kg/day (**Table 1**).

Curative Effect

In the univariate analysis of the curative effect 90 days after the beginning of the treatment, there was no difference between the two groups (p = 0.196) (**Table 1**). In the M+P group, 69.23% of the patients were cured; in the A+P group, 66.66% of the patients were cured. In the secondary analysis of the result 180 days after the beginning of treatment, the finding remained the same. Complete healing within 30 days from the beginning of treatment was achieved by 27% of the patients in the M+P group and 38% of the patients in the A+P group (p = 0.452) (**Table 1**).

In multivariate analysis of the curative effect, there were no significant differences between the two groups (HR = 2.44 (CI: 0.97 - 6.14); p = 0.058) based on the adjusted Cox regression model. Patients who had previously undergone antileishmanial treatment more than 6 months before had a higher cure rate (HR = 7.91 (CI: 1.27 – 49.41); p = 0.026), as did patients with only cutaneous lesions (HR = 7.73 (CI: 1.07 – 55.72); p = 0.042). (**Table 2**).

Adverse Effects

In univariate analysis of AEs, 50% of the patients in the M+P group experienced AEs, while 90.47% of the patients in group A+P experienced AEs; the difference was significant (p = 0.003) (**Table 1**). The AEs in the M+P group were as follows, in descending order of frequency: nausea (n = 10), vomiting (n = 8), asthenia (n = 3), stomachache (n = 2), elevated transaminase levels (n =1) and dizziness (n = 1). In the A+P group, the AEs in descending order of frequency were myalgia (n = 12), elevated transaminase levels (n = 7), asthenia (n = 5), renal alterations (n = 3), elevated amylase levels (n = 2), anemia (n = 2), cardiac alterations with QTc interval enlargement (n = 1) and stomachache (n = 1). Only one patient had severe AEs in the M+P group, while 12 patients in the A+P group had at least one severe AE.

In multivariate analysis of the risk of adverse effects with the Cox regression model, patients treated with A+P had a higher risk of adverse effects (HR 3.22 (CI: 1.10 – 9.40); p = 0.032) than those treated with M+P. Additionally, patients with only CL had a higher risk of adverse effects (HR = 10.32 (CI: 1.21 - 88.20); p = 0.033) than those with ML, as did patients who had previously received treatment with antileishmanial drugs (HR = 15.20 (CI: 1.97 – 117.07); p = 0.009) (**Table 2**).

DISCUSSION

Current Treatments and Supporting Evidence

Leishmaniasis, despite its increasing incidence, is included in the WHO list of neglected tropical diseases. Cochrane database systematic reviews and recent updates about interventions and treatments for both Old World and New World leishmaniasis have shown that the level of evidence in most publications was low or moderate due to methodological shortcomings that made it impossible to draw reliable conclusions (González et al., 2008; González et al., 2009; Heras-Mosteiro et al., 2017; Pinart et al., 2020). The most recent Cochrane review of New World leishmaniasis included 75 studies and concluded that intravenous meglumine antimoniate and oral miltefosine yield the best cure rates and are currently the most highly recommended treatments (Pinart et al., 2020). The association of pentavalent antimonials with drugs with immunomodulatory effects has already been tested with encouraging results (Ventin et al., 2018). It seems that penthoxyfiline reduces vacuolation of macrophages, making active drugs more effective in achieving clinical cure (de Sá Oliveira et al., 2000).

To achieve more robust evidence, it is important to standardize clinical studies about ATL, as proposed in a recent expert consensus (Olliaro et al., 2018). Harmonizing the criteria used to identify patients and to measure treatment effects can

TABLE 2 | Multivariate analysis results showing hazard ratios for cure and adverse effects in patients treated with miltefosine and pentoxifylline and in patients treated with pentavalent antimonial and pentoxifylline.

Cure	**Crude Hazard Ratio**		**Adjusted Hazard Ratio**	
	PR (CI 95%)	**p-value**	**RR (CI 95%)**	**p-value**
Specific previous treatment		0.5158		0.0269
No	1	–	1	–
Yes	1.63 (0.37; 7.08)	0.5158	7.91 (1.27; 49.41)	0.0269
Clinical presentation		0.0161		0.0425
Mucosal	1	–	1	–
Cutaneous	3.27 (1.25; 8.58)	0.0161	7.73 (1.07; 55.72)	0.0425
Treatment Group		0.0949		0.0589
M + P	1	–	1	–
A + P	1.99 (0.89; 4.44)	0.0949	2.44 (0.97; 6.14)	0.0589
Adverse effects	**Crude Hazard Ratio**		**Adjusted Hazard Ratio**	
Specific previous treatment		0.4608		0.0090
No	1	–	1	–
Yes	1.74 (0.40; 7.60)	0.4608	15.20 (1.97; 117.07)	0.0090
Clinical presentation		0.0029		0.0330
Mucosal	1	–	1	–
Cutaneous	5.10 (1.74; 14.93)	0.0029	10.32 (1.21; 88.20)	0.0330
Treatment Group		0.0379		0.0322
M + P	1	–	1	–
A + P	2.53 (1.05; 6.08)	0.0379	3.22 (1.10; 9.40)	0.0322

The influence of relevant variables was also included.

help provide more convincing evidence of treatment efficacy (Olliaro et al., 2018). In this RCT, recommendations were followed concerning the diagnostic parameters and cure criteria.

Oral Combination Treatment

New antileishmanial drugs are rarely developed, and treatment failure due to drug resistance and host immune response is a growing concern in endemic regions (Ponte-Sucre et al., 2017). ATL, especially ML, needs to be addressed in well-designed, robust RCTs (González et al., 2008; González et al., 2009; Reveiz et al., 2013; Heras-Mosteiro et al., 2017; Carvalho et al., 2018; Pinart et al., 2020). Injectable PAs have been used since the 1940s to treat ATL and are currently the recommended first-line treatments in Brazil (Ministério da Saúde, 2017). Treatment with PAs requires daily intravenous or intramuscular injections for 20 to 30 days in areas with a high risk of ML, which means that patients have to go every day during the treatment period to a healthcare facility to receive the medication, which can impose additional burdens on the healthcare system and the patient (Burza et al., 2018; Chakravarty and Sundar, 2019; Carvalho et al., 2021).

In 2021, the estimated cost of treating patients with ML in Brazil with PAs and pentoxifylline for 30 days was US$167.66, while the cost of treatment with 150 mg/day miltefosine for 28 days was US$259.92 (Carvalho et al., 2021). However, in that cost evaluation, the eventual expenses arising from the occurrence of AEs, treatment interruptions and treatment failure with the subsequent need for other treatments were not considered, and these expenses can be relatively higher with PAs. It is known that treatment with PAs can lead to severe AEs, such as cardiac arrythmias, pancreatitis, acute renal failure, and hepatic toxicity (Chakravarty and Sundar, 2019). In addition, in that cost evaluation, the miltefosine dosage was higher than the one we propose, and the combination with pentoxifylline was not considered, which would affect the cost.

There are still few published data on the use of miltefosine for the treatment of ATL, and combined treatment with miltefosine and oral pentoxifylline in mice yielded encouraging results, with a greater reduction in viable Leishmania than achieved with miltefosine alone (Santarem et al., 2014). The idea of combining treatments to reduce AEs, increase cure rates, and reduce drug resistance is promising (Santarem et al., 2014). The possibility of using only oral drugs has the benefit of facilitating drug administration and increasing treatment adherence (Carvalho et al., 2021). As the real effect of combined treatment with miltefosine and pentoxifylline is unknown and no data have been published, we relied on a *post hoc* analysis, effect sizes and confidence intervals to assess the feasibility of future trials.

This pilot trial based on a *post hoc* analysis reflects the reported epidemiology of ATL, with a male predominance and an older age of patients with ML than of those with CL. Additionally, patients with ML have a longer delay in treatment and diagnosis than those with CL, which is characterized by visible lesions. The M+P and A+P groups were comparable, with no significant differences in demographic and epidemiological characteristics between the groups, indicating that the randomization was successful.

The treatment duration was considerably longer in the A+P group due to the higher rate of treatment interruption. These interruptions were necessary because of AEs, especially elevated levels of hepatic markers, that were significantly more frequent in the A+P group. Some of these AEs led to the need for permanent treatment suspension and treatment with LAB. This reveals the potential risks associated with this treatment (Chakravarty and Sundar, 2019).

Curative Effect

The miltefosine dosage used in this trial was fixed at 100 mg daily, and it ranged between 1.13 mg and 1.79 mg/kg/day, which is lower than the initial dosage described as monotherapy of 2.5 mg/kg/day (Sundar et al., 2002; Sindermann et al., 2004; Soto et al., 2004; Machado et al., 2010; Chrusciak-Talhari et al., 2011) but is compatible with a more recently published dosage that yielded good results (Sampaio et al., 2019). The dosage of APs was the previously described standard and ranged from 13.96 to 19.91 mg Sb5+/kg/day.

There was no significant difference in the cure rate 90 days after the start of treatment, indicating that the proposed combination oral treatment is effective. These results were maintained 180 days after the start of treatment, indicating that the curative effect persists. There was no significant difference in the cure rate 30 days after the start of treatment, indicating that there was no difference in the speed of healing between the two evaluated treatments.

ML is more severe and difficult to treat than CL (Burza et al., 2018; Chakravarty and Sundar, 2019; Sampaio et al., 2019); therefore, it is expected that patients with CL would have a higher cure rate, even after a shorter duration of treatment (**Figure 2**). Indeed, the multivariate analysis showed that patients with cutaneous lesions had a higher cure rate in both groups. *L. (V.) braziliensis* is the main causative agent of leishmaniasis in the Americas and the pathogen most often related to ML; therefore, in areas in which this pathogen is endemic, ML should always be suspected.

Patients who had previously received antileishmanial treatment more than 6 months before entering the trial also had a higher chance of achieving a cure, possibly because previous treatment may have triggered the host immune system, leading to a better response to subsequent treatment. Another possible explanation for this result is a residual effect of previous treatment with PAs.

Adverse Effects Analysis

The incidence of AEs was significantly higher in the A+P group ($p = 0.032$ in the multivariate analysis and $p = 0.003$ in the univariate analysis), and the most frequent AEs in this group were intense myalgia and elevated hepatic transaminase levels. The most frequent AEs in patients in the M+P group were nausea and vomiting, which usually improved after a few days, allowing the patients to complete treatment and indicating that oral treatment was well tolerated (Machado et al., 2010). In the M+P group, most of the AEs were mild (nausea and vomiting), and no patient in this group had cardiac, renal or amylase alterations, while more than half of the patients in the A+P group had at least one severe AE. Only one patient had a severe AE in the M+P group (transaminase level elevation),

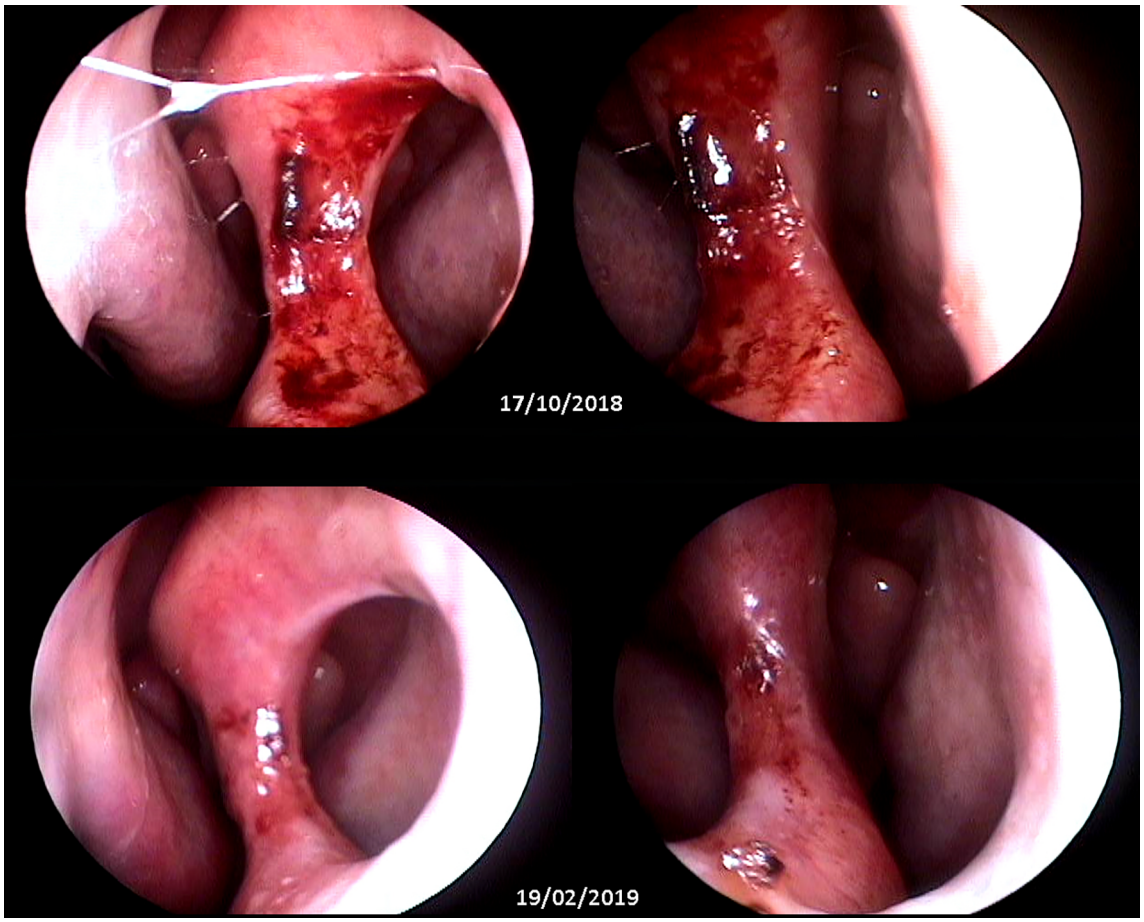

FIGURE 2 | Top: wide septal perforation with infiltrated borders and granulomatous ulcerated aspect (pretreatment). Bottom: septal perforation with smooth borders without ulceration and with cicatricial aspect (90 days after treatment). Images obtained with nasofibroscopy and provided by Dr. Gustavo Subtil.

while 12 patients in the A+P group had severe AEs, indicating a difference in the severity of the AEs associated with the treatment regimens.

Although the mean number of days of treatment interruption was not significantly different between groups, the mean interruption duration in the M + P group was below 1 day, representing a clinically significant difference once most patients in this group did not interrupt treatment. When analyzing frequency, more patients had to interrupt treatment due to AEs in the A+P group (57% x 14%), and more patients could not finish treatment due to AEs in the A+P group (23% x 9%). Those patients were treated with intravenous LAB. Among the patients who could complete treatment, the duration of treatment was shorter in the M+P group (20-28 days *vs.* 20-94 days).

The independent characteristics that were associated with a higher risk of AEs were CL instead of ML and prior antileishmanial treatment. When we analyzed the type of AEs in the CL and ML groups, we found that in those with CL, most of the AEs were mild, such as nausea, vomiting and myalgia, while in the ML group, the AEs were more severe, such as hepatic and renal toxicity. This difference may not be related to the actual severity of the AEs and may instead reflect a reporting bias, since the patients with ML had more severe symptoms at baseline, making them less likely to report symptoms of AEs than those with CL. The increase in the occurrence of AEs associated with previous antileishmanial treatment may be due to residual toxicity from previous treatments, especially with PAs, which persist in the human body.

Limitations

This pilot study was conducted in two referral centers for the diagnosis and treatment of LTA, which may have resulted in selection bias. Additionally, it was an open-label RCT in which both the patients and the doctors knew which medication was being used. This lack of blinding could have also led to bias. Only the statistical analysis was blinded. A convenience sample was adopted due to the limitations on the availability of miltefosine in the country. Although reduced sample sizes are frequently found in studies targeting mucous leishmaniasis because of its relative rarity, we must reinforce that treatment comparison in the multivariate analysis was followed by considerably narrow confidence intervals, enhancing confidence in the present results.

Final Considerations

This pilot, open-label RCT with 43 ATL patients showed that the oral combination of miltefosine and pentoxifylline has a cure rate equivalent to that of traditional intravenous A+P in this population, with the additional benefit of fewer AEs. Further studies with more patients and a longer follow-up duration are needed to evaluate this promising oral treatment.

DATA AVAILABILITY STATEMENT

The raw data supporting the conclusions of this article will be made available by the authors, without undue reservation.

ETHICS STATEMENT

The studies involving human participants were reviewed and approved by Brazilian ethics committee - Comitê de Ética em Pesquisa da Faculdade de Medicina da Universidade de Brasília CAAE: 40068714.1.1001.5558. The patients/participants provided their written informed consent to participate in this study.

AUTHOR CONTRIBUTIONS

SM: conducting the clinical trial, including and following up patients, gathering and analyzing data, drafting, and refining the manuscript. DB: performing mucosal clinical examination, supervising, and executing molecular examinations. BR: selecting and including patients, gathering clinical data, and performing the literature review. JM and PK: supervising patients' diagnosis and inclusion. GF: performing all nasofibroscopy exams and analyzing and interpreting mucosal images. LP: executing the study arm in the Hospital Estadual de Doenças Tropicais Dr. Anuar Auad. CG: co-coordinating the trial design and methodology, supervising parasitological and molecular diagnoses, and critically supervising manuscript writing. RS: coordinating the study, conceiving of and designing the study, analyzing and interpreting the data, supervising the manuscript writing, reviewing the manuscript, performing the final review of the article, and acting as the beneficiary of the main financial support. All authors contributed to the article and approved the submitted version.

FUNDING

Received funding from: Fundação de Apoio a Pesquisa do Distrito Federal (FAP- DF) no Edital n° 03/2016; Conselho Nacional de Desenvolvimento Científico e Tecnológico (CNPq) process 309439/2018-3 and CNPq process 307358/2017-8 researcher scolarship; and Fundação de Apoio a Pesquisa em Dermatologia (FUNADERM) de 2016.

ACKNOWLEDGMENTS

We would like to thank the dermatology interns, medical and administrative staff of our leishmaniasis clinic and the pathology unit staff for their support in the clinical trial.

REFERENCES

Bergmann, J. O., de Castro Moreira Dos Santos Júnior, A., Santos, L. S., Silva, V. M., Pompeu, C. B., Arabi, A. Y. M., et al. (2019). Accuracy of a TaqMan-based Real-Time Polymerase Chain Reaction Combined to a Novy-MacNeal-Nicolle Medium Culture for the Diagnosis of American Tegumentary Leishmaniasis. *J. Eur. Acad. Dermatol. Venereol* 33 (5), e188–e190. doi: 10.1111/jdv.15440

Berman, J. J. (2008). Treatment of Leishmaniasis With Miltefosine: 2008 Status. *Expert Opin. Drug Metab. Toxicol.* 4 (9), 1209–1216. doi: 10.1517/17425255.4.9.1209

Burza, S., Croft, S. L., and Boelaert, M. (2018). Leishmaniasis. *Lancet* 392 (10151), 951–970. doi: 10.1016/S0140-6736(18)31204-2

Carvalho, J. P., Assis, T. M., Simões, T. C., Simões, T. C., and Cota, G. (2021). Estimating Direct Costs of the Treatment for Mucosal Leishmaniasis in Brazil. *Rev. Soc. Bras. Med. Trop.* 54, e04542020. doi: 10.1590/0037-8682-0454-2020

Carvalho, E. M., Llanos-Cuentas, A., and Romero, G. A. S. (2018). Mucosal Leishmaniasis: Urgent Need for More Research. *Rev. Soc. Bras. Med. Trop.* 51 (1), 120–121. doi: 10.1590/0037-8682-0463-2017

Chakravarty, J., and Sundar, S. (2019). Current and Emerging Medications for the Treatment of Leishmaniasis. *Expert Opin. Pharmacother* 20 (10), 1251–1265. doi: 10.1080/14656566.2019.1609940

Chrusciak-Talhari, A., Dietze, R., Talhari, S., Chrusciak Talhari, C., da Silva, R. M., Gadelha Yamashita, E. P., et al. (2011). Randomized Controlled Clinical Trial to Access Efficacy and Safety of Miltefosine in the Treatment of Cutaneous Leishmaniasis Caused by Leishmania (Viannia) Guyanensis in Manaus, Brazil. *Am. J. Trop. Med. Hygiene* 84 (2), 255–260. doi: 10.4269/ajtmh.2011.10-0155

de Sá Oliveira, T., Capp Neto, M., Martins, B. J., Rodrigues, H. A., Antonino, R. M., and Magalhães, A. V. (2000). Action of Pentoxifylline on Experimental Cutaneous Leishmaniasis Due to Leishmania (Leishmania) Amazonensis. *Mem Inst Oswaldo Cruz* 95 (4), 477–482. doi: 10.1590/S0074-02762000000400006

Dorlo, T. P. C., Balasegaram, M., Beijnen, J. H., and de Vries, P. J. (2012). Miltefosine: A Review of its Pharmacology and Therapeutic Efficacy in the Treatment of Leishmaniasis. *J. Antimicrobial Chemother.* 67 (11), 2576–2597. doi: 10.1093/jac/dks275

Fernández, O. L., Diaz-Toro, Y., Ovalle, C., Valderrama, L., Muvdi, S., Rodríguez, I., et al. (2014). Miltefosine and Antimonial Drug Susceptibility of Leishmania Viannia Species and Populations in Regions of High Transmission in Colombia. *PloS Negl. Trop. Dis.* 8 (5), e2871–e2811. doi: 10.1371/journal.pntd.0002871

Gomes, C. M., Cesetti, M. V., de Paula, N. A., Vernal, S., Gupta, G., Sampaio, R. N. R., et al. (2017). Field Validation of SYBR Green- and TaqMan-Based Real-Time PCR Using Biopsy and Swab Samples To Diagnose American Tegumentary Leishmaniasis in an Area Where Leishmania (Viannia) Braziliensis is Endemic. *J. Clin. Microbiol.* 55 (2), 526–534. doi: 10.1128/JCM.01954-16

Gomes, C. M., de Paula, N. A., de Morais, O. O., Soares, K. A., Roselino, A. M., and Sampaio, R. N. R. (2014). Complementary Exams in the Diagnosis of American Tegumentary Leishmaniasis. *Bras. Dermatol.* 89 (5), 701–709. 2nd ed. Sociedade Brasileira de Dermatologia;. doi: 10.1590/abd1806-4841.20142389

González, U., Pinart, M., Rengifo-Pardo, M., Macaya, A., Alvar, J., and Tweed, J. A. (2009). Interventions for American Cutaneous and Mucocutaneous Leishmaniasis. *Cochrane Database Syst. Rev.* 2, CD004834. doi: 10.1002/14651858.CD004834.pub2

González, U., Pinart, M., Reveiz, L., and Alvar, J. (2008). Interventions for Old World Cutaneous Leishmaniasis. *Cochrane Database Syst. Rev.* 4, CD004834. doi: 10.1002/14651858.CD005067.pub3

Heras-Mosteiro, J., Monge-Maillo, B., Pinart, M., Lopez Pereira, P., Garcia-Carrasco, E., Campuzano Cuadrado, P., et al. (2017). Interventions for Old World Cutaneous Leishmaniasis. *Cochrane Database Syst. Rev.* 12 (12), CD005067. doi: 10.1002/14651858.CD005067.pub5

Machado, P. R., Ampuero, J., Guimaraes, L. H., Villasboas, L., Rocha, A. T., Schriefer, A., et al. (2010). Miltefosine in the Treatment of Cutaneous Leishmaniasis Caused by Leishmania Braziliensis in Brazil: A Randomized and Controlled Trial. *PloS Negl. Trop. Dis.* 4 (12), e912–e916. doi: 10.1371/journal.pntd.0000912

Ministério da Saúde. (2017). Brasil. Ministério Da Saúde. Secretaria de Vigilância em Saúde. Departamento de Vigilância das Doenças Transmissíveis. Manual de vigilância da leishmaniose tegumentar [recurso eletrônico] / Ministério da Saúde, Secretaria de Vigilância em Saúde, Departamento de Vigilância das Doenças Transmissíveis: il. Edição eletrônica da 2ª edição do livro: *Manual de Vigilância da Leishmaniose Tegumentar Americana*, atualizado. (Brasília: Ministério da Saúde), 189 p.

Olliaro, P., Grogl, M., Boni, M., Carvalho, E. M., Chebli, H., Cisse, M., et al. (2018). Harmonized Clinical Trial Methodologies for Localized Cutaneous Leishmaniasis and Potential for Extensive Network With Capacities for Clinical Evaluation. *PloS Negl. Trop. Dis. Public Library Sci* 12 (1), e0006141. doi: 10.1371/journal.pntd.0006141

Organização Pan-Americana da Saúde (2019). *Leishmanioses: Informe Epidemiológico Nas Américas* (Washington, D.C: OPAS). Available at: http://iris.paho.org/xmlui/handle/123456789/50505. Disponível em: incluir.

Pinart, M., Rueda, J.-R., Romero, G. A., Pinzón-Flórez, C. E., Osorio-Arango, K., Silveira Maia-Elkhoury, A. N., et al. (2020). Interventions for American Cutaneous and Mucocutaneous Leishmaniasis. *Cochrane Database Syst. Rev.* 8 (8), CD004834. doi: 10.1002/14651858.CD004834.pub3

Ponte-Sucre, A., Gamarro, F., Dujardin, J.-C., Barrett, M. P., López-Vélez, R., García-Hernández, R., et al. (2017). Drug Resistance and Treatment Failure in Leishmaniasis: A 21st Century Challenge. *PLoS Negl. Trop. Dis.* 11 (12), e0006052–24. doi: 10.1371/journal.pntd.0006052

Reveiz, L., Maia-Elkhoury, A. N. S., Nicholls, R. S., Sierra Romero, G. A., and Yadon, Z. E. (2013). Interventions for American Cutaneous and Mucocutaneous Leishmaniasis: A Systematic Review Update. *PLoS One* 8 (4), e61843–e61814. doi: 10.1371/journal.pone.0061843

Rugani, J. N., Quaresma, P. F., Gontijo, C. F., Soares, R. P., and Monte-Neto, R. L. (2018). Intraspecies Susceptibility of Leishmania (Viannia) Braziliensis to Antileishmanial Drugs: Antimony Resistance in Human Isolates From Atypical Lesions. *Biomed. Pharmacother.* 108, 1170–1180. doi: 10.1016/j.biopha.2018.09.149

Sampaio, R. N. R., Silva, J. S. F. E., de, P. C. D. R., Porto, C., Motta J de, O. C. D., Pereira LI de, A., et al. (2019). A Randomized, Open-Label Clinical Trial Comparing the Long-Term Effects of Miltefosine and Meglumine Antimoniate for Mucosal Leishmaniasis. *Rev. Soc. Bras. Med. Trop. SBMT* 52 (5), 701–708. doi: 10.1590/0037-8682-0292-2018

Santarem, A. A. A., Greggianin, G. F., Debastiani, R. G., Ribeiro, J. B. P., Polli, D. A., and Sampaio, R. N. R. (2014). Effectiveness of Miltefosine-Pentoxifylline Compared to Miltefosine in the Treatment of Cutaneous Leishmaniasis in C57Bl/6 Mice. *Rev. Soc. Bras. Med. Trop. SBMT* 47 (4), 517–520. doi: 10.1590/0037-8682-0202-2013

Sindermann, H., Croft, S. L., Engel, K. R., Bommer, W., Eibl, H. J., Unger, C., et al. (2004). Miltefosine (Impavido): The First Oral Treatment Against Leishmaniasis. *Med. Microbiol. Immunol.* 193 (4), 173–180. doi: 10.1007/s00430-003-0201-2

Soto, J., Arana, B. A., Toledo, J., Rizzo, N., Vega, J. C., Diaz, A., et al. (2004). Miltefosine for New World Cutaneous Leishmaniasis. *Clin. Infect. Dis.* 38 (9), 1266–1272. doi: 10.1086/383321

Sundar, S., Jha, T. K., Thakur, C. P., Engel, J., Sindermann, H., Fischer, C., et al. (2002). Oral Miltefosine for Indian Visceral Leishmaniasis. *N. Engl. J. Med.* 347 (22), 1739–1746. doi: 10.1056/NEJMoa021556

Ventin, F., Cincurá, C., and Machado, P. R. L. (2018). Safety and Efficacy of Miltefosine Monotherapy and Pentoxifylline Associated With Pentavalent Antimony in Treating Mucosal Leishmaniasis. *Expert Rev. Anti-infective Ther.* 0 (0), 1–26. doi: 10.1080/14787210.2018.1436967

Conflict of Interest: The authors declare that the research was conducted in the absence of any commercial or financial relationships that could be construed as a potential conflict of interest.

frontiers in Cellular and Infection Microbiology

ORIGINAL RESEARCH
published: 14 July 2021
doi: 10.3389/fcimb.2021.687499

A New Target Organ of *Leishmania (Viannia) braziliensis* Chronic Infection: The Intestine

Amanda Gubert Alves dos Santos[1], *Maria Gabriela Lima da Silva*[1], *Erick Lincoln Carneiro*[2], *Lainy Leiny de Lima*[3], *Andrea Claudia Bekner Silva Fernandes*[2], *Thaís Gomes Verzignassi Silveira*[2], *Debora de Mello Gonçales Sant'Ana*[1,3] *and Gessilda de Alcantara Nogueira-Melo*[1,2*]

[1] Biosciences and Physiopathology Program, Universidade Estadual de Maringá, Maringá, Brazil, [2] Department of Clinical Analysis and Biomedicine, Universidade Estadual de Maringá, Maringá, Brazil, [3] Department of Morphological Sciences, Universidade Estadual de Maringá, Maringá, Brazil

OPEN ACCESS

Edited by:
Wander Pavanelli, State University of Londrina, Brazil

Reviewed by:
Saikat Majumder, University of Pittsburgh, United States
Michael Lewis, University of London, United Kingdom

***Correspondence:**
Gessilda de Alcantara Nogueira-Melo
ganmelo2@uem.br

Specialty section:
This article was submitted to Parasite and Host, a section of the journal Frontiers in Cellular and Infection Microbiology

Received: *29 March 2021*
Accepted: *22 June 2021*
Published: *14 July 2021*

Citation:
Santos AGA, da Silva MGL, Carneiro EL, de Lima LL, Fernandes ACBS, Silveira TGV, Sant'Ana DMG and Nogueira-Melo GA (2021) A New Target Organ of Leishmania (Viannia) braziliensis Chronic Infection: The Intestine. Front. Cell. Infect. Microbiol. 11:687499. doi: 10.3389/fcimb.2021.687499

Leishmania (Viannia) braziliensis is one of the main causes of cutaneous leishmaniasis in the Americas. This species presents genetic polymorphism that can cause destructive lesions in oral, nasal, and oropharyngeal tracts. In a previous study, the parasite caused several histopathological changes to hamster ileums. Our study evaluates immune response components, morphological changes, and effects on neurons in the ileums of hamsters infected by three different strains of *L. (V.) braziliensis* in two infection periods. For the experiment, we separated hamsters into four groups: a control group and three infected groups. Infected hamsters were euthanized 90- or 120-days post infection. We used three strains of *L. (V.) braziliensis*: the reference MHOM/BR/1975/M2903 and two strains isolated from patients who had different responses to Glucantime® treatment (MHOM/BR/2003/2314 and MHOM/BR/2000/1655). After laparotomy, ileums were collected for histological processing, biochemical analysis, and evaluation of neurons in the myenteric and submucosal plexuses of the enteric nervous system (ENS). The results demonstrated the increase of blood leukocytes after the infection. Optical microscopy analysis showed histopathological changes with inflammatory infiltrates, edemas, ganglionitis, and *Leishmania* amastigotes in the ileums of infected hamsters. We observed changes in the organ histoarchitecture of infected hamsters when compared to control groups, such as thicker muscular and submucosa layers, deeper and wider crypts, and taller and broader villi. The number of intraepithelial lymphocytes and TGF-β-immunoreactive cells increased in all infected groups when compared to the control groups. Mast cells increased with longer infection periods. The infection also caused remodeling of intestinal collagen and morphometry of myenteric and submucosal plexus neurons; but this effect was dependent on infection duration. Our results show that *L. (V.) braziliensis* infection caused time-dependent alterations in hamster ileums. This was demonstrated by the reduction of inflammatory cells and the increase of tissue regeneration factors at 120 days of infection. The infected groups demonstrated

different profiles in organ histoarchitecture, migration of immune cells, and morphometry of ENS neurons. These findings suggest that the small intestine (or at least the ileum) is a target organ for *L. (V.) braziliensis* infection, as the infection caused changes that were dependent on duration and strain.

Keywords: leishmaniasis, small intestine, inflammation, enteric nervous system, TGF-beta

INTRODUCTION

Leishmania (Viannia) braziliensis is one of the main species that causes cutaneous and mucocutaneous leishmaniasis in the Americas (Patino et al., 2020). In 2018, the World Health Organization reported 253,435 new cases of cutaneous leishmaniasis. More than 46,000 of these cases were in the Americas (World Health Organization, 2020); 84% of these cases occurred in Brazil (Pan American Health Organization, 2019), that is considered a "high burden country" for leishmaniasis (World Health Organization, 2020). The disease primarily affects poor segments of the population and results in negative social and economic impacts (Ministério da Saúde, 2017).

The diversity of clinical forms of leishmaniasis caused by *L. (V.) braziliensis* and disease severity are related to the immune system (Fernandes et al., 2016), genetic factors, the clinical condition of the host (Quaresma et al., 2018), and the inoculum (Ribeiro-Romão et al., 2014) and strain of the parasite (Vieira et al., 2019); this species presents high levels of genetic polymorphism (Patino et al., 2020). Different strains found in the same region can cause different clinical forms (Guimarães et al., 2016; Quaresma et al., 2018; Rugani et al., 2018) and therapeutic responses (Fernandes et al., 2016; Gagini et al., 2017), even in the same patient (Hoyos et al., 2019). Lesions are destructive and principally affect the skin and mucus membranes in the oral, nasal, and oropharyngeal tracts (Ministério da Saúde, 2017; Conceição-Silva and Morgado, 2019). Furthermore, studies have reported the occurrence of lesions in the eye (Cruz et al., 2017) and larynx (Silva et al., 2017). The DNA of the parasite has also been detected in bone marrow of immunocompromised patients (Gontijo et al., 2002; Silva et al., 2002).

Studies have reported the presence of amastigotes of the parasite in spleens, lymph nodes (Almeida et al., 1996; Gomes-Silva et al., 2013; Ribeiro-Romão et al., 2014), and livers (Barral et al., 1996) of animals infected with *L. (V.) braziliensis*. In chronically-infected hamsters, our research group detected the DNA of the parasite in ileums and mesenteric lymph nodes, amastigotes in the ileums, and alterations to intestinal architecture (Santos et al., 2018b). Hamsters are good models for *L. (V.) braziliensis* infection research, as they develop lesions (De Oliveira et al., 2004; Gomes-Silva et al., 2013), clinical and histopathological manifestations (Almeida et al., 1996; Gomes-Silva et al., 2013), and immune responses (Ribeiro-Romão et al., 2014) that are similar to those observed in human leishmaniasis. With hamsters, the parasites can migrate to the viscera or other skin sites, where the parasites replicate (Almeida et al., 1996).

The effect of *Leishmania* infection in the gastrointestinal tract is the topic of studies that evaluated different segments of the intestine of dogs (Figueiredo et al., 2014; Silva et al., 2016; Silva et al., 2018) and rodents (Souza et al., 2019; Lewis et al., 2020; Passos et al., 2020) with visceral leishmaniasis (VL). In human VL, the presence of amastigote forms in intestinal tissues may be related to episodes of diarrhea (Baba et al., 2006; Soria López et al., 2016; Raina et al., 2017) or not (Chattopadhyay et al., 2020). The findings have reported higher villi and moderate inflammatory infiltrate composed mainly of mononuclear cells in the lamina propria of the duodenum (Chattopadhyay et al., 2020) and mild ulcers in the colon (Baba et al., 2006).

The intestine is the largest immune organ in mammals; it helps to maintain the equilibrium of the organism (Chassaing et al., 2014). The ileum is the final segment of the small intestine and plays an important role in its immunity. The ileum has more Peyer patches (Mowat and Agace, 2014), the highest concentration of Paneth cells (Santaolalla et al., 2011; Mowat and Agace, 2014), lymphoid aggregates (Mowat and Agace, 2014), which may be related to the highest number of bacteria in this portion of the intestine (Santaolalla et al., 2011). Specialized cells (e.g., enterocytes, goblet cells, Paneth cells, and enteroendocrines) in its epithelium participate in the innate immune response. These cells secrete substances with various functions, such as glycoproteins, antimicrobial substances, cytokines, and hormones. The lamina propria has a high quantity and variety of immune cells, such as mast cells, macrophages, dendritic cells, and lymphocytes, among others (Abbas et al., 2017). Epithelial cells and the innate and adaptive immune systems interact with the ENS to promote immune tolerance, defense, and organ regeneration (Jacobson et al., 2021).

The ENS sends and receives nerve impulses from other organs and is responsible for digestion, motility (Yoo and Mazmanian, 2017), and maintenance of intestinal homeostasis (Drokhlyansky et al., 2020). Studies have shown that the intestine is affected by *L. (V.) braziliensis* infection (Santos et al., 2018a; Santos et al., 2018b) thus, evaluating the effects of the infection from different parasite strains on histoarchitecture and immune response of the organ and ENS are essential for the understanding of the complex *Leishmania*-host relationship. As in previous studies we detected changes in the ileum (Santos et al., 2018a; Santos et al., 2018b), we carried out this research to confirm that the intestine is a target organ for infection by *L. (V.) braziliensis*. Thus, the objective of this work was to evaluate some components of the immune response, morphological and neuronal alterations in this organ of hamsters infected by other three different strains of the parasite at two different periods.

MATERIALS AND METHODS

Ethics Statement

The animal studies were previously approved by the Ethical Committee on Animal Use of the Universidade Estadual de Maringá (UEM) under protocol number 7587260416.

Parasites

For the infection, we used three different strains of *L. (V.) braziliensis*: The World Health Organization reference strain MHOM/BR/1975/M2903 (2903) and two strains isolated from patients treated at the Laboratório de Ensino e Pesquisa em Análises Clínicas (LEPAC/UEM). The two strains from UEM came from patients who had different responses to Glucantime® treatment. The patient who was infected with the MHOM/BR/2003/2314 (2314) strain showed good therapeutic response with complete lesion regression after the first treatment. The MHOM/BR/2000/1655 (1655) strain was isolated from a patient whose infection was considered resistant by reactivation of the previously-healed lesion. These isolates were cultured, cryopreserved, and identified by the Oswaldo Cruz Institute, Rio de Janeiro, Brazil (Fernandes et al., 2016).

Experimental Design and Infection

For the infection, we used promastigotes in the stationary growth phase from the fifth *in vitro* passage. The parasites were cryopreserved in the Leishmaniasis Laboratory of UEM. For culture they were thawed and reactivated. They were then kept in a culture of 199 medium (Gibco Laboratories®, Grand Island, USA) and supplemented with 1% human urine, 10% fetal bovine serum, and 1% L-glutamine. For infection preparation, the hamsters were anesthetized with a combination of ketamine (Francotar®-Virbac Animal health) and xylazine (Calmiun Agener-Union Animal Health).

We used 48 female hamsters (*Mesocricetus auratus*) (21-day-old). The hamsters were randomly separated into four groups (n = 12/group): the control group and three groups inoculated with different isolates of *L. (V.) braziliensis*. The control group received an intradermal injection of 100 µl of phosphate-buffered saline (PBS) in the left hindpaw. The infected group received an intradermal injection of each isolate ($2x10^7$/100 µl) in the left hindpaw. Once a week, both paws were measured using a digital pachymeter and analyzed for edema and lesions. The hamsters were weighed before infection and before euthanasia.

The hamsters were kept in a temperature-controlled environment with a light/dark cycle (12/12 hr). To avoid external contamination, we housed the animals in individually ventilated cages with autoclaved wood shavings and filtered air and water. Food and water were available *ad libitum*. The hamsters were euthanized 90- or 120-days post infection, thus forming a total of eight groups. For all experiments, we used 4–6 animals per group.

Euthanasia and Tissue Collection

Before euthanasia, blood samples were collected from the retro orbital sinus and total leukocytes were counted using a Neubauer chamber. The differential leukocyte count was determined in blood smears (May-Grünwald-Giemsa staining technique) using light microscopy. The data is represented in box plots (median with 25 to 75 percentile), whiskers (2.5 to 97.5 percentile), and mean (+).

The hamsters were euthanized under deep anesthesia. We then performed the laparotomies and collected and measured the ileums. Approximately 1 cm of the ileum was collected for histology. The ileum samples were fixed in buffered paraformaldehyde, dehydrated, diaphanized, and embedded in paraffin. One segment (0.5 cm) was used for biochemical analyses; this fragment was washed with PBS, frozen in liquid nitrogen, and stored in a freezer at -80°C. A different segment (2 cm) was used for the evaluation of enteric neurons. This segment was fixed in 4% paraformaldehyde and immersed in the same fixative solution for 3 hours at room temperature. It was then opened along the mesenteric border, washed twice for 10 minutes with PBS, and stored in PBS with 0.08% sodium azide at 4°C.

Histological Processing and Immunohistochemistry

To evaluate ileum morphology and cellularity, sets with semi-serial 5 µm transverse histological sections were prepared and stained using different techniques. Histopathological evaluations and morphometric analyses of ileal walls, enterocytes, and intraepithelial lymphocytes (IELs) were performed on sets stained with hematoxylin and eosin (HE) (Santos et al., 2018b; Passos et al., 2020). Goblet cells producing different mucins were counted in Alcian blue pH 1.0 (AB 1.0), Alcian blue pH 2.5 (AB 2.5), and periodic acid-Schiff (PAS) stained sets (1; Santos et al., 2018b). Total mast cells were counted with the toluidine blue technique (Yu et al., 2016; Pastre et al., 2019), and collagen fibers were analyzed in picrosirius red (Pastre et al., 2019; Panza et al., 2021).

The immunohistochemistry technique was used to label TGF-β and *Leishmania* amastigotes, as described by Santos et al. (2018b). Briefly, the slides were separately exposed to primary anti-*Leishmania* (1:200 dilution) produced in infected *L. (L.) amazonensis* mice and purified with intestines of healthy hamsters (Santos et al., 2018b) and anti-TGF-β (1:100 dilution; Thermo Fisher Scientific, Rockford, IL, EUA) antibodies. After incubation with the primary antibody, the sets were incubated with horseradish peroxidase polymer conjugate (Life Technologies Corp., Frederick, MD, USA) and stable DAB (Invitrogen™, Carlsbad, CA, USA), counterstained with Mayer's hematoxylin, and mounted with coverslips. A brown color in the sets indicated a positive reading.

Morphometric Analyses

Motic Images Plus (version 2.0) software was used to measure ileal walls and enterocytes. For these analyses, images were captured with a digital camera (Moticam 2000, 2.0 Megapixel) coupled to an optical microscope (MOTIC B5). Morphometries of ileal walls were performed in 16 images captured with a 10x objective lens. We performed 64 measurements of each of the following parameters for each animal: total thickness of intestinal walls, muscular tunics, and submucosa; widths and depths of

crypts (**Figure 1**). The heights and widths of villi were measured using the same images. The base, middle, and apex of villi were measured first, and then the average of these values resulted in the final value (Santos et al., 2018b; Passos et al., 2020). For each animal, the heights and widths of 80 enterocytes and their respective nuclei were measured in images captured with a 100x objective lens (Santos et al., 2018b).

Image-Pro® Plus (version 4.5.0.29) software was used for the evaluation of collagen fibers and HuC/HuD immunostaining neurons. In the slides stained with picrosirius red, 16 images were captured with a 20x objective lens in a light microscope (Olympus BX50 - Minato-Ku, Japan) with the use of a polarizing filter (Olympus U-POT, Japan) for measurement of type I and III collagen fibers. We captured 16 images without the polarizer for the measurement of total fibrillar collagen (μm²) (Pastre et al., 2019; Panza et al., 2021).

Cell Counting

For the quantification of goblet cells, IELs, and mast cells, we used a Nikon Eclipse E200 optical microscope. Using the 40x objective lens, we counted the number of IELs and goblet cells in 2,560 epithelial cells of each hamster (160 epithelial cells/quadrant/cut). For statistical analysis, we calculated the ratio to 100 epithelial cells (Santos et al., 2018b). Total mast cells were counted in 100 microscopic fields using the 100x objective lens (Pastre et al., 2019). From ileal mucosa and submucosa, TGF-β-immunoreactive cells (TGF-β-IR) were counted in 16 images captured by an Olympus CX31 microscope attached to a digital camera (Moticam 2000, 2.0 Megapixel). Quantities of mast cells and TGF-β-IR cells in 1 mm^2 were calculated.

Leishmania Amastigote Analysis

From each hamster, four histological sections stained with HE were analyzed to verify amastigote forms. The positive hamsters had their histological slides submitted to immunohistochemistry with anti-*Leishmania* antibodies. Five immunostained tissue sections were examined for the presence of extra- or intramacrophagic amastigote forms. Positive (sections of popliteal lymph nodes) and negative controls (sections without the primary antibody) were used.

Biochemical Analyses

Fragments of the ileum were homogenized with PBS (4mM) and centrifuged. The supernatant was then used for the measurement of nitric oxide (NO) and evaluation of enzyme myeloperoxidase (MPO) activity. The pellet was resuspended in PBS with hexadecyltrimethylammonium bromide (8mM), homogenized, and centrifuged to measure the enzymatic activity of N-acetyl-β-D-glucosaminidase (NAG). All analyses were performed in duplicate in a 96-well microplate, and their absorbances were measured in a microplate reader (Spectra Max Plus).

For the measurement of MPO, 10 μL of the sample reacted with the o-dianisidine solution (16.7 mg O-dianisidine dihydrochloride, 90 ml double-distilled water, 10 ml PBS, and 50 μl of 1% H_2O_2) for 5 minutes with protection from light. The enzymatic reaction was stopped by the addition of acetate solution, and the reading was performed at 450 nm. The results were expressed in optical density (OD).

The estimation of NO was performed indirectly by the determination of nitrite (NO^{2-}) with the Griess method. 50 μL of the sample was incubated with Griess solution (1%

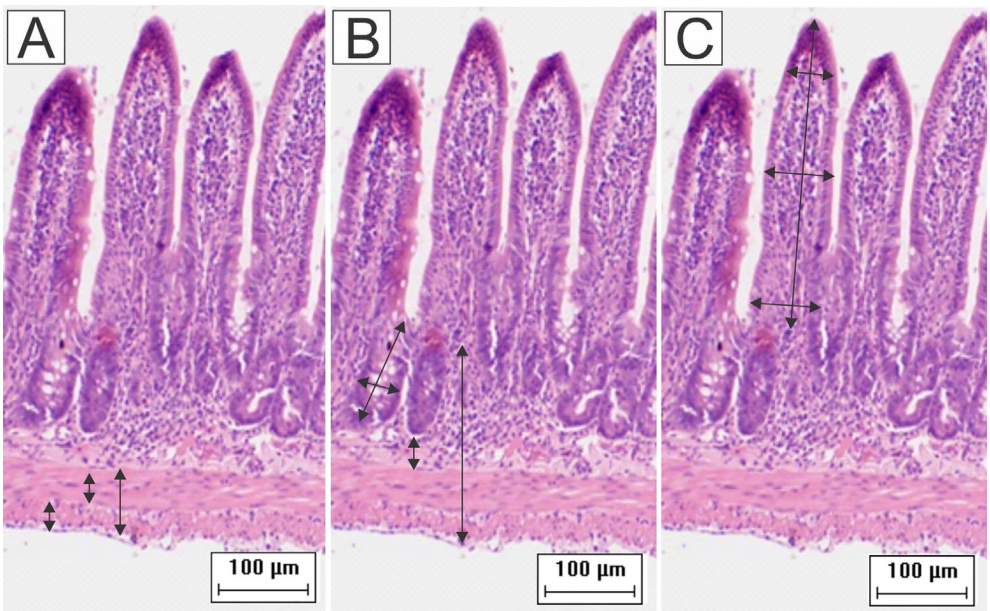

FIGURE 1 | Schematic representation of the measurement of **(A)** muscular layers, **(B)** submucosa, total wall, depth and width of the crypts, and **(C)** height and width of the villi. Were performed 64 measurements of each parameter for each animal. To obtain the width of the villi, the base, middle, and apex were measured and then the average of these values resulted in the final value (HE staining, 20× magnification, scale bar = 100 μm, Olympus CX31).

sulfanilamide in 5% phosphoric acid, and 0.1% N-1-naphthylethylenediamine dihydrochloride in water) at room temperature. The NO concentration was calculated based on the sodium nitrite standard curve. The absorbance was measured at 550 nm; the results were expressed in μM concentration of NO^{2-}.

Finally, the measurement of NAG enzymatic activity was performed with a 25 μL sample that remained incubated for 1 hour at 37°C with a citrate buffer and NAG solution (1.14 mg of p-nitrophenyl-N-acetyl-β-D- glucosamine in distilled water). Before the reading at 405 nm, glycine buffer was added. The result was expressed in OD/g of wet tissue.

Neuron Counting and Morphometry

Small fractions of ileums were dissected under stereomicroscopy to obtain whole mount preparations of enteric plexuses. To mark the total population of HuC/HuD neurons, whole mounts of myenteric and submucosal plexuses were washed 3 times for 5 minutes with PBS (0.1M pH 7.4) and incubated separately in microtubes with an antigen blocking solution containing 3% bovine serum albumin (BSA; Sigma, St. Louis, MO, USA) and 0.1% Triton X100 (Sigma, St. Louis, MO, USA) diluted in PBS for 1 hour at room temperature. After this, the membranes were incubated in a solution containing the primary mouse anti-HuC/HuD (1:300; Molecular Probes, Eugene, OR, USA) antibody, 3% BSA, and 0.1% Triton X100 diluted in PBS for 48 hours under stirring at room temperature. After this period, the samples were washed 3 times for 5 minutes with PBS and incubated in a solution containing the secondary Alexa Fluor 488 donkey anti-mouse antibody (1:300; Molecular Probes, Eugene, OR, USA), 3% BSA, and 0.1% Triton X100 diluted in PBS for 2 hours at room temperature under agitation and protection from light. Then, the membrane preparations were washed 3 times for 5 minutes in PBS, mounted on glass slides with Prolong Gold Antifade (Molecular Probes, Eugene, OR, USA), and stored at 4°C (light-protected).

The counting of HuC/HuD-immunoreactive neurons from myenteric and submucosal plexuses was performed on 32 images captured randomly with a 20x objective lens in all areas of the ileum circumference using the FSXBSW Image Browser integrated in an Olympus FSX100 light microscope (Olympus, Tokyo, Japan) with immunofluorescence filters. In the submucosal plexus, we counted the neurons inside and outside the ganglia and the total number of ganglias. These results were expressed in cells/mm². The areas of 100 neurons (μm^2) of submucosal and myenteric neurons per animal were measured in the same images. For both analyses, we used Image-Pro® Plus (version 4.5.0.29) software.

Statistical Analysis

The statistical analyses were performed using the data of the individual animals and were determined based on the data distribution, which was verified using the Shapiro-Wilk or D'Agostino Pearson tests (BioEstat 5.3 software). Comparisons between the groups were verified with two-way analysis of variance (ANOVA) followed by Tukey's multiple-comparison test or Fisher's *post hoc* test; the Kruskal-Wallis test followed by Dunn's pos hoc test was also used (GraphPad Prism 8.0.1 software). We compared the control groups to the infected groups in the two experimental periods (90 or 120 days) and the 90-day infected group to the 120-day group. Values of $p < 0.05$ were considered statistically significant.

RESULTS

Clinical Signs

The infection was confirmed by the development of the lesion at the site of inoculation of the parasite, therefore, only animals with lesions on the left hindpaw were used. Body weight, consistency of feces, and appearance of hair did not change during the experimental period when compared the groups. Edema was observed in infected paws in the first days after infection. The lesions started to appear between the third and fourth week after infection and no statistical differences were observed among the infected groups. All infected hamsters showed difficulty in mobility due to lesion progression (**Figure 2**).

Infection Increased Leukocytes in Peripheral Blood

Global leukocyte counts increased in all infected groups (90 days) when compared to control group (2903: $p = 0.007$; 2314: $p = 0.033$; 1655: $p = 0.039$). In differential leukocyte counts, we observed an increase in neutrophils ($p = 0.029$), lymphocytes ($p < 0.03$), and monocytes ($p < 0.001$) in the 2903 group at 90 days of infection when compared to the control group. When compared to the control group, monocyte quantities were also significantly higher at 120 days of infection in the 2903 group ($p = 0.034$) and 90 days in the 2314 group ($p = 0.012$); 1655 group presented $p = 0.058$ when compared to the CG. Lymphocytes also increased in the 1655 group at 90 days of infection when compared to the control group ($p = 0.046$); but lymphocyte numbers decreased between 90 and 120 days of infection for this group (1655; $p = 0.029$) (**Figure 3**).

After Infection, Intestinal Walls Were Thicker, Crypts Were Deeper and Wider, and Villi Were Longer and Wider

Ileums showed no significant macroscopic changes after infection. However, we measured intestinal walls to analyze the morphology of the organ and significant changes were found. We observed thicker muscular layers in groups 2903 and 2314 in both infection periods when compared to the control groups ($p < 0.001$). In groups 2903 and 2314, increases of approximately 20% and 29% of total muscle thickness were observed at 90 and 120 days of infection, respectively, when compared to the control groups. Group 1655 had values similar to the control group, with the exception of an increase to longitudinal layers at 90 days ($p = 0.003$). Submucosal layers were thicker in all infected groups and increased by an average of 25% at 90 days (2903 and 2314: $p < 0.001$; 1655: $p = 0.023$) and 42% at 120 days of infection ($p < 0.001$) and when compared to the control groups (**Figures 4** and **5**).

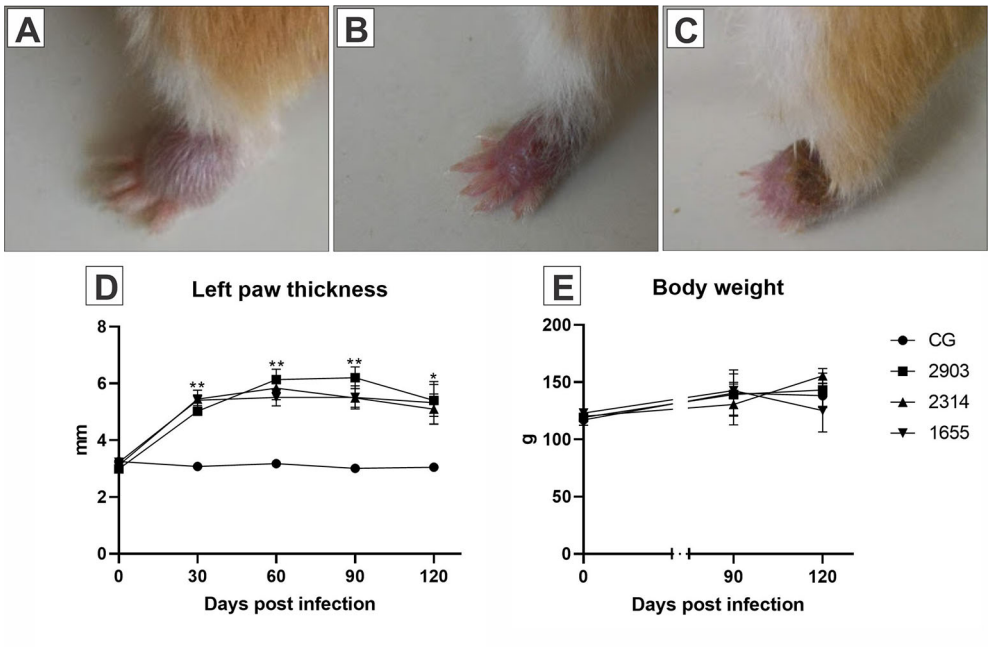

FIGURE 2 | Images **(A–C)** represent the evolution of the paw lesion after the infection by *L.* (*V.*) *braziliensis* (MHOM/BR/2000/1655 strain): **(A)** initial edema, **(B)** initial lesion, **(C)** ulcerated lesion. **(D)** Represents the evaluation of the clinical course of lesions through the 120 days following the infections. The size of the lesions was measured with a digital pachymeter by evaluating the dorsal-ventral thickness of the infected paw (mm). *p < 0.05; **p < 0.001 when compared the infected groups to the respective control. **(E)** Demonstrates the body weight (g) of the hamsters before parasite inoculation and at 90- and 120-days post infection (n = 4). CG, control group. 2903: group infected with MHOM/BR/1975/M2903. 2314: group infected with MHOM/BR/2003/2314. 1655: group infected with MHOM/BR/2000/1655.

Crypts of group 2314 in the two infection periods and groups 2903 and 1655 at 120 days were deeper and wider than in control group hamsters ($p < 0.001$). Total organ wall size in groups 2903 and 2314 increased in both experimental periods when compared to the control groups ($p < 0.001$). We recorded an average increase of 16% and 35% in height and 15% and 22% in width at 90 and 120 days of infection, respectively, when compared to the control groups ($p < 0.001$). Thus, infection

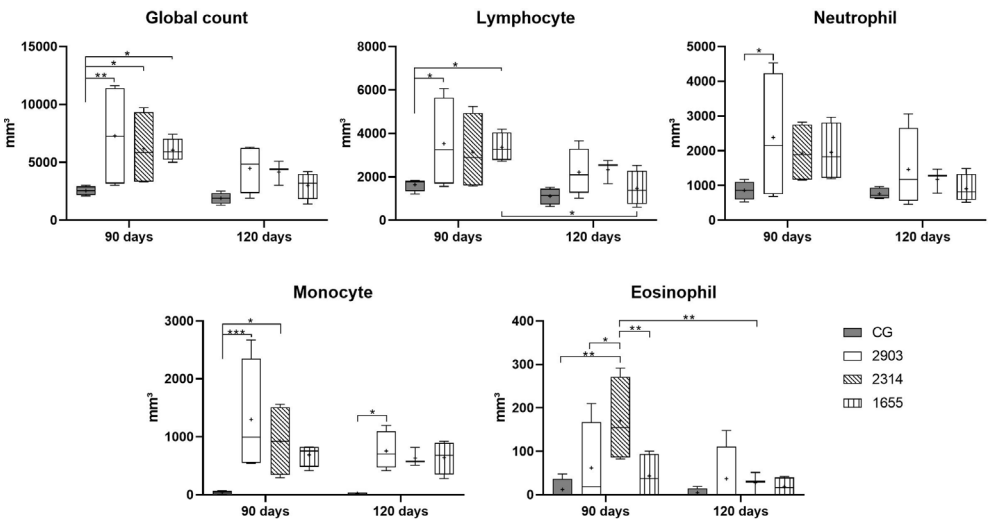

FIGURE 3 | Global and differential leucocyte counts in peripheral blood in hamsters infected with three strains of *L. (V.) braziliensis* for 90 and 120 days. Data is represented in box plots (median with 25 to 75 percentile), whiskers (2.5 to 97.5 percentile), and mean (+) (n = 4). *$p < 0.05$; **$p < 0.01$; ***$p < 0.001$. CG, control group. 2903: group infected with MHOM/BR/1975/M2903. 2314: group infected with MHOM/BR/2003/2314. 1655: group infected with MHOM/BR/2000/1655.

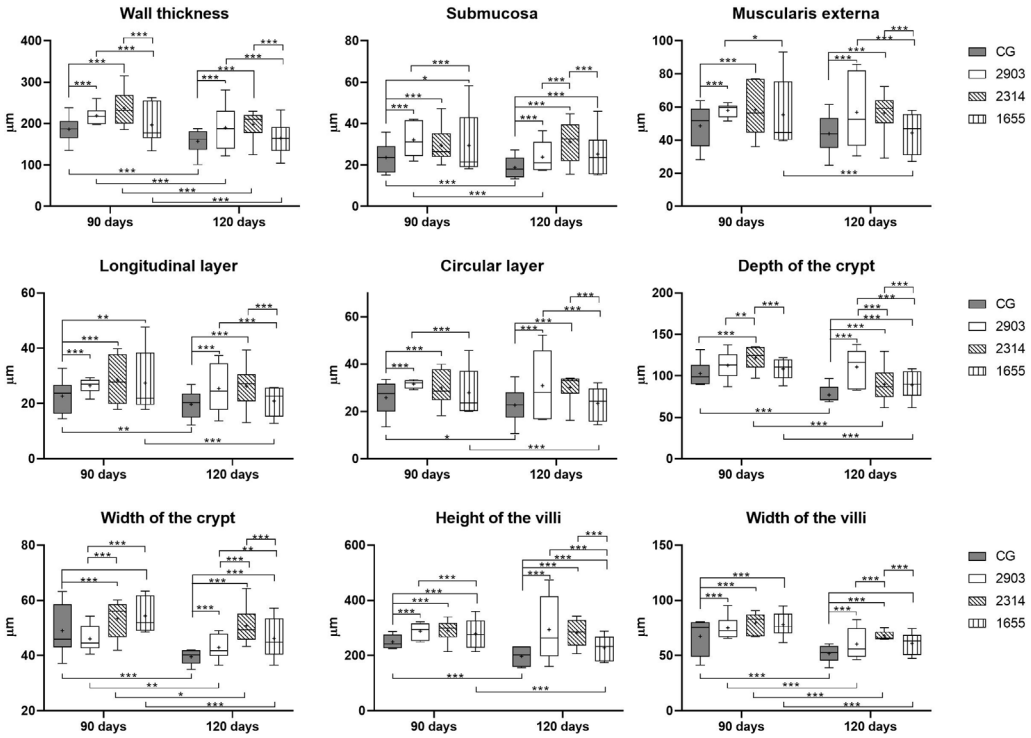

FIGURE 4 | Morphometry of wall, villi, and crypts of ileums of hamsters infected by *L. (V.) braziliensis* for 90 or 120 days (µm). Data represented in box plots (median with 25 to 75 percentile), whiskers (2.5 to 97.5 percentile), and mean (+) ($n = 6$). *$p < 0.05$; **$p < 0.01$; ***$p < 0.001$. CG, control group. 2903: group infected with MHOM/BR/1975/M2903. 2314: group infected with MHOM/BR/2003/2314. 1655: group infected with MHOM/BR/2000/1655.

duration seemed to be a determining factor in organ response (**Figures 4** and **5**).

The Infection Caused Morphometric and Quantitative Changes to Epithelial Cells in Hamster Ileums

We measured enterocytes to verify the impacts of the infection on epithelial cells in the ileum. Enterocytes are the most abundant cell type in the intestinal epithelium. As shown in **Figure 6**, enterocytes increased in height ($p < 0.05$) and decreased in width ($p < 0.05$) in all infected groups when compared to the controls. We observed increases to the nuclei of these cells only in group 2314 (in both infection periods) when compared to the respective controls ($p < 0.001$). For group 2314, the longer infection period (120 days) resulted in a 29% increase to nuclei size when compared to the 90-day group (**Figure 6**).

In goblet cell quantification, we observed a 41% increase in the number of sulfomucin producers (AB 1.0; $p = 0.028$) and a 38% reduction in the neutral producers (PAS; $p = 0.003$) in group 1655 that were infected for 120 days when compared to the 90-day group. The 1655 group reduced the PAS goblet cells when compared to the 2314 group infected by 120 days ($p = 0.007$). No alterations were observed in the goblet cells that produce sialomucins (AB 2.5; $p > 0.1$) (**Figure 7**).

Intraepithelial Lymphocytes and TGF-β-Immunoreactive Cells Increased After Infection

When compared to the control, we observed an average increase of IELS of approximately 70% in the groups infected for 90 days ($p < 0.001$) and of 36%, 74%, and 51% in hamsters infected for 120 days in groups 2903 ($p = 0.013$), 2314 ($p < 0.001$), and 1655 ($p < 0.001$), respectively. Mast cell quantities significantly increased in the 2314 ($p = 0.002$) and 1655 ($p < 0.001$) groups at 120 days of infection when compared to 90 days. The number of TGF-β-IR cells increased in all infected groups when compared to the control groups (90 days – 2903: $p = 0.009$; 2314: $p = 0.003$; 1655: $p = 0.012$; 120 days – 2903: $p = 0.020$; 2314: $p = 0.001$; 1655: $p = 0.009$). The two-way ANOVA analyses revealed a significant main effect for the time [$F_{(1,40)} = 16.5$, $p < 0.001$] and infection [$F_{(3,40)} = 24.2$, $p < 0.001$] in IELs; for the time [$F_{(1,40)} = 26.3$, $p < 0.001$] in mast cells; and for the infection [$F_{(3,25)} = 9.02$, $p < 0.001$] in the TGF-β-IR cells (**Figure 8**).

Infection and Experimental Duration Affect Collagen Fiber Remodeling

To understand the effects of the infection on the ileum cellular matrix, we used histochemistry to evaluate the areas occupied by collagen fibers. Hamsters from group 2903 showed higher total fibrillar collagen at 120 days of infection than at 90 days ($p < 0.001$). At 120 days of infection, group 2903 had higher total

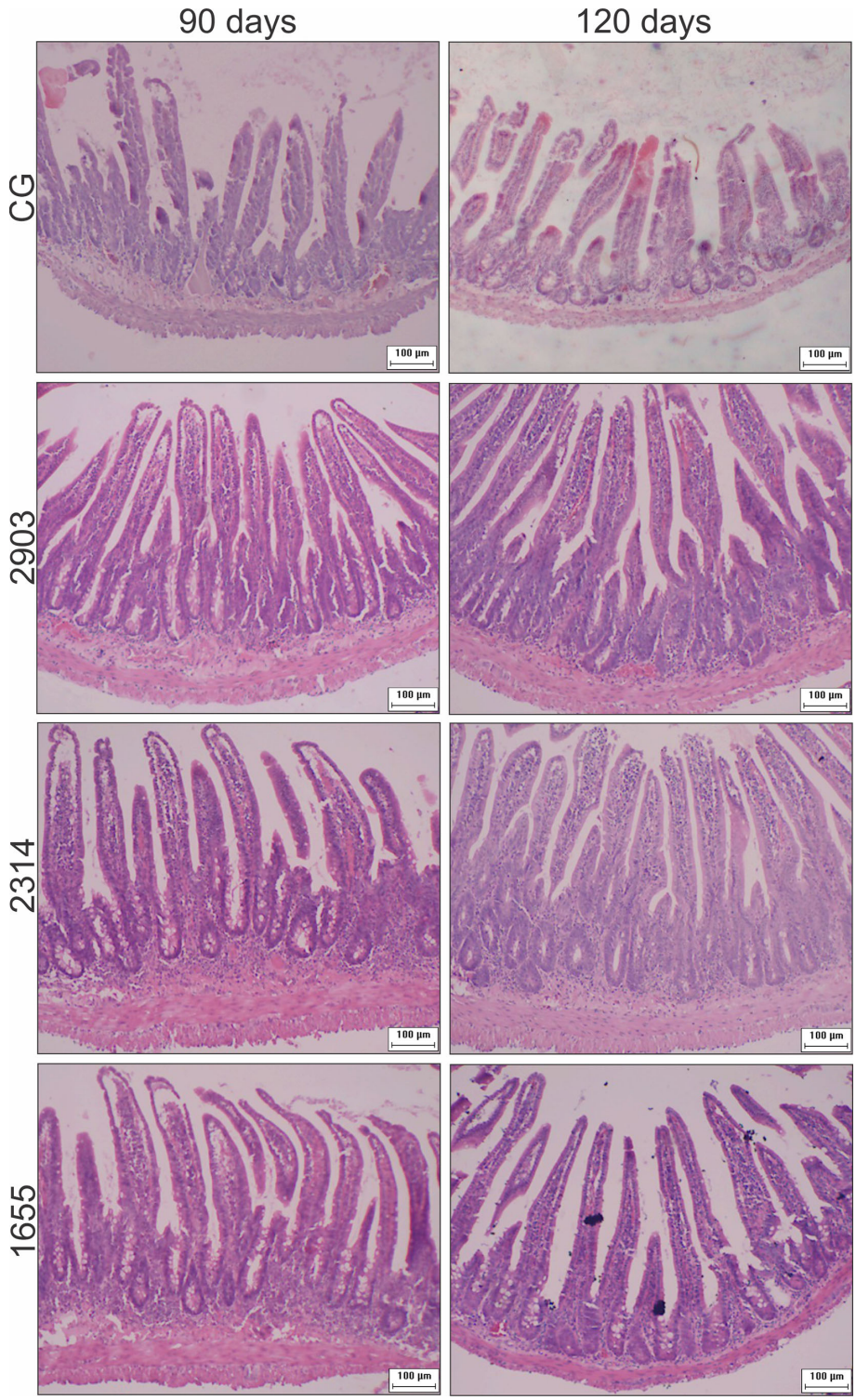

FIGURE 5 | Photomicrograph of cross-sections representing the ileum wall, villi, and crypts of hamsters infected by *L. (V.) braziliensis* (HE staining, 10× magnification, scale bar = 100 µm, Olympus CX31). CG, control group. 2903: group infected with MHOM/BR/1975/M2903. 2314: group infected with MHOM/BR/2003/2314. 1655: group infected with MHOM/BR/2000/1655.

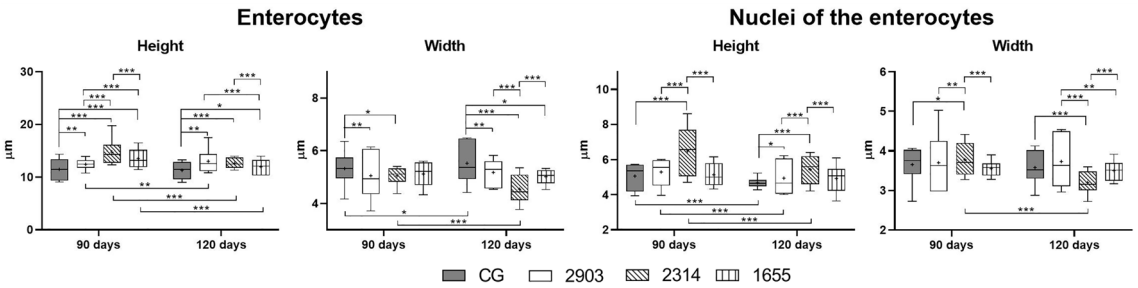

FIGURE 6 | Morphometry of ileum enterocytes from hamsters infected with different *L.* (*V.) braziliensis* strains at 90 or 120 days of infection (µm). Data represented in box plots (median with 25 to 75 percentile), whiskers (2.5 to 97.5 percentile), and mean (+) ($n = 6$). *$p < 0.05$; **$p < 0.01$; ***$p < 0.001$. CG, control group. 2903: group infected with MHOM/BR/1975/M2903. 2314: group infected with MHOM/BR/2003/2314. 1655: group infected with MHOM/BR/2000/1655.

fibrillar collagen than all other groups in the experiment ($p < 0.001$). The two-way ANOVA demonstrated a significant main effect for the time [$F_{(1,40)} = 4.70$, $p = 0.036$] and infection [$F_{(3,40)} = 3.35$, $p = 0.028$] without interaction between the variables. At 90 days of infection, type I collagen fiber decreased in 2903 ($p = 0.015$), 2314 ($p = 0.001$) and 1655 ($p < 0.001$) groups when compared to the control. Hamsters in groups 2903 ($p = 0.039$) and 2314 ($p = 0.012$) had reductions in type III collagen fiber at 90 days of infection when compared to the controls, but type III fibers increased for both groups in the period between 90 to 120 days of infection (2903: $p = 0.015$; 2314: $p = 0.008$). In the type III collagen fibers was observed the interaction between the variables [$F_{(3,40)} = 4.34$, $p = 0.009$] by two-way ANOVA; while the type I demonstrated a significant main effect only for the infection [$F_{(3,40)} = 4.06$, $p = 0.013$] (**Figure 9**).

Presence of Amastigotes and Inflammatory Changes in Ileums of Infected Hamsters

As demonstrated in **Table 1** after 120 days of infection, NO levels in hamster ileums in group 1655 were higher than in the control group. We observed an increase in myeloperoxidase enzyme activity in group 2903 when compared to group 1655 at 90 days of infection; the opposite was observed for NAG enzymatic activity.

Figure 10 shows an infiltration of mononuclear cells in the mucous layer formed mostly by lymphocytes, plasmocytes, and (to a lesser extent) polymorphonuclear leukocytes. In addition, we observed signs of inflammatory infiltrates in mucosa, submucosa and in crypts, and edemas in villi. Our findings of immune cells inside and around ganglia suggest that ganglionitis and periganglionitis could be correlated with changes observed in the ENS. While using hematoxylin and eosin staining, we also found forms that suggested amastigote presence; this presence was later confirmed by immunohistochemistry.

The Infection Caused Morphometric Changes in Neurons in the Myenteric and Submucosal Plexuses

No quantitative changes in neurons or ganglias were observed in the evaluation of total neuronal populations (immunostained analysis with HuC/HuD) (**Table 2**).

In the myenteric plexus, the bodies of neurons in groups 2314 ($p = 0.023$) and 1655 ($p < 0.001$) at 90 days of infection were larger than the controls. However, significant reductions to cellular bodies were recorded thereafter (2314: $p = 0.014$; 1655: $p < 0.001$); at 120 days after infection, the cellular body sizes of infected groups were similar to the control groups. However, neuronal body sizes in the submucosal plexus at 120 days of infection decreased by approximately 15% in group 2903, 30% in 2314, and 26% in 1655 when compared to the 120 days control group ($p < 0.001$) (**Figure 11**).

DISCUSSION

Due to the clinical/epidemiological importance (Ministério da Saúde, 2017; Conceição-Silva and Morgado, 2019; World Health Organization, 2020) of the disease and its ability to use genetic diversity to create more aggressive forms (Guimarães et al., 2016; Rugani et al., 2018), our study evaluated the changes in hamster ileums at 90 days and 120 days of infection from one reference parasite strain and two clinically-isolated strains.

In infection-related lesions, different *L. (V.) braziliensis* strains have presented different biological behaviors (Rêgo et al., 2018) and cytokine and chemokine gene expressions in skin lesions in hamsters (Rêgo et al., 2019). For example, in BALB/c and C57BL/6 mice, different profiles of inflammatory infiltrates in livers and spleens were found with or without the presence of parasite (Pereira et al., 2009). Fernandes et al. (2016) demonstrated various cytokine expressions and macrophage-infectivity rates in *in vitro* experiments with the same strains used in our study.

Almeida and collaborators Almeida et al. (1996) reported the presence of *L. (V.) braziliensis* species in the spleens and livers of hamsters that could multiply *in situ*, which enables the production of secondary metastatic visceral lesions from a primary skin lesion (the reverse could also be possible). We found some *Leishmania* amastigote forms in infected hamster ileums with all strains analyzed in our study. The changes observed in this specific organ cannot be solely linked to the presence of the protozoan, but as a systemic consequence of

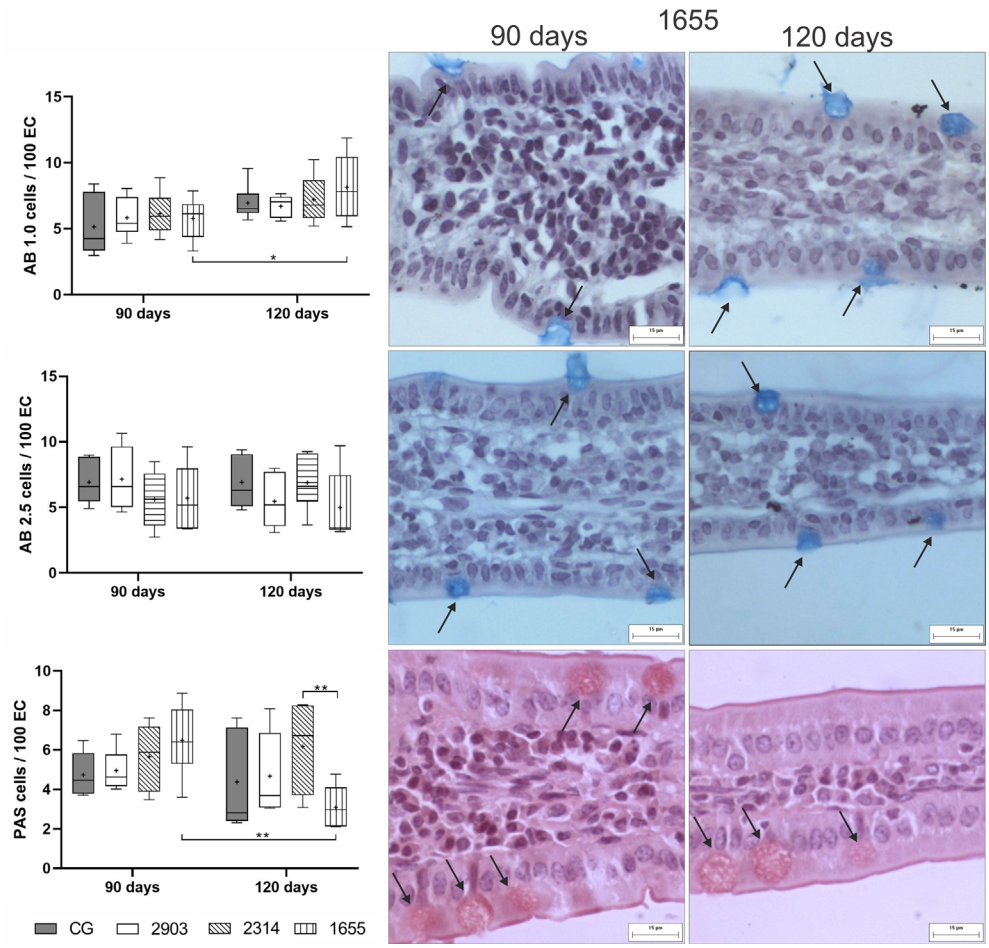

FIGURE 7 | Ratio of globlet cells/100 of epithelial cells (EC) stained using the histochemical techniques of Alcian Blue (AB) pH 1.0, AB pH 2.5, and periodic acid-Schiff (PAS). Data is represented in box plots (median with 25 to 75 percentile), whiskers (2.5 to 97.5 percentile), and mean (+) ($n = 6$). *$p < 0.05$; **$p < 0.01$. Representative photomicrograph of the group 1655 at 90- and 120-days post infection showing goblet cells (black arrows) in each technique (AB pH 1.0 and 2.5 and PAS staining, 40× magnification, scale bar = 15 µm, Olympus BX50). CG, control group. 2903: group infected with MHOM/BR/1975/M2903. 2314: group infected with MHOM/BR/2003/2314. 1655: group infected with MHOM/BR/2000/1655.

infection. Pereira et al. (2009) also reported changes to livers and spleens of mice infected with different *L. (V.) braziliensis* strains, and Passos and collaborators Passos et al. (2020) demonstrated changes to hamster colons infected with *L. infantum*.

Increases of blood leukocytes confirmed the systemic effects of infection and necessity for mobilization of these cells to the site of initial infection and possibly other organs, such as the intestine. The presence of inflammatory infiltrates and increases to submucosa, muscular layers, and villi in the present study and other research (Góis et al., 2016; Santos et al., 2018a; Santos et al., 2018b) support this hypothesis. These effects enable the presence of the parasite in other organs, as defense cells maintain viable parasitic forms in the interior and are used as vehicles of the parasite to infect macrophages (Bogdan, 2020). When migrating from the infection site to the lymph nodes, macrophages and other immune cells can transport the parasite to other organs *via* the lymphatic system, as evidenced by the presence of amastigote forms in the popliteal lymph and the DNA of the parasite in mesenteric lymph nodes of hamsters chronically-infected with *L. (V.) braziliensis* (Santos et al., 2018b).

The inflammatory infiltrates observed in the lamina propria of infected hamsters mainly contained mononuclear cells, similar to observed in the duodenum of a patient infected by *L. donovani* (Chattopadhyay et al., 2020). At 120 days of infection, decreases were observed in various parameters of the intestinal wall and blood leukocytes when compared to groups infected for 90 days. This might be a natural part of the aging process, as this reduction was also seen in the control groups.

Ganglionitis and periganglionitis have been reported in hamsters infected with *L. (V.) braziliensis* (Santos et al., 2018b) and *L. infantum* (Passos et al., 2020), but our article is the first to numerically and morphometrically evaluate the neurons of both ENS plexuses. The infiltration of immune cells in the ganglia can lead to neuronal degeneration and consequently cause cell dysfunction and loss (De Giorgio et al., 2004). However, the

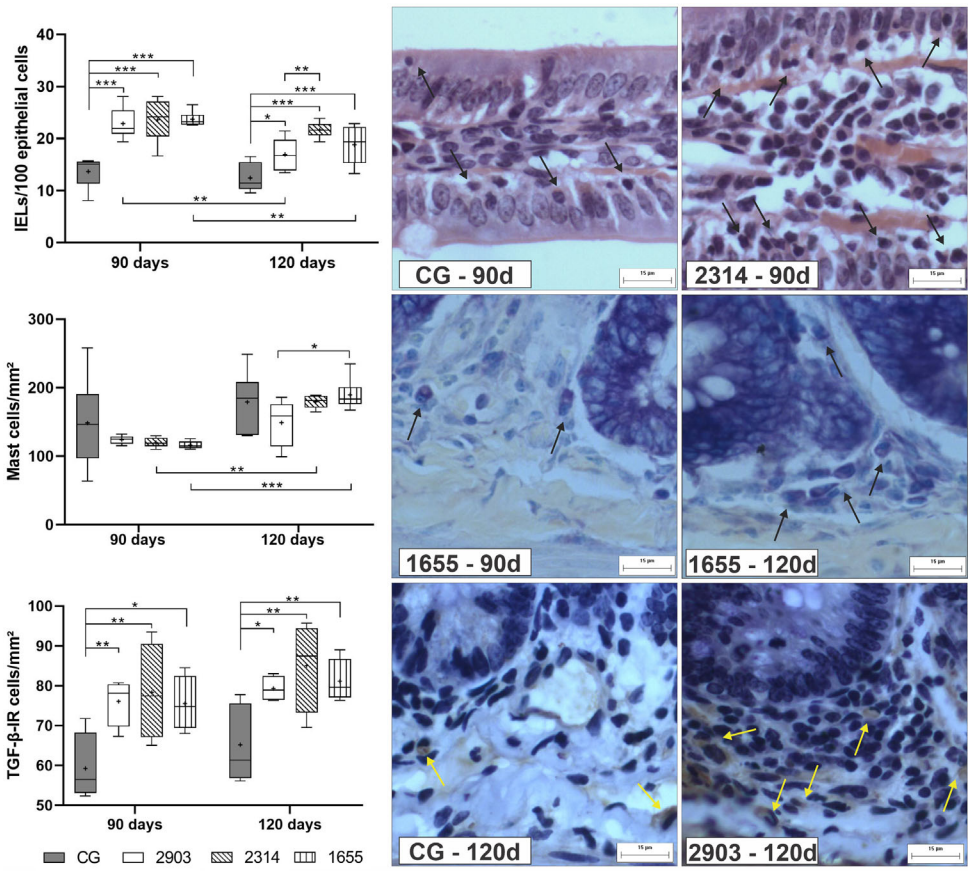

FIGURE 8 | Proportion of intraepithelial lymphocytes (IELs) in 100 epithelial cells, mast cells, and TGF-β-immunoreactive cells (TGF-β-IR) per mm². Data represented in box plots (median with 25 to 75 percentile), whiskers (2.5 to 97.5 percentile), and mean (+) ($n = 6$). *$p < 0.05$; **$p < 0.01$; ***$p < 0.001$. Representative photomicrograph of IELs in the control group and 2314 at 90-days post infection (black arrows; HE staining, 40× magnification, scale bar = 15 µm, Olympus BX50); mast cells in group 1655 at 90- and 120-days post infection (black arrows; blue toluidine staining, 40× magnification, scale bar = 15 µm, Olympus BX50); TGF-β-IR of the control group and 2903 at 120-days post infection (yellow arrows; immunohistochemistry, 40× magnification, scale bar = 15 µm, Olympus BX50). CG, control group. 2903: group infected with MHOM/BR/1975/M2903. 2314: group infected with MHOM/BR/2003/2314. 1655: group infected with MHOM/BR/2000/1655.

neuroplastic response to inflammation enables intestinal homeostasis (Mawe et al., 2009).

Hypertrophy of neuron bodies in the myenteric plexus at 90 days of infection suggests an increase in their metabolic activity; this acts as a mechanism of adaptation to adverse conditions suffered by these cells (Araújo, 2015; Trevizan et al., 2019). Such alterations can interfere with intestinal motility and consequently lead to an increase in muscle layers, as this plexus is responsible for the coordinating movements of intestinal relaxation and contraction (Nezami and Srinivasan, 2010; Machado et al., 2021). This relationship has been observed with other protozoa (Araújo, 2015; Machado et al., 2021). At 120 days of infection, we observed reduction in neuronal bodies and muscle layers in group 1655; this may be related to more acidic mucus, and consequently, more fluid and easier secretion (Góis et al., 2016).

The increase in immune cells and the presence of edemas in the mucosal and submucosal layers contributed to the thickening of both layers in the ileal wall. The migration of these cells may have contributed to reductions to the body sizes of submucosal neurons in all infected groups at 120 days of infection. These data corroborate with those of other authors (da Silva et al., 2017; Schneider et al., 2018) who demonstrated that submucosal neurons are directly affected by intestinal inflammation. The submucosal plexus controls the function of epithelial cells *via* the lumen (Nezami and Srinivasan, 2010), chemical stimuli, and distension of intestinal mucosa (Christofi, 2008). The loss of normal functions of these neurons can cause dysfunction in intestinal permeability and secretion. We evaluated the total population of neurons (marked by HuC/HuD); other markers can also be used to detect possible changes in specific neuronal populations and ENS components.

The increase in cellularity in the lamina propria occurred together with large increases of IELs, demonstrating the attraction of immune cells to the epithelium (Santos et al., 2018a; Santos et al., 2018b). This effect corroborates with the previously discussed changes in submucosal neurons. IELs can play a protective role on enterocytes in the maintenance of epithelial integrity (Hu and Edelblum, 2017), an effect typically

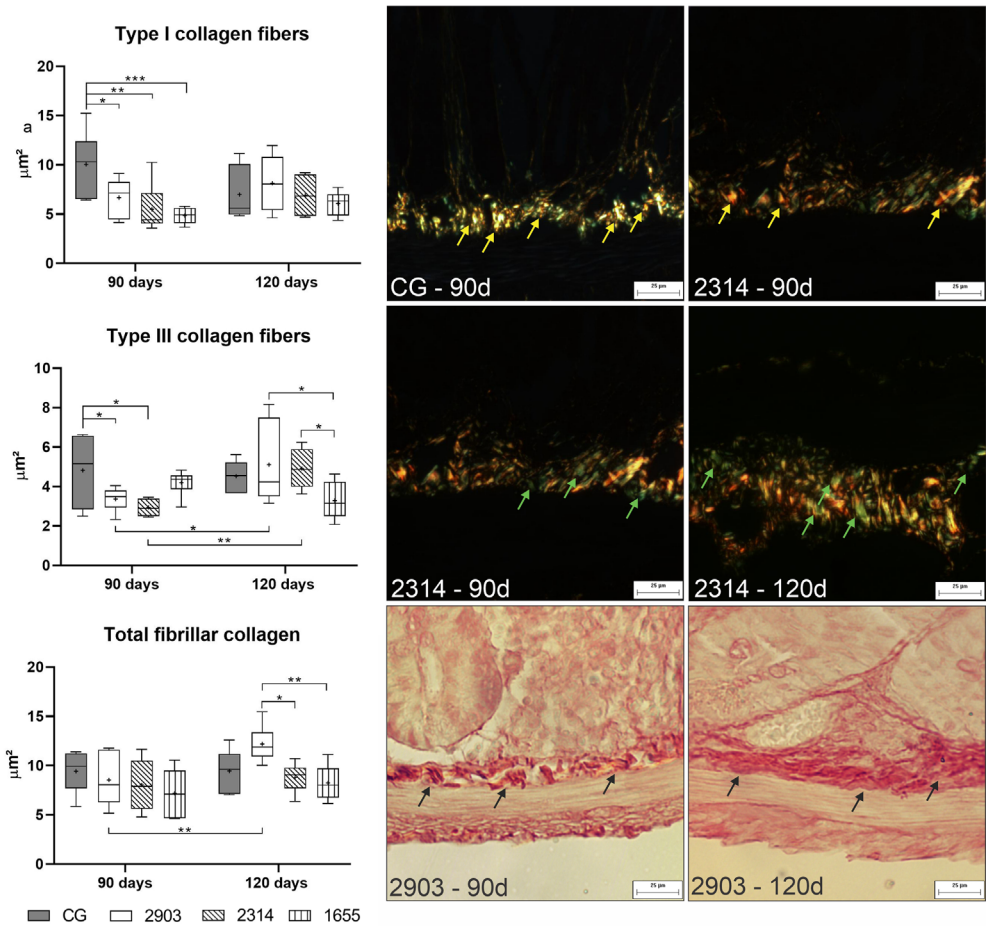

FIGURE 9 | Area occupied by type I, type III, and total fibrillar collagen fibers (μm^2). Data represented in box plots (median with 25 to 75 percentile), whiskers (2.5 to 97.5 percentile), and mean (+) ($n = 6$). *$p < 0.05$; **$p < 0.01$; ***$p < 0.001$. Photomicrograph of the area occupied by type I collagen fibers (yellow arrow) in control group and 2314 at 90-days post infection; by type III collagen fibers (green arrow) in group 2314 at 90- and 120-days post infection; and of total fibrillar collagen (black arrow) in group 2903 at 90- and 120-days post infection (Picrosirius Red staining, 20× magnification, scale bar = 25 µm, Olympus BX50). CG, control group. 2903: group infected with MHOM/BR/1975/M2903. 2314: group infected with MHOM/BR/2003/2314. 1655: group infected with MHOM/BR/2000/1655.

TABLE 1 | Biochemical analyses of the ileums of hamsters infected with different *L. (V.) braziliensis* strains at 90 and 120 days of infection.

		NO (µM)	MPO (OD)	NAG (OD/g of wet tissue)
	CG	47.41 ± 8.03	0.19 ± 0.02	23.23 ± 0.53
90	**2903**	57.25 ± 4.59	(0.24 ± 0.02)	(19.37 ± 2.01)
days	**2314**	68.29 ± 8.72	0.20 ± 0.03	25.17 ± 2.52
	1655	58.31 ± 13.27	(0.14 ± 0.02)$^{\#}$	(28.52 ± 1.85)$^{\#}$
	CG	(31.02 ± 6.20)	0.12 ± 0.02	17.87 ± 2.72
120	**2903**	51.32 ± 12.85	0.17 ± 0.03	21.71 ± 4.13
days	**2314**	38.76 ± 13.26	0.15 ± 0.06	22.28 ± 2.25
	1655	(66.51 ± 17.34)*	0.15 ± 0.03	21.76 ± 2.42

*The data are expressed as mean ± SE ($n = 4$). *$p < 0.05$ comparing 1665 to CG at 120 days. $^{\#}p < 0.05$ comparing 1655 to 2903 at 90 days. CG, control group. 2903: group infected with MHOM/BR/1975/M2903. 2314, group infected with MHOM/BR/2003/2314. 1655, group infected with MHOM/BR/2000/1655. NO, nitric oxide dosage; MPO, enzymatic activity of myeloperoxidase; NAG, enzymatic activity of N-acetyl-β-D-glucosaminidase; OD, optical density.*

associated with inflammatory intestinal diseases (Mahadeva et al., 2002; Ahn et al., 2014; Sergi et al., 2017). Passos and collaborators (2020) found similar results in hamster colons after four months of *L. infantum* infection. In infected hamsters, we observed deeper crypts, longer and larger villis, and an increase of TGF-β-IR cells (a cytokine that controls growth and differentiation of enterocytes) (Sangild et al., 2009). These effects suggest there was a large proliferation of epithelial cells

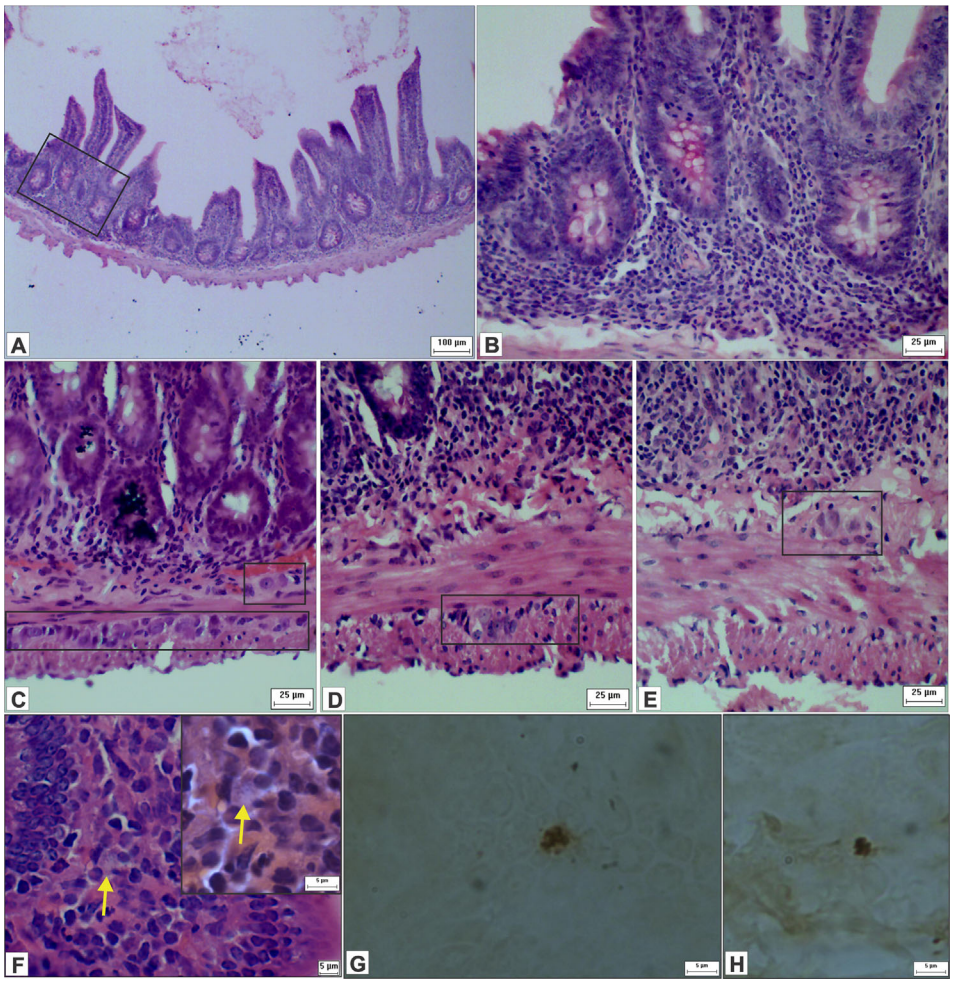

FIGURE 10 | Photomicrograph of cross-sections of the ileum of hamsters infected by *L. (V.) braziliensis*. **(A)** Presence of inflammatory infiltrates in the intestinal wall and in the crypts (HE staining, 10× magnification, scale bar = 100 µm; Olympus CX31). **(B)** Higher magnification of image A (HE staining, 40× magnification, scale bar = 25 µm; Olympus CX31). **(C–E)** Inflammatory cells within and close to the myenteric and submucosal ganglia, suggestive of ganglionitis and periganglionitis (HE staining, 40× magnification, scale bar = 25 µm; Olympus CX31). **(F)** Suggestive amastigotes forms (arrow), presence of immune cells and IELs (HE staining, 100× magnification, scale bar = 5 µm; Olympus CX31) with a higher magnification (HE staining, 100× magnification, scale bar = 5 µm; Olympus BX50). **(G, H)** *Leishmania* amastigotes in the ileum (immunohistochemistry, 100× magnification, scale bar = 5 µm; Olympus BX50).

TABLE 2 | Counting of neurons in the myenteric and submucosal plexuses (marked by HuC/HuD) in the ileum of hamsters infected with different *L. (V.) braziliensis* strains at 90 and 120 days of infection.

		Myenteric neurons (mm^2)	Submucosal plexus (mm^2)			
			Number of ganglia	Neurons inside ganglia	Neurons outside ganglia	Submucous neurons
90 days	CG	239.22 ± 4.62	9.13 ± 0.55	45.26 ± 3.27	15.43 ± 0.44	60.70 ± 3.61
	2903	238.96 ± 5.54	11.10 ± 0.40	54.11 ± 1.04	15.26 ± 0.58	69.37 ± 0.87
	2314	241.59 ± 5.00	10.12 ± 0.15	47.98 ± 1.72	14.80 ± 1.02	62.78 ± 1.45
	1655	229.74 ± 1.12	10.87 ± 0.38	51.45 ± 1.50	15.32 ± 0.72	66.77 ± 2.05
120 days	CG	243.27 ± 3.08	9.94 ± 0.25	49.60 ± 0.79	16.36 ± 0.11	65.96 ± 0.87
	2903	245.66 ± 11.40	9.40 ± 0.07	48.40 ± 0.90	16.49 ± 0.07	64.90 ± 0.88
	2314	250.83 ± 7.28	10.02 ± 0.78	48.33 ± 3.26	14.88 ± 0.65	63.21 ± 3.91
	1655	242.65 ± 2.67	10.86 ± 0.35	50.72 ± 1.35	14.56 ± 0.58	65.28 ± 1.93

The data are expressed as mean ± SE in 1 mm^2 (n = 4). GC, control group. 2903, group infected with MHOM/BR/1975/M2903. 2314, group infected with MHOM/BR/2003/2314. 1655, group infected with MHOM/BR/2000/1655. Number of neuron totals were counted in the myenteric plexus. Number of ganglia, the quantity of neurons inside and outside the ganglia, and the total number of neurons in the plexus were counted in the submucosal plexus.

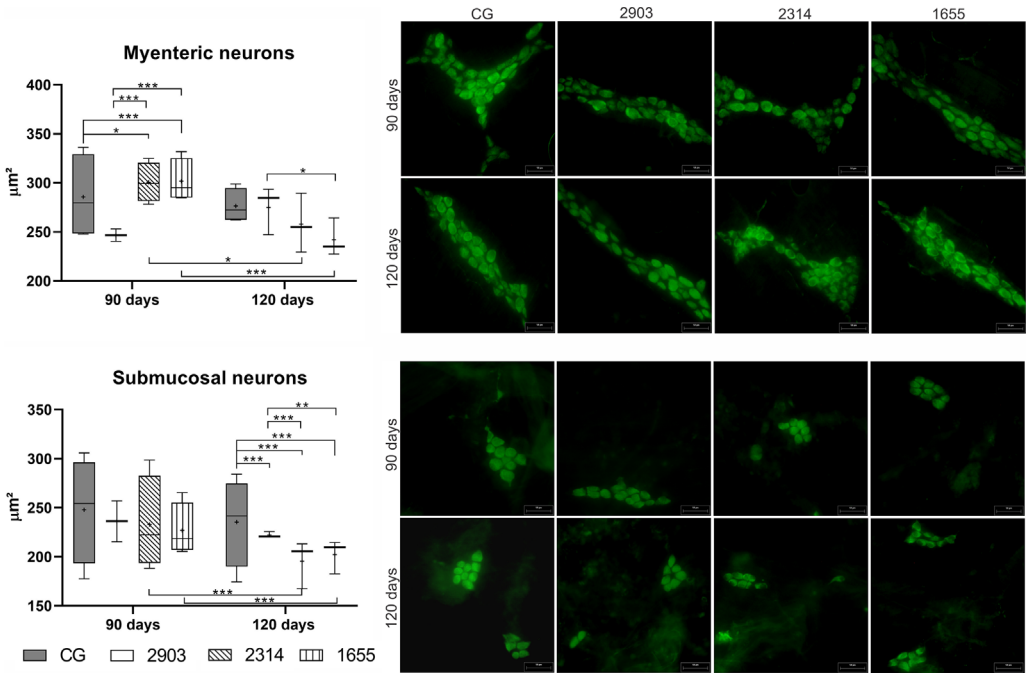

FIGURE 11 | Size of neuron bodies (µm²) in the myenteric and submucosal plexuses of ileums of hamsters infected by *L. (V.) braziliensis* for 90 or 120 days. Data represented in box plots (median with 25 to 75 percentile), whiskers (2.5 to 97.5 percentile), and mean (+) ($n = 4$). *$p < 0.05$; **$p < 0.01$; ***$p < 0.001$. Photomicrograph of neurons from both plexuses (HuC/HuD immunohistochemistry, 20× magnification, scale bar = 50 µm, Olympus FSX100). CG, control group. 2903: group infected with MHOM/BR/1975/M2903. 2314: group infected with MHOM/BR/2003/2314. 1655: group infected with MHOM/BR/2000/1655.

(Trevizan et al., 2016; Santos et al., 2018b); this may have led to the changes observed in the absorptive cells.

TGF-β may have contrasting roles in intestinal inflammation (Feagins, 2010). It possibly maintains intestinal homeostasis (Troncone et al., 2018). On the other hand, increased levels of this cytokine are found in areas of active intestinal inflammation (Feagins, 2010). It also has a role in the susceptibility of infection by *L. (V.) braziliensis* (Barral-Netto et al., 1992; Barral et al., 1995) and other species of *Leishmania* (Li et al., 1999; Gantt et al., 2003; Saha et al., 2007; Farage Frade et al., 2011). TGF-β performs the negative regulation of various macrophase-related microbicidal functions (Gantt et al., 2003; de Oliveira and Brodskyn, 2012). This includes decreasing NO production (Vodovotz et al., 1993; Bogdan, 2020), which is one of the principal defense mechanisms against infection (Bogdan, 2020). *In vitro* studies using the same strains as our study have not detected NO production by macrophages (Fernandes et al., 2016).

TGF-β acts on mast cells and performs opposite roles that may induce chemotaxis (Caslin et al., 2018). It is also capable of inhibiting the proliferation and development of mast cells and suppressing their function and survival (Ryan et al., 2007; Fernando et al., 2013; Caslin et al., 2018). Mast cells are important for tissue regeneration, as they enable the remodeling of collagen fibers (Hamilton et al., 2014). A positive correlation exists between the quantity of mast cells and immature collagen fibers (Ribeiro et al., 2018), which can be observed in group 2314 at 120 days of infection. Mature collagen fibers decreased after infection, demonstrating tissue remodeling (Pastre et al., 2019).

In the experimental conditions used in our study, *L. (V.) braziliensis* infection caused distinct alterations dependent by strain and infection duration in hamster ileum. In fact, in group 1655, some changes observed at 90 days of infection, approached values of the control group at 120 days.Ileums generally seemed to adapt to infection, considering the reduction of inflammatory cells and increase of elements involving tissue regeneration at 120 days of infection. The changes observed in hamsters infected with the MHOM/BR/2000/1655 strain were milder, although this strain was isolated from a patient with a reactivation of a lesion that had been previously considered cured. The groups infected with the strain isolated from a patient effectively treated with Glucantime® (MHOM/BR/2003/2314) presented a greater effect in the ileum histoarchitecture that remained at 120 days of infection. These results show the significance of the host and their specific response to infection by different strains of the parasite.

Our results revealed that *L. (V.) braziliensis* infection leads to different morphological, cellular, biochemical and ENS neurons changes in hamster ileum. Although clinical signs were not observed during the experimental period, our results show that the intestine is a possible target for future studies of the *L. (V.) braziliensis* host relationship. Further studies are needed to clarify the impacts of these changes on the function of the organ and the mechanisms involved in the process.

DATA AVAILABILITY STATEMENT

The raw data supporting the conclusions of this article will be made available by the authors, without undue reservation.

ETHICS STATEMENT

The animal study was reviewed and approved by Ethical Committee on Animal Use of the Universidade Estadual de Maringá under protocol number 7587260416.

AUTHOR CONTRIBUTIONS

AS, AF, TS, DS, and GN-M contributed to the conception, experimental design and implementation of the study. AS, MS, EC, and LL contributed to methodology and analyses. AS and GN-M was responsible for interpretation of data. AS and GN-M wrote the article. All authors contributed to the article and approved the submitted version.

FUNDING

This study was financed in part by the Coordenação de Aperfeiçoamento de Pessoal de Nível Superior - Brasil (CAPES) - Finance Code 001 and by the Conselho Nacional de Desenvolvimento Científico e Tecnológico - Brasil (CNPq) - Grant Number: 4226522016-4.

ACKNOWLEDGMENTS

The authors thank the Coordenação de Aperfeiçoamento de Pessoal de Nível Superior, the Conselho Nacional de Desenvolvimento Científico e Tecnológico, the Leishmaniasis Laboratory, and the Laboratories of Parasitology and Clinical Parasitology, especially the Professor Max Jean de Ornelas Toledo. Also, the Department of Morphological Sciences and the Department of Clinical Analysis and Biomedicine at Universidade Estadual de Maringá.

REFERENCES

Abbas, A., Lichtman, A., and Pillai, S. (2017). *Cellular and Molecular Immunology. 9th ed* (Philadelphia: Elsevier).

Ahn, J. Y., Lee, K. H., Choi, C. H., Kim, J. W., Lee, H. W., Kim, J. W., et al. (2014). Colonic Mucosal Immune Activity in Irritable Bowel Syndrome: Comparison With Healthy Controls and Patients With Ulcerative Colitis. *Dig. Dis. Sci.* 59, 1001–1011. doi: 10.1007/s10620-013-2930-4

Almeida, M. C., Cuba-Cuba, C. A., Moraes, M. A. P., and Miles, M. A. (1996). Dissemination of *Leishmania (Viannia) braziliensis*. *J. Comp. Pathol.* 115, 311–316. doi: 10.1016/S0021-9975(96)80088-0

Araújo, E.J.d. (2015). *Toxoplasma Gondii* Causes Death and Plastic Alteration in the Jejunal Myenteric Plexus. *World J. Gastroenterol.* 21:4829. doi: 10.3748/wjg.v21.i16.4829

Baba, C. S., Makharia, G. K., Mathur, P., Ray, R., Gupta, S. D., and Samantaray, J. C. (2006). Chronic Diarrhea and Malabsorption Caused by *Leishmania Donovani*. *Indian J. Gastroenterol.* 25, 309–310.

Barral, A., de Freitas, L. A. R., Carvalho, E. M., Almeida, R. P., Barral-Netto, M., and de Jesus, A. M. R. (1996). Biological Behavior of *Leishmania Amazonensis* Isolated From Humans With Cutaneous, Mucosal, or Visceral Leishmaniasis in Balb/C Mice. *Am. J. Trop. Med. Hyg.* 54, 178–184. doi: 10.4269/ajtmh.1996.54.178

Barral-Netto, M., Barral, A., Brownell, C. E., Skeiky, Y. A. W., Ellingsworth, L. R., Twardzik, D. R., et al. (1992). Transforming Growth Factor-β in Leishmanial Infection: A Parasite Escape Mechanism. *Sci. (80-.)* 257, 545–548. doi: 10.1126/science.1636092

Barral, A., Teixeira, M., Reis, P., Vinhas, V., Costa, J., Lessa, H., et al. (1995). Transforming Growth Factor-Beta in Human Cutaneous Leishmaniasis. *Am. J. Pathol.* 147, 947–954.

Bogdan, C. (2020). Macrophages as Host, Effector and Immunoregulatory Cells in Leishmaniasis: Impact of Tissue Micro-Environment and Metabolism. *Cytokine X* 2:100041. doi: 10.1016/j.cytox.2020.100041

Caslin, H. L., Kiwanuka, K. N., Haque, T. T., Taruselli, M. T., MacKnight, H. P., Paranjape, A., et al. (2018). Controlling Mast Cell Activation and Homeostasis: Work Influenced by Bill Paul That Continues Today. *Front. Immunol.* 9, 868. doi: 10.3389/fimmu.2018.00868

Chassaing, B., Kumar, M., Baker, M. T., Singh, V., and Vijay-Kumar, M. (2014). Mammalian Gut Immunity. *Biomed. J.* 37, 246–258. doi: 10.4103/2319-4170.130922

Chattopadhyay, A., Mittal, S., Gupta, K., Dhir, V., and Jain, S. (2020). Intestinal Leishmaniasis. *Clin. Microbiol. Infect.* 26, 1345–1346. doi: 10.1016/j.cmi.2020.05.003

Christofi, F. L. (2008). Purinergic Receptors and Gastrointestinal Secretomotor Function. *Purinergic Signal.* 4, 213–236. doi: 10.1007/s11302-008-9104-4

Conceição-Silva, F., and Morgado, F. N. (2019). *Leishmania* Spp-Host Interaction: There Is Always an Onset, But Is There An End? *Front. Cell. Infect. Microbiol.* 9, 330. doi: 10.3389/fcimb.2019.00330

Cruz, A. A. V., Alves-Ferreira, E. V. C., Milbratz-Moré, G., Chahud, F., Ruy, P. C., Duarte, M. I. S., et al. (2017). Case Report: Sclerosing Orbital Inflammation Caused by *Leishmania braziliensis*. *Am. J. Trop. Med. Hyg.* 96, 197–199. doi: 10.4269/ajtmh.16-0389

da Silva, M. V., Marosti, A. R., Mendes, C. E., Palombit, K., and Castelucci, P. (2017). Submucosal Neurons and Enteric Glial Cells Expressing the P2X7 Receptor in Rat Experimental Colitis. *Acta Histochem.* 119, 481–494. doi: 10.1016/j.acthis.2017.05.001

De Giorgio, R., Guerrini, S., Barbara, G., Stanghellini, V., De Ponti, F., Corinaldesi, R., et al. (2004). Inflammatory Neuropathies of the Enteric Nervous System. *Gastroenterology* 126, 1872–1883. doi: 10.1053/j.gastro.2004.02.024

de Oliveira, C. I., and Brodskyn, C. I. (2012). The Immunobiology of *Leishmania braziliensis* Infection. *Front. Immunol.* 3:145. doi: 10.3389/fimmu.2012.00145

De Oliveira, C. I., Teixeira, M. J., Gomes, R., Barral, A., and Brodskyn, C. (2004). Animal Models for Infectious Diseases Caused by Parasites: Leishmaniasis. *Drug Discovery Today Dis. Model.* 1, 81–86. doi: 10.1016/j.ddmod.2004.07.005

Drokhlyansky, E., Smillie, C. S., Van Wittenberghe, N., Ericsson, M., Griffin, G. K., Eraslan, G., et al. (2020). The Human and Mouse Enteric Nervous System at Single-Cell Resolution. *Cell* 182, 1606–1622.e23. doi: 10.1016/j.cell.2020.08.003

Farage Frade, A., Campos de Oliveira, L., Lamounier Costa, D., Henrique Nery Costa, C., Aquino, D., Van Weyenbergh, J., et al. (2011). TGFB1 and IL8 Gene Polymorphisms and Susceptibility to Visceral Leishmaniasis. *Infect. Genet. Evol.* 11, 912–916. doi: 10.1016/j.meegid.2011.02.014

Feagins, L. A. (2010). Role of Transforming Growth Factor-β in Inflammatory Bowel Disease and Colitis-Associated Colon Cancer. *Inflamm. Bowel Dis.* 16, 1963–1968. doi: 10.1002/ibd.21281

Fernandes, A. C. B. S., Pedroso, R. B., de Mello, T. F. P., Donatti, L., Venazzi, E. A. S., Demarchi, I. G., et al. (2016). *In Vitro* Characterization of *Leishmania (Viannia) braziliensis* Isolates From Patients With Different Responses to Glucantime ® Treatment From Northwest Paraná, Brazil. *Exp. Parasitol.* 167, 83–93. doi: 10.1016/j.exppara.2016.05.003

Fernando, J., Faber, T. W., Pullen, N. A., Falanga, Y. T., Kolawole, E. M., Oskeritzian, C. A., et al. (2013). Genotype-Dependent Effects of TGF-β1 on Mast Cell Function: Targeting the Stat5 Pathway. *J. Immunol.* 191, 4505–4513. doi: 10.4049/jimmunol.1202723

Figueiredo, M. M., Deoti, B., Amorim, I. F., Pinto, A. J. W., Moraes, A., Carvalho, C. S., et al. (2014). Expression of Regulatory T Cells in Jejunum, Colon, and Cervical and Mesenteric Lymph Nodes of Dogs Naturally Infected With *Leishmania Infantum*. *Infect. Immun.* 82, 3704–3712. doi: 10.1128/IAI.01862-14

Gagini, T., De Oliveira Schubach, A., De Fatima Madeira, M., Valete-Rosalino, C. M., Pimentel, M. I. F., and Da Silva Pacheco, R. (2017). Genotypic Profiles of Leishmania (Viannia) braziliensis Strains From Cutaneous Leishmaniasis Patients and Their Relationship With the Response to Meglumine Antimoniate Treatment: A Pilot Study. *Parasite* 24, 1–11. doi: 10.1051/parasite/2017035

Gantt, K. R., Schultz-Cherry, S., Rodriguez, N., Jeronimo, S. M. B., Nascimento, E. T., Goldman, T. L., et al. (2003). Activation of TGF-β by *Leishmania Chagasi*: Importance for Parasite Survival in Macrophages. *J. Immunol.* 170, 2613–2620. doi: 10.4049/jimmunol.170.5.2613

Góis, M. B., Hermes-Uliana, C., Barreto Zago, M. C., Zanoni, J. N., da Silva, A. V., de Miranda-Neto, M. H., et al. (2016). Chronic Infection With *Toxoplasma Gondii* Induces Death of Submucosal Enteric Neurons and Damage in the Colonic Mucosa of Rats. *Exp. Parasitol.* 164, 56–63. doi: 10.1016/j.exppara.2016.02.009

Gomes-Silva, A., Valverde, J. G., Ribeiro-Romão, R. P., Plácido-Pereira, R. M., and da-Cruz, A. M. (2013). Golden Hamster (*Mesocricetus Auratus*) as an Experimental Model for *Leishmania (Viannia) braziliensis* Infection. *Parasitology* 140, 771–779. doi: 10.1017/S0031182012002156

Gontijo, C. M., Pacheco, R. S., Oréfice, F., Lasmar, E., Silva, E. S., and Melo, M. N. (2002). Concurrent Cutaneous, Visceral and Ocular Leishmaniasis Caused by *Leishmania (Viannia) braziliensis* in a Kidney Transplant Patient. *Mem. Inst. Oswaldo Cruz* 97, 751–753. doi: 10.1590/S0074-02762002000500029

Guimarães, L. H., Queiroz, A., Silva, J. A., Silva, S. C., Magalhães, V., Lago, E. L., et al. (2016). Atypical Manifestations of Cutaneous Leishmaniasis in a Region Endemic for *Leishmania braziliensis*: Clinical, Immunological and Parasitological Aspects. *PloS Negl. Trop. Dis.* 10, e0005100. doi: 10.1371/journal.pntd.0005100

Hamilton, M. J., Frei, S. M., and Stevens, R. L. (2014). The Multifaceted Mast Cell in Inflammatory Bowel Disease. *Inflamm. Bowel Dis.* 20, 2364–2378. doi: 10.1097/MIB.0000000000000142

Hoyos, C. L., Quipildor, M., Bracamonte, E., Lauthier, J. J., Cajal, P., Uncos, A., et al. (2019). Simultaneous Occurrence of Cutaneous and Mucocutaneous Leishmaniasis Caused by Different Genotypes of *Leishmania (Viannia) braziliensis*. *J. Dermatol.* 46, e320–e322. doi: 10.1111/1346-8138.14866

Hu, M. D., and Edelblum, ,. K. L. (2017). Sentinels at the Frontline: The Role of Intraepithelial Lymphocytes in Inflammatory Bowel Disease. *Curr. Pharmacol. Rep.* 3, 321–334. doi: 10.1007/s40495-017-0105-2

Jacobson, A., Yang, D., Vella, M., and Chiu, ,. I. M. (2021). The Intestinal Neuro-Immune Axis: Crosstalk Between Neurons, Immune Cells, and Microbes. *Mucosal Immunol.* 14, 555–565. doi: 10.1038/s41385-020-00368-1

Lewis, M. D., Paun, A., Romano, A., Langston, H., Langner, C. A., Moore, I. N., et al. (2020). Fatal Progression of Experimental Visceral Leishmaniasis is Associated With Intestinal Parasitism and Secondary Infection by Commensal Bacteria, and is Delayed by Antibiotic Prophylaxis. *PloS Pathog.* 16, e1008456. doi: 10.1371/journal.ppat.1008456

Li, J., Hunter, C. A., and Farrell, J. P. (1999). Anti-TGF-Beta Treatment Promotes Rapid Healing of *Leishmania Major* Infection in Mice by Enhancing *In Vivo* Nitric Oxide Production. *J. Immunol.* 162, 974–979.

Machado, C. C. A., Watanabe, P., Mendes, d., de L, J. D., Pupim, A. C. E., Ortigoza, S. M., et al. (2021). *Toxoplasma Gondii* Infection Impairs the Colonic Motility of Rats Due to Loss of Myenteric Neurons. *Neurogastroenterol. Motil.* 33:13967. doi: 10.1111/nmo.13967

Mahadeva, S., Wyatt, J. I., and Howdle, P. D. (2002). Is a Raised Intraepithelial Lymphocyte Count With Normal Duodenal Villous Architecture Clinically Relevant? *J. Clin. Pathol.* 55, 424–428. doi: 10.1136/jcp.55.6.424

Mawe, G. M., Strong, D. S., and Sharkey, K. A. (2009). Plasticity of Enteric Nerve Functions in the Inflamed and Postinflamed Gut. *Neurogastroenterol. Motil.* 21, 481–491. doi: 10.1111/j.1365-2982.2009.01291.x

Ministério da Saúde (2017). "Manual de Vigilância da Leishmaniose Tegumentar Americana," *1st ed* (Brasília: Ministério da Saúde). Available at: http://bvsms.saude.gov.br/bvs/publicacoes/manual_vigilancia_leishmaniose_tegumentar_americana.pdf.

Mowat, A. M., and Agace, W. W. (2014). Regional Specialization Within the Intestinal Immune System. *Nat. Rev. Immunol.* 14, 667–685. doi: 10.1038/nri3738

Nezami, B. G., and Srinivasan, S. (2010). Enteric Nervous System in the Small Intestine: Pathophysiology and Clinical Implications. *Curr. Gastroenterol. Rep.* 12, 358–365. doi: 10.1007/s11894-010-0129-9

Pan American Health Organization (2019). *Leishmaniasis: Epidemiological Report in the Americas* (Washington, D.C). Available at: http://iris.paho.org/xmlui/handle/123456789/50505.

Panza, S. B., Vargas, R., Balbo, S. L., Bonfleur, M. L., Granzotto, D. C. T., Sant'Ana, D. M. G., et al. (2021). Perinatal Exposure to Low Doses of Glyphosate-Based Herbicide Combined With a High-Fat Diet in Adulthood Causes Changes in the Jejunums of Mice. *Life Sci.* 275, 119350. doi: 10.1016/j.lfs.2021.119350

Passos, F. C., Gois, M. B., Sousa, A. D., de Marinho, A. I. L., Corvo, L., Soto, M., et al. (2020). Investigating Associations Between Intestinal Alterations and Parasite Load According to Bifidobacterium Spp. And Lactobacillus Spp. Abundance in the Gut Microbiota of Hamsters Infected by *Leishmania Infantum*. *Mem. Inst. Oswaldo Cruz* 115, 1–11. doi: 10.1590/0074-02760200377

Pastre, M. J., Casagrande, L., Gois, M. B., Pereira-Severi, L. S., Miqueloto, C. A., Garcia, J. L., et al. (2019). *Toxoplasma Gondii* Causes Increased ICAM-1 and Serotonin Expression in the Jejunum of Rats 12 H After Infection. *Biomed. Pharmacother.* 114:108797. doi: 10.1016/J.BIOPHA.2019.108797

Patino, L. H., Muñoz, M., Cruz-Saavedra, L., Muskus, C., and Ramírez, J. D. (2020). Genomic Diversification, Structural Plasticity, and Hybridization in *Leishmania (Viannia) braziliensis*. *Front. Cell. Infect. Microbiol.* 10, 582192. doi: 10.3389/fcimb.2020.582192

Pereira, C. G., Silva, A. L. N., de Castilhos, P., Mastrantonio, E. C., Souza, R. A., Romão, R. P., et al. (2009). Different Isolates From *Leishmania braziliensis* Complex Induce Distinct Histopathological Features in a Murine Model of Infection. *Vet. Parasitol.* 165, 231–240. doi: 10.1016/j.vetpar.2009.07.019

Quaresma, P. F., De Brito, C. F. A., Rugani, J. M. N., Freire, J. D. M., Baptista, R. D. P., Moreno, E. C., et al. (2018). Distinct Genetic Profiles of *Leishmania (Viannia) braziliensis* Associate With Clinical Variations in Cutaneous-Leishmaniasis Patients From an Endemic Area in Brazil. *Proc. Int. Astron. Union* 145, 1161–1169. doi: 10.1017/S0031182018000276

Raina, S., Raina, R. K., Bodh, A., Rana, B. S., and Sharma, R. (2017). Gastrointestinal Leishmaniasis in Non-Endemic Region. *J. Assoc. Phys. India* 65, 106–107.

Rêgo, F. D., da Rocha Lima, A. C. V. M., Pereira, A. A. S., Quaresma, P. F., Pascoal-Xavier, M. A., Shaw, J. J., et al. (2018). Genetic Variant Strains of *Leishmania (Viannia) braziliensis* Exhibit Distinct Biological Behaviors. *Parasitol. Res.* 117, 3157–3168. doi: 10.1007/s00436-018-6014-4

Rêgo, F. D., Fradico, J. R. B., Teixeira-Carvalho, A., and Gontijo, C. M. F. (2019). Molecular Variants of *Leishmania (Viannia) braziliensis* Trigger Distinct Patterns of Cytokines and Chemokines Expression in Golden Hamster. *Mol. Immunol.* 106, 36–45. doi: 10.1016/j.molimm.2018.12.013

Ribeiro, L. S. F., dos Santos, J. N., Rocha, C. A. G., and Cury, P. R. (2018). Association Between Mast Cells and Collagen Maturation in Chronic Periodontitis in Humans. *J. Histochem. Cytochem.* 66, 467–475. doi: 10.1369/0022155418765131

Ribeiro-Romão, R. P., Moreira, O. C., Osorio, E. Y., Cysne-Finkelstein, L., Gomes-Silva, A., Valverde, J. G., et al. (2014). Comparative Evaluation of Lesion Development, Tissue Damage, and Cytokine Expression in Golden Hamsters (*Mesocricetus Auratus*) Infected by Inocula With Different *Leishmania (Viannia) braziliensis* Concentrations. *Infect. Immun.* 82, 5203–5213. doi: 10.1128/IAI.02083-14

Rugani, J. N., Quaresma, P. F., Gontijo, C. F., Soares, R. P., and Monte-Neto, R. L. (2018). Intraspecies Susceptibility of *Leishmania (Viannia) braziliensis* to Antileishmanial Drugs: Antimony Resistance in Human Isolates From Atypical Lesions. *Biomed. Pharmacother.* 108, 1170–1180. doi: 10.1016/j.biopha.2018.09.149

Ryan, J. J., Kashyap, M., Bailey, D., Kennedy, S., Speiran, K., Brenzovich, J., et al. (2007). Mast Cell Homeostasis: A Fundamental Aspect of Allergic Disease. *Crit. Rev. Immunol.* 27, 15–32. doi: 10.1615/critrevimmunol.v27.i1.20

Saha, S., Mondal, S., Ravindran, R., Bhowmick, S., Modak, D., Mallick, S., et al. (2007). IL-10- and TGF-β-Mediated Susceptibility in Kala-Azar and Post-Kala-Azar Dermal Leishmaniasis: The Significance of Amphotericin B in the Control of *Leishmania Donovani* Infection in India. *J. Immunol.* 179, 5592–5603. doi: 10.4049/jimmunol.179.8.5592

Sangild, P. T., Mei, J., Fowden, A. L., and Xu, R. J. (2009). The Prenatal Porcine Intestine has Low Transforming Growth Factor-Beta Ligand and Receptor Density and Shows Reduced Trophic Response to Enteral Diets. *Am. J. Physiol. Integr. Comp. Physiol.* 296, R1053–R1062. doi: 10.1152/ajpregu.90790.2008

Santaolalla, R., Fukata, M., and Abreu, M. T. (2011). Innate Immunity in the Small Intestine. *Curr. Opin. Gastroenterol.* 27, 125–131. doi: 10.1097/MOG.0b013e3283438dea

Santos, A.G.A.d., Ferlini, J. de P., Vicentino, S. L., Lonardoni, M. V. C., Sant'Ana, D., de, M. G., et al. (2018a). Alterations Induced in the Ileum of Mice Upon Inoculation With Different Species of *Leishmania*: A Preliminary Study. *Rev. Soc Bras. Med. Trop.* 51, 537–541. doi: 10.1590/0037-8682-0348-2017

Santos, A.G.A.d., Lima, L.L. de, Mota, C. A., Gois, M. B., Fernandes, A. C. B. S., Silveira, T. G. V., et al. (2018b). Insights of *Leishmania (Viannia) braziliensis* Infection in Golden Hamster (*Mesocricetus Auratus*) Intestine. *Biomed. Pharmacother.* 106, 1624–1632. doi: 10.1016/j.biopha.2018.07.120

Schneider, L. C. L., do Nascimento, J. C. P., Trevizan, A. R., Góis, M. B., Borges, S. C., Beraldi, E. J., et al. (2018). *Toxoplasma Gondii* Promotes Changes in VIPergic Submucosal Neurons, Mucosal Intraepithelial Lymphocytes, and Goblet Cells During Acute Infection in the Ileum of Rats. *Neurogastroenterol. Motil.* 30, e13264. doi: 10.1111/nmo.13264

Sergi, C., Shen, F., and Bouma, G. (2017). Intraepithelial Lymphocytes, Scores, Mimickers and Challenges in Diagnosing Gluten-Sensitive Enteropathy (Celiac Disease). *World J. Gastroenterol.* 23, 573–589. doi: 10.3748/wjg.v23.i4.573

Silva, D.T. da, Alves, M. L., Spada, J. C. P., Silveira, R. de C.V., Oliveira, T.M.F.d., and Starke-Buzetti, ,. W. A. (2018). Neutrophils, Eosinophils, and Mast Cells in the Intestinal Wall of Dogs Naturally Infected With *Leishmania Infantum*. *Rev. Bras. Parasitol. Vet.* 27, 430–438. doi: 10.1590/s1984-296120180085

Silva, L., Damrose, E., and Fernandes, , A.-M.-F. (2017). Laryngeal Leishmaniasis, a Rare Manifestation of an Emerging Disease. *Eur. Ann. Otorhinolaryngol. Head Neck Dis.* 134, 211–212. doi: 10.1016/j.anorl.2015.11.013

Silva, D. T., Neves, M. F., Queiroz, N. M. G. P., de Spada, J. C. P., Alves, M. L., Flóro e Silva, M., et al. (2016). Correlation Study and Histopathological Description of Intestinal Alterations in Dogs Infected With Leishmania Infantum. *Rev. Bras. Parasitol. Vet.* 25, 24–36. doi: 10.1590/S1984-29612016009

Silva, E.S. da, Pacheco, R. S., Gontijo, C. M. F., Carvalho, I. R., and Brazil, R. P. (2002). Visceral Leishmaniasis Caused by *Leishmania (Viannia) braziliensis* in a Patient Infected With Human Immunodeficiency Virus. *Rev. do Inst. Med. Trop. São Paulo* 44, 145–149. doi: 10.1590/S0036-46652002000300006

Soria López, E., Olalla Sierra, J., Del Arco Jiménez, A., Pereda Salguero, T., Abitei, C., and de la Torre Lima, J. (2016). Colonic Leishmaniasis in a Patient With HIV: A Case Report. *Rev. Esp. Enferm. Dig.* 108, 838–840. doi: 10.17235/reed.2016.4038/2015

Souza, K. D., Fernandes, E. P. A., Santos, A. G. A., Lima, L. L., Gonzaga, W. F. K. M., Xander, P., et al. (2019). Infection by *Leishmania (Leishmania) Infantum Chagasi* Causes Intestinal Changes B-1 Cells Dependent. *Parasit. Immunol.* 41, e12661. doi: 10.1111/pim.12661

Trevizan, A. R., Schneider, L. C. L., Araújo, E. J., de, A., Garcia, J. L., Buttow, N. C., et al. (2019). Acute *Toxoplasma Gondii* Infection Alters the Number of Neurons and the Proportion of Enteric Glial Cells in the Duodenum in Wistar Rats. *Neurogastroenterol. Motil.* 31, e13523. doi: 10.1111/nmo.13523

Trevizan, A. R., Vicentino-Vieira, S. L., da Silva Watanabe, P., Góis, M. B., de Melo, G., de, A. N., et al. (2016). Kinetics of Acute Infection With *Toxoplasma Gondii* and Histopathological Changes in the Duodenum of Rats. *Exp. Parasitol.* 165, 22–29. doi: 10.1016/j.exppara.2016.03.015

Troncone, E., Marafini, I., Stolfi, C., and Monteleone, G. (2018). Transforming Growth Factor-β1/Smad7 in Intestinal Immunity, Inflammation, and Cancer. *Front. Immunol.* 9, 1407. doi: 10.3389/fimmu.2018.01407

Vieira, T., da, S., Rugani, J. N., Nogueira, P. M., Torrecilhas, A. C., Gontijo, C. M. F., et al. (2019). Intraspecies Polymorphisms in the Lipophosphoglycan of *L. braziliensis* Differentially Modulate Macrophage Activation via TLR4. *Front. Cell. Infect. Microbiol.* 9, 240. doi: 10.3389/fcimb.2019.00240

Vodovotz, Y., Bogdan, C., Paik, J., Xie, Q. W., and Nathan, C. (1993). Mechanisms of Suppression of Macrophage Nitric Oxide Release by Transforming Growth Factor γ. *J. Exp. Med.* 178, 605–613. doi: 10.1084/jem.178.2.605

World Health Organization (2020). *Global Leishmaniasis Surveillance 2017–2018, and First Report on 5 Additional Indicators* (Genebra). Available at: https://apps.who.int/iris/bitstream/handle/10665/339849/WER9608-eng-fre.pdf.

Yoo, B. B., and Mazmanian, S. K. (2017). The Enteric Network: Interactions Between the Immune and Nervous Systems of the Gut. *Immunity* 46, 910–926. doi: 10.1016/j.immuni.2017.05.011

Yu, Y., Daly, D. M., Adam, I. J., Kitsanta, P., Hill, C. J., Wild, J., et al. (2016). Interplay Between Mast Cells, Enterochromaffin Cells, and Sensory Signaling in the Aging Human Bowel. *Neurogastroenterol. Motil.* 28, 1465–1479. doi: 10.1111/nmo.12842

Conflict of Interest: The authors declare that the research was conducted in the absence of any commercial or financial relationships that could be construed as a potential conflict of interest.

frontiers in Cellular and Infection Microbiology

ORIGINAL RESEARCH
published: 19 August 2021
doi: 10.3389/fcimb.2021.702676

Thermoresponsive Copolymer Nanovectors Improve the Bioavailability of Retrograde Inhibitors in the Treatment of *Leishmania* Infections

Evan Craig[1], *Anna Calarco*[2], *Raffaele Conte*[2], *Veronica Ambrogi*[3], *Giovanna Gomez d'Ayala*[4], *Philip Alabi*[5], *Jason K. Sello*[5], *Pierfrancesco Cerruti*[4*] and *Peter E. Kima*[1*]

[1] Department of Microbiology and Cell Science, University of Florida, Gainesville, FL, United States, [2] Research Institute on Terrestrial Ecosystems (IRET-CNR), Napoli, Italy, [3] Department of Chemical, Materials and Production Engineering (DICMaPI) – University of Naples Federico II, Napoli, Italy, [4] Institute for Polymers, Composites and Biomaterials (IPCB-CNR), Pozzuoli, Italy, [5] Department of Pharmaceutical Chemistry, University of California, San Francisco, San Francisco, CA, United States

OPEN ACCESS

Edited by:
Izabel Galhardo Demarchi, Federal University of Santa Catarina, Brazil

Reviewed by:
Danilo Ciccone Miguel, State University of Campinas, Brazil
Mauro Javier Cortez Veliz, University of São Paulo, Brazil

***Correspondence:**
Peter E. Kima
pkima@ufl.edu
Pierfrancesco Cerruti
cerruti@ipcb.cnr.it

Specialty section:
This article was submitted to Parasite and Host, a section of the journal Frontiers in Cellular and Infection Microbiology

Received: *29 April 2021*
Accepted: *09 July 2021*
Published: *19 August 2021*

Citation:
Craig E, Calarco A, Conte R, Ambrogi V, d'Ayala GG, Alabi P, Sello JK, Cerruti P and Kima PE (2021) Thermoresponsive Copolymer Nanovectors Improve the Bioavailability of Retrograde Inhibitors in the Treatment of Leishmania Infections. Front. Cell. Infect. Microbiol. 11:702676. doi: 10.3389/fcimb.2021.702676

Clinical manifestations of leishmaniasis range from self-healing, cutaneous lesions to fatal infections of the viscera. With no preventative *Leishmania* vaccine available, the frontline option against leishmaniasis is chemotherapy. Unfortunately, currently available anti-*Leishmania* drugs face several obstacles, including toxicity that limits dosing and emergent drug resistant strains in endemic regions. It is, therefore, imperative that more effective drug formulations with decreased toxicity profiles are developed. Previous studies had shown that 2-(((5-Methyl-2-thienyl)methylene)amino)-N-phenylbenzamide (also called Retro-2) has efficacy against *Leishmania* infections. Structure–activity relationship (SAR) analogs of Retro-2, using the dihydroquinazolinone (DHQZ) base structure, were subsequently described that are more efficacious than Retro-2. However, considering the hydrophobic nature of these compounds that limits their solubility and uptake, the current studies were initiated to determine whether the solubility of Retro-2 and its SAR analogs could be enhanced through encapsulation in amphiphilic polymer nanoparticles. We evaluated encapsulation of these compounds in the amphiphilic, thermoresponsive oligo (ethylene glycol) methacrylate-*co*-pentafluorostyrene (PFG30) copolymer that forms nanoparticle aggregates upon heating past temperatures of 30°C. The hydrophobic tracer, coumarin 6, was used to evaluate uptake of a hydrophobic molecule into PFG30 aggregates. Mass spectrometry analysis showed considerably greater delivery of encapsulated DHQZ analogs into infected cells and more rapid shrinkage of *L. amazonensis* communal vacuoles. Moreover, encapsulation in PFG30 augmented the efficacy of Retro-2 and its SAR analogs to clear both *L. amazonensis* and *L. donovani* infections. These studies demonstrate that encapsulation of compounds in PFG30 is a viable approach to dramatically increase bioavailability and efficacy of anti-*Leishmania* compounds.

Keywords: *Leishmania*, Retro-2, retrograde inhibitors, thermoresponsive polymers, nanoaggregates, encapsulation, bioavailability, drug release

INTRODUCTION

Leishmania are flagellated, obligate, protozoan parasites in the Trypanosomatidae family. They are the causative agents of leishmaniases that manifest as three major clinical entities: cutaneous, mucocutaneous, and visceral infection. The prevalence of leishmaniasis is estimated at 12 to 15 million cases with 350 million people at risk worldwide. Annually, 1.5 to 2 million new leishmaniasis cases occur with approximately 70,000 deaths. In 2016, the World Health Organization (WHO) reported that of 200 countries, 87 (44%) and 75 (38%) countries were classified as endemic for cutaneous leishmaniasis (CL) or visceral leishmaniasis (VL), respectively (Arenas et al., 2017; World Health Organization, 2018; Inceboz, 2019). While CL cases are often self-limiting, VL cases are lethal requiring curative treatment with anti-leishmanial drugs. The WHO has classified leishmaniasis as a neglected disease. The few available drugs have important shortcomings, including high cost, toxicity, and the emergence of resistance strains. Control of VL has been further complicated in regions, including sub-Saharan Africa, that have high rates of human immunodeficiency virus (HIV) infection. HIV-VL-coinfection significantly increases the risk of development of VL as well as decreasing the efficacy of therapeutic responses (Alvar et al., 2008). As there is currently no clinically approved *Leishmania* vaccine, the discovery of new anti-*Leishmania* compounds or strategies to improve current treatments is sorely needed.

A few studies have reported on the antileishmanial efficacy of Retro-2, a small, organic, retrograde pathway inhibitor. Retro-2 was initially identified using high-throughput screens of a chemical library to identify compounds that could limit the toxicity of *Shiga* toxin [*Shiga*-like toxin 1 (SLT1) and 2 (SLT2)], a toxin from enterohemorrhagic *Escherichia coli* or *Shigella dysenteriae*, as well as the plant toxin, ricin. Retro-2 appeared to function through prevention of retrograde transport of these toxins (Stechmann et al., 2010). The efficacy of Retro-2 on *Leishmania* infections was subsequently demonstrated (Canton and Kima, 2012). Craig et al. and other reports later showed that the structural–activity relationship (SAR) analogs, DHQZ 36 and DHQZ 36.1, were more efficacious against both *L. amazonensis* and *L. donovani* infections (Canton and Kima, 2012; Craig et al., 2017; Gupta et al., 2017). While the precise mechanism of action of Retro-2 and its SAR analogs in *Leishmania* infections is not known, its application was shown to result in the shrinkage of the communal *Leishmania* parasitophorous vacuoles (LPVs) that harbor *L. pifanoi* or *L. amazonensis* amastigotes. LPVs had been demonstrated to be hybrid compartments that in addition to their extensive interactions with the endocytic pathway, they also displayed secretory pathway molecules (Canton et al., 2012). Acquisition of secretory pathway molecules was shown to be dependent on the actions of syntaxin 5 (Stx5), a SNARE that participates in vesicle transport and fusion at several points in the secretory pathway (Canton and Kima, 2012; Canton et al., 2012; Arango Duque et al., 2019). Loss of Stx5 function through the expression of a dominant-negative mutant or by siRNA silencing of Stx5 or treatment with Retro-2 resulted in decreased localization of Stx5 to the LPV membrane, as well as a significant decrease in vacuole size and parasite burden (Ndjamen et al., 2010; Canton and Kima, 2012; Canton et al., 2012). Unlike Retro-2, the SAR DHQZ analogs, DHQZ 36 and DHQZ 36.1, are directly *Leishmania*-cidal (Craig et al., 2017).

While improvements in efficacy through SAR analog development are encouraging, Retro-2 and the SAR analogs are limited by their hydrophobic nature. Retro-2 solubility is estimated at <0.4 mg/ml in H_2O (Carney et al., 2014; Gandhi et al., 2019). It, therefore, requires the use of an organic solvent, such as dimethyl sulfoxide (DMSO), for solubilization and uptake by mammalian cells. One method to significantly improve solubility of hydrophobic compounds while also ensuring protection against degradation is the encapsulation of the drug within nanoparticles. The latter may be made of inorganic or organic, inert, biodegradable materials that form a capsule-like structure around the compound. The benefits of encapsulation include increased solubility and bioavailability, protection against degradation, and the potential for modified release kinetics or targeting to specific sites in the body, thereby reducing toxicity of the compound of interest (Banik et al., 2016; Barouti et al., 2017). This increase in bioavailability while limiting toxicity has resulted in improved safety profiles and efficacy of a multitude of anti-*Leishmania* compounds including liposomal AmB that is currently approved for clinical use (Croft and Coombs, 2003; Nafari et al., 2020). Thus, it is likely that Retro-2 and SAR DHQZ analogs would greatly benefit from nanoparticle encapsulation to improve efficacy of these compounds through improved solubility and delivery.

In this regard, amphiphilic, thermoresponsive polymers are suitable as encapsulation vectors for hydrophobic SAR analogs. They are soluble in organic solvents, while their solubility in water dramatically depends on the temperature. In particular, below a critical temperature (defined as low critical solution temperature, LCST), they form water-soluble nanosized micelles, which are able to encapsulate hydrophobic guest molecules in their hydrophobic core (Almeida et al., 2012). When the temperature exceeds the LCST, hydrogen-bonding interactions between hydrophilic micelle shell and water molecules weaken, and those between hydrophobic moieties become dominant leading to a collapse of polymer chains. The resulting intermicellar aggregates can aptly be used as intracellular drug delivery vectors (Sponchioni et al., 2019).

Recently, it was shown that an amphiphilic statistical copolymer based on oligo(ethylene glycol) methacrylate (OEGMA, M_n = 300 g/mol) and 30%mol pentafluorostyrene (PFS) (known as PFG30) forms micelles of about 10 nm at room temperature, which self-assemble into 200-nm-sized intermicellar nanoaggregates at temperatures greater than 30°C (Zuppardi et al., 2017). Another study showed that PFG copolymers of different molecular weights were able to efficiently encapsulate and remove a hydrophobic dye, Nile Red, from aqueous solutions by up to 90% removal (Zuppardi et al., 2020). Based on these results, this study evaluates the potential application of PFG30 for the delivery of Retro-2 and its

SAR analogs, DHQZ 36 and DHQZ 36.1, to *Leishmania*-infected cells.

MATERIALS AND METHODS

Cell Lines

RAW264.7 murine macrophages were obtained from ATCC (ATCC TIB-71, ATCC, USA) and maintained in Dulbecco's Modified Eagle's Medium (DMEM) supplemented with 10% fetal bovine serum (FBS) and 100 μg/ml streptomycin-penicillin. They were cultured in a humidified atmosphere at 37°C with 5% CO_2.

Parasites

Promastigotes of *L. amazonensis* strain RAT/BA/74/LV78 (LV78) obtained from Dr. Lynn Soong (UTMB, TX) were maintained at 26°C in Schneider's Drosophila medium supplemented with 10% heat-inactivated FBS and 10 μg/ml Gentamycin. Promastigotes of *L. donovani* [MHOM/SD/62/1S-C12D (SD)] obtained from Dr. Hira L. Nakhasi laboratory (FDA, MD) was maintained at 26°C in M199 medium supplemented with 10% heat-inactivated FBS and 1% penicillin/streptomycin.

Materials Preparation and Stock Solutions

Retro-2, DHQZ 36, and DHQZ 36.1 were synthesized by Dr. Jason Sello at Brown University as described previously (Carney et al., 2014; Craig et al., 2017). Stock solutions were prepared in DMSO at concentrations of 20 or 30 mM. Retro-2 was also purchased from Sigma-Aldrich (CAS: 1429192-00-6) and prepared in DMSO, as well as at a concentration of 20 mM. Miltefosine was purchased from Sigma-Aldridge (catalog m5571), and a stock solution was prepared in filtered NanoPure diH_2O at a concentration of 10 mM. Coumarin 6 (C6) was purchased from Sigma-Aldrich (catalog 546283) and a stock solution was made in DMSO at a 5.3-mM solution. The tetrazolium salt MTT [3-(4,5-dimethylthiazol-2-yl)-2,5-diphenyl tetrazolium bromide] Cell Viability Assay Kit was purchased from Biotium (Fremont, CA).

PFG30 was prepared *via* radical polymerization under nitrogen in DMF as described previously (Zuppardi et al., 2017). PFG30 was dried *via* nitrogen until weight remained constant into a gel-like solid and stored at 4°C. Stock solutions were prepared in sterile-filtered, NanoPure diH_2O at concentrations of 10 mg/ml *via* gentle mixing in an Eppendorf tube at room temperature overnight. The 10-mg/ml stocks were then stored at 4°C prior to mixing with drugs or C6.

Modeling Drug Uptake Into PFG30 With C6

C6 solutions were prepared at concentrations between 0.5 and 50 μM in filter-sterilized, NanoPure diH_2O or incomplete DMEM. C6-loaded PFG30 aggregates were prepared by mixing volumes of a 5.3-mM C6 in DMSO stock solution with a 10-mg/ml PFG30 stock (at a 1:10 w/w C6:polymer ratio) to produce a 20- or 50-μM working PFG30 encapsulated C6 stock solution. This mixture was cooled at 4°C to allow solubilization of any PFG30 precipitate due to DMSO addition, and then heated at 37°C for 5 min to induce polymer self-assembly and C6 encapsulation. Additional warm (37°C) diH_2O or incomplete DMEM was added for a final volume of 1 ml at a C6 concentration of 20 or 50 μM, respectively. This solution was then serially diluted in warm diH_2O or incomplete DMEM to produce lower C6-loaded PFG30 aggregate concentrations as described in the text.

For fluorescence or NanoSight experiments, additional C6-free vehicle controls were prepared with DMSO with or without PFG30 encapsulation procedures to account for any signal due to clouding of the solution by polymer or DMSO alone. Both C6 and PFG30-C6 samples had their respective vehicle control fluorescence readings subtracted out to control for any vehicle signal.

To determine if a significant proportion of C6 was not encapsulated, centrifugation experiments were performed alongside C6-loaded PFG30 aggregate samples in fluorescence experiments. Samples for centrifugation were made as described above with aggregates prepared at a 1:10 w/w ratio in filter-sterilized diH_2O at 37°C. Prior to serial dilution, the stock PFG30:C6 solution made at 50 μM was centrifuged at 10,000*g* in a microcentrifuge for 3 min at 37°C to produce a pellet. Supernatant was then collected from the pellet to remove any free C6 unassociated with the PFG30 pellet. The pellet was then resolubilized in an equal part of diH_2O and chilled with gentle mixing. This solution was then reheated at 37°C for 5 min to encapsulate the remaining C6, and this solution and the supernatant were diluted in warm diH_2O for a final nominal concentration of 50 μM. Both sample pellets and the respective supernatants were then diluted to a nominal concentration of 5 μM for fluorescence measurements and compared with the non-centrifuged 5 μM PFG30-C6 sample to estimate the efficiency of the PFG30 encapsulation procedure.

Both sets of samples were then read on a BioTek Cytation™ 5 microplate reader with excitation and emission wavelengths set to 420 and 500 nm, respectively. Vehicle controls with equal portions of DMSO and PFG30 were used to correct for background signal caused through clouding of PFG30 polymers. These values were subtracted out of their respective C6 or PFG30-C6 measurements. Statistically significant changes in fluorescence were calculated through way ANOVA with multiple comparisons using the Holm-Šídák two method.

PFG30 Encapsulation Procedure

DHQZ analog-loaded PFG30 nanoparticles were prepared by mixing 5 μl of a 20-mM Retro-2, DHQZ 36 or DHQZ 36.1 stock with 32 to 45 μl of a 10-mg/ml PFG30 stock (at a 1:10 w/w drug: polymer ratio). This mixture was cooled at 4°C to remove any PFG30 precipitate and then heated at 37°C for 5 min to induce polymer self-assembly and drug encapsulation. This solution was then raised to a 1-ml volume with warm, complete DMEM to produce a 100-μM DHQZ drug solution loaded into PFG30 aggregates.

When noted, additional PFG30 aggregates housing Retro-2 or miltefosine were sedimented down as described above to pellet PFG30 capsules, and the supernatant was removed by pipette.

The pellet was then resolubilized in an equivalent volume of complete DMEM as described above to make a nominal 50 or 10 μM working solution of Retro-2 or miltefosine, respectively. These centrifuged samples were run in tandem as described below with non-centrifuged samples for comparison of PFG30 loading efficiency between the hydrophobic compound, Retro-2, and the hydrophilic compound, miltefosine.

Nanoparticle Size Characterization and Tracking Analysis

The self-assembly behavior of PFG30 was investigated by dynamic light scattering (DLS), performed with a Malvern Zetasizer Nano ZS instrument (Cambridge, UK) equipped with a 4-mV HeNe laser operating at $\lambda = 633$ nm, with a measurement angle of 173°. The measurements were carried out at 20°C and 37°C on a solution made up of 3.4 μl of a 30-mM Retro-2 stock in DMSO, 32 μl of a 10-mg/ml PFG30 stock, and 964.6 ml incomplete DMEM.

To determine if C6 was taken up into the intermicellar aggregates of PFG30, we used NanoSight to visualize and measure PFG30 particles with or without C6. DMSO vehicle or C6 were encapsulated in PFG30 aggregates as described above and diluted in incomplete DMEM without supplementation of 10% FBS because of the high amounts of particles from FBS. After preparation of samples, a dilution was prepared at 1:50 and then run for Nanoparticle Tracking Analysis (NTA, Malvern NanoSight NS300) at 37°C for particle size and concentration at 60 s per replicate. A second 1:50 dilution was then prepared and re-measured with a 500 nm green filter to measure the fraction of particles positive for containing C6. At least two replicates were run in these experiments.

Immunofluorescence Assay for Drug Susceptibility

RAW264.7 macrophages were plated in 100-mm dishes over glass coverslips at 1×10^6 cells/dish. After 24 h incubation, cells were infected with 96 h stationary phase *L. amazonensis* or 96 h PNA-selected, metacyclic *L. donovani* promastigotes at a 20:1 MOI for 4 h prior to two phosphate-buffered saline (PBS) washes to remove external parasites. Infected macrophages were incubated at 34°C or 37°C, respectively, with 5% CO_2.

Infected cells were treated with free DHQZ analogs or with PFG30 encapsulated Retro-2, DHQZ 36, or DHQZ 36.1 at a 1:10 w/w (drug:PFG30) ratio as described above. When noted, some samples were centrifuged and supernatant removed as described above prior to treatment. Treatments were performed for 48 h at concentrations ranging from 100 nM to 100 μM. Miltefosine, with or without PFG30 encapsulation, was used as a positive control for parasite clearance from concentrations ranging from 100 nM to 15 μM. Cells were incubated with free drugs or PFG30 encapsulated drugs at 34°C or 37°C for *L. amazonensis* or *L. donovani* infections, respectively, for 48 h. Coverslips were fixed in 4% paraformaldehyde (PFA) in PBS for 1 h prior to storage at 4°C in PBS. Coverslips were then processed in immunofluorescence assays (IFAs) to visualize the distribution of LAMP-1 as described previously (Craig et al., 2017). IFAs were visualized and captured using a QImaging Retiga 1300C cooled CCD camera mounted on an Olympus BX50 microscope equipped with automated filters with 100× NA 1.30 oil-immersion objective. Scored LPVs were delimited by LAMP-1 reactivity and contained at least one parasite nucleus visualized by 4′,6-diamidino-2-phenylindole (DAPI) stain. The percentage of infected macrophages and the average number of parasites was determined by counting at least 100 macrophages per coverslip. Counts were done in duplicate over at least three experiments and EC_{50} values were determined in GraphPad Prism 8 using a four-parameter dose-response best-fit curve line. Statistical significance between treated infected cells, and the control was measured using a one-way ANOVA in GraphPad Prism 8, and multiple comparisons were measured for statistical significance using the Holm-Šídák method.

Centrifugation Assay for the Estimation of Drug Uptake by PFG30 Aggregates

As described above, PFG30 encapsulated Retro-2 or miltefosine were prepared at 100 μM or 10 μM concentrations, respectively, in warm, complete DMEM. A second set of encapsulated Retro-2 or miltefosine was subjected to centrifugation to form a pellet prior to dilution in DMEM, and the supernatant was discarded. This mixture was re-encapsulated as described above and diluted in warm, complete DMEM prior to treatment of *L. amazonensis*-infected macrophages in tandem with non-centrifuged samples for comparison.

RAW264.7 macrophages were plated and infected with *L. amazonensis* at a 20:1 MOI as described previously. Coverslips were then treated in duplicate with Retro-2 or Miltefosine alone, PFG30-encapsulated Retro-2 or Miltefosine, or centrifugation products of PFG30-encapsulated Retro-2 or Miltefosine for 48 h at 34°C with 5% CO_2. Cells were then fixed with 2% PFA in PBS and IFA stained for LAMP-1 and DAPI for estimation of infection rates as described above. Statistical significance was measured by one-way ANOVA and the Holm-Šídák method for multiple comparisons.

Quantitative Uptake of C6-Loaded PFG30 Aggregates Into RAW264.7 Macrophages

To assess the cellular uptake of PFG30 aggregates, RAW264.7 cells were seeded on round, glass coverslips at a density of 4.5×10^4 cells in 24-well plates. On the second day, each well was incubated at 37°C for 0, 30, 60, and 180 min, with 500 ml of a solution made up of 1.7 μl of a 30-mM C6 stock in DMSO, 16 μL of a 10-mg/ml PFG30 stock, and 482.3 ml incomplete DMEM.

Post-treatment at the desired time points, cells were washed twice with PBS and fixed (3.7% formaldehyde in PBS) for 15 min at room temperature. Coverslips were mounted onto microscope slides using ProLong Gold Antifade reagent with DAPI (Thermo Fisher Scientific, Milan, Italy).

Cell-associated fluorescence was qualitatively and quantitatively detected by a Cytation 3 Cell Imaging Multi-Mode Reader fluorescence microscope (Biotek) at 480 nm as previously reported (Calarco et al., 2013).

Estimation of Retro-2 Incorporation Into RAW264.7 Macrophages by Mass Spectrometry

RAW264.7 macrophages were plated in six-well plates at 1×10^6 cells/well overnight and infected with stationary stage *L. amazonensis* promastigotes as described previously. Cells were then treated 24 h-post infection with 5 or 50 μM free Retro-2 or PFG30-encapuslated Retro-2 in warm, complete DMEM. Treatments were performed at 34°C from 4 to 12 h before preparations of cell lysates with RIPA Buffer (10 mM Tris, pH 7.4, 100 mM NaCl, 1 mM EDTA, 1 mM NaF, 20 mM $Na_4P_2O_7$, 2 mM Na_3VO_4, 1% NP-40, 0.5% deoxycholate) supplemented with 1 mM PMSF and protease cocktail inhibitor, purchased from Sigma Aldrich, prior to use. Lysates were sonicated for 15 s prior to centrifugation to remove cellular debris. Supernatants and cell lysates were frozen at −80°C until ready for analysis.

Mass spectrometry analysis of the cell lysates was performed on a Shimadzu Ultra-High-Performance Liquid Chromatography (Nexera XR LC 40), coupled to an MS/MS detector (LCMS 8060, Shimadzu), and controlled by Lab Solution software. The MS/MS was operated in positive electrospray ionization (ESI+), setting the nebulizing gas flow at 3 L/min, heating gas flow 10 L/min, interface temperature 370°C, DL temperature 250°C, heat block temperature 450°C, and drying gas flow 10 L/min. Analyzed fragments of Retro-2 (343.00 > 39.05; 343.00 > 23.15; 343.00 > 284.3) were selected by flow injection analysis mass identification, while quantification was operated after chromatographic separation of acetonitrile treated lysates (1:1 v/v) on a Phenomenex Kinetex polar C18 column (3 × 100 mm, 2.6 μm, Phenomenex, USA) with mobile phase consisting of acetonitrile: water + 0.01% formic acid (70:30, v/v; isocratic). A bar graph with estimated internal Retro-2 concentrations was generated in GraphPad Prism 8 and statistical significance measured *via* two-way ANOVA and the Tukey method for multiple comparisons.

Measurement of Vacuole Size

LPV size measurements were performed as described previously (Craig et al., 2017). Briefly, RAW264.7 macrophages on coverslips were infected with stationary *L. amazonensis* promastigotes at 10:1 MOI for 4 h after which parasites were washed off and DHQZ analogs, PFG30 encapsulated DHQZ analogs or miltefosine were added for an additional 24 h. Infected macrophages were fixed with 2% PFA in PBS then processed in IFAs to visualize the distribution of LAMP-1. IFAs were visualized and captured using a QImaging Retiga 1300C cooled CCD camera mounted on an Olympus BX50 microscope equipped with automated filters with 100× NA 1.30 oil-immersion objective. Scored LPVs were delimited by LAMP-1 reactivity and contained at least one parasite nucleus visualized by DAPI stain. Vacuole size was determined by measuring vacuole area *via* ImageJ. At least 30 vacuoles were measured per coverslip of which there were three per concentration per biological repeat. Statistical significance between treated infected cells and the control was measured using a one-way ANOVA in GraphPad Prism 8 with the Dunnett test for multiple comparisons.

Estimation of PFG30 Cytotoxicity

RAW264.7 macrophages were seeded at 1×10^4 cells/well in 96-well plates in complete DMEM at 37°C with 5% CO_2 for 2 to 4 h to allow adherence, but not replication. Cells were then treated with filter-sterilized, NanoPure diH_2O vehicle or PFG30 at concentrations ranging from 450 to 1 mg/ml for 48 h prior to MTT assay. After treatment, cells were incubated an additional 4 h with MTT before addition of 10% SDS in PBS with 5 N HCl to dissolve formazan crystals overnight. Absorbances were read at 570 nm with a 630 nm background subtracted out. Cell numbers were estimated based on a standard curve and statistical significance was measured *via* one-way ANOVA with multiple comparisons using the Holm-Šídák method.

RESULTS

PFG30 Enhances C6 Solubility Through Efficient Uptake Into Nanoaggregates

Previous studies had shown that Retro-2 and two SAR analogs, DHQZ 36 and DHQZ 36.1 are effective compounds against *L. amazonensis* and *L. donovani* infections (Canton and Kima, 2012; Craig et al., 2017; Gupta et al., 2017). However, these compounds are hydrophobic with low solubility in aqueous solutions. It is, therefore, likely that the efficacy of these compounds could be further enhanced by increasing their solubility through polymer-based encapsulation. Polymer encapsulation has been shown to increase hydrophobic drug solubility, drug delivery, and protection from degradation *in vivo* (Huh and Kwon, 2011; Costa Lima et al., 2012; Nafari et al., 2020). Previously, amphiphilic co-polymers made from OEGMA and 30% PFS were found to be responsive to temperatures greater than 30°C, leading to stable nanoaggregates with a hydrophobic interior (Lutz, 2011; Kwan and Marić, 2016; Welsch and Lyon, 2017). Therefore, it is expected that these nanoparticles may enhance solubility and bioavailability of hydrophobic Retro-2 and SAR analogs.

In the first series of experiments, the uptake of poorly soluble, hydrophobic molecules into PFG30 thermoresponsive aggregates was assessed. As Retro-2 is not fluorescent and its UV absorption spectrum overlaps with that of PFG30, we evaluated PFG30's ability to encapsulate and deliver the green laser dye, coumarin 6 (C6), to obtain further insight into its efficiency of encapsulating hydrophobic compounds (Zuppardi et al., 2020). The fluorescence of C6 is low in polar solvents bcause of its poor solubility; however, its fluorescence can be restored by using amphiphilic hosts that have hydrophobic cavities (Banerjee et al., 2016). The solubility of C6 in water with or without PFG30 encapsulation was measured through changes in the fluorescent profile. Fluorescence of 5 and 10 μM C6 in the presence of PFG30 was significantly greater at RFU values of 24,381 and 76,430, respectively, than water-dispersed C6, which barely fluoresced at 810 and 1,319 RFU, respectively (**Figure 1A**). The experiment was stopped at 10 μM because of the values reaching overflow in PFG30 encapsulated C6 samples.

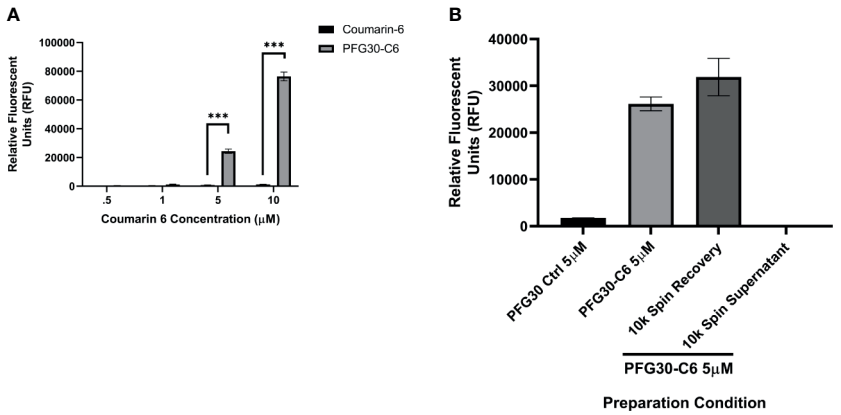

FIGURE 1 | Encapsulation of hydrophobic molecules in PFG30 increases their solubility. **(A)** Increasing concentrations of C6 alone or PFG30 + C6 was measured at 420 nm excitation and 500 nm emission. **(B)** 50 μM PFG30-C6 preparations were centrifuged after which the supernatant fluid and pellets were diluted to 5 μM for measurement of fluorescence at 420/500 nm. Experiments were run in triplicate with at least two technical replicates each. Statistical significance was determined by two-way ANOVA in GraphPad Prism 8 with the Holm-Šídák posthoc test for multiple comparisons (***p-value < 0.001).

To determine if increased fluorescence of C6 was due to PFG30 encapsulation, we elected to separate free C6 in solution from encapsulated C6 *via* centrifugation. After removal of the supernatant and resuspension of the pellet, there was no significant drop in the fluorescence of the pellet of the 5 μM sample at 31,888 RFU compared to the control 5 μM sample (26,160 RFU) without centrifugation. In addition, the supernatant contained very little C6 with a fluorescent value of only 189 RFU (**Figure 1B**).

Because of the increase in C6 solubility and association with the PFG30 pellet in centrifugation experiments, DLS was used to assess whether PFG30 was able to retain its thermally triggered self-assembly properties in DMEM solution, as well as in the presence of the hydrophobic compound Retro-2. To that end, the size distribution of a PFG30 solution containing Retro-2 in DMEM was measured by DLS at 20°C and 37°C. At 20°C, polymer micelles having average hydrodynamic diameter of 10 nm were detected, with monomodal distribution and low polydispersity. When the temperature was raised to 37°C, the particle size increased up to about 200 nm, due to formation of intermicellar aggregates, demonstrating that Retro-2 did not affect the self-assembly behavior of PFG30 (**Supplemental Figure 1**).

To further affirm that the increased solubility of C6 was indeed due to encapsulation of C6 into PFG30, the sizes of PFG30 intermicellar aggregates, with or without C6, were assessed by NanoSight. PFG30 aggregates without C6 were about 200 nm in size. Encapsulation of C6 with PFG30 resulted in increased particle sizes ranging from 200 to 400 nm in size. The incomplete DMEM vehicle included a small population of particles. However, they were distinctly different from PFG30 nanoparticles with sizes less than 100 nm (**Figure 2A**). Furthermore, the addition of PFG30 significantly increased the magnitude of particles compared to incomplete DMEM or incomplete DMEM with free C6 (**Figure 2B**). Using a 500 nm wavelength filter for green fluorescence in the NanoSight, we found that there was a significant increase in the number of green fluorescent particles in PFG30 encapsulated C6 samples as compared with PFG30 or C6 alone. These results suggests that C6 is encapsulated within PFG30 aggregates.

Considering the observations on the encapsulation of C6, the encapsulation of Retro-2 and its SAR derivatives, DHQZ 36 and DHQZ 36.1 were evaluated. 50 μM Retro-2, DHQZ 36 or DHQZ 36.1 mixed with C6 were encapsulated by PFG30 at a 1:10 w/w ratio. A 1:50 dilution in incomplete DMEM was prepared for evaluation by NanoSight. Mixing of C6, DHQZ analogs, and PFG30 resulted in an increase in the size of the particles that were formed (**Figure 2A**). There was also an increase in the number of PFG30 aggregates that were formed (**Figure 2B**). Interestingly, PFG30 particles formed upon addition of DHQZ 36 and DHQZ 36.1, were smaller but more numerous (**Figures 2A, B**). Retro-2 and the two DHQZ analogs mixed with C6 had a similar increase in the concentrations of green-positive particles as compared to PFG30 encapsulation of C6 alone, suggesting that the addition of drug did not affect C6 loading into PFG30 aggregates (**Figure 2C**).

PFG30 Enhances Efficacy of SAR DHQZ Analogs of Retro-2 Against *L. donovani* and *L. amazonensis* Infections of RAW264.7 Macrophages

We commenced these studies by assessing whether Retro-2 efficacy against intracellular *Leishmania* amastigotes would be improved by encapsulation in PFG30 polymeric nanoparticles.

RAW264.7 macrophages plated on coverslips in six-well plates were infected with *L. donovani* parasites for 24 h. Thereafter, several concentrations of Retro-2, DHQZ 36, or DHQZ 36.1 encapsulated in PFG30 were added to infections. After an additional 48 h, the infections were fixed by adding 2% PFA. Coverslips with infected cells were then processed by immunofluorescence labeling to detect the contours of the LPV and to visualize parasite nuclei. After enumerating the number of cells harboring intracellular *Leishmania*, the data were

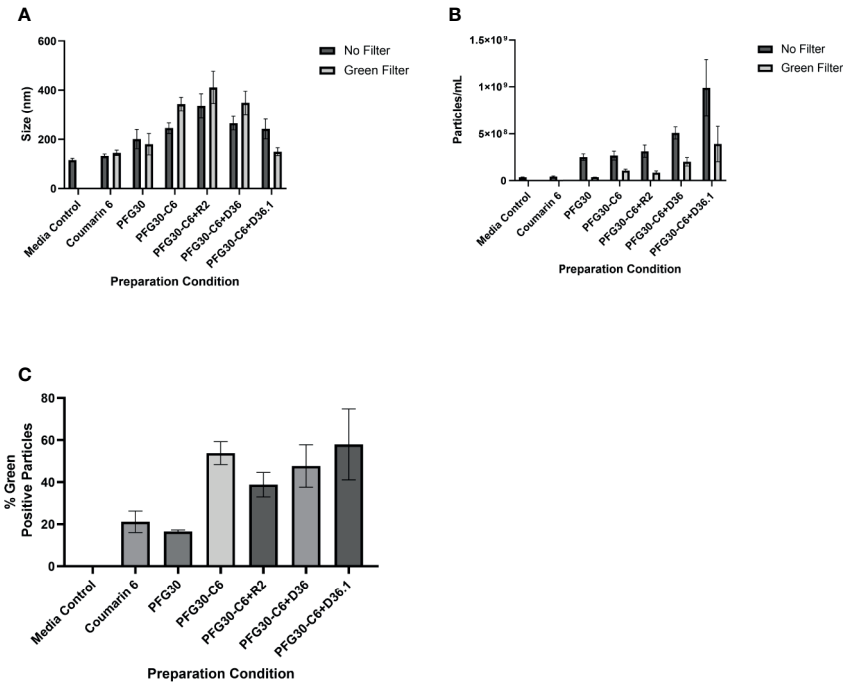

FIGURE 2 | NanoSight measurements of PFG30 encapsulated compounds. The size and number of particles produced after encapsulation in PFG30 were analyzed as follows: C6 alone (20 μM); PFG30 alone; PFG30 + C6 (20 μM); PFG30 + C6 + Retro-2 (50 μM R2); PFG30 + C6 + DHQZ 36 (50 μM); PFG30 + C6 + DHQZ 36.1 (50 μM). Encapsulation mixtures were prepared at 1:50 dilution for NanoSight analysis. **(A)** The size measurements of polymer aggregates with or without the use of a 500 nm green filter for fluorescence. **(B)** The number of particles within the samples with or without the use of a 500 nm green filter for fluorescence. **(C)** Particles observed in samples using a 500-nm green filter were compared with the total particles in the sample observed without the filter to generate a percentage estimation of C6 uptake within PFG30 aggregates. Data were obtained from at least two biological replicates.

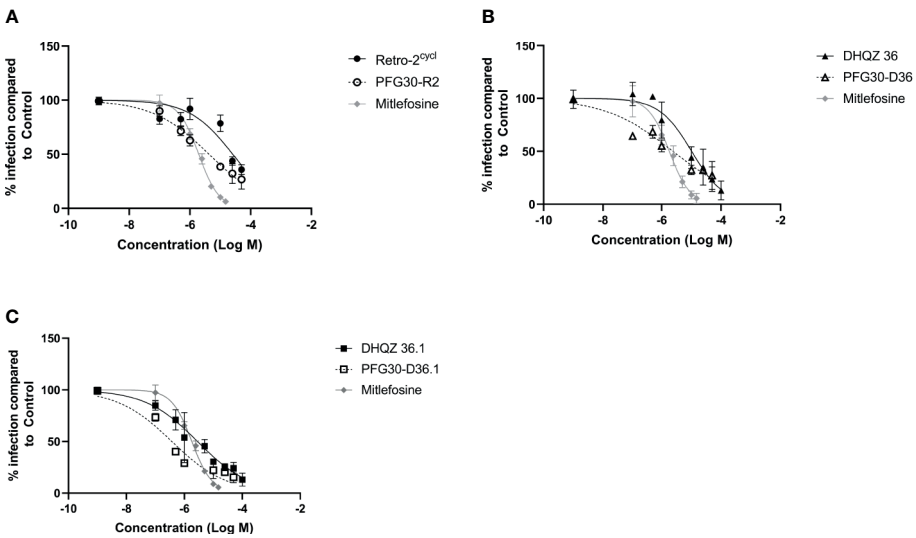

FIGURE 3 | Evaluation of polymer-encapsulated compounds on *L. donovani*-infected RAW264.7 macrophages. *L. donovani*-infected macrophages were treated for 48 h with the following compounds: **(A)** free Retro-2 or PFG30 + Retro-2 (PFG30-R2); **(B)** free DHQZ 36 or PFG30 + DHQZ 36 (PFG30-D36); **(C)** free DHQZ 36.1 or PFG30 + DHQZ 36.1 (PFG30-D36.1) at concentrations ranging from 100 nM to 100 μM. Miltefosine (100 nM to 15 μM) treatment was used as a positive control for parasite clearance. Cells were fixed in 2% PFA in PBS. IFAs were performed for detection of LAMP-1 and cell and parasite nuclei with DAPI. At least 200 cells were scored per coverslip and infection rates were standardized to a vehicle control before EC_{50} estimation. Data were compiled from at least three biological repeats.

plotted (**Figure 3**). PFG30 encapsulation of Retro-2 significantly augmented the EC_{50} value calculated at 4.46 ± 0.94 μM compared to unencapsulated Retro-2 at 22.73 ± 3.44 μM. Due to the increased efficacy observed of Retro-2 encapsulated in PFG30 to clear *L. donovani* infections, we proceeded to test the efficacy of DHQZ 36 and DHQZ 36.1 encapsulated in PFG30. After processing in immunofluorescence assays and enumeration of infected macrophages, we determined that DHQZ 36 encapsulated in PFG30 had an EC_{50} value of 1.07 ± 0.98 μM (**Figure 3B**). Encapsulated DHQZ 36.1 had an EC_{50} value of 0.27 ± 0.09 μM, (**Figure 3C**). **Table 1** shows the EC_{50} of DHQZ 36 and DHQZ 36.1 without encapsulation. The efficacy of DHQZ compounds and encapsulated formulations were run alongside miltefosine. The EC_{50} of miltefosine in these experiments was determined to be 1.96 ± 0.38 μM. As shown in **Table 1**, the EC_{50} values of the PFG30 encapsulated compounds on *L. donovani* infections were much improved and were effective at lower concentrations than miltefosine.

TABLE 1 | Estimation of the efficacy of PFG30 encapsulated DHQZ analogs on *L. donovani* infections.

Treatment	EC_{50} (μM)	
	PFG30 (–)	PFG30 (+)
Retro-2	22.73 ± 3.44	4.46 ± 0.94***
DHQZ 36	11.70 ± 0.33	1.07 ± 0.98***
DHQZ 36.1	1.80 ± 0.20	0.27 ± 0.09***
Miltefosine	1.96 ± 0.38	

R2, Retro-2; D36, DHQZ 36; D36.1, DHQZ 36.1.
*EC_{50} values were calculated for the plots in **Figure 3** generated in GraphPad Prism 8. Statistical significance was measured between $LogEC_{50}$ values between DHQZ compounds and encapsulated DHQZ compounds though the Extra Sum-of-Squares F test (***p-value < 0.001).*

We then proceeded to test the efficacy of the encapsulated compounds just described, on *L. amazonensis* infections. We wanted to determine if using the same methodology for PFG30 encapsulation would improve the efficacy Retro-2 and the DHQZ analogs on *L. amazonensis* infections. The drug killing curves that were generated for the studies on *L. amazonensis* infections are shown in **Figure 4**. From these curves we calculated the EC_{50} for PFG30 encapsulated Retro-2 to be 26.15 ± 2.46 μM; the EC_{50} of encapsulated DHQZ 36 was 2.42 ± 2.12 μM; the EC_{50} of PFG30 encapsulated DHQZ 36.1 was 0.36 ± 0.13 μM. These results are presented in **Table 2** alongside the EC_{50} values of these compounds without encapsulation. **Supplemental Figure 2** and **Table 2** show that encapsulation of miltefosine, using the encapsulation protocol described above, did not result in a significant change in the EC_{50} of miltefosine. The EC_{50} of miltefosine on *L. amazonensis* infections is 2.50 ± 0.37 μM.

We proceeded to rule out the possibility that the increase in efficacy of the encapsulated compounds was not due to toxicity of PFG30 on RAW264.7 macrophages, which may lead to stress of the parasites during infection. This was determined by using a MTT assay to measure RAW264.7 cell viability with PFG30 treatment over 48 h. In this experiment, we included much higher concentrations of PFG30 along with a filter-sterilized, NanoPure diH_2O vehicle control. No significant loss in cell viability was observed at 48 h treatments of RAW264.7

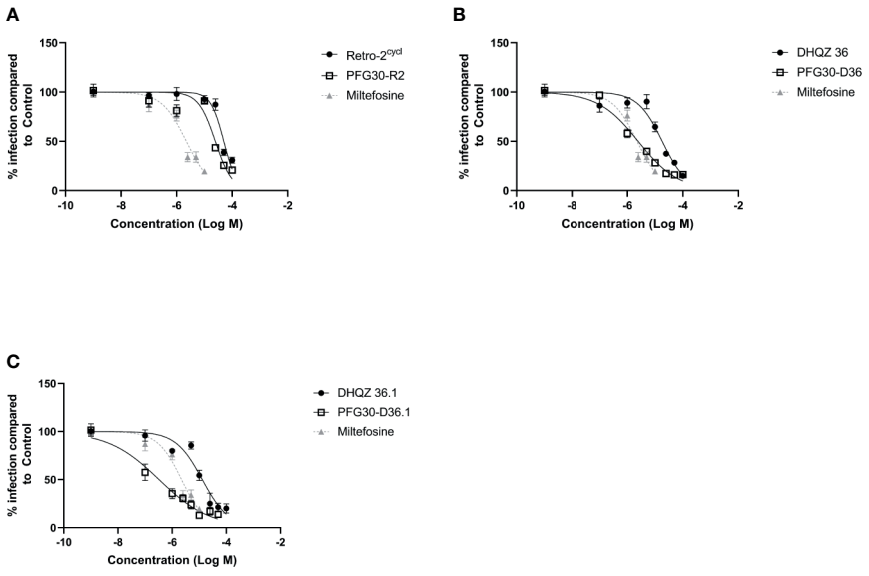

FIGURE 4 | Evaluation of polymer-encapsulated compounds on *L. amazonensis*-infected RAW264.7 macrophages. To *L. amazonensis*-infected RAW264.7 macrophages, the following drug/polymer mixtures were added then incubated for an additional 48 h. **(A)** Retro-2 in DMSO or Retro-2 + PFG30; **(B)** DHQZ 36 in DMSO or DHQZ 36 + PFG30; **(C)** DHQZ 36.1 in DMSO or DHQZ 36.1 + PFG30 at concentrations of 100 nM to 100 μM. Miltefosine (100 nM to 15 μM) treatment served as a positive control for parasite clearance. Cells were fixed in 2% PFA in PBS. IFAs were performed for detection of LAMP-1 and cell and parasite nuclei with DAPI. At least 200 cells were scored per coverslip and infection rates were standardized to a vehicle control before EC_{50} estimation. Data were compiled from at least three biological repeats.

TABLE 2 | Estimated efficacy on *L. amazonensis* infections of Retro-2 and DHQZ analogs with or without PFG30.

Treatment	EC_{50} (μM)	
	PFG30 (–)	PFG30 (+)
Retro-2	50.29 ± 5.91	26.15 ± 2.46***
DHQZ 36	18.00 ± 2.54	2.42 ± 2.12***
DHQZ 36.1	13.05 ± 0.49	0.36 ± 0.13***
Miltefosine	2.23 ± 0.27	2.11 ± 0.26

*EC_{50} values were calculated from fitted-line dose-response curves in **Figure 4** of R2, Retro-2; D36, DHQZ 36; D36.1, DHQZ 36.1 Plots and analysis were performed in GraphPad Prism7. Statistical significance was measured between $LogEC_{50}$ values between Retro-2 and encapsulated Retro-2 though the Extra Sum-of-Squares F test (***p-value < 0.001).*

macrophages, even at 1 mg/ml concentrations of PFG30 (**Supplemental Figure 3**).

Retro-2 SAR Analogs Are Efficiently Packaged in PFG30 Aggregates and Delivered Into Macrophages *In Vitro*

While PFG30 encapsulation experiments against *L. donovani* and *L. amazonensis* infections indicate improved efficacy, it is uncertain how much DHQZ analogs are retained in the PFG30 polymer capsules and how much drug is excluded. Therefore, we reasoned that due to the physical aggregation of the capsules, these could be centrifuged into a pellet allowing for the removal of the supernatant fluid containing any free drug unassociated with the polymers. Once free drug was removed, the remaining drug associated with the polymer could be tested against *L. amazonensis* infections and potential loss of efficacy determined. We observed that with 10,000*g* centrifugation at 37°C, pelleted Retro-2 encapsulated in PFG30 had no significant loss in efficacy after supernatant was discarded (**Figure 5A**). In contrast, centrifugation of PFG30 encapsulated miltefosine and removal of supernatant from the PFG30 pellet resulted in significant loss of efficacy even at 10 μM (**Figure 5B**), likely because of the hydrophilicity of the compound.

Because of the results with C6 solubility and centrifugation experiments, it is likely that Retro-2 SAR analogs are also solubilized and packaged into PFG30 nanoaggregates. Therefore, PFG30 encapsulation and uptake could facilitate Retro-2 entry into infected cells leading to the observed increase in efficacy. To first estimate PFG30 uptake into cells, RAW264.7 macrophages were treated with PFG30 encapsulated C6 up to 180 min prior to fixation. These cells were then stained with DAPI and visualized *via* fluorescence microscopy to assess PFG30 uptake by macrophages. The intracellular C6-associated fluorescence was visualized as early as 30 min post-treatment and increased gradually until 180 min (**Figures 6A–I**). The increasing amount of C6 uptake into cells was confirmed by fluorescence quantification (**Figure 6J**). Additional experiments related to C6-loaded PFG30 uptake were performed on mouse fibroblast cell line (L929). The result clearly demonstrated that PFG30 nanoparticles efficiently enter the cells, suggesting that the PFG30 cellular uptake is not related to the phagocytic nature of the cell (**Supplemental Figure S4**).

Based on these results, the concentration of Retro-2 uptaken by cells after PFG30 encapsulation, was then evaluated by LC/MS (**Figure 6K**). Infected cells were treated with various amounts of PFG30 encapsulated Retro-2 for 4 and 12 h before lysis by the addition of RIPA buffer and sonication. Early timepoints were used to limit potential drug loss from drug turnover within cellular compartments, as this compound is relatively stable in acidic conditions (Gandhi et al., 2019). Mass spectrometry analysis of the cell lysates found that levels of Retro-2 treatments of 5 and 50 μM in macrophage lysates were detectable at 4 h post-treatment with cellular uptake at 0.14 ± 0.04 μM and 3.83 ± 1.15 μM, respectively. These concentrations

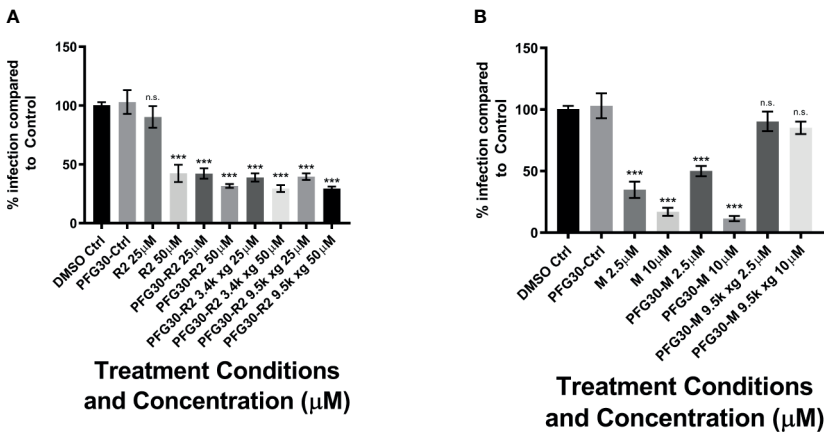

FIGURE 5 | Evaluation of PFG30 encapsulation efficiency of Retro-2 and miltefosine through centrifugation separation of free and encapsulated drug. *L. amazonensis*-infected RAW264.7 macrophages were treated for 48 h with the following preparations: **(A)** Retro-2, PFG30 + Retro-2 or PFG30 + Retro-2 post-centrifugation; **(B)** miltefosine, PFG30 + miltefosine or PFG30 + miltefosine post-centrifugation. Cells were fixed in 2% PFA in PBS. IFA's were performed for detection of LAMP-1 and cell and parasite nuclei with DAPI. Statistical significance was determined by one-way ANOVA in GraphPad Prism 8 with the Holm-Šídák posthoc test for multiple comparisons (n.s., not statistically significant, ***p-value < 0.001). Data were compiled from three biological experiments with at least two technical replicates.

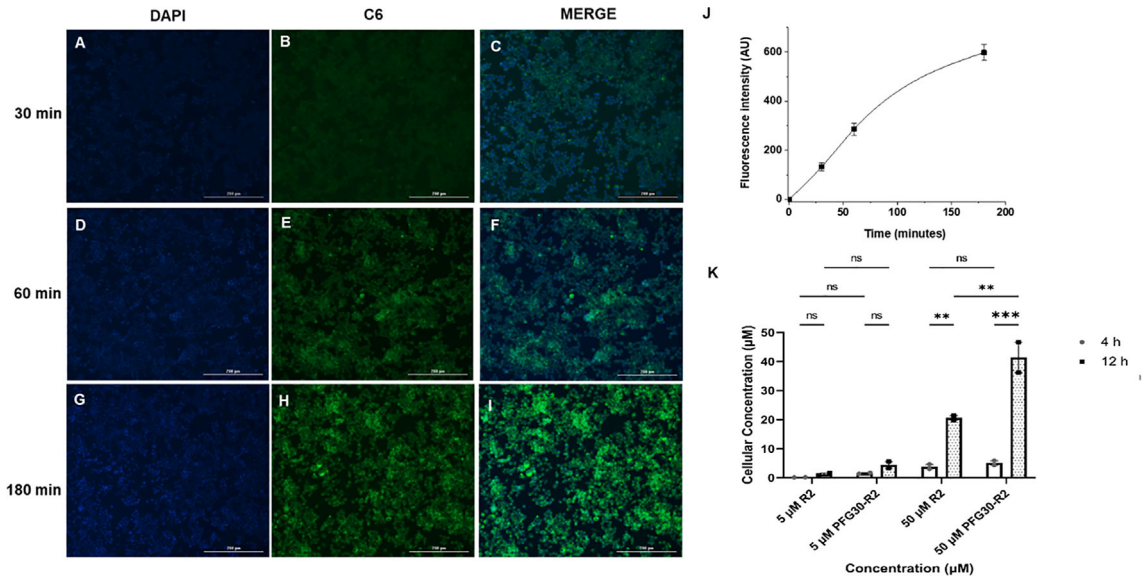

FIGURE 6 | PFG30 encapsulation of Retro-2 (R2) increases uptake of the drug into RAW264.7 macrophages. **(A–I)** Representative microscope images (magnification 10X) of PFG30 + C6 nanoparticle uptake by RAW264.7 macrophages at different incubation time. RAW264.7 macrophages were incubated at 37°C with PFG30 encapsulated C6 at the following time points: **(A–C)** 30 min, **(D–F)** 60 min, and **(G–I)** 180 min. **(J)** Cell-associated fluorescence quantification calculated as a function of time. The curve was generated by performing image analysis (ImageJ software). Results are expressed as the mean of three biological replicates ± standard deviation (n = 3). **(K)** LC/MS quantification of R2 concentration in *L. amazonensis*-infected RAW264.7 macrophages. Cells were treated with R2 or PFG30 encapsulated R2 (PFG30-R2) for 4 or 12 h. At the indicated times, cells were recovered and supernatant was collected. The cell pellets were lysated in RIPA buffer and then sonicated for 15 s twice prior to storage at –80°C. Statistical significance was determined by two-way ANOVA in GraphPad Prism 8 with the Tukey posthoc test for multiple comparisons (ns, not statistically significant where p-value > 0.05, **p-value < 0.01, ***p-value < 0.001). Data were compiled from two biological replicates.

increased over time at 12 h post-treatment to 1.18 ± 0.59 μM in the 5-μM treated sample and 20.62 ± 1.11 μM in the 50-μM treated sample. Drug levels in cells were found to be elevated with PFG30 encapsulation at all time points. At 4 h, PFG30-Retro-2 treatments of 5 and 50 μM resulted in intracellular Retro-2 levels at 1.55 ± 0.28 μM and 5.1 ± 1.13 μM, respectively. This effect was more pronounced at 12 h post-treatment with intracellular Retro-2 concentrations of 4.43 ± 1.59 μM and 41.45 ± 7.42 μM in the 5 and 50 μM PFG30-Retro-2 treated samples, respectively (**Figure 6K**).

PFG30 Aggregates Improve Effects of DHQZ Analogs on LPV Maturation Through Prevention of Vacuole Size Increases During *L. amazonensis* Infection

Previously, we showed that treatment with Retro-2 and the DHQZ analogs, DHQZ 36 and DHQZ 36.1, resulted in reduced sizes of maturing *L. amazonensis* LPVs (Craig et al., 2017). Considering those observations, we wanted to determine if the effects on maturing LPVs DHQZ analogs could be enhanced with PFG30 encapsulation. RAW264.7 cells were infected with *L. amazonensis* promastigotes for 4 h prior to treatment with DHQZ analogs, alone or PFG30 encapsulated, for an additional 24 h. We found that PFG30 enhanced the vacuole size reduction results observed previously with drug alone with all three compounds. Free Retro-2 significantly reduced vacuole size in *L. amazonensis*-infected RAW264.7 macrophages at 25 and 50 μM by 16.6% and 41.2%, respectively. PFG30 encapsulated Retro-2 increased this effect with significant loss of vacuole size by 21.2% at 10 μM (**Figure 7A**). DHQZ 36 also showed significant vacuole size reductions at 25 and 50 μM by 28.3% and 42.7%, respectively. PFG30 encapsulation of DHQZ 36 improved this effect significantly at concentrations as low as 1 μM with a size reduction of 33.1% compared with the PFG30-treated control (**Figure 7B**). Free DHQZ 36.1 only showed significant size reduction at 50 μM by 41.5%. However, PFG30 encapsulation of DHQZ 36.1 showed similar results to DHQZ 36 with 1 μM significantly reducing vacuole size by 35.0% compared to the control (**Figure 7C**).

CONCLUSIONS/DISCUSSION

With no preventative vaccine available for leishmaniasis, chemotherapy is the front-line option for treatment of this potentially deadly disease. However, the pool of clinically-available anti-*Leishmania* compounds remains relatively small. One major issue in drug development of new potentially effective compounds is the problem of solubility. It is estimated that approximately 40% of market compounds and up to 90% of pipeline candidate drugs are poorly soluble in water (Kalepu and Nekkanti, 2015). Although repurposing drugs is a viable strategy

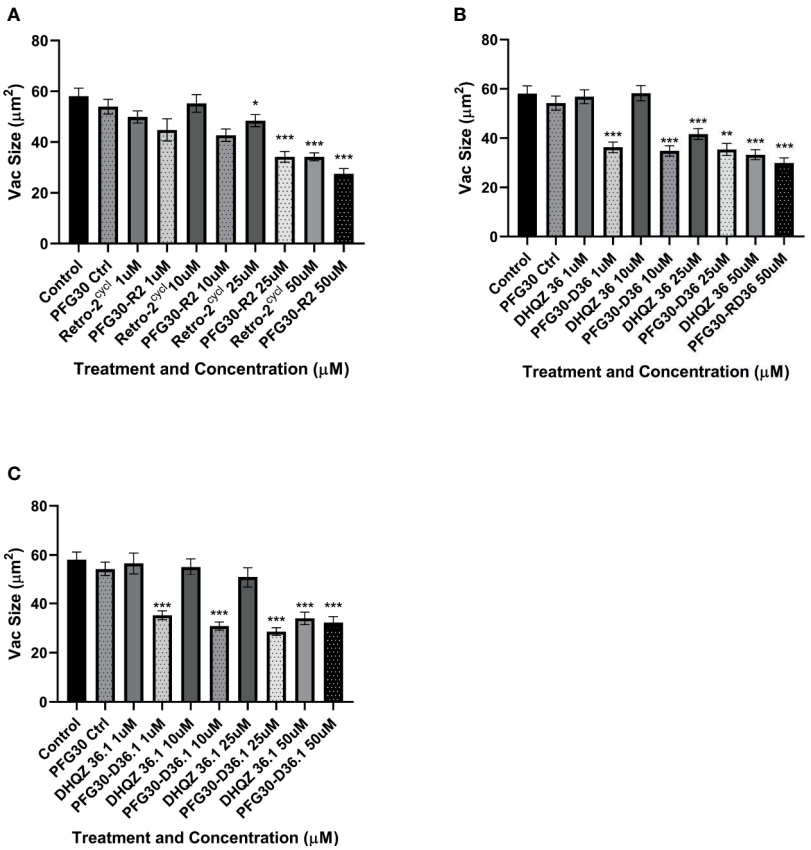

FIGURE 7 | Vacuole size measurements of drug treated *L. amazonensis* LPVs. RAW264.7 macrophages were infected for 24 h after which they were treated Retro-2 or DHQZ analogs, with or without encapsulation in PFG30. **(A)** Treatment with Retro-2 (0–50 μM) with or without PFG30 encapsulation. **(B)** Treatment with DHQZ 36 (0–50 μM) with or without encapsulation. **(C)** Treatment DHQZ 36.1 (0–50 μM) with or without PFG30 encapsulation. Data were compiled from three experiments. At least 30 vacuoles were measured per treatment *via* one-way ANOVA with the Šídák correction for multiple comparisons. (*p-value < 0.05, **p-value < 0.01, ***p-value < 0.001).

for discovery of anti-*Leishmania* candidates because of the preceding studies of their bioavailability and toxicity *in vivo*, it would nonetheless be beneficial to utilize the large pool of hydrophobic compounds in the discovery pipeline. One way to overcome the hurdle of water solubility is the encapsulation of drugs in water-soluble, inert, biodegradable nanoparticle capsules to enhance drug solubility (Zhang et al., 2008; Rao and Geckeler, 2011). In this manuscript, we evaluated PFG30 for their capacity to encapsulate and enhance the efficacy of Retro-2 and its DHQZ SAR analogs to clear *L. donovani* and *L. amazonensis* infections of macrophages *in vitro*.

We first decided to explore the efficiency of PFG30 to encapsulate hydrophobic compounds. C6 was selected due to its fluorescent properties and low solubility in aqueous solution. In addition, Zuppardi et al. recently used PFG preparations of different polyfluorostyrene concentrations with a similar dye, Nile Red, to demonstrate efficient removal of the dye from aqueous solution (Zuppardi et al., 2020). When encapsulated by PFG30, C6 solubility was significantly increased in water compared with C6 alone as measured by 420/500 nm excitation and emission fluorescence. This increase in solubility appears to be due to C6 encapsulation into PFG30 aggregates as tested through centrifugation and NanoSight experiments. Despite removal of the supernatant, C6 fluorescence did not significantly change compared to PFG30 encapsulated C6 without centrifugation. While PFG30 did cause some background fluorescent particles likely through light refraction, the magnitude of green fluorescent particles measured on NanoSight were higher in PFG30 encapsulated C6 samples compared to C6 or PFG30 alone. DLS experiments with PFG30 encapsulation of Retro-2 at 20°C and 37°C show that thermosensitive polymer self-assembly was not impeded upon uptake of hydrophobic cargo.

Because of the improved solubility of the hydrophobic molecule, C6, after encapsulation by PFG30, we tested the improved efficacy of encapsulated Retro-2, DHQZ 36, and DHQZ 36.1 against *L. donovani* and *L. amazonensis in vitro* infections of RAW264.7 macrophages. PFG30 encapsulation was found to enhance the efficacy of all three DHQZ compounds with DHQZ 36.1 EC_{50} values in the nanomolar range, surpassing that of miltefosine, which is used clinically. It is likely that these compounds are encapsulated within PFG30 aggregates similar to

encapsulation of C6 as centrifugation experiments and sampling of the pellet did not affect the EC_{50} of DHQZ analogs encapsulated in PFG30. This suggests that these compounds are likely enclosed in the hydrophobic portion of the PFG30 aggregate. Conversely, the EC_{50} of miltefosine against *L. amazonensis* was not significantly affected by PFG30 encapsulation, and efficacy was lost upon centrifugation and sampling of the pellet. These results suggest that miltefosine was not efficiently encapsulated within PFG30 aggregates. Likely, because of its hydrophilic nature, miltefosine remained in the aqueous supernatant, which was removed post-centrifugation.

Because of the increase in solubility of C6 and the increased efficacy of Retro-2 DHQZ SAR analogs, we decided to test if this effect was due to improved delivery of Retro-2 by uptake of PFG30 aggregates using LC/MS. Small, but not significant, increases were observed as early as 4 h post-treatment with PFG30 encapsulated Retro-2 compared to free Retro-2. However, this increase was much more pronounced by 12 h post-treatment especially in the 50-μM sample where 82.9% of the encapsulated Retro-2 was associated with the cellular lysate. This result suggests that PFG30 aggregates are efficiently taken up by RAW264.7 macrophages and that encapsulation of Retro-2 is a viable strategy for improving its delivery to infected cells. However, the dynamics of uptake and release of Retro-2 encapsulated in PFG30 aggregates remains unknown. The dramatically increased reduction of LPV size by PFG30 encapsulated DHQZ 36 and DHQZ 36.1 at 24 h post-treatment suggests that a large proportion of the compounds are able to target the host secretory pathway machinery. Additionally, due to the reported direct activity of Retro-2 analogs against *Leishmania*, it is possible that encapsulation increases delivery of Retro-2 directly to amastigotes residing within the LPV (Canton and Kima, 2012; Craig et al., 2017). *Leishmania* LPVs acquire large amounts of LAMP-1-associated membrane which may lead to the direct delivery of endocytic vesicles containing PFG30 encapsulated DHQZ analogs.

This study presents PFG30 as a potential candidate copolymer for biological application as a drug carrier. Further studies should elucidate its uptake and release mechanisms within cells as well as its viability for use in *in vivo* studies. In addition, this study highlights the significant improvement of DHQZ analog efficacy with polymer encapsulation. It is likely that other nanocarrier options would provide similar improvements. As an organic polymer, PFG30 may also be further improved through the addition of targeting mechanisms to increase uptake and cell specificity. These methods may further enhance drug delivery and bioavailability within an *in vivo* model.

DATA AVAILABILITY STATEMENT

The original contributions presented in the study are publicly available. This data can be found here: https://figshare.com/articles/dataset/Thermoresponsive_copolymer_nanovectors_improve_the_bioavailability_of_retrograde_inhibitors_LC-MS_dataset_xlsx/14553783.

AUTHOR CONTRIBUTIONS

EC performed experiments and wrote manuscript: RC, GG performed experiments. VA and AC performed experiments and contributed analysis and writing. PA and JS synthesized most drugs used in study. PC made intellectual contributions to the study and wrote and edited manuscript. PK made intellectual contributions to the study and wrote and edited manuscript and was responsible for the overall execution of the study. All authors contributed to the article and approved the submitted version.

ACKNOWLEDGMENTS

The authors acknowledge the H2020 - MSCA-RISE-Marie Sklodowska-Curie Actions (MSCA) Research and Innovation Staff Exchange (RISE) for funding this work in the framework of the Project VAHVISTUS - Project Number: 734759.

SUPPLEMENTARY MATERIAL

The Supplementary Material for this article can be found online at: https://www.frontiersin.org/articles/10.3389/fcimb.2021.702676/full#supplementary-material

Supplementary Figure 1 | Size distribution of PFG30 + Retro-2 particles measured by DLS at 20°C and 37°C. The self-assembly behavior of PFG30 was investigated by DLS performed at 20°C and 37°C on a solution containing Retro-2, PFG30, and incomplete DMEM. At 20°C, 10 nm polymer micelles were detected, whereas at 37°C intermicellar aggregates of about 200 nm in size formed, demonstrating that encapsulation of Retro-2 did not affect the self-assembly behavior of PFG30. The reported size distribution curves are averaged from 3 experiments.

Supplementary Figure 2 | Evaluation of polymer-encapsulated miltefosine on *L. amazonensis*-infected RAW264.7 macrophages. To *L. amazonensis*-infected RAW264.7 macrophages, free or PFG30 encapsulated miltefosine was added. After 48 h treatment, cells were fixed in 2% PFA in PBS. IFA's were performed for detection of LAMP-1 and cell and parasite nuclei with DAPI. At least 200 cells were scored per coverslip and infection rates were standardized to a vehicle control before EC_{50} estimation. Data were compiled from at least three biological repeats.

Supplementary Figure 3 | MTT assay of RAW264.7 macrophages treated with vehicle or PFG30 aggregates. Macrophages were treated with PFG30 at concentrations ranging from 450 ng/ml to 1 mg/ml for 48 h at 37°C with 5% CO_2. Cells were then incubated with MTT for 4 h before addition of 10% SDS in PBS with 5 N HCl to dissolve formazan crystals overnight. Absorbances were read at 570 nm with a 630 nm background. Cell numbers were estimated based on a standard curve from at least 3 technical replicates each over triplicate experiments.

Supplementary Figure 4 | L929 cellular uptake of C6-loaded PFG30 nanoparticles. **(A–C)** R Representative microscope images (magnification 10X) of PFG30 + C6 nanoparticle uptake by L929 mouse fibroblast cell line after 60 min incubation time. L929 cells were incubated at 37°C with PFG30 encapsulated C6 as reported in materials and methods section for RAW264.7 macrophages.

REFERENCES

Almeida, H., Amaral, M. H., and Lobão, P. (2012). Temperature and pH Stimuli-Responsive Polymers and Their Applications in Controlled and Self-Regulated Drug Delivery. *J. Appl. Pharm. Sci.* 02 (06), 01–10. doi: 10.7324/JAPS.2012.2609

Alvar, J., Aparicio, P., Aseffa, A., Den Boer, M., Cañavate, C., Dedet, J. P., et al. (2008). The Relationship Between Leishmaniasis and AIDS: The Second 10 Years. *Clin. Microbiol. Rev.* 21 (2), 334–359. doi: 10.1128/CMR.00061-07

Arango Duque, G., Jardim, A., Gagnon, É., Fukuda, M., and Descoteaux, A. (2019). The Host Cell Secretory Pathway Mediates the Export of Leishmania Virulence Factors Out of the Parasitophorous Vacuole. *PloS Pathog.* 15 (7), 1–25. doi: 10.1371/journal.ppat.1007982

Arenas, R., Torres-Guerrero, E., Quintanilla-Cedillo, M. R., and Ruiz-Esmenjaud, J. (2017). Leishmaniasis: A Review. *F1000Research* 6, 750. doi: 10.12688/f1000research.11120.1

Banerjee, R., Mondal, S., and Purkayastha, P. (2016). Revival{}, Enhancement and Tuning of Fluorescence From Coumarin 6: Combination of Host–Guest Chemistry{}, Viscosity and Collisional Quenching. *RSC Adv.* 6 (107), 105347–105349. doi: 10.1039/C6RA20884C

Banik, B. L., Fattahi, P., and Brown, J. L. (2016). Polymeric Nanoparticles: The Future of Nanomedicine. *Wiley. Interdiscip. Rev.: Nanomed. Nanobiotechnol.* 8 (2), 271–99. doi: 10.1002/wnan.1364

Barouti, G., Jaffredo, C. G., and Guillaume, S. M. (2017). Advances in Drug Delivery Systems Based on Synthetic Poly(Hydroxybutyrate) (Co)Polymers. *Prog. Polymer. Sci.* 73, 1–31. doi: 10.1016/j.progpolymsci.2017.05.002

Calarco, A., Bosetti, M., Margarucci, S., Fusaro, L., Nicolì, E., Petillo, O., et al. (2013). The Genotoxicity of PEI-Based Nanoparticles Is Reduced by Acetylation of Polyethylenimine Amines in Human Primary Cells. *Toxicol. Lett.* 218 (1), 10—17. doi: 10.1016/j.toxlet.2012.12.019

Canton, J., and Kima, P. E. (2012). Targeting Host Syntaxin-5 Preferentially Blocks Leishmania Parasitophorous Vacuole Development in Infected Cells and Limits Experimental Leishmania Infections. *Am. J. Pathol.* 181 (4), 1348–1355. doi: 10.1016/j.ajpath.2012.06.041

Canton, J., Ndjamen, B., Hatsuzawa, K., and Kima, P. E. (2012). Disruption of the Fusion of Leishmania Parasitophorous Vacuoles With ER Vesicles Results in the Control of the Infection. *Cell Microbiol.* 14 (6), 937–948. doi: 10.1111/j.1462-5822.2012.01767.x

Carney, D. W., Nelson, C. D. S., Ferris, B. D., Stevens, J. P., Lipovsky, A., Kazakov, T., et al. (2014). Structural Optimization of a Retrograde Trafficking Inhibitor That Protects Cells From Infections by Human Polyoma- and Papillomaviruses. *Bioorg. Med. Chem.* 22 (17), 4836–4847. doi: 10.1016/j.bmc.2014.06.053

Costa Lima, S. A., Resende, M., Silvestre, R., Tavares, J., Ouaissi, A., Lin, P. K. T., et al. (2012). Characterization and Evaluation of BNIPDaoct-Loaded PLGA Nanoparticles for Visceral Leishmaniasis: *In Vitro* and *In Vivo* Studies. *Nanomedicine* 7 (12), 1839–1849. doi: 10.2217/nnm.12.74

Craig, E., Huyghues-Despointes, C. E., Yu, C., Handy, E. L., Sello, J. K., and Kima, P. E. (2017). Structurally Optimized Analogs of the Retrograde Trafficking Inhibitor Retro-2cycl Limit Leishmania Infections. *PloS Negl. Trop. Dis.* 11 (5), e0005556. doi: 10.1371/journal.pntd.0005556

Croft, S. L., and Coombs, G. H. (2003). Leishmaniasis - Current Chemotherapy and Recent Advances in the Search for Novel Drugs. *Trends Parasitol.* 19 (11), 502–508. doi: 10.1016/j.pt.2003.09.008

Gandhi, T., Patki, M., Kong, J., Koya, J., Yoganathan, S., Reznik, S., et al. (2019) Development of an Arginine Anchored Nanoglobule With Retrograde Trafficking Inhibitor (Retro-2) for the Treatment of an Enterohemorrhagic Escherichia Coli Outbreak. *Mol. Pharm.* 16 (10), 4405–4415. doi: 10.1021/acs.molpharmaceut.9b00727

Gupta, N., Noël, R., Goudet, A., Hinsinger, K., Michau, A., Pons, V., et al. (2017). Inhibitors of Retrograde Trafficking Active Against Ricin and Shiga Toxins Also Protect Cells From Several Viruses, Leishmania and Chlamydiales. *Chem. Biol. Interact.* 267, 96–103. doi: 10.1016/j.cbi.2016.10.005

Huh, A. J., and Kwon, Y. J. (2011). "Nanoantibiotics": A New Paradigm for Treating Infectious Diseases Using Nanomaterials in the Antibiotics Resistant Era. *J. Control Release* 156 (2), 128–145. doi: 10.1016/j.jconrel.2011.07.002

Inceboz, T. (2019). "Epidemiology and Ecology of Leishmaniasis", in *Current Topics in Neglected Tropical Diseases*. p. 1–15. doi: 10.5772/intechopen.86359

Kalepu, S., and Nekkanti, V. (2015). Insoluble Drug Delivery Strategies: Review of Recent Advances and Business Prospects. *Acta Pharm. Sin. B.* 5 (5), 442–453. doi: 10.1016/j.apsb.2015.07.003

Kwan, S., and Marić, M. (2016). Thermoresponsive Polymers With Tunable Cloud Point Temperatures Grafted From Chitosan *via* Nitroxide Mediated Polymerization. *Polymer. (Guildf.)* 86, 69–82. doi: 10.1016/j.polymer.2016.01.039

Lutz, J. F. (2011). Thermo-Switchable Materials Prepared Using the OEGMA-Platform. *Adv. Mater.* 23 (19), 2237–2243. doi: 10.1002/adma.201100597

Nafari, A., Cheraghipour, K., Sepahvand, M., Shahrokhi, G., Gabal, E., and Mahmoudvand, H. (2020). Nanoparticles: New Agents Toward Treatment of Leishmaniasis. *Parasite Epidemiol. Control* e00156. doi: 10.1016/j.parepi.2020.e00156

Ndjamen, B., Kang, B. H., Hatsuzawa, K., and Kima, P. E. (2010). Leishmania Parasitophorous Vacuoles Interact Continuously With the Host Cell's Endoplasmic Reticulum; Parasitophorous Vacuoles are Hybrid Compartments. *Cell Microbiol.* 12 (10), 1480–1494. doi: 10.1111/j.1462-5822.2010.01483.x

Rao, J. P., and Geckeler, K. E. (2011). Polymer Nanoparticles: Preparation Techniques and Size-Control Parameters. *Prog. Polymer. Sci. (Ox.)* 36 (7), 887–913. doi: 10.1016/j.progpolymsci.2011.01.001

Sponchioni, M., Capasso Palmiero, U., and Moscatelli, D. (2019). Thermo-Responsive Polymers: Applications of Smart Materials in Drug Delivery and Tissue Engineering. *Mater. Sci. Eng. C.* 102, 589–605. doi: 10.1016/j.msec.2019.04.069

Stechmann, B., Bai, S. K., Gobbo, E., Lopez, R., Merer, G., Pinchard, S., et al. (2010). Inhibition of Retrograde Transport Protects Mice From Lethal Ricin Challenge. *Cell* 141 (2), 231–242. doi: 10.1016/j.cell.2010.01.043

Welsch, N., and Lyon, L. A. (2017). Oligo(ethylene Glycol)-Sidechain Microgels Prepared in Absence of Cross-Linking Agent: Polymerization, Characterization and Variation of Particle Deformability. *PloS One* 12 (7), e0181369. doi: 10.1371/journal.pone.0181369

World Health Organization (2018). Global Leishmaniasis Surveillance Update, 1998–2016. *Wkly. Epidemiol. Rec. Relev. épidémiologique. Hebd.* 93 (40), 530–540

Zhang, L., Gu, F. X., Chan, J. M., Wang, A. Z., Langer, R. S., and Farokhzad, O. C. (2008). Nanoparticles in Medicine: Therapeutic Applications and Developments. *Clin. Pharmacol. Ther.* doi: 10.1038/sj.clpt.6100400

Zuppardi, F., Chiacchio, F. R., Sammarco, R., Malinconico, M., Gomez d'Ayala, G., and Cerruti, P. (2017). Fluorinated Oligo(Ethylene Glycol) Methacrylate-Based Copolymers: Tuning of Self Assembly Properties and Relationship With Rheological Behavior. *Polymer. (Guildf.)* 112, 1697–179. doi: 10.1016/j.polymer.2017.01.080

Zuppardi, F., Malinconico, M., D'agosto, F., D'ayala, G. G., and Cerruti, P. (2020). Well-Defined Thermo-Responsive Copolymers Based on Oligo(Ethylene Glycol) Methacrylate and Pentafluorostyrene for the Removal of Organic Dyes From Water. *Nanomaterials* 10 (9), 1779. doi: 10.3390/nano10091779

Conflict of Interest: The authors declare that the research was conducted in the absence of any commercial or financial relationships that could be construed as a potential conflict of interest.

frontiers in Cellular and Infection Microbiology

ORIGINAL RESEARCH
published: 07 September 2021
doi: 10.3389/fcimb.2021.687607

Early Leukocyte Responses in *Ex-Vivo* Models of Healing and Non-Healing Human *Leishmania (Viannia) panamensis* Infections

Maria Adelaida Gomez[1,2*], *Ashton Trey Belew*[3,4], *Adriana Navas*[1], *Mariana Rosales-Chilama*[1,2], *Julieth Murillo*[1,5], *Laura A. L. Dillon*[3,4], *Theresa A. Alexander*[3], *Alvaro Martinez-Valencia*[1] *and Najib M. El-Sayed*[3,4*]

[1] Centro Internacional de Entrenamiento e Investigaciones Médicas (CIDEIM), Cali, Colombia, [2] Universidad Icesil, Cali, Colombia, [3] Department of Cell Biology and Molecular Genetics, University of Maryland, College Park, MD, United States, [4] Center for Bioinformatics and Computational Biology, University of Maryland, College Park, MD, United States, [5] Pontificia Universidad Javeriana, Cali, Colombia

OPEN ACCESS

Edited by:
Wander Pavanelli,
State University of Londrina, Brazil

Reviewed by:
Izabela Marques Dourado Bastos,
University of Brasilia, Brazil
Walderez Ornelas Dutra,
Federal University of Minas Gerais, Brazil
Maria Fernanda Laranjeira-Silva,
University of São Paulo, Brazil

***Correspondence:**
Maria Adelaida Gomez
mgomez@cideim.org.co
Najib M. El-Sayed
elsayed@umd.edu

Specialty section:
This article was submitted to Parasite and Host, a section of the journal Frontiers in Cellular and Infection Microbiology

Received: 29 March 2021
Accepted: 16 August 2021
Published: 07 September 2021

Citation:
Gomez MA, Belew AT, Navas A, Rosales-Chilama M, Murillo J, Dillon LAL, Alexander TA, Martinez-Valencia A and El-Sayed NM (2021) Early Leukocyte Responses in Ex-Vivo Models of Healing and Non-Healing Human Leishmania (Viannia) panamensis Infections. Front. Cell. Infect. Microbiol. 11:687607. doi: 10.3389/fcimb.2021.687607

Early host-pathogen interactions drive the host response and shape the outcome of natural infections caused by intracellular microorganisms. These interactions involve a number of immune and non-immune cells and tissues, along with an assortment of host and pathogen-derived molecules. Our current knowledge has been predominantly derived from research on the relationships between the pathogens and the invaded host cell(s), limiting our understanding of how microbes elicit and modulate immunological responses at the organismal level. In this study, we explored the early host determinants of healing and non-healing responses in human cutaneous leishmaniasis (CL) caused by *Leishmania (Viannia) panamensis.* We performed a comparative transcriptomic profiling of peripheral blood mononuclear cells from healthy donors (PBMCs, n=3) exposed to promastigotes isolated from patients with chronic (CHR, n=3) or self-healing (SH, n=3) CL, and compared these to human macrophage responses. Transcriptomes of *L. V. panamensis*-infected PBMCs showed enrichment of functional gene categories derived from innate as well as adaptive immune cells signatures, demonstrating that *Leishmania* modulates adaptive immune cell functions as early as after 24h post interaction with PBMCs from previously unexposed healthy individuals. Among differentially expressed PBMC genes, four broad categories were commonly modulated by SH and CHR strains: cell cycle/proliferation/differentiation, metabolism of macromolecules, immune signaling and vesicle trafficking/transport; the first two were predominantly downregulated, and the latter upregulated in SH and CHR as compared to uninfected samples. Type I IFN signaling genes were uniquely up-regulated in PBMCs infected with CHR strains, while genes involved in the immunological synapse were uniquely downregulated in SH infections. Similarly, pro-inflammatory response genes were upregulated in isolated macrophages infected with CHR strains. Our data demonstrate that early responses during *Leishmania* infection extend beyond innate cell and/or phagocytic host cell

functions, opening new frontiers in our understanding of the triggers and drivers of human CL.

Keywords: *Leishmania Viannia*, PBMCs, leukocytes, host-pathogen interactions, RNA-Seq

INTRODUCTION

Clinical manifestations of human infections with *Leishmania Viannia* species (primarily *L. V. braziliensis* and *L.V. panamensis*) range from single self-healing skin lesions, to severe and chronic cutaneous or mucosal disease (Weigle et al., 1993; Murray et al., 2005). Contrary to infections where microorganisms inflict direct damage to the host *via* toxins or cellular injury, symptomatic dermal leishmaniasis (cutaneous, mucosal or muco-cutaneous) results from parasite-elicited immunopathology, and disease severity depends on the degree of immunopathology and concomitant immunoregulation (Murray et al., 2005; Rodriguez-Pinto et al., 2012). For these immunopathologically-driven infections, the early host-microbe interactions and the elicited innate immune responses, together with specific features of the anatomical sites and tissues affected, shape the adaptive responses that contribute to pathology and disease severity. However, the triggers and drivers of immunopathology of dermal leishmaniasis remain largely unknown.

Genotypic and phenotypic variability among *Leishmania* isolates of the same species has been long-recognized. Within the *L. Viannia* subgenus, a number of phenotypically discernable populations (zymodemes) co-circulate in endemic foci of transmission, with *L. V braziliensis* and *L.V. panamensis* being the two species with the highest heterogeneity (Saravia et al., 1998). Distinct host responses as well as intrinsic parasite phenotypes have been correlated with different zymodemes. Disease caused by *L. V. braziliensis* zymodeme 1.1 has been associated with a longer time of evolution in humans (Saravia et al., 1998), and *L. V. panamensis* zymodeme 2.3 has been identified as a population intrinsically resistant to antimony (Fernandez et al., 2014). Thus, parasite factors, as well as their interaction with the host may contribute to the distinct immunological responses unleashed upon infection with different strains of the same *Leishmania* species. Although the specific determinants of such responses are currently unknown, variations in virulence factors involved in modulating the early stages of the host-pathogen interaction [e.g. GP63 copy number or function (Gomez and Olivier, 2010)], could contribute to divergent clinical outcomes of disease.

Characterization of the early *Leishmania*-host interactions has been primarily conducted in the context of isolated phagocyte infections [macrophages, dendritic cells and neutrophils, and predominantly using murine or human cell lines (Cohen-Freue et al., 2007; Ovalle-Bracho et al., 2015)]. We have previously shown that *L. V. panamensis* strains isolated from patients with chronic cutaneous leishmaniasis (CL) induced significantly more expression of pro-inflammatory chemokines and cytokines in human macrophages (Navas et al., 2014), consistent with parasite-elicited hyperactivation of the host-cell inflammatory response driving disease severity. However, during natural vector-borne infections, the initial host-parasite interaction involves a multitude of other immune and non-immune cells, which constitute the cellular micro-environment to which, promastigotes are exposed after inoculation into the human host. Murine models of infection have provided evidence of the early participation of keratinocytes in susceptibility to *L. major* via induction of pro-inflammatory chemokines and cytokines (Ehrchen et al., 2010; Ronet et al., 2019). In humans, keratinocytes were proposed to participate in the development of post-kala azar dermal leishmaniasis, and in the pathologic changes of ulcerating skin lesions (Gasim et al., 1998; Tasew et al., 2010). The participation of non-immune and non-phagocytic immune cells in the early interactions of *L. Viannia* species and the host, and the contribution of those responses to development of symptomatic disease and in disease severity, are not completely understood.

Gene expression profiling of peripheral blood mononuclear cells (PBMCs) responses, both at the basal level and after antigenic recall, has been successfully implemented as a tool to identify immunological gene signatures of clinical and therapeutic outcomes in human infections. Illustrating this, transcriptional profiling of PBMCs has revealed gene signatures associated with immunological protection in human malaria vaccine studies (Moncunill et al., 2020), responsiveness to antiviral treatment in human hepatitis C infections (Orr et al., 2020), and long-lasting immune dysfunction in patients with chronic ebola infection (Wiedemann et al., 2020), among others. More recently, consistency between results from bulk RNA-seq and single cell sequencing has been demonstrated with PBMCs from COVID-19 patients (Arunachalam et al., 2020), supporting the use of bulk transcriptomics to explore immunological signatures of infectious diseases and disease severity.

Antigen-specific recall responses of PBMCs from CL patients has demonstrated that a mixed T_h1/T_h2 response, accompanied by immune deregulation, participates in the clinical manifestations and disease severity caused by *L. Viannia* (Carvalho et al., 1985; Saravia et al., 1989; Diaz et al., 2010). In this study, we examined how clinical strains of *L.V. panamensis* which cause different degrees of severity of CL in humans (chronic or self-healing CL), modulate the early responses of PBMCs within the first 24 hours of parasite-host interaction. We hypothesize that these initial PBMC-promastigote interactions contribute to define the nature and magnitude of activated or repressed host functions, ultimately determining the clinical outcome of infection. Identification of immunological signatures associated with development of more severe disease manifestations and triggered during the early phases of infection, will serve as a knowledge base for the development of prognostic tools, ultimately allowing timely intervention for these cases,

known to be more refractory to first-line antileishmanial drugs (Amato et al., 2008; Maurer-Cecchini et al., 2009; Bamorovat et al., 2021).

MATERIALS AND METHODS

Isolation of Total WBCs and PBMCs

Peripheral blood samples from healthy volunteers without history of CL and residing in an urban non-endemic city, were collected and processed to obtain total WBCs and PBMCs. WBCs were isolated by centrifugation at 400 g for 15 min at RT and cells were collected from the interface between the plasma and red blood cells. WBCs were incubated in RBC lysis buffer ([150 mM] NH_4CL, [10 mM] $KHCO_3$, [0.1 mM] Na_2EDTA) for 5 min at RT, washed with PBS, and resuspended in RPMI supplemented with 10% FBS for subsequent procedures. PBMCs were obtained by centrifugation of PBS-diluted (1:1) blood samples over a Ficoll-Hypaque gradient (Sigma-Aldrich) following the manufacturer's instructions.

Leishmania Strains

Clinical strains were obtained from the CIDEIM BioBank. Strains were originally isolated by needle aspirate of cutaneous lesions or from biopsies of mucosal lesions, propagated in Senekjie´s biphasic blood agar and immediately stored in liquid nitrogen until use. Strains were typed by immunoreactivity to monoclonal antibodies. *L. V. panamensis* strains MHOM/CO/11/5430 (5430chr), MHOM/CO/08/5433 (5433chr) and MHOM/CO/08/5397 (5397chr) were isolated from patients with chronic CL of > 6 months´ evolution. MHOM/CO/87/1320 (1320chr) and MHOM/CO/85/2504 (2504chr) were isolated from lesion biopsies of nasal mucosa from patients with >10 years of muco-cutaneous disease. Strains MHOM/CO/85/2272 (2272sh), MHOM/CO/85/2271 (2271sh), MHOM/CO/89/2189 (2189sh) and MHOM/CO/83/1022 (1022sh) were isolated from CL patients who clinically resolved disease in the absence of any treatment (self-healing CL).

Infection

Promastigotes were grown at 25°C in Senekjie's biphasic medium and passed for a maximum of two sub-passages into RPMI 1640 supplemented with 10% heat-inactivated FBS and 5 mg/ml hemin. Ten million WBCs or PBMCs were infected at a 10:1 parasite-to-monocyte ratio with human AB+ serum-opsonized stationary phase promastigotes for 24h. Selection of 24 hours post infection (hpi) as the time to characterize the early interaction of PBMCs and *Leishmania*, was based on prior transcriptomic data showing a strong modulation of gene expression at 4 hpi, and stabilization of these responses at 24 hpi, remaining essentially unaltered up to 72 hpi (Dillon et al., 2015; Fernandes et al., 2016).

Macrophage Samples

All macrophage samples used were those previously collected and characterized in a previous study from our group (Navas et al., 2014). Briefly, macrophages were differentiated from PBMCs by adherence to cell culture plasticware in serum-free RPMI for 2h, followed by culture for 7 days in RPMI supplemented with 20% FBS at 37°C and 5% CO_2. Cells were infected for 24h at a 1:10 ratio as described above.

RNA Isolation and cDNA Synthesis

Total RNA was extracted from uninfected and infected cultured cells using Trizol (Invitrogen, USA) followed by RNA cleanup with RNeasy Mini Kit columns (Qiagen, USA). RNA integrity was assessed using an Agilent 2100 bioanalyzer. For RNA-seq, poly(A)-enriched cDNA libraries were generated using the Illumina TruSeq v2 sample preparation kit (San Diego, CA) and checked for quality and quantity using bioanalyzer and quantitative PCR. For qRT-PCR analyses, RNA was reverse transcribed with RT First Strand Kit (SABiosciences-Qiagen).

Gene Expression by qRT-PCR

Gene expression analysis of 84 inflammatory genes and receptors was conducted by qRT-PCR using Qiagen PCR Arrays (PAHS-077Z) on a BioRad® CFX-96 detection platform. Gene expression was normalized to a five gene panel composed of β2-microglobulin, hypoxanthine phosphoribosyltransferase-1, β-actin, GAPDH and ribosomal protein L13a. Data was analyzed using the ΔΔCt method and fold change calculated compared to uninfected cells and expressed as $2^{-\Delta\Delta Ct}$. Data was processed and analyzed on the RT² Profiler™ PCR Array Data Analysis online tool provided by the manufacturer.

RNA-Seq Data Generation, Preprocessing, and Quality Trimming

Paired-end reads (100 bp) were obtained using an Illumina HiSeq 1500. Trimmomatic (Bolger et al., 2014) was used to remove Illumina adapter sequences from reads and to trim bases off the start or the end of a read when the quality score fell below a threshold of 25. Sequence quality metrics were assessed using FastQC (http://www.bioinformatics.babraham.ac.uk/projects/fastqc/).

Mapping cDNA Fragments, Abundance Estimation, and Data Normalization

Reads were aligned against the human (hg38 revision 91), *L.V. panamensis* (TriTrypDb release 36), and *L.V. braziliensis* (release 26) genomes with TopHat (2.1.0) (Trapnell et al., 2012) using parameters to randomly place multi-matches (-g 1), using an existing set of splice junctions (-G), and using the more sensitive bowtie2 options (–b2-very-sensitive). The resulting accepted hits and mapped reads were sorted and indexed *via* SAMtools (Li et al., 2009) and passed to HTSeq (Anders et al., 2015) for generating count tables.

Global Data Assessment, Visualization and Differential Expression Analysis

Biological replicates and batch effects were assessed and visualized using the hpgltools (https://github.com/elsayed-lab/hpgltools) R package. The process included creating density plots, boxplots of depth, coefficient of variance, hierarchical clustering analyses based on Pearson's correlation coefficient

and Euclidean distance, variance partition analyses (Hoffman and Schadt, 2016), and principal component analyses before and after normalization. Several combinations of normalization and batch adjustment strategies were evaluated. The normalization methods tested included trimmed median of M-values, relative log expression, and quantile. These were combined with different batch evaluation strategies including: surrogate variable analysis (SVA) (Leek et al., 2012), ComBat (in sva), RUV (Risso et al., 2014), and batch factor removal *via* residuals (performed manually and *via* limma's (Ritchie et al., 2015) removeBatchEffect function). Normalized data were visualized using $\log_2$ transformed counts per million reads following filtering to remove low counts (defined as any gene with fewer counts than twice the number of samples or when any sample had fewer than 2 counts).

Differential expression analyses were performed using a single pipeline which performed all pairwise comparisons using the Bioconductor packages: limma, edgeR (Robinson et al., 2010), DESeq2 (Love et al., 2014), EBSeq (Leng et al., 2013), and a statistically uninformed basic analysis. In each case (except EBSeq and the basic analysis), the surrogate variable estimates provided by SVA were used to adjust the statistical model in an attempt to address the batch/surrogate effects. The quality of each contrast was evaluated by the degree of agreement among methods, but the interpretations were primarily informed by the DESeq2 results. Detailed information on the analytical pipeline and scripts is available at (https://github.com/abelew/cideim_early_leukocyte).

Genes with significant changes in abundance (fold change $\geq |1.5|$ and false discovery rate adjusted P values ≤ 0.05) were passed to a few gene set enrichment methods including: GOseq (Young et al., 2010), clusterprofiler (Yu et al., 2012), topGO, GOstats (Falcon and Gentleman, 2007), gProfileR (Reimand et al., 2016) and gene set variation analysis (GSVA) (Hanzelmann et al., 2013). Gene ontology analyses were supplemented with manual data curation. GSVA was performed to produce an enrichment score for each gene set per sample. These scores were passed to limma to evaluate the difference in GSVA score distributions for each gene set in the samples. Limma results were then filtered according to log2 fold change, adjusted p-value, and maximum GSVA score mean. GSVA was conducted using the immunologic signature gene sets publicly available at GSEA|MSigDB (C7 collection) (Liberzon et al., 2011). Network analyses were done with STRING 11.0 (Szklarczyk et al., 2019).

Detection of *Leishmania* RNA Virus (LRV)

Total RNA was extracted from stationary-phase promastigotes using TRIzol (Invitrogen, USA), and cDNA was synthesized using a high-capacity cDNA reverse transcription kit (Applied Biosystems). LRV was detected by qRT-PCR using the primer sets described by (Zangger et al., 2013): Forward 5′-CTG ACT GGA CGG GGG GTA AT-3′ and Reverse 5′-CAA AAC ACT CCC TTA CGC-3′, derived from LRV1-4 genome sequences (GenBank accession number: NC_003601). As a quality control procedure for nucleic acids, a 372 bp fragment of the *Leishmania* β-tubulin gene was also amplified. Positive and negative controls for LRV were included in each run: *L. V. guyanensis* M5313 (WHI/BR/78/M5313 – LRV+) and *L. V. panamensis* (MHOM/CO/2002/3594 stably transfected with the luciferase reporter gene, L.p.LUC 001, LRV-).

RESULTS AND DISCUSSION

Profiling of Inflammatory Mediators in WBCs and PBMCs Reveals a Similar Signature

The macrophage-*Leishmania* infection model has been consistently used as the preferred *in vitro* and *ex vivo* experimental system, because it portrays the interaction of the parasite and its primary host cell. However, recruitment of other cells to the inflammatory microenvironment generated during the vector blood meal, implies that the early interaction between the parasite and the host extends beyond the macrophage-*Leishmania* contact. Different experimental approaches and cell preparations can be used to explore these *Leishmania*-leukocyte interactions (e.g. whole blood, total white blood cells -buffy coat-, isolated PBMCs). To select the *ex vivo* cellular system for our experiments, we performed a comparative expression profiling of 84 immune response genes in total human white blood cells (WBCs) and PBMCs collected from healthy donors (n=3), which were then exposed to *L.V. panamensis* promastigotes for 24 hours. Eleven genes (*ccl11, ccl16, ccl21, ccl8, crp, IL17a, il23r, il9, kng1, nos2* and *sele*) were not detected in either PBMCs or WBCs. *Il22* was only detected in infected PBMCs from one donor, and *ccl19* was not detected in WBCs, but was induced in infected PBMCs (**Table S1**). 56 genes were modulated by exposure to *L. V. panamensis* (fold change, FC $\geq |1.5|$), and 39 were common in PBMCs and WBCs (28 upregulated and 11 downregulated). Modulation of *il1r, il1rap* and *tlr1* was mainly found in WBCs, which is consistent with the predominant expression in granulocytes (Uhlen et al., 2015). The magnitude of modulation was consistently higher in PBMCs than WBCs, in line with higher transcriptional activity of mononuclear compared to polymorphonuclear cells (Ericson et al., 2014; Grassi et al., 2018) (**Figure 1**). The similarity of gene expression profiles supports the use of PBMCs as an informative cell population to explore the predominant immunological signatures elicited during the early stages of *L.V. panamensis* infections.

Exposure of PBMCs to *L. Viannia* Modulates Transcriptional Signatures of Lymphocyte Activation

PBMCs from three healthy donors from a non-endemic area, were exposed for 24h to stationary phase promastigotes isolated from patients with chronic (CHR, n=3) or self-healing (SH, n=3) CL. *Leishmania* virulence factors such as the major surface metalloprotease GP63, lipophosphoglycan (LPG), and the *Leishmania* RNA virus (LRV), contribute to disease severity in murine models of infection (Beverley and Turco, 1998; Gomez et al., 2009; Ives et al., 2011). However, a clear relationship of these and other virulence determinants in the clinical outcome of human infections remains elusive. We evaluated the presence of LRV in all clinical strains used in this study. All strains except

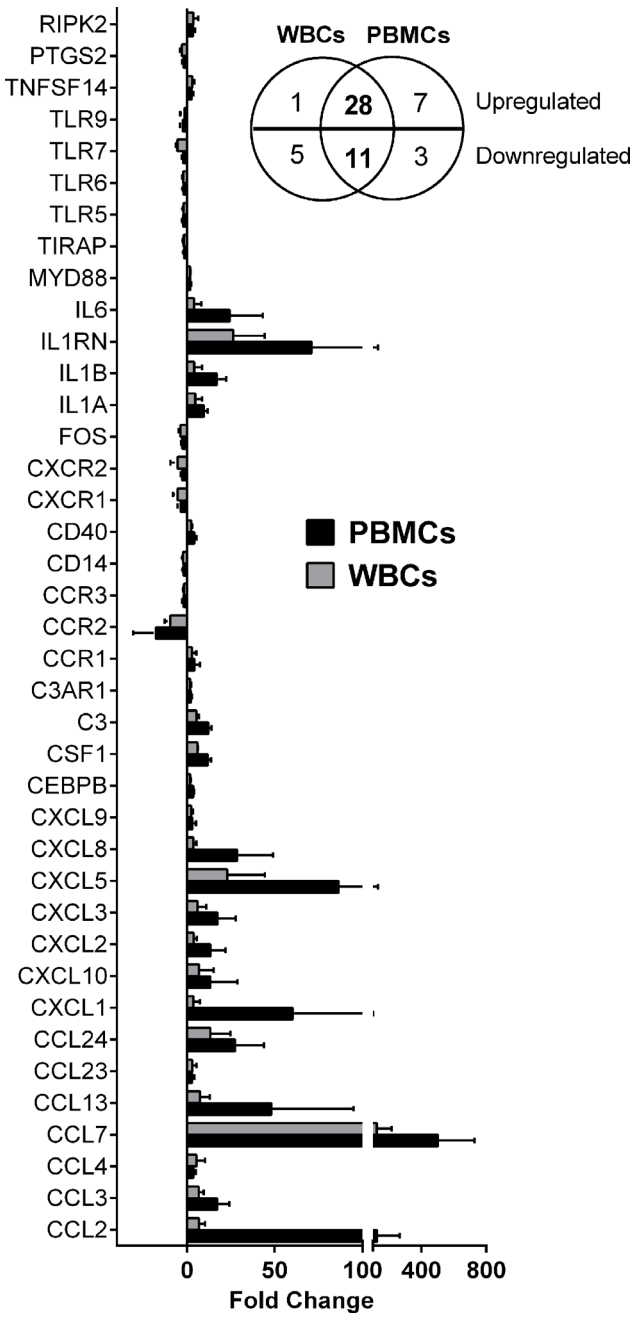

FIGURE 1 | Differentially expressed genes in WBCs and PBMCs upon *L. V. panamensis* infection. Fold change gene expression (infected *vs.* uninfected) of genes modulated in WBCs and PBMCs from three healthy donors after *ex vivo* infection with *L. V. panamensis* for 24h. Insert: Venn diagram representing the number of upregulated and downregulated genes.

for the positive control *L. V. guyanensis* M5313, which was LRV (+) with an avergae Ct value of 24,3.

Poly(A)-enriched cDNA libraries were constructed and 100 bp paired-end reads were generated (**Table S2** and **Figure S1**). Each sample from infected cells consisted of a pool of mixed RNAs from parasites and human macrophages. Post-experimental authentication of *Leishmania* strains used in these experiments was carried out by SNP profiling of parasite-derived sequences. This confirmed that all strains used corresponded to *L.V. panamensis*, except for strain MHOM/CO/11/5430 which was identified as a mixed *L. V. panamensis/L. V. braziliensis* isolate.

A principal component analysis (PCA) showed that a significant amount of the variance observed in the host transcriptomic data resulted from either the infection status (infected *vs.* uninfected, **Figure 2A**) or, in the absence of uninfected samples, from inter-donor variability (**Figure 2B**). To account for these sources of variance, an adjusted statistical model was developed using SVA. A PCA of the SVA-adjusted data showed a partial separation of samples based on infection with CHR *vs.* SH strains (**Figure 2C**).

Differential expression (DE) analysis of the transcriptomes from PBMCs exposed to SH strains against CHR strains yielded no statistically significant DE genes. Considering that most of the variance between samples was attributed to either donor variability or infection status, we conducted three additional analyses: 1) an independent DE analysis of infection with CHR *vs.* SH strains for each donor; 2) a grouped analysis of PBMCs from the three donors infected with SH strains against uninfected controls, and 3) a grouped analysis of PBMCs from the three donors infected with CHR strains against uninfected controls. For the independent donor analyses, transcriptomes of PBMCs from one donor did not identify statistically significant DE genes. For the second and third donors, only 3 and 28 DE genes were found respectively (**Table S3**). Grouped analysis of infected PBMCs against uninfected controls yielded over 2800 significantly DE genes in infections with either SH or CHR strains. Of these, 2208 (78.8%) were common to CHR and SH infections: 1408 upregulated and 800 downregulated (cut off values: $p \leq 0.05$; $\log_2 FC \geq |0.58|$, i.e. fold change $\geq |1.5|$), **Figure 2D**. Despite the statistical significance of this enrichment analysis, the biological information extracted from these GO categories is limited.

Among up- and down-regulated genes, the top 10 significantly enriched categories (ranked by % representation within the dataset) corresponded to broad categories related to immune functions, cell signaling, transcription, and cell proliferation, among others (**Table S4**).

To provide a more insightful biological interpretation of the effect of early exposure of PBMCs to *L.V. panamensis*, and to explore the potential contribution of specific cell types to the bulk transcriptomic profile of PBMCs, we conducted gene set variation analysis (GSVA) using the immunologic signature gene sets publicly available at GSEA|MSigDB (C7 collection) (Liberzon et al., 2011). 140 categories were significantly and differentially enriched in *L.V. panamensis* infected *vs.* uninfected PBMCs (**Figure 3** and **Table S5**), independent of whether cells were exposed to CHR or SH strains. Interestingly, 37 gene sets were derived from experiments involving microbial agents, including infections with old world *Leishmania* species (*L. donovani and L. major*) and other intracellular microbes

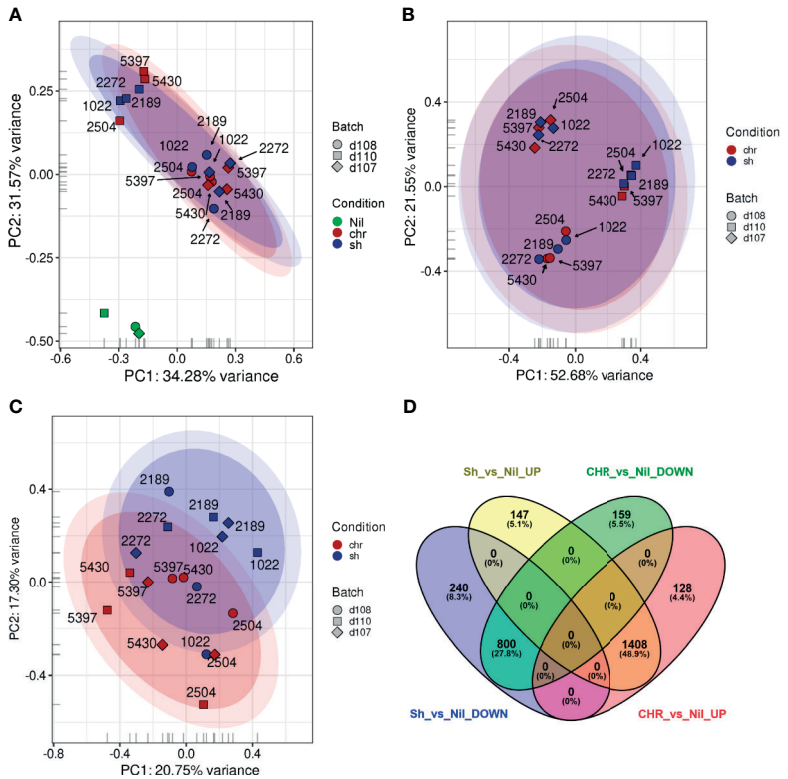

FIGURE 2 | Principal Component Analysis plots and Differential Expression analyses of PBMCs exposed to SH and CHR strains. An initial PCA was performed **(A)** using log_2, quantile, count per million (cpm), low-count-filtered data and displayed a strong clustering with respect to the three donors (represented as the different symbol shapes). **(B)** This donor-specific effect was made even clearer when the uninfected samples (green) were removed from the analysis. **(C)** When surrogate variable estimates from SVA were included, it became possible to visualize differences between the PBMCs exposed to CHR (red) and self-healing (blue) strains. **(D)** Venn diagrams showing the relationships between the overlaps of differentially expressed genes in SH *vs.* uninfected (Nil) and CHR *vs.* uninfected samples.

(*Toxoplasma gondii* and *Mycobacterium tuberculosis*). This potentially shows common early response mechanisms against intracellular pathogens.

Among enriched categories, 47 corresponded exclusively to innate cell signatures (monocytes, macrophages, NK cells, dendritic cells), while 56 were related to signatures derived from adaptive immune cells (CD8 and CD4 T cells, Th17, Tregs, T follicular cells, B cells) **(Table S5)**. This indicates that as early as 24h after interaction, *Leishmania* modulates adaptive immune cell functions in PBMCs from previously unexposed healthy individuals, revealing a largely unexplored and exploitable dimension of the host-pathogen interactome in Leishmania infections. The mechanism(s) mediating this rapid activation, especially of naïve T cells, remains to be determined, but could occur *via* bystander (antigen-independent) activation of naïve or memory T cells (Kim and Shin, 2019; Lee et al., 2020), cross-reactivity of memory T cells, or potentially *via* antigen-presentation by circulating fibrocytes (Chesney et al., 1997; Grab et al., 2004). Interestingly, bystander activation of *Lysteria*-specific and *LCMV*-specific memory T-cells has been reported in chronic *L. donovani* infection of *Lysteria*-immune mice (Polley et al., 2005), and in acutely *L. major* infected mice, respectively (Crosby et al., 2014).

Exposure of PBMCs to SH and CHR Strains Differentially Modulate Genes Related to IFN Responses and the T Cell Synapse

We next analyzed the gene set differentially modulated by SH and CHR infections. A total of 387 genes were uniquely modulated in PBMCs after exposure to SH strains (240 down- and 157 up-regulated), and 287 were unique to infection with CHR strains (159 down- and 128 upregulated) **(Table S6).** Functional interpretation of DE genes was performed *via* GO enrichment, complemented by network analyses and manual curation. For infections with SH strains, no significantly enriched GO categories were found. For infections with CHR strains, a single GO category was enriched (FDR=0.00029): Type I IFN signaling (reactome pathway HSA-1606322) (**Table S7**).

Upon manual curation, 17 functional categories were defined (all containing ≥ 5 genes, except for "antimicrobial activity"). Four categories (metabolism of macromolecules, cell cycle/proliferation/differentiation, immune signaling and vesicle trafficking/transport) were common to infections with SH and CHR strains (**Table S7**). Genes involved in metabolism of macromolecules (lipid, glycan and nucleic acids metabolism)

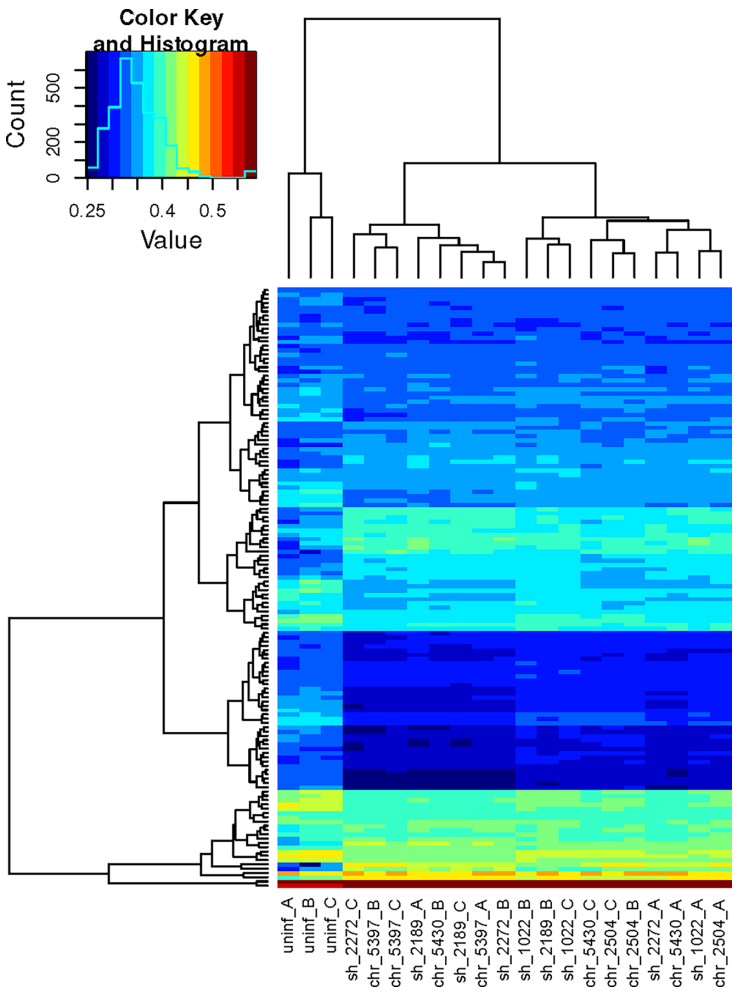

FIGURE 3 | Hierarchical clustering heatmap of significant mSigDB c7 gene sets. GSVA was performed using the normalized expression data and the mSigDB c7 gene sets. The resulting scored gene sets were examined using limma and by *de-novo* comparisons of the mean group scores in order to extract the most significant gene sets. The remaining scores were passed to a hierarchical clustering algorithm and plotted. Each column corresponds to an independent sample, each row to a unique gene set. Columns 1- 3, uninfected PBMCs from three independent healthy donors (A–C). Columns 4-18, infected PBMCs. Sample codes correspond to the phenotype of the disease caused by the *Leishmania* strain (sh, self healing; chr, chronic), followed by the strain code and the PBMC donor.

were found in both upregulated and downregulated gene lists, however, most of these genes were significantly downregulated in infected PBMCs. Rapid downregulation (at 4hpi) of fatty acid metabolism, amino acid catabolism and glycan degradation has been previously documented in murine and human macrophages infected with *L. major* (Dillon et al., 2015; Fernandes et al., 2016); here we show that this is maintained as long as 24hpi. This suggests that basic metabolic functions are stalled during the early time-points of *Leishmania* infection in both phagocytic host cells and other blood leukocytes, potentially revealing an early re-programming of basic metabolic functions towards a state of immune cell activation (O'Neill et al., 2016).

Downregulation of central elements of cell cycle progression and pro-growth signaling (MAPK and PI3K), and concomitant induction of genes involved in oxidative phosphorylation and intracellular vesicle trafficking, were also observed (**Table S7**). Downregulation of genes involved in cell cycle and metabolism of macromolecules, and induction of genes of the tricarboxylic acid (TCA) cycle, is consistent with a state of arrested cell cycle progression. High metabolic demands (provided by metabolism of macromolecules, and not the TCA cycle) are required during cell proliferation and differentiation, while oxidative phosphorylation is a major metabolic pathway in non-proliferative cells (O'Neill et al., 2016). These data further support that the early interaction of *L. Viannia* with PBMCs leads to reduced metabolic capacity, potentially skewing immune cells towards mechanisms of fast energy production to support rapid immune cell activation in otherwise metabolically "paused" cells (Alonso and Nungester, 1956; Newsholme et al., 1986).

Among the uniquely downregulated genes in PBMCs infected with SH strains were primary cilium proteins (**Table S7**). The primary cilium was long considered a vestigial organelle

(Cassioli and Baldari, 2019), and re-discovered as a signaling hub (Nachury and Mick, 2019). Although hematopoietic cells do not have primary cilia, a more recent understanding of the T cell immunological synapse (IS) suggests participation of ciliary proteins in IS formation (Cassioli and Baldari, 2019). The assembly and function of the IS and the primary cilium depend on cytoskeleton dynamics and polarized vesicle trafficking, and evidence of strong modulation of these processes was found in the transcriptomic profiles of *L. Viannia*-infected PBMCs (**Table S7**). Within the first hour of interaction between T-cells and antigen presenting cells (APC), an actin-rich invasive pseudopodia emerges from T-cells and probes deep within the APC. The actin cap is then cleared to allow orientation of the microtubule organization center (MTOC) to the IS, resulting in a matured IS (Ueda et al., 2015). Interestingly, disruption of the MTOC does not impact the level of cytokine production in T cells; however, it does change the "directionality" of cytokine secretion so that it is no longer directed at the IS (Ueda et al., 2015). Dampened expression of molecules involved in primary cilia/IS formation during infection of PBMCs with SH strains suggests a cytokine micro-environment that may lead to subtler activation of APCs during interaction with T cells, potentially limiting excessive pro-inflammatory cytokine production that can result in uncontrolled inflammation and immunopathology (Scott and Novais, 2016).

Macrophage Functions Are Central Drivers of the Divergent Immune Responses Elicited Upon SH and CHR Infections

We explored the effect of SH and CHR infections in macrophages as one of the central APCs and principal host cells for *Leishmania*. Total transcriptomic profiles were obtained from primary macrophages infected for 24 h with SH and CHR strains [RNA samples used here were those previously reported in (Navas et al., 2014)]. PCA showed clustering of samples by disease phenotype (**Figures 4A** and **S2**). Macrophages infected with SH strains clustered together and close to uninfected cells, indicating minimal modulation of macrophage gene expression by SH strains, and supporting the controlled APC response that also emerged from SH-infected PBMC transcriptomes.

Differential gene expression analysis of macrophages infected with CHR *vs.* SH strains identified 884 DE genes (**Figure 4B** and **Table S8**), representing 30% more DE genes compared to those in PBMCs. The macrophage DE gene profile consisted predominantly of upregulated inflammatory response genes in infections with CHR *vs.* SH strains [also previously reported in microarray and qRT-PCR datasets of *L.V. panamensis* infected macrophages (Ramirez et al., 2012; Navas et al., 2014)]. In infections with CHR strains, up-regulation of chemokines involved in monocyte (CCL2, CCL13 and CCR1) and $CD4^+$-T_H1 (CXCL10) activation and recruitment (**Figure 5** and **Table S8**), as well as genes associated with TLR and IFN signaling (TLR4, CD14, TLR1, IFNGR1, IFNAR1, JAK2) were found. In addition, an upregulation of complement components including C3, C1QA, C1QC, CFD and CFP (complement factors D and properdin), ficolin (FCN1), CR1 and the anaphylatoxin receptor C5AR1 (and downstream signaling molecules Rap1b, Rap2a) was observed, which have been associated with a potent induction of inflammation and cell recruitment during acute and chronic inflammatory processes.

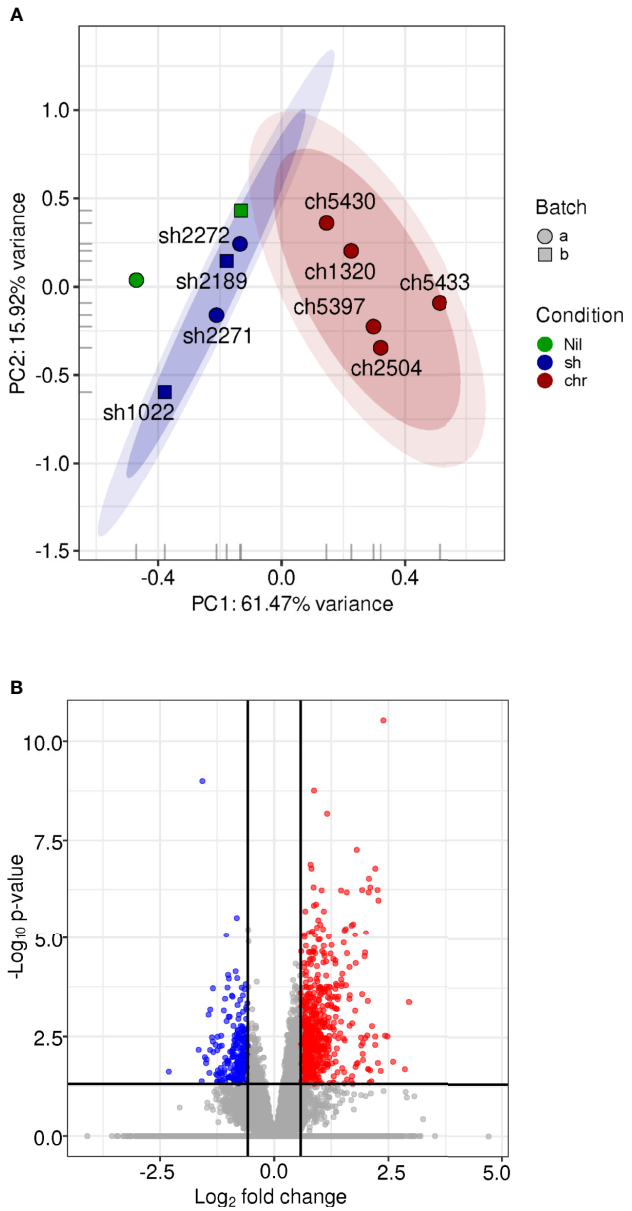

FIGURE 4 | Gene expression profiles of human macrophages infected with SH and CHR L. V. panamensis strains CL. The *(H)* sapiens RNA-seq expression data for annotated coding genes after low-count filtering (7,019 genes remaining) and log_2[quantile(cpm)] normalization was examined *via* PCA **(A)**. Each glyph represents an experimental sample where the color represents the infection state, the shape represents the experimental batch. The 0.90, 0.95 confidence intervals are shown as shaded ovals. Differential expression analysis was performed using DESeq2, including experimental date (batch) in the statistical model. The volcano plot **(B)** shows the distribution of significance (-log adjusted *P* value) with respect to log_2-fold change. Points colored in blue are deemed significantly downregulated in the macrophage samples infected with CHR *vs.* SH strains while those in red are significantly up-regulated.

Genes involved in opsonophagocytosis and vesicle mediated transport were also induced in CHR-infected macrophages relative to SH-infected cells (**Figure 5** and **Table S8**). Among those were CR1, properdin and C3b, which have been associated with opsonophagocytosis of intracellular pathogens (Rosales and Uribe-Querol, 2017; Lu et al., 2018). Complement receptors participate in uptake of *Leishmania* by macrophages, and a direct relationship between permissiveness of macrophage infection, CR1 and CR3 activity, and chronic CL caused by *L. V. panamensis* has been reported (Robledo et al., 1994). Increased C3 gene expression has been demonstrated in lesion biopsies from CL patients unresponsive to antimonial treatment, potentially leading to enhanced recruitment of polymorphonuclear cells to the affected tissues, promoting immunopathology and a non-healing phenotype (Navas et al., 2020). Induction of multiple Fc gamma receptors (FcgR, including the high affinity receptor FcgR1 as well as low affinity receptors 2a, 2b, 3a and 3b), and a number of genes involved in vesicle-mediated transport (sortins, syntaxins), phagolysosomal acidification (Rab39A, Rab32, Rab20, Vamp7, lamp1, lamp2, V-ATPase subunits among others), and antigen processing and presentation (MHC-II molecules, lyzozyme, cathepsine L) was also observed in macrophages infected with CHR strains, supporting enhanced opsonophagocytosis (Lu et al., 2018) and intracellular parasite killing. Consistent with this hypothesis was the finding that parasite loads were lower in primary human macrophages infected with CHR compared to SH strains (**Table S2**, **Figure S3**).

CONCLUDING REMARKS

The exploration of transcriptomic signatures from both isolated human primary macrophages and PBMCs consistently provides evidence that pathology and severity of CL infection is determined, at least in part, by the immune response. Chronic CL is characterized by the induction of pro-inflammatory leukocyte

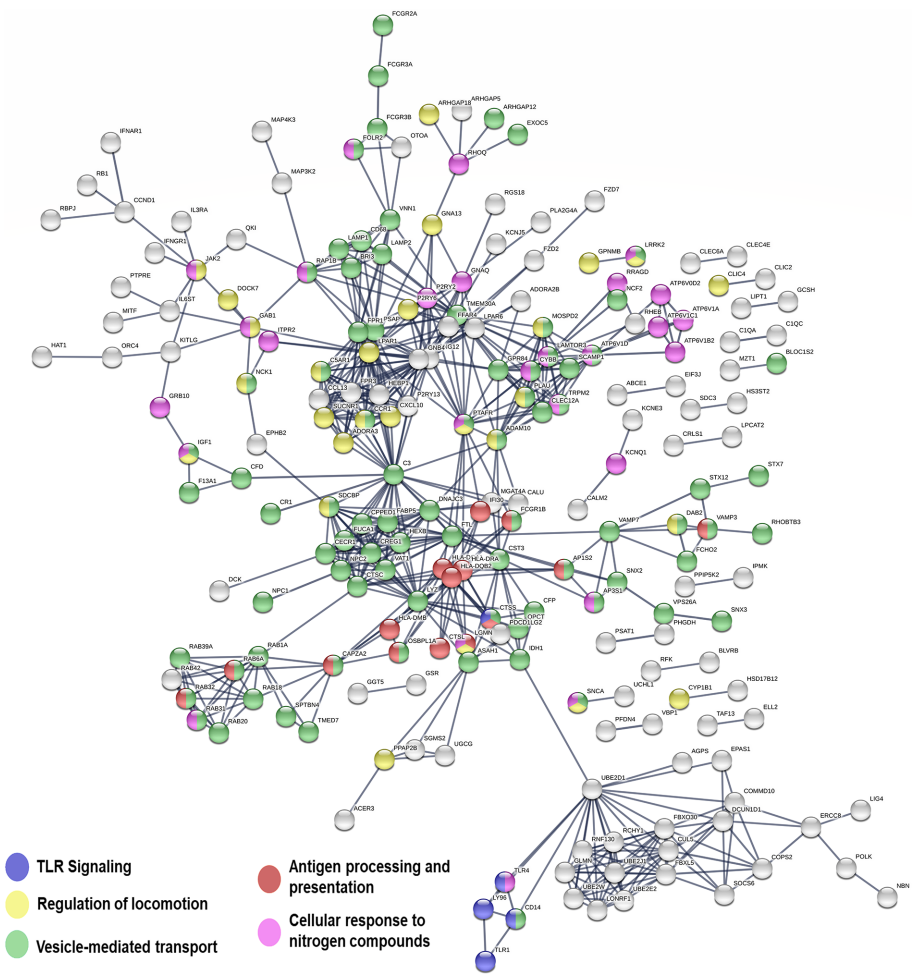

FIGURE 5 | Network representation of genes significantly upregulated in macrophages infected with CHR *vs.* SH strains. Line thickness represents the strength of data support (displaying relationships > 0.9 confidence value). Interaction sources for network building in STRING included experiments, databases, co-expression, neighborhood, gene fusion and co-occurrence. Nodes not in networks are hidden.

responses, while benign, self-resolving CL, may be primarily marked by limited and controlled T-cell and APC activation. The early interaction of PBMCs and *L. Viannia* provides a more comprehensive view of additional mechanisms involved in the establishment of infection in the human host. Downregulation of genes involved in biosynthesis and metabolism of macromolecules, cell cycle progression and cellular proliferation, together with upregulation of functional categories related to glycolysis and oxidative phosphorylation, suggest that the parasite-host interplay of *Leishmania* and PBMCs drives cellular functions and energy production towards immunological activation rather than to promote metabolism of macromolecules. Whether this immunological activity is skewed towards a pro-inflammatory environment or a controlled adaptive response, emerges as a potential key aspect for defining the course of human CL. Results from this study instigate further explorations of the *Leishmania*-host interactions involving functional aspects of B and T lymphocytes in the early response to infection (within the first 24 hours of contact). Whether the functions modulated in these cells are dependent on APCs, are a direct effect elicited by the parasite, or are a bystander mechanism of adaptive cell activation, remains to be determined.

DATA AVAILABILITY STATEMENT

All sequence data is publicly available in NCBI's Short Read Archive (SRA) under bioproject PRJNA685835 (https://www.ncbi.nlm.nih.gov/bioproject/?term=PRJNA685835).

ETHICS STATEMENT

This study was approved and monitored by the institutional review board for ethical conduct of research involving human subjects of the Centro Internacional de Entrenamiento e Investigaciones Médicas (CIDEIM) in accordance with national (Resolution 008430, República de Colombia, Ministry of Health, 1993) and international (Declaration of Helsinki and amendments, World Medical Association, Fortaleza, Brazil, October 2013) guidelines. All individuals voluntarily participated in the study and written informed consent was obtained from each participant.

AUTHOR CONTRIBUTIONS

MG, MR-C, AN, and NE-S contributed to conception and design of the study. AM-V conducted patient recruitment and all clinical management of study participants. AN, MR-C, JM, AB, and LD performed the experiments. AB, MG, and NE-S performed the statistical analysis. MG wrote the first draft of the manuscript. AB, AN, JM, LD, TA, and NE-S wrote sections of the manuscript. All authors contributed to the article and approved the submitted version.

FUNDING

This research was funded in part by the American Society of Tropical Medicine and Hygiene Gorgas Memorial Institute Research Award, and received support from NIAID/NIH U19AI129910 and Wellcome Trust 107595/Z/15/Z.

SUPPLEMENTARY MATERIAL

The Supplementary Material for this article can be found online at: https://www.frontiersin.org/articles/10.3389/fcimb.2021.687607/full#supplementary-material

REFERENCES

Alonso, D., and Nungester, W. J. (1956). Comparative Study of Host Resistance of Guinea Pigs and Rats: V. The Effect of Pneumococcal Products on Glycolysis and Oxygen Uptake by Polymorphonuclear Leucocytes. *J. Infect. Dis.* 99 (2), 174–181.

Amato, V. S., Tuon, F. F., Bacha, H. A., Neto, V. A., and Nicodemo, A. C. (2008). Mucosal Leishmaniasis . Current Scenario and Prospects for Treatment. *Acta Trop.* 105 (1), 1–9. doi: 10.1016/j.actatropica.2007.08.003

Anders, S., Pyl, P. T., and Huber, W. (2015). HTSeq–a Python Framework to Work With High-Throughput Sequencing Data. *Bioinformatics* 31 (2), 166–169. doi: 10.1093/bioinformatics/btu638

Arunachalam, P. S., Wimmers, F., Mok, C. K. P., Perera, R., Scott, M., Hagan, T., et al. (2020). Systems Biological Assessment of Immunity to Mild *Versus* Severe COVID-19 Infection in Humans. *Science* 369 (6508), 1210–1220. doi: 10.1126/science.abc6261

Bamorovat, M., Sharifi, I., Dabiri, S., Shamsi Meymandi, S., Karamoozian, A., et al. (2021). Major Risk Factors and Histopathological Profile of Treatment Failure, Relapse and Chronic Patients With Anthroponotic Cutaneous Leishmaniasis: A Prospective Case-Control Study on Treatment Outcome and Their Medical Importance. *PloS Negl. Trop. Dis.* 15 (1), e0009089. doi: 10.1371/journal.pntd.0009089

Beverley, S. M., and Turco, S. J. (1998). Lipophosphoglycan (LPG) and the Identification of Virulence Genes in the Protozoan Parasite Leishmania. *Trends Microbiol.* 6 (1), 35–40. doi: 10.1016/S0966-842X(97)01180-3

Bolger, A. M., Lohse, M., and Usadel, B. (2014). Trimmomatic: A Flexible Trimmer for Illumina Sequence Data. *Bioinformatics* 30 (15), 2114–2120. doi: 10.1093/bioinformatics/btu170

Carvalho, E. M., Johnson, W. D., Barreto, E., Marsden, P. D., Costa, J. L., Reed, S., et al. (1985). Cell Mediated Immunity in American Cutaneous and Mucosal Leishmaniasis. *J. Immunol.* 135 (6), 4144–4148.

Cassioli, C., and Baldari, C. T. (2019). A Ciliary View of the Immunological Synapse. *Cells* 8 (8), 1–24. doi: 10.3390/cells8080789

Chesney, J., Bacher, M., Bender, A., and Bucala, R.. (1997). The Peripheral Blood Fibrocyte is a Potent Antigen-Presenting Cell Capable of Priming Naive T Cells in Situ. *Proc. Natl. Acad. Sci. U. S. A.* 94 (12), 6307–6312. doi: 10.1073/pnas.94.12.6307

Cohen-Freue, G., Holzer, T. R., Forney, J. D., and McMaster, W. R. (2007). Global Gene Expression in Leishmania. *Int. J. Parasitol.* 37 (10), 1077–1086. doi: 10.1016/j.ijpara.2007.04.011

Crosby, E. J., Goldschmidt, M. H., Wherry, E. J., and Scott, P. (2014). Engagement of NKG2D on Bystander Memory CD8 T Cells Promotes Increased Immunopathology Following Leishmania Major Infection. *PloS Pathog.* 10 (2), e1003970. doi: 10.1371/journal.ppat.1003970

Diaz, Y. R., Rojas, R., Valderrama, L., and Saravia, N. G. (2010). T-Bet, GATA-3, and Foxp3 Expression and Th1/Th2 Cytokine Production in the Clinical Outcome of Human Infection With Leishmania (Viannia) Species. *J. Infect. Dis.* 202 (3), 406–415. doi: 10.1086/653829

Dillon, L. A., Suresh, R., Okrah, K., Corrada Bravo, H., Mosser, D. M., and El-Sayed, N. M. (2015). Simultaneous Transcriptional Profiling of Leishmania Major and Its Murine Macrophage Host Cell Reveals Insights Into Host-Pathogen Interactions. *BMC Genomics* 16, 1108. doi: 10.1186/s12864-015-2237-2

Ehrchen, J. M., Roebrock, K., Foell, D., Nippe, N., von Stebut, E., Weiss, J. M., et al. (2010). Keratinocytes Determine Th1 Immunity During Early Experimental Leishmaniasis. *PloS Pathog.* 6 (4), e1000871. doi: 10.1371/journal.ppat.1000871

Ericson, J. A., Duffau, P., Yasuda, K., Ortiz-Lopez, A., Rothamel, K., Rifkin, I. R., et al. (2014). Gene Expression During the Generation and Activation of Mouse Neutrophils: Implication of Novel Functional and Regulatory Pathways. *PloS One* 9 (10), e108553. doi: 10.1371/journal.pone.0108553

Falcon, S., and Gentleman, R. (2007). Using GOstats to Test Gene Lists for GO Term Association. *Bioinformatics* 23 (2), 257–258. doi: 10.1093/bioinformatics/btl567

Fernandes, M. C., Dillon, L. A., Belew, A. T., Bravo, H. C., Mosser, D. M., and El-Sayed, N. M. (2016). Dual Transcriptome Profiling of Leishmania-Infected Human Macrophages Reveals Distinct Reprogramming Signatures. *mBio* 7 (3). doi: 10.1128/mBio.00027-16

Fernandez, O. L., Diaz-Toro, Y., Ovalle, C., Valderrama, L., Muvdi, S., Rodriguez, I., et al. (2014). Miltefosine and Antimonial Drug Susceptibility of Leishmania Viannia Species and Populations in Regions of High Transmission in Colombia. *PloS Negl. Trop. Dis.* 8 (5), e2871. doi: 10.1371/journal.pntd.0002871

Gasim, S., Elhassan, A. M., Khalil, E. A., Ismail, A., Kadaru, A. M., Kharazmi, A., et al. (1998). High Levels of Plasma IL-10 and Expression of IL-10 by Keratinocytes During Visceral Leishmaniasis Predict Subsequent Development of Post-Kala-Azar Dermal Leishmaniasis. *Clin. Exp. Immunol.* 111 (1), 64–69. doi: 10.1046/j.1365-2249.1998.00468.x

Gomez, M. A., Contreras, I., Halle, M., Tremblay, M. L., McMaster, R. W., and Olivier, M. (2009). Leishmania GP63 Alters Host Signaling Through Cleavage-Activated Protein Tyrosine Phosphatases. *Sci. Signal.* 2 (90), ra58. doi: 10.1126/scisignal.2000213

Gomez, M. A., and Olivier, M. (2010). Proteases and Phosphatases During Leishmania-Macrophage Interaction: Paving the Road for Pathogenesis. *Virulence* 1 (4), 314–318. doi: 10.4161/viru.1.4.12194

Grab, D. J., Salem, M. L., Dumler, J. S., and Bucala, R. (2004). A Role for the Peripheral Blood Fibrocyte in Leishmaniasis? *Trends Parasitol.* 20 (1), 12. doi: 10.1016/j.pt.2003.10.012

Grassi, L., Pourfarzad, F., Ullrich, S., Merkel, A., Were, F., Carrillo-de-Santa-Pau, E., et al. (2018). Dynamics of Transcription Regulation in Human Bone Marrow Myeloid Differentiation to Mature Blood Neutrophils. *Cell Rep.* 24 (10), 2784–2794. doi: 10.1016/j.celrep.2018.08.018

Hanzelmann, S., Castelo, R., and Guinney, J. (2013). GSVA: Gene Set Variation Analysis for Microarray and RNA-Seq Data. *BMC Bioinf.* 14, 7. doi: 10.1186/1471-2105-14-7

Hoffman, G. E., and Schadt, E. E. (2016). Variancepartition: Interpreting Drivers of Variation in Complex Gene Expression Studies. *BMC Bioinf.* 17 (1), 483. doi: 10.1186/s12859-016-1323-z

Ives, A., Ronet, C., Prevel, F., Ruzzante, G., Fuertes-Marraco, S., Schutz, F., et al. (2011). Leishmania RNA Virus Controls the Severity of Mucocutaneous Leishmaniasis. *Science* 331 (6018), 775–778. doi: 10.1126/science.1199326

Kim, T. S., and Shin, E. C. (2019). The Activation of Bystander CD8(+) T Cells and Their Roles in Viral Infection. *Exp. Mol. Med.* 51 (12), 1–9. doi: 10.1038/s12276-019-0316-1

Lee, H. G., Cho, M. Z., and Choi, J. M. (2020). Bystander CD4(+) T Cells: Crossroads Between Innate and Adaptive Immunity. *Exp. Mol. Med.* 52 (8), 1255–1263. doi: 10.1038/s12276-020-00486-7

Leek, J. T., Johnson, W. E., Parker, H. S., Jaffe, A. E., and Storey, J. D. (2012). The Sva Package for Removing Batch Effects and Other Unwanted Variation in High-Throughput Experiments. *Bioinformatics* 28 (6), 882–883. doi: 10.1093/bioinformatics/bts034

Leng, N., Dawson, J. A., Thomson, J. A., Ruotti, V., Rissman, A. I., Smits, B. M., et al. (2013). EBSeq: An Empirical Bayes Hierarchical Model for Inference in RNA-Seq Experiments. *Bioinformatics* 29 (8), 1035–1043. doi: 10.1093/bioinformatics/btt087

Liberzon, A., Subramanian, A., Pinchback, R., Thorvaldsdottir, H., Tamayo, P., and Mesirov, J. P. (2011). Molecular Signatures Database (MSigDB) 3.0. *Bioinformatics* 27 (12), 1739–1740. doi: 10.1093/bioinformatics/btr260

Li, H., Handsaker, B., Wysoker, A., Fennell, T., Ruan, J., Homer, N., et al. (2009). The Sequence Alignment/Map Format and SAMtools. *Bioinformatics* 25 (16), 2078–2079. doi: 10.1093/bioinformatics/btp352

Love, M. I., Huber, W., and Anders, S. (2014). Moderated Estimation of Fold Change and Dispersion for RNA-Seq Data With Deseq2. *Genome Biol.* 15 (12), 550. doi: 10.1186/s13059-014-0550-8

Lu, J., Mold, C., Du Clos, T. W., and Sun, P. D. (2018). Pentraxins and Fc Receptor-Mediated Immune Responses. *Front. Immunol.* 9, 2607. doi: 10.3389/fimmu.2018.02607

Maurer-Cecchini, A., Decuypere, S., Chappuis, F., Alexandrenne, C., De Doncker, S., Boelaert, M., et al. (2009). Immunological Determinants of Clinical Outcome in Peruvian Patients With Tegumentary Leishmaniasis Treated With Pentavalent Antimonials. *Infect. Immun.* 77 (5), 2022–2029. doi: 10.1128/IAI.01513-08

Moncunill, G., Scholzen, A., Mpina, M., Nhabomba, A., Hounkpatin, A. B., Osaba, L., et al. (2020). Antigen-Stimulated PBMC Transcriptional Protective Signatures for Malaria Immunization. *Sci. Transl. Med.* 12 (543). doi: 10.1126/scitranslmed.aay8924

Murray, H. W., et al. (2005). Advances in Leishmaniasis. *Lancet* 366 (9496), 1561–1577. doi: 10.1016/S0140-6736(05)67629-5

Nachury, M. V., and Mick, D. U. (2019). Establishing and Regulating the Composition of Cilia for Signal Transduction. *Nat. Rev. Mol. Cell Biol.* 20 (7), 389–405. doi: 10.1038/s41580-019-0116-4

Navas, A., Vargas, D. A., Freudzon, M., McMahon-Pratt, D., Saravia, N. G., et al. (2014). Chronicity of Dermal Leishmaniasis Caused by Leishmania Panamensis Is Associated With Parasite-Mediated Induction of Chemokine Gene Expression. *Infect. Immun.* 82 (7), 2872–2880. doi: 10.1128/IAI.01133-13

Navas, A., Fernandez, O., Gallego-Marin, C., Castro, M. D. M., Rosales-Chilama, M., Murillo, J., et al. (2020). Profiles of Local and Systemic Inflammation in the Outcome of Treatment of Human Cutaneous Leishmaniasis Caused by Leishmania (Viannia). *Infect. Immun.* 88 (3). doi: 10.1128/IAI.00764-19

Newsholme, P., Curi, R., Gordon, S., and Newsholme, E. A. (1986). Metabolism of Glucose, Glutamine, Long-Chain Fatty Acids and Ketone Bodies by Murine Macrophages. *Biochem. J.* 239 (1), 121–125. doi: 10.1042/bj2390121

O'Neill, L. A., Kishton, R. J., and Rathmell, J. (2016). A Guide to Immunometabolism for Immunologists. *Nat. Rev. Immunol.* 16 (9), 553–565. doi: 10.1038/nri.2016.70

Oliveros, J. C. *Venny. An Interactive Tool for Comparing Lists With Venn's Diagrams. (2007-2015)*. Available at: https://bioinfogp.cnb.csic.es/tools/venny/index.html.

Orr, C., Xu, W., Masur, H., Kottilil, S., and Meissner, E. G. (2020). Peripheral Blood Correlates of Virologic Relapse After Sofosbuvir and Ribavirin Treatment of Genotype-1 HCV Infection. *BMC Infect. Dis.* 20 (1), 929. doi: 10.1186/s12879-020-05657-5

Ovalle-Bracho, C., Franco-Munoz, C., Londono-Barbosa, D., Restrepo-Montoya, D., and Clavijo-Ramirez, C. (2015). Changes in Macrophage Gene Expression Associated With Leishmania (Viannia) Braziliensis Infection. *PloS One* 10 (6), e0128934. doi: 10.1371/journal.pone.0128934

Polley, R., Sanos, S. L., Prickett, S., Haque, A., and Kaye, P. M. (2005). Chronic Leishmania Donovani Infection Promotes Bystander CD8+-T-Cell Expansion and Heterologous Immunity. *Infect. Immun.* 73 (12), 7996–8001. doi: 10.1128/IAI.73.12.7996-8001.2005

Ramirez, C., Diaz-Toro, Y., Tellez, J., Castilho, T. M., Rojas, R., Ettinger, N. A., et al. (2012). Human Macrophage Response to L. (Viannia) Panamensis: Microarray Evidence for an Early Inflammatory Response. *PloS Negl. Trop. Dis.* 6 (10), e1866. doi: 10.1371/journal.pntd.0001866

Reimand, J., Arak, T., Adler, P., Kolberg, L., Reisberg, S., Peterson, H., et al. (2016). G:Profiler-A Web Server for Functional Interpretation of Gene Lists (2016 Update). *Nucleic Acids Res.* 44 (W1), W83–W89. doi: 10.1093/nar/gkw199

Risso, D., Ngai, J., Speed, T. P., and Dudoit, S. (2014). Normalization of RNA-Seq Data Using Factor Analysis of Control Genes or Samples. *Nat. Biotechnol.* 32 (9), 896–902. doi: 10.1038/nbt.2931

Ritchie, M. E., Phipson, B., Wu, D., Hu, Y., Law, C. W., Shi, W., et al. (2015). Limma Powers Differential Expression Analyses for RNA-Sequencing and Microarray Studies. *Nucleic Acids Res.* 43 (7), e47. doi: 10.1093/nar/gkv007

Robinson, M. D., McCarthy, D. J., and Smyth, G. K. (2010). Edger: A Bioconductor Package for Differential Expression Analysis of Digital Gene Expression Data. *Bioinformatics* 26 (1), 139–140. doi: 10.1093/bioinformatics/btp616

Robledo, S., Wozencraft, A., Valencia, A. Z., and Saravia, N. (1994). Human Monocyte Infection by Leishmania (Viannia) Panamensis. Role of Complement Receptors and Correlation of Susceptibility *In Vitro* With Clinical Phenotype. *J. Immunol.* 152 (3), 1265–1276.

Rodriguez-Pinto, D., Navas, A., Blanco, V. M., Ramirez, L., Garcerant, D., Cruz, A., et al. (2012). Regulatory T Cells in the Pathogenesis and Healing of Chronic Human Dermal Leishmaniasis Caused by Leishmania (Viannia) Species. *PloS Negl. Trop. Dis.* 6 (4), e1627. doi: 10.1371/journal.pntd.0001627

Ronet, C., Passelli, K., Charmoy, M., Scarpellino, L., Myburgh, E., Hauyon La Torre, Y., et al. (2019). TLR2 Signaling in Skin Nonhematopoietic Cells Induces Early Neutrophil Recruitment in Response to Leishmania Major Infection. *J. Invest. Dermatol.* 139 (6), 1318–1328. doi: 10.1016/j.jid.2018.12.012

Rosales, C., and Uribe-Querol, E. (2017). Phagocytosis: A Fundamental Process in Immunity. *BioMed. Res. Int* 2017, 9042851. doi: 10.1155/2017/9042851

Saravia, N. G., Valderrama, L., Labrada, M., Holguin, A. F., Navas, C., Palma, G., et al. (1989). The Relationship of Leishmania Braziliensis Subspecies and Immune Response to Disease Expression in New World Leishmaniasis. *J. Infect. Dis.* 159 (4), 725–735. doi: 10.1093/infdis/159.4.725

Saravia, N. G., Segura, I., Holguin, A. F., Santrich, C., Valderrama, L., and Ocampo, C. (1998). Epidemiologic, Genetic, and Clinical Associations Among Phenotypically Distinct Populations of Leishmania (Viannia) in Colombia. *Am. J. Trop. Med. Hyg.* 59 (1), 86–94. doi: 10.4269/ajtmh.1998.59.86

Scott, P., and Novais, F. O. (2016). Cutaneous Leishmaniasis: Immune Responses in Protection and Pathogenesis. *Nat. Rev. Immunol.* 16 (9), 581–592. doi: 10.1038/nri.2016.72

Szklarczyk, D., Gable, A. L., Lyon, D., Junge, A., Wyder, S., Huerta-Cepas, J., et al. (2019). STRING V11: Protein-Protein Association Networks With Increased Coverage, Supporting Functional Discovery in Genome-Wide Experimental Datasets. *Nucleic Acids Res.* 47 (D1), D607–D613. doi: 10.1093/nar/gky1131

Tasew, G., Nylen, S., Lieke, T., Lemu, B., Meless, H., Ruffin, N., et al. (2010). Systemic FasL and TRAIL Neutralisation Reduce Leishmaniasis Induced Skin Ulceration. *PloS Negl. Trop. Dis.* 4 (10), e844. doi: 10.1371/journal.pntd.0000844

Trapnell, C., Roberts, A., Goff, L., Pertea, G., Kim, D., Kelley, R., et al. (2012). Differential Gene and Transcript Expression Analysis of RNA-Seq Experiments With TopHat and Cufflinks. *Nat. Protoc.* 7 (3), 562–578. doi: 10.1038/nprot.2012.016

Ueda, H., Zhou, J., Xie, J., and Davis, M. M. (2015). Distinct Roles of Cytoskeletal Components in Immunological Synapse Formation and Directed Secretion. *J. Immunol.* 195 (9), 4117–4125. doi: 10.4049/jimmunol.1402175

Uhlen, M., Fagerberg, L., Hallstrom, B. M., Lindskog, C., Oksvold, P., Mardinoglu, A., et al. (2015). Proteomics. Tissue-Based Map of the Human Proteome. *Science* 347 (6220), 1260419. doi: 10.1126/science.1260419

Weigle, K. A., Santrich, C., Martinez, F., Valderrama, L., and Saravia, N. G. (1993). Epidemiology of Cutaneous Leishmaniasis in Colombia: A Longitudinal Study of the Natural History, Prevalence, and Incidence of Infection and Clinical Manifestations. *J. Infect. Dis.* 168 (3), 699–708. doi: 10.1093/infdis/168.3.699

Wiedemann, A., Foucat, E., Hocini, H., Lefebvre, C., Hejblum, B. P., Durand, M., et al. (2020). Long-Lasting Severe Immune Dysfunction in Ebola Virus Disease Survivors. *Nat. Commun.* 11 (1), 3730. doi: 10.1038/s41467-020-17489-7

Young, M. D., Wakefield, M. J., Smyth, G. K., and Oshlack, A. (2010). Gene Ontology Analysis for RNA-Seq: Accounting for Selection Bias. *Genome Biol.* 11 (2), R14. doi: 10.1186/gb-2010-11-2-r14

Yu, G., Wang, L. G., Han, Y., and He, Q. Y. (2012). Clusterprofiler: An R Package for Comparing Biological Themes Among Gene Clusters. *OMICS* 16 (5), 284–287. doi: 10.1089/omi.2011.0118

Zangger, H., Ronet, C., Desponds, C., Kuhlmann, F. M., Robinson, J., Hartley, M. A., et al. (2013). Detection of Leishmania RNA Virus in Leishmania Parasites. *PloS Negl. Trop. Dis.* 7 (1), e2006. doi: 10.1371/journal.pntd.0002006

Author Disclaimer: The content is solely the responsibility of the authors and does not necessarily represent the official views of the National Institutes of Health or other agencies.

Conflict of Interest: The authors declare that the research was conducted in the absence of any commercial or financial relationships that could be construed as a potential conflict of interest

Publisher's Note: All claims expressed in this article are solely those of the authors and do not necessarily represent those of their affiliated organizations, or those of the publisher, the editors and the reviewers. Any product that may be evaluated in this article, or claim that may be made by its manufacturer, is not guaranteed or endorsed by the publisher.

frontiers in Cellular and Infection Microbiology

ORIGINAL RESEARCH
published: 22 September 2021
doi: 10.3389/fcimb.2021.710006

Neutrophil Activation: Influence of Antimony Tolerant and Susceptible Clinical Strains of *L. (V.) panamensis* and Meglumine Antimoniate

Olga Lucía Fernández[1,2]*, *Lady Giovanna Ramírez*[1,2], *Míriam Díaz-Varela*[3], *Fabienne Tacchini-Cottier*[3] *and Nancy Gore Saravia*[1,2]

[1] Centro Internacional de Entrenamiento e Investigaciones Médicas (CIDEIM), Cali, Colombia, [2] Universidad Icesi, Cali, Colombia, [3] Department of Biochemistry, University of Lausanne, Epalinges, Switzerland

OPEN ACCESS

Edited by:
Izabel Galhardo Demarchi, Federal University of Santa Catarina, Brazil

Reviewed by:
Beatriz Simonsen Stolf, University of São Paulo, Brazil
Sara M. Robledo, University of Antioquia, Colombia

***Correspondence:**
Olga Lucía Fernández
ofernandez@cideim.org.co

Specialty section:
This article was submitted to Parasite and Host, a section of the journal Frontiers in Cellular and Infection Microbiology

Received: *14 May 2021*
Accepted: *31 August 2021*
Published: *22 September 2021*

Citation:
Fernández OL, Ramírez LG, Díaz-Varela M, Tacchini-Cottier F and Saravia NG (2021) Neutrophil Activation: Influence of Antimony Tolerant and Susceptible Clinical Strains of L. (V.) panamensis and Meglumine Antimoniate. Front. Cell. Infect. Microbiol. 11:710006. doi: 10.3389/fcimb.2021.710006

Emerging evidence indicates that innate host response contributes to the therapeutic effect of antimicrobial medications. Recent studies have shown that *Leishmania* parasites derived by *in vitro* selection for resistance to pentavalent antimony (SbV) as meglumine antimoniate (MA) modulate the activation of neutrophils. However, whether modulation of neutrophil activation extends to natural resistance to this antileishmanial drug has not been established. We have evaluated the influence of clinical strains of *L. (V.) panamensis* having intrinsic tolerance/resistance to SbV, on the inflammatory response of neutrophils during *ex vivo* exposure to MA. Accordingly, neutrophils obtained from healthy donors were infected with clinical strains that are sensitive (n = 10) or intrinsically tolerant/resistant to SbV (n = 10) and exposed to a concentration approximating the maximal plasma concentration (Cmax) of SbV (32 µg/ml). The activation profile of neutrophils was evaluated as the expression of the surface membrane markers CD66b, CD18, and CD62L by flow cytometry, measurement of reactive oxygen species (ROS) by luminometry, and NET formation using Picogreen to measure dsDNA release and quantification of NETs by confocal microscopy. These parameters of activation were analyzed in relation with parasite susceptibility to SbV and exposure to MA. Here, we show that clinical strains presenting intrinsic tolerance/resistance to SbV induced significantly lower ROS production compared to drug-sensitive clinical strains, both in the presence and in the absence of MA. Likewise, analyses of surface membrane activation markers revealed significantly higher expression of CD62L on cells infected with intrinsically SbV tolerant/resistant *L. (V.) panamensis* than cells infected with drug-sensitive strains. Expression of other activation markers (CD18 and CD66b) and NET formation were similar for neutrophils infected with SbV sensitive and tolerant clinical strains under the conditions evaluated. Exposure to MA broadly impacted the activation of neutrophils, diminishing NET formation and the expression of CD62L, while augmenting ROS production and CD66b expression, independently of the parasite susceptibility phenotype. These results demonstrated that activation of human neutrophils *ex vivo* is

differentially modulated by infection with clinical strains of *L. (V.) panamensis* having intrinsic tolerance/resistance to SbV compared to sensitive strains, and by exposure to antimonial drug.

Keywords: neutrophil activation, *Leishmania*, meglumine antimoniate, antileishmanial drug susceptibility, intrinsic drug resistance

INTRODUCTION

Cutaneous leishmaniasis (CL) is a neglected tropical disease of emerging or reemerging public health importance in 98 countries, with more than a million new cases reported annually (Alvar et al., 2012; Pace, 2014). First-line treatment in Latin America is parentally administered meglumine antimoniate (MA), and orally administered miltefosine (ML) is recommended for individuals with contraindication for antimonial drugs. Case identification and treatment are the principal control measures for CL; however, treatment failure within efficacy trials is frequent (17 to 47%) (Palacios et al., 2001; Soto et al., 2008; Velez et al., 2010; Chrusciak-Talhari et al., 2011; Rubiano et al., 2012). The determinants of antileishmanial treatment failures are multiple, complex, and poorly understood; however, it is clear that both parasite and host factors including innate and adaptive immune response contribute to therapeutic outcome (Rojas et al., 2006; Goyeneche-Patino et al., 2008; Obonaga et al., 2014; Palic et al., 2019).

Evidence of parasite resistance to SbV and MIL has been reported globally from major endemic regions. Differences in susceptibility to SbV were found among clinical strains of *L. (V.) panamensis* circulating in Colombia that are distinguished by isoenzyme profiles that define discrete natural parasite populations discernable as zymodemes (Saravia et al., 1998). Subpopulations of *L. (V.) panamensis* belonging to zymodeme 2.3 were subsequently found to be associated with tolerance/resistance to SbV, while those belonging to zymodeme 2.2 were associated with sensitivity (Fernandez et al., 2014). The relationship between drug susceptibility of *Leishmania* as conventionally measured *in vitro* and therapeutic response remains unclear for all forms of human leishmaniasis. The multifactorial bases of the response to treatment confound the understanding of parasite drug susceptibility as a determinant of therapeutic outcome. However, the importance of the host cell in determining susceptibility is illustrated by the distinct EC_{50} of antileishmanial drugs for the same parasite in different host cells (primary macrophages or mononuclear phagocytic cell lines (Seifert et al., 2010)), and the divergence of drug screening results based on intracellular amastigotes, promastigotes, and axenic amastigotes (Vermeersch et al., 2009; De Muylder et al., 2011; Zahid et al., 2019). Furthermore, growing evidence indicates that neutrophils, the first host cells recruited to the site of infection, may play a role in the pathogenesis of leishmaniasis depending on the infecting *Leishmania* spp (Afonso et al., 2008; Carlsen et al., 2013; Hurrell et al., 2015; Charmoy et al., 2016; Hurrell et al., 2016; Passelli et al., 2021). Despite their important role in cutaneous leishmaniasis, the involvement of neutrophils in the response to antileishmanial drugs has not been examined.

Neutrophils are the most abundant cells in human blood, are terminally differentiated cells, and are rapidly recruited to sites of infection. Their antimicrobial mechanisms include phagocytosis, the formation of radical oxygen species (ROS), and the release of neutrophil extracellular traps (NETs) (Brinkmann et al., 2004) as well as antimicrobial agents stored in neutrophil granules that can be rapidly released into the phagosomes (Borregaard, 2010). Previous studies have shown that elimination or survival of *Leishmania* parasites by or within neutrophils differs among parasite species or even strains of the same species (Hurrell et al., 2016; Regli et al., 2017). *Leishmania* may be killed or inhibit the otherwise very efficient killing machinery of these cells (Passelli et al., 2021) and effectively mediate the transfer of parasites to macrophages (van Zandbergen et al., 2004; Chaves et al., 2020). Infection of human neutrophils with laboratory-derived MIL and SbV resistant lines of *L. (V.) panamensis* elicited significantly greater NET formation by both murine and human neutrophils compared to infections with the wild-type (WT) sensitive line, while the MIL resistant line, but not SbV resistant line, also elicited significantly higher ROS production than SbV resistant or sensitive lines (Regli et al., 2018). The potential of naturally resistant *Leishmania* populations to modulate neutrophil activation has not been previously evaluated and is relevant to treatment since mechanisms of resistance derived by *in vitro* drug selection have not replicated intrinsic or acquired resistance mechanisms evidenced during treatment or *in vitro* evaluation of drug susceptibility (Goyeneche-Patino et al., 2008).

In this study, we have evaluated the influence of clinical strains of having intrinsic tolerance/resistance to SbV on the inflammatory response of neutrophils during *ex vivo* infection and treatment with MA.

MATERIALS AND METHODS

Study Design

Human neutrophils were infected *ex vivo* with SbV sensitive (n = 10) or resistant (n = 10) clinical strains of *L. (V.) panamensis*. Neutrophil effector functions were assessed by analyzing the production of reactive oxygen species (ROS), the formation of neutrophil extracellular traps (NETs), and the expression of cell surface activation markers (CD18, CD62L, and CD66b). Susceptibility phenotype of clinical strains as intracellular amastigotes was previously evaluated *in vitro* as described (Fernandez et al., 2014) and confirmed within the scope of this study using macrophages differentiated from U937 human promonocytic cells.

Cell Donors

To characterize the phenotype and functionality of human neutrophils during infection with *L. (V.) panamensis* strains and their relation with parasite drug susceptibility, 13 volunteer healthy donors without history of leishmaniasis were recruited to participate in this study. The inclusion criteria were as follows: 18–60 years of age, absence of active or healed lesions suggestive of leishmaniasis, voluntary participation, and hemoglobin levels > 11 mg/dl in women and >12 mg/dl in men.

Ethics Statement

The institutional ethical review board of Centro Internacional de Entrenamiento e Investigaciones Médicas (CIDEIM) approved all study procedures in accordance with national guidelines: CEIH approval code: 1274, and was conducted in compliance with the legislation of the Canton of Vaud and the Swiss Confederation (CER-VD 2017-00182) and in accordance with the international guidelines: WMA Helsinki Declaration, 2013 declaration of Helsinki. Written informed consent was obtained from all donors who participated voluntarily in the study.

Leishmania (Viannia) panamensis Internal Reference Lines and Clinical Strains

Internal controls included a wild-type (WT) antimony-sensitive line of *L. (V.) panamensis* transfected with the luciferase reporter gene (luc), MHOM/COL/03/1166, prepared as previously described (Roy G, Dumas 2000), and antimony resistant laboratory line of *L. (V.) panamensis* (MHOM/COL/03/1166-1000.1). Clinical strains of *L. (V.) panamensis* previously defined as sensitive or resistant to antimony were obtained from CIDEIM Biobank. Susceptibility to the C_{max} of SbV, zymodeme, clinical outcome of treatment with MA of the corresponding patient, and geographic origin of strains included in the study are summarized in **Table 1**. *Leishmania* strains were propagated in culture at 25°C in Senejke's diphasic blood agar medium with 5 ml of PBS for 6 days. Parasites were opsonized in 10% human AB serum for 60 min 34°C prior to exposure to neutrophils.

In Vitro Assay for SbV Susceptibility Using Intracellular Amastigotes

The *in vitro* susceptibility of clinical strains of *L. (V.) panamensis* was determined as intracellular amastigotes. Susceptibility was based on the percent reduction of intracellular parasite burden in U-937 macrophages (ATCC CRL-159.3) by 72 h of exposure to 32 μg Sb^V/ml as meglumine antimoniate as previously described (Fernandez et al., 2012). Briefly, 1.2 x 10^5 U-937 cells cultured in 24-well plates containing glass coverslips were differentiated to macrophages by treatment with phorbol 12-myristate 13-acetate (PMA; 100 ng/ml; Sigma) and infected with opsonized promastigotes at a ratio of 5 parasites per macrophage. After 2 h of co-culture at 34°C in 5% CO_2, extracellular parasites were removed by washing with PBS, and infected cells were cultured in RPMI-1640 medium (Sigma-Aldrich) supplemented with 10% heat-inactivated fetal bovine serum (FBS; 10082; Gibco), 1% Penicillin/Streptomycin solution (10,000 U/ml Penicillin G/ 10,000 μg/ml Streptomycin; Gibco BRL), and 1% glutamine during 24 h to allow differentiation of intracellular parasites to amastigotes. The medium was replaced with complete RPMI containing 32 μg Sb^V/ml and replenished 48 h later, followed by incubation for an additional 24 h.

Glass coverslips with infected cells were fixed with methanol and stained with 3% Giemsa (Sigma Aldrich) prior to blinded evaluation by one of the two experienced microscopists who evaluated all of the slides for this study. Six replicates of cells

TABLE 1 | Characteristics of clinical strains of *L. (V.) panamensis*.

Strain code	Zymodeme	% Reduction of parasite burden(32 μg SbV/mL)		Treatment outcome	Department
		Historical data[a]	Confirmation of susceptibility		
MHOM/CO/2014/12309	2.2	99	80	Cure	Nariño
MHOM/CO/2015/12345	2.2	99	89	Cure	Nariño
MHOM/CO/2011/10763	2.2	99	75	Failure	Nariño
MHOM/CO/2014/11126	2.2	97	92	Failure	Nariño
MHOM/CO/2015/12367	2.2	97	85	Cure	Valle
MHOM/CO/2013/11006	2.2	99	91	Failure	Nariño
MHOM/CO/2014/11075	2.2	99	97	Failure	Nariño
MHOM/CO/2013/11031	2.2	98	97	Failure	Nariño
MHOM/CO/2013/10977	2.2	99	97	Cure	Nariño
MHOM/CO/2014/11109	2.2	99	83	Cure	Nariño
MHOM/CO/2015/12355	2.3	45	45	Cure	Nariño
MHOM/CO/2014/12251	2.3	46	48	Cure	Valle
MHOM/CO/2011/10772	2.3	14	45	Failure	Nariño
MHOM/CO/2013/11045	2.3	45	43	Failure	Nariño
MHOM/CO/1984/2169	2.3	0	28	Failure	Nariño
MHOM/CO/2013/12116	2.3	49	24	Failure	Chocó
MHOM/CO/2013/11024	2.3	45	58	Failure	Nariño
MHOM/CO/2013/11026	2.3	46	60	Failure	Nariño
MHOM/CO/2014/11152	2.3	56	26	Cure	Nariño
MHOM/CO/2013/7158	2.3	70	33	Cure	Chocó

[a]*Historical data correspond to previously determined drug susceptibility, and confirmation refers to the result obtained within the scope of this study.*

exposed to the discriminatory drug concentrations and infected control macrophages not exposed to the drugs were evaluated. The number of intracellular amastigotes per cell was determined for 100 macrophages per replica. Susceptibility results were expressed as percent reduction of infection, determined by comparing the parasite burden of infected cells exposed to SbV *versus* the parasite burden of infected cells cultured without drug.

Human Neutrophil Isolation

Peripheral blood neutrophils were isolated from the venous blood of healthy volunteers. Blood volume ranged from 20 to 200 ml according to the experimental protocol. Density gradient centrifugation using polymorphprep (Progen) was performed, and neutrophils were isolated according to the manufacturer's instructions.

NET Detection

NET formation was first assessed by the measurement of dsDNA in culture supernatants using the QuantiT PicoGreen kit (Thermo Fisher) as previously described (Regli et al., 2018). Briefly, for each condition, 2 million (2×10^6/500 µl) neutrophils were primed with GM-CSF (25 ng/ml) for 20 min at 37°C. The neutrophils were incubated for 4 h in the *ex vivo* medium (Lonza Bioscience) with (100 ng/ml) PMA, *L. (V.) panamensis* strains, or without stimulus at 34°C, with rotation. After incubation, DNAse (2.5 UI/ml) was added to the cell suspensions. The reaction was stopped using EDTA (2.5 mM). The supernatants were collected and transferred to black 96-well plates. Picogreen dye was added, and fluorescence was measured using a plate reader (Chamaleon) at an excitation wavelength of 480 nm and an emission wavelength of 520 nm.

NET release and quantification was also assessed by confocal microscopy. Human neutrophils (2.5×10^5 per well) were seeded on poly-L-lysine (Sigma) coated microscope slides (Thermo Scientific) in RPMI 1640 (Gibco) supplemented with 2% heat-inactivated AB human serum (Sigma). Neutrophils were exposed for 4 h to either *L. (V.) p*. at a parasite/cell ratio of 5:1 in the presence or absence of 32 µg SbV per ml during the last 2 h of infection. In parallel, cells were exposed to 100 ng/ml PMA, 100 ng/ml PMA plus 100 ng/ml DNase I, or the culture medium alone. After incubation, cells were fixed with 4% paraformaldehyde, washed and blocked with PBS containing 3% BSA. Cells were incubated with goat antihuman MPO primary antibody (R&D, AF3667), extensively washed, and incubated with Alexa-Fluor 488 anti-goat IgG (H+L) secondary antibody (Invitrogen, A-11055). Coverslips were mounted on slides with Fluoromount-G with DAPI (Invitrogen) and analyzed by confocal microscopy (Zeiss LSM 880). Frequencies of NET-producing cells were determined by counting at least 200 cells per condition. Each condition was evaluated in triplicate in a blinded manner by coding of samples. Neutrophils that released filamentous structures containing DNA and MPO were considered as NET-forming cells.

Reactive Oxygen Species (ROS) Production

ROS production was measured using a luminol-based chemiluminescence assay, as previously described (Regli et al., 2018). Neutrophils were resuspended in an RPMI medium at 3 x 10^6 c/ml and distributed into the wells of white opaque 96-well plates. Cells were infected with *L. (V.) panamensis* lines or clinical strains, and ROS production was evaluated immediately and 2 h after infection over 60-min periods in the absence or presence of 32 µg SbV/ml as MA. Luminol Sodium Salt (Carbosynth Limited) was added at a final concentration of 20 µg/ml, and luminescence induced by ROS was measured every 2.5 min for periods of 60 min using a plate reader (Chamaleon). Positive control for ROS production was induced with 100 ng/ml PMA.

Neutrophil Membrane Activation Marker Staining

To evaluate the viability of neutrophils, cells were stained with the LIVE/DEAD TM Fixable Green Dead Cell Stain Kit (Life Technologies) for 15 min at 4°C and washed once with PBS. Neutrophils were distributed at $5x10^5$ cells per tube and stained for 20 min at 4°C with a negative cocktail of antihuman CD3/CD19/CD14 (PerCP); positive staining of neutrophils was performed with antihuman CD15 (APC) and activation markers as follows: antihuman CD66b, CD18, and CD62L (PE). Flow cytometry was performed using a Becton Dickinson Accuri C6 Flow Cytometer, and data were analyzed using FlowJo V10 (Tree Star). For each experimental sample, 100,000 events were acquired based on the neutrophils CD15+ gate.

Data Analysis

The Mann–Whitney U test or unpaired t test was used to establish statistical differences between neutrophil activation induced by sensitive and resistant strains. To compare two related groups (the same sample of neutrophils in the absence or presence of drug), Wilcoxon matched-pairs signed rank test or paired t was used according to the parametric or nonparametric distribution of data. Statistical differences among groups for dsDNA release in supernatant were analyzed by Kruskal–Wallis followed by Dunn's multiple comparison test. Two-way ANOVA was used to compare NET release assessed by microscopy in the absence or presence of drug. Analyses were performed with the GraphPad Prism 6 software (GraphPad Inc., San Diego, CA), and P values < 0.05 were considered significant.

RESULTS

Infection of Neutrophils by Intrinsically Sensitive and SbV Resistant Clinical Strains of *L. (V.) panamensis* Differentially Elicit ROS Induction

Neutrophils were infected with clinical strains of *L. (V.) panamensis* having intrinsic sensitivity (zymodeme 2.2) or resistance (zymodeme 2.3) to SbV over a period of 3 h. A trend toward a lower generation of ROS by neutrophils exposed to intrinsically SbV tolerant/resistant strains compared to drug-sensitive clinical strains was evident at 60 min (**Figure 1A**) and

reached significance during the interval from 2 to 3 h of infection (**Figures 1B, C**), both in the presence of the C_{max} of SbV (32 μg/ml) or in the absence of drug (**Figures 1B, C**). An exploratory comparison of ROS induction by clinical strains in relation with the treatment outcome of the corresponding patient with MA did not reveal significant differences in ROS induction by clinical strains from patients who failed or responded to treatment (**Figure 1D**). This was ascertained in the absence of drug (at 2 to 3 h/AUC median: Failure 5.4 x 10^5 *vs* Cure AUC 5.7 x 10^5, P = 0.5 as well as at 60 min/AUC mean: Failure 2.0 x 10^7 *vs* Cure 1.9 x 10^7, P = 0.2962); and the presence of MA (at 2 to 3 h/AUC median: Failure AUC 0.7 x 10^6 *vs* Cure AUC 1.0 x 10^6, P = 0.3520). Independently of the susceptibility phenotype of the infecting parasites, exposure of infected neutrophils to MA at a concentration of 32 ug SbV/ml elicited a significant increase in ROS production compared to infected neutrophils cultured without drug (**Figure 2A**). The modulation of ROS production by MA exposure of neutrophils infected with *L. (V.) panamensis* was confirmed by the dose-dependent response to four clinically relevant concentrations of SbV (**Figure 2B**). These results were replicated using neutrophils obtained from three healthy donors.

NET Formation by Neutrophils Is Similar Following Infection by SbV Sensitive and Resistant Clinical Strains of *L. (V.) panamensis*

Neutrophils were infected during 4 h with sensitive or resistant clinical strains in the absence or presence of 32 μg SbV/ml during the last 2 h of culture. Release of DNA was analyzed as a surrogate of NETs at the end of 4 h. Neutrophils exposed to sensitive or resistant clinical strains of *L. (V.) panamensis* released similar concentrations of DNA into the culture supernatant (**Figure 3A**). Neutrophils infected with antimony-resistant and sensitive laboratory lines, which were included in each experiment with clinical strains, also showed no differences in DNA release (**Figure 3A**). As the picogreen assay may detect DNA release not specific to NETs, we further visualized *L. (V.) panamensis* induced NET formation by confocal microscopy. To this end, neutrophils were exposed to sensitive or resistant clinical strains, and formation of NETs was assessed by confocal immunofluorescent microscopy using DAPI to detect filamentous DNA structures and an antibody against MPO to detect the MPO associated with these structures. As a positive control, neutrophils were exposed to PMA, and as negative controls

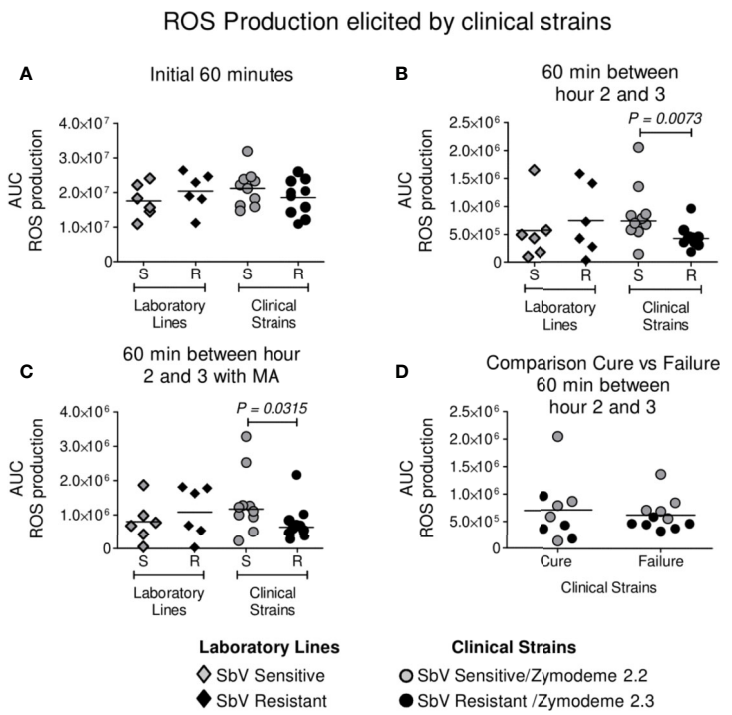

FIGURE 1 | ROS production by neutrophils during infection with intrinsically SbV sensitive (S) (zymodeme 2.2) and tolerant/resistant (R) (zymodeme 2.3) clinical strains of *L. (V.) panamensis*. ROS production was evaluated over 60 min immediately after infection **(A)** and between hours 2 and 3 following infection in the absence **(B)** or presence of antimony **(C)**. Comparison of ROS induction by clinical strains in relation with treatment outcome (11 failures, 9 cures) of the corresponding patient during 60 min between hours 2 and 3 **(D)**. Neutrophils isolated from healthy donors were infected with sensitive (n = 10) and antimony-resistant (n = 10) clinical strains; susceptible and resistant laboratory lines were included in each experiment. ROS production was determined independently in neutrophils from three healthy donors. Data analysis was conducted using unpaired t test **(A)** or the Mann–Whitney **(B, C)** according to the parametric or nonparametric distribution of data. P value shown for comparisons presenting significant differences.

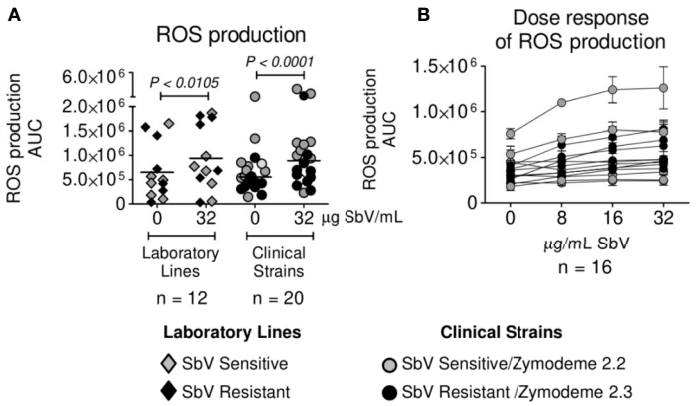

FIGURE 2 | Antimony effect on ROS production by neutrophils infected with sensitive and antimony tolerant/resistant clinical strains of *L. (V.) panamensis*. Effect of SbV at Cmax: 32 ug SbV/ml on ROS production **(A)**. Dose response of ROS production by infected neutrophils over a range of clinically relevant concentrations of antimony **(B)**. ROS production is expressed as AUC. Data correspond to ROS production by neutrophils from three donors.

to PMA and DNAse, or the medium only. We observed that all the clinical strains analyzed induced NET formation independently of their intrinsic or natural susceptibility phenotype (**Figure 3B**). Neutrophils infected with laboratory-adapted lines also produced NETs, in particular, when exposed to the SbV-resistant laboratory strain as previously observed (Regli et al., 2018) (**Figure 3C**).

NET Release by Infection With Clinical Strains of *L. (V.) panamensis* Is Modulated by SbV as MA

Next, we evaluated whether MA exposure would alter NET formation. Neutrophils were exposed to sensitive or resistant clinical strains, in the absence or presence of 32 µg SbV/ml or a

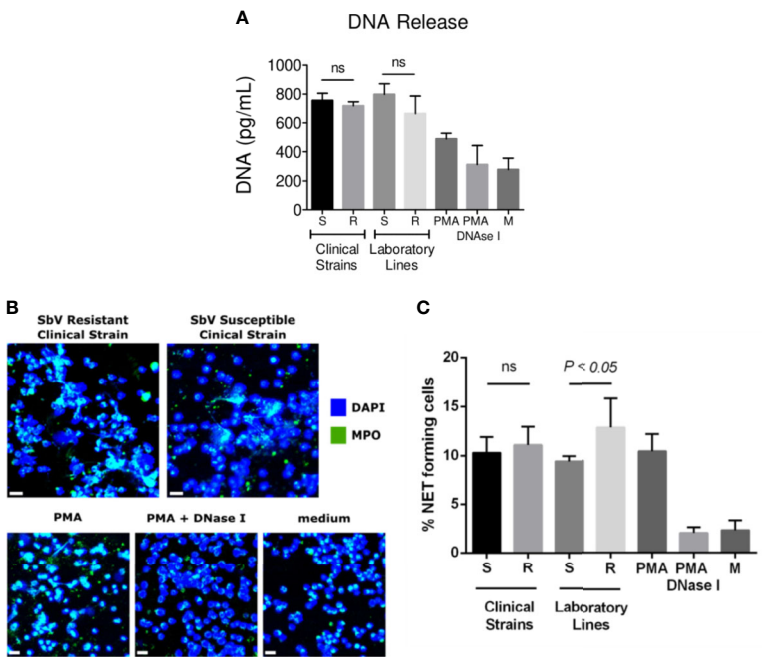

FIGURE 3 | NET release by neutrophils infected with sensitive and antimony tolerant/resistant clinical strains of *L. (V.) panamensis*. Neutrophils were exposed to *L. (V.) p.* parasites of the indicated susceptibility. Four hours later, NET formation was evaluated. Levels of dsDNA released in the culture supernatant by fluorescent picogreen assay **(A)**. Confocal microscopy images of neutrophils seeded on poly-L-lysine wells and exposed to *L. (V.) p.* parasites. As controls, neutrophils were exposed to PMA, PMA + DNase I, or the medium alone. Cells were fixed and stained for human MPO (green) and DNA (blue). The scale bar represents 20 µm **(B)**. Frequency of NET-forming neutrophils assessed by confocal microscopy **(C)**. Data are the mean frequency of NET-producing neutrophils observed in three different neutrophil donors. M, medium; ns, not significant.

range of relevant drug concentrations, during the last 2 h of culture. Picogreen assay revealed a diminished DNA release in infected neutrophils cultured with drug compared to those cultured without drug, both at Cmax and over a range of clinically relevant concentrations (**Figures 4A, B**). These results were corroborated by the analysis of NET formation by confocal microscopy, where all clinical and laboratory lines assessed induced a lower amount of NETs upon MA exposure (**Figure 4C**). Although MA exposure resulted in reduced NET release, the response was not dose-dependent, as reduction of NETs observed over the concentration range of 8 to 32 μg SbV/ml was similar (**Figure 4B**). Viability of neutrophils under the conditions and over the time course of assays of ROS and NET production was evaluated by MTT assay and shown to be >90%.

Neutrophil Surface Activation Marker Expression Is Modulated by Infection With SbV Sensitive or Resistant Strains of *L. (V.) panamensis*, and Exposure to MA

Neutrophils infected with SbV sensitive and resistant clinical strains of *L. (V.) panamensis*, in the absence of drug exposure, exhibited similar expression of CD18 and CD66b activation markers, whereas the expression of CD62L, a marker that is lost during cell homing and diapedesis into peripheral tissues, was significantly higher in neutrophils infected with SbV resistant strains (**Figure 5A**). Exposure of infected neutrophils to antimonial drug resulted in a higher expression of the activation marker CD66b, reaching significance for neutrophils infected with SbV sensitive strains (**Figure 5B**), and significantly diminished the expression of CD62L in neutrophils infected with drug sensitive as well as resistant strains (**Figures 5B, C**).

DISCUSSION

The results of this study show that infection of neutrophils with phenotypically/genotypically distinguishable clinical strains of *L. (V.) panamensis* that are intrinsically sensitive or resistant to SbV differentially modulates neutrophil activation. These findings obtained with clinical strains extend prior observations based on laboratory-derived lines (Regli et al., 2018) by substantiating that parasite adaptations that have occurred over time during the natural cycle of transmission contribute to or confer tolerance or resistance to antileishmanial drugs and are associated with modified host cell responses to infection. Naturally occurring adaptations of *Leishmania* populations causing cutaneous leishmaniasis that enhance intracellular survival despite antimicrobial defense mechanisms, can also contribute to the effect of drug exposure on host cells as well as the parasite responses to antileishmanial drugs. This phenomenon has been previously evidenced in the modulation of drug transport by SbV in infected host macrophages (Gomez et al., 2014) and as cross-

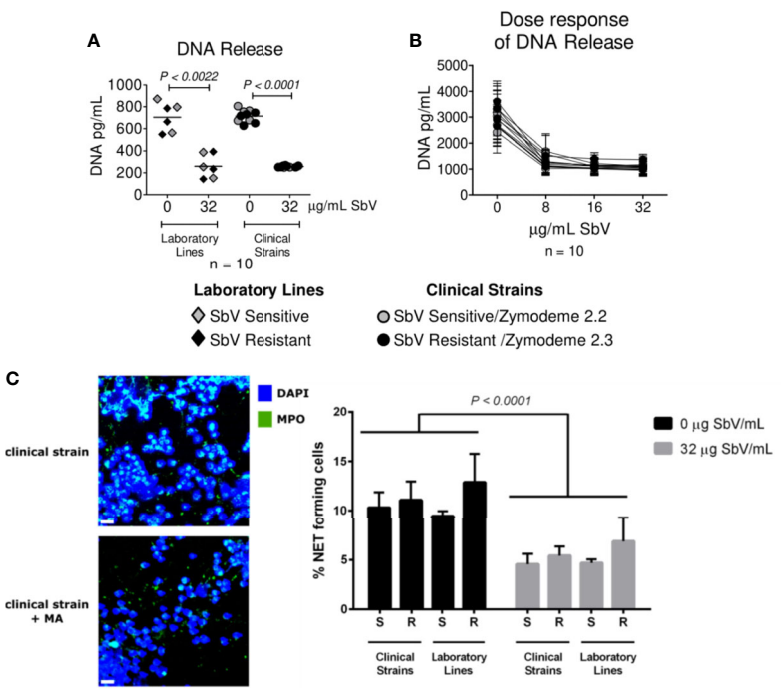

FIGURE 4 | Antimony effect on NET release by neutrophils infected with sensitive and antimony tolerant/resistant clinical strains of *L. (V.) panamensis*. Effect of SbV at Cmax: 32 ug SbV/ml on DNA release **(A)**. Dose response effect on DNA release **(B)**. Effect of SbV exposure on NET formation evaluated with confocal microscopy. On the left, representative confocal images of neutrophils exposed to the clinical strain of *L. (V.) p.* in the absence or presence of SbV. On the right, quantification of NET-forming neutrophils **(C)**. Data are the mean frequency of NET-producing neutrophils observed in three different neutrophil donors.

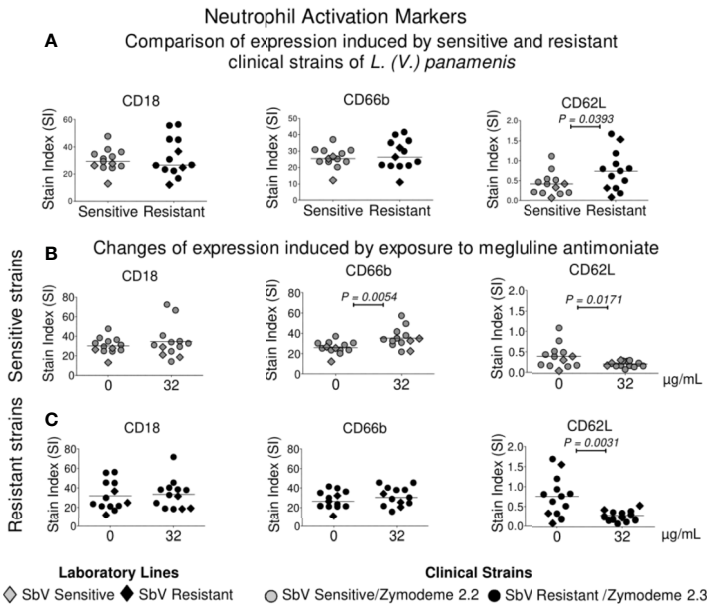

FIGURE 5 | Modulation of activation markers in neutrophils following infection with sensitive and resistant strains of *L. (V.) panamensis* and antimony exposure. Expressions of CD18, CD66b, and CD62L were compared in neutrophils infected with intrinsically SbV sensitive and resistant clinical strains of *L. (V.) panamensis* **(A)**, and after exposure to 32 µg SbV/ml of neutrophils infected with sensitive (n = 10) **(B)** and resistant strains (n = 10) **(C)**. Orange circles represent sensitive and resistant laboratory lines of *L. (V.) panamensis*. Each point corresponds to the mean or median of marker expression on neutrophils from three healthy donors. Statistical significance was defined using paired t test or Wilcoxon test according to the distribution of the data.

tolerance to nitric oxide (NO) reported among strains of *L. (V.) braziliensis* from a group of patients who failed antimonial treatment (Souza et al., 2010). However, parasite susceptibility to SbV was not evaluated in the latter study. Similarly, four clinical strains of *Leishmania infantum* isolated from patients who relapsed following treatment with MA drug presented tolerance to NO and to trivalent antimony (Sb^{III}). Modulation of neutrophil responses by our cohort of 20 clinical strains of *L. (V.) panamensis* was associated with intrinsic drug susceptibility phenotype for SbV, though not with outcome of treatment, which is multifactorial. Adherence to treatment, age-related pharmacokinetics, chronicity and location of lesions, and concurrent conditions influence and can confound the therapeutic response (Castro et al., 2017).

The intrinsic nature of the difference in susceptibility to SbV of the *L. (V.) panamensis* populations (zymodeme 2.2 and 2.3) represented by the clinical strains included in this study is supported by their sympatric prevalence and distribution throughout the Pacific Coast region of Colombia (Saravia et al., 1998). Furthermore, classification of the represented populations within distinct zymodemes was established during the 1990s and reported in 1998 (Saravia et al., 1998), 15 years before our large-scale drug susceptibility evaluation revealed their disparate susceptibility phenotype for antimonial drugs (Fernandez et al., 2014). Although the bases of the tolerant/resistant phenotype are not known, the results of this study support the participation of the elicited response of host neutrophils to the distinct parasite populations and to MA, as well as intrinsic parasite susceptibility to SbV, underscoring the interdependency of the host–parasite–drug interaction.

The observed induction of lower ROS production by SbV resistant clinical strains is potentially a manifestation of an adaptive phenotype that would diminish the effectiveness of this neutrophil defense mechanism during intracellular infection and contribute to tolerance to Sb. Notably the induction of ROS by SbV as MA, which has been previously documented for macrophages infected with *Leishmania donovani* (Mandal et al., 2007), did not override the diminished ROS induction by SbV resistant clinical strains of *L. (V.) panamensis*. In contrast, ROS induction was not modulated by infection with the SbV resistant laboratory derived line of *L. (V.) panamensis*, consistent with the intrinsic basis of the diminished ROS induction by the SbV resistant clinical strains. Although resistance mechanisms experimentally selected by long term, incremental drug pressure have been informative of factors involved in intracellular distribution, metabolism, and elimination of antileishmanials, they have not modeled natural resistance (Goyeneche-Patino et al., 2008). Hence, the mechanism(s) underlying tolerance to SbV in these clinical strains offers a window on the pathways to intracellular survival of *Leishmania* in the presence of this antileishmanial as well as in the absence of drug.

The participation of modulated host cell responses in treatment outcome was not discernable in the limited number of clinical strains from patients whose treatment outcome was available for inclusion in this analysis. The multiplicity of host,

parasite, and herein demonstrable parasite-mediated host responses confound and challenge the association of specific factors with therapeutic outcome. Nevertheless, the evidence of down-modulation of ROS production and increased expression of the surface activation marker and L-selectin associated with homing and migration to inflammatory sites in neutrophils infected with clinical strains that are intrinsically resistant is consistent with adaptations that favor the establishment of infection. The lower ROS induction by SbV tolerant/resistant clinical strains compared to sensitive strains extends prior findings with laboratory-derived lines to epidemiologically and clinically relevant parasite populations. The nature and mechanism of intrinsic tolerance/resistance are likely to be distinct from mechanisms derived by experimental selection based on direct and specific drug pressure and motivate further examination of neutrophil responses to phenotypically distinctive natural populations of *Leishmania* infecting patients.

SbV as meglumine antimoniate modulated some of the principal antimicrobial mechanisms of neutrophils, augmenting ROS production and reducing NET formation. These contrasting effects on neutrophil activation were consistently manifest independently of the susceptibility phenotype, whether laboratory derived or intrinsic to naturally circulating populations of *L. (V.) panamensis*. Several mechanisms may induce NET release that may be ROS-dependent (suicidal NETosis) (Fuchs et al., 2007) or ROS-independent (vital NETosis) (Pilsczek et al., 2010; Rochael et al., 2015). NET formation was induced in response to all the clinical *L. (V.) panamensis* strains tested irrespective of their sensitivity phenotype. Here, despite an increase in ROS production observed in the presence of parasites and MA, we observed decreased release of NETs following infection of drug-exposed neutrophils of both sensitive and resistant *L. (V.) panamensis* strains. It has been shown that the requirement of ROS for NET formation depends on the stimulus (Parker et al., 2012); in this regard, *L. amazonensis* has been reported to induce both the formation of ROS-dependent and ROS-independent NET release. As the increased ROS production induced by SbV did not correlate with increased NET release, our data suggest that the negative impact of MA on NET induction is ROS-independent.

The *in vitro* antimony concentrations, 8 to 32 μg SbV/ml, used in this study are achieved in plasma during treatment (Cruz et al., 2007). However, the implications of these drug-mediated effects on neutrophil defense mechanisms in relation with therapeutic response will require the evaluation of neutrophil responses of patients during treatment. The differential neutrophil activation observed following infection with clinical strains of *L. (V.) panamensis* that are intrinsically resistant to SbV illustrates the interplay of naturally occurring parasite adaptations and the elicited host cell response in antileishmanial drug susceptibility and resistance. This finding together with the evidence that antimonial drug also modulates neutrophil antimicrobial mechanisms enlightens approaches to optimizing therapeutic strategies.

Healing of CL is dependent upon the control of pro- and anti-inflammatory host defense mechanisms (Lakhal-Naouar et al., 2015). Consequently, antileishmanial drugs alone are often insufficient to clinically resolve disease even in immuno-competent individuals. Differential effects of intrinsically SbV tolerant/resistant *L. (V.) panamensis* on neutrophil activation and antimicrobial responses such as decreased ROS may influence therapeutic response to this drug. Modulation of host responses that impede lesion resolution and mobilization of regulatory mechanisms that promote healing may be achievable through co-adjuvant immunotherapeutic approaches to the treatment of cutaneous leishmaniasis (Ehrlich et al., 2017; Thacker et al., 2020).

DATA AVAILABILITY STATEMENT

The raw data supporting the conclusions of this article will be made available by the authors, without undue reservation.

ETHICS STATEMENT

The studies involving human participants were reviewed and approved by the Institutional Ethical Review Board of Centro Internacional de Entrenamiento e Investigaciones Médicas (CIDEIM) and by the Ethical Committee of the Canton of Vaud and the Swiss Confederation (CER-VD 2017-00182). The patients/participants provided their written informed consent to participate in this study.

AUTHOR CONTRIBUTIONS

NGS, FT-C, OF, LR, and MD-V contributed to the design and interpretation of the experiments. LR, OF, and MD-V performed the experiments and analyzed the data. NGS, OF, and LR wrote the manuscript. FT-C and MD-V contributed to and critically reviewed the manuscript. All authors contributed to the article and approved the submitted version.

FUNDING

This work was supported by the SPIRIT Swiss Programme for International Research by Scientific Investigation Teams, number IZSTZO_1190140 to FT-C and NGS, and in part by the Swiss National Science Foundation grant number 310030_184751 to FT-C and by the Global Infectious Research Training Program of the Fogarty International Center of the U.S. National Institutes of Health under award number SD43TW006589 and NIH/NIAID Tropical Medicine Research Centers (TMRC) grant U19AI129910 to NGS.

ACKNOWLEDGMENTS

We thank our colleagues in the CIDEIM Clinical Research Unit, David Esteban Rebellon, MD and Jimena Jojoa, MSc, for their assistance in the enrollment of volunteers, Paola Gómez for

technical assistance in the development of experiments, and Liliana Fernanda López and Isabel Guasaquillo for technical assistance in *Leishmania* propagation and characterization. At the University of Lausanne, we also gratefully acknowledge the training in the analysis of neutrophil activation provided by Ivo B. Regli, MD-PhD, and Yazmin Hauyon La Torre for technical assistance in the management of the *Leishmania* strains, and the Cellular Imaging Facility of the University of Lausanne, Switzerland. Preliminary results of this work were previously presented in the ASTMH Annual Meeting in November 2020.

REFERENCES

Afonso, L., Borges, V. M., Cruz, H., Ribeiro-Gomes, F. L., DosReis, G. A., Dutra, A. N., et al. (2008). Interactions With Apoptotic But Not With Necrotic Neutrophils Increase Parasite Burden in Human Macrophages Infected With Leishmania Amazonensis. *J. Leukoc. Biol.* 84 (2), 389–396. doi: 10.1189/jlb.0108018

Alvar, J., Velez, I. D., Bern, C., Herrero, M., Desjeux, P., Cano, J., et al. (2012). Leishmaniasis Worldwide and Global Estimates of Its Incidence. *PLoS One* 7 (5), e35671. doi: 10.1371/journal.pone.0035671

Borregaard, N. (2010). Neutrophils, From Marrow to Microbes. *Immunity* 33 (5), 657–670. doi: 10.1016/j.immuni.2010.11.011

Brinkmann, V., Reichard, U., Goosmann, C., Fauler, B., Uhlemann, Y., Weiss, D. S., et al. (2004). Neutrophil Extracellular Traps Kill Bacteria. *Science* 303 (5663), 1532–1535. doi: 10.1126/science.1092385

Carlsen, E. D., Hay, C., Henard, C. A., Popov, V., Garg, N. J., and Soong, L. (2013). Leishmania Amazonensis Amastigotes Trigger Neutrophil Activation But Resist Neutrophil Microbicidal Mechanisms. *Infect. Immun.* 81 (11), 3966–3974. doi: 10.1128/IAI.00770-13

Castro, M. D. M., Cossio, A., Velasco, C., and Osorio, L. (2017). Risk Factors for Therapeutic Failure to Meglumine Antimoniate and Miltefosine in Adults and Children With Cutaneous Leishmaniasis in Colombia: A Cohort Study. *PLoS Negl. Trop. Dis.* 11 (4), e0005515. doi: 10.1371/journal.pntd.0005515

Charmoy, M., Hurrell, B. P., Romano, A., Lee, S. H., Ribesiro-Gomes, F., Riteau, N., et al. (2016). The Nlrp3 Inflammasome, IL-1beta, and Neutrophil Recruitment Are Required for Susceptibility to a Nonhealing Strain of Leishmania Major in C57BL/6 Mice. *Eur. J. Immunol.* 46 (4), 897–911. doi: 10.1002/eji.201546015

Chaves, M. M., Lee, S. H., Kamenyeva, O., Ghosh, K., Peters, N. C., and Sacks, D. (2020). The Role of Dermis Resident Macrophages and Their Interaction With Neutrophils in the Early Establishment of Leishmania Major Infection Transmitted by Sand Fly Bite. *PLoS Pathog.* 16 (11), e1008674. doi: 10.1371/journal.ppat.1008674

Chrusciak-Talhari, A., Dietze, R., Chrusciak Talhari, C., da Silva, R. M., Gadelha Yamashita, E. P., de Oliveira Penna, C., et al. (2011). Randomized Controlled Clinical Trial to Access Efficacy and Safety of Miltefosine in the Treatment of Cutaneous Leishmaniasis Caused by Leishmania (Viannia) Guyanensis in Manaus, Brazil. *Am. J. Trop. Med. Hyg.* 84 (2), 255–260. doi: 10.4269/ajtmh.2011.10-0155

Cruz, A., Rainey, P. M., Herwaldt, B. L., Stagni, G., Palacios, R., Trujillo, R., et al. (2007). Pharmacokinetics of Antimony in Children Treated for Leishmaniasis With Meglumine Antimoniate. *J. Infect. Dis.* 195 (4), 602–608. doi: 10.1086/510860

De Muylder, G., Ang, K. K., Chen, S., Arkin, M. R., Engel, J. C., and McKerrow, J. H. (2011). A Screen Against Leishmania Intracellular Amastigotes: Comparison to a Promastigote Screen and Identification of a Host Cell-Specific Hit. *PLoS Negl. Trop. Dis.* 5 (7), e1253. doi: 10.1371/journal.pntd.0001253

Ehrlich, A. K., Fernandez, O. L., Rodriguez-Pinto, D., Castilho, T. M., Corral Caridad, M. J., Goldsmith-Pestana, K., et al. (2017). Local Delivery of the Toll-Like Receptor 9 Ligand CpG Downregulates Host Immune and Inflammatory Responses, Ameliorating Established Leishmania (Viannia) Panamensis Chronic Infection. *Infect. Immun.* 85 (3), e00981-16. doi: 10.1128/IAI.00981-16

Fernandez, O. L., Diaz-Toro, Y., Ovalle, C., Valderrama, L., Muvdi, S., Rodriguez, I., et al. (2014). Miltefosine and Antimonial Drug Susceptibility of Leishmania Viannia Species and Populations in Regions of High Transmission in Colombia. *PLoS Negl. Trop. Dis.* 8 (5), e2871. doi: 10.1371/journal.pntd.0002871

Fernandez, O., Diaz-Toro, Y., Valderrama, L., Ovalle, C., Valderrama, M., Castillo, H., et al. (2012). Novel Approach to *In Vitro* Drug Susceptibility Assessment of Clinical Strains of Leishmania Spp. *J. Clin. Microbiol.* 50 (7), 2207–2211. doi: 10.1128/JCM.00216-12

Fuchs, T. A., Abed, U., Goosmann, C., Hurwitz, R., Schulze, I., Wahn, V., et al. (2007). Novel Cell Death Program Leads to Neutrophil Extracellular Traps. *J. Cell Biol.* 176 (2), 231–241. doi: 10.1083/jcb.200606027

Gomez, M. A., Navas, A., Marquez, R., Rojas, L. J., Vargas, D. A., Blanco, V. M., et al. (2014). Leishmania panamensis Infection and Antimonial Drugs Modulate Expression of Macrophage Drug Transporters and Metabolizing Enzymes: Impact on Intracellular Parasite Survival. *J. Antimicrob. Chemother.* 69 (1), 139–149. doi: 10.1093/jac/dkt334

Goyeneche-Patino, D. A., Valderrama, L., Walker, J., and Saravia, N. G. (2008). Antimony Resistance and Trypanothione in Experimentally Selected and Clinical Strains of Leishmania panamensis. *Antimicrob. Agents Chemother.* 52 (12), 4503–4506. doi: 10.1128/AAC.01075-08

Hurrell, B. P., Regli, I. B., and Tacchini-Cottier, F. (2016). Different Leishmania Species Drive Distinct Neutrophil Functions. *Trends Parasitol.* 32 (5), 392–401. doi: 10.1016/j.pt.2016.02.003

Hurrell, B. P., Schuster, S., Grun, E., Coutaz, M., Williams, R. A., Held, W., et al. (2015). Rapid Sequestration of Leishmania Mexicana by Neutrophils Contributes to the Development of Chronic Lesion. *PLoS Pathog.* 11 (5), e1004929. doi: 10.1371/journal.ppat.1004929

Lakhal-Naouar, I., Slike, B. M., Aronson, N. E., and Marovich, M. A. (2015). The Immunology of a Healing Response in Cutaneous Leishmaniasis Treated With Localized Heat or Systemic Antimonial Therapy. *PLoS Negl. Trop. Dis.* 9 (10), e0004178. doi: 10.1371/journal.pntd.0004178

Mandal, G., Wyllie, S., Singh, N., Sundar, S., Fairlamb, A. H., and Chatterjee, M. (2007). Increased Levels of Thiols Protect Antimony Unresponsive Leishmania Donovani Field Isolates Against Reactive Oxygen Species Generated by Trivalent Antimony. *Parasitology* 134 (Pt 12), 1679–1687. doi: 10.1017/S0031182007003150

Obonaga, R., Fernandez, O. L., Valderrama, L., Rubiano, L. C., Castro, M., Barrera, M. C., et al. (2014). Treatment Failure and Miltefosine Susceptibility in Dermal Leishmaniasis Caused by Leishmania Subgenus Viannia Species. *Antimicrob. Agents Chemother.* 58 (1), 144–152. doi: 10.1128/AAC.01023-13

Pace, D. (2014). Leishmaniasis. *J. Infect.* 69 Suppl 1, S10–S18. doi: 10.1016/j.jinf.2014.07.016

Palacios, R., Osorio, L. E., Grajalew, L. F., and Ochoa, M. T. (2001). Treatment Failure in Children in a Randomized Clinical Trial With 10 and 20 Days of Meglumine Antimonate for Cutaneous Leishmaniasis Due to Leishmania Viannia Species. *Am. J. Trop. Med. Hyg.* 64 (3-4), 187–193. doi: 10.4269/ajtmh.2001.64.187

Palic, S., Bhairosing, P., Beijnen, J. H., and Dorlo, T. P. C. (2019). Systematic Review of Host-Mediated Activity of Miltefosine in Leishmaniasis Through Immunomodulation. *Antimicrobial. Agents Chemother.* 63 (7), e02507-18. doi: 10.1128/AAC.02507-18

Parker, H., Dragunow, M., Hampton, M. B., Kettle, A. J., and Winterbourn, C. C. (2012). Requirements for NADPH Oxidase and Myeloperoxidase in Neutrophil Extracellular Trap Formation Differ Depending on the Stimulus. *J. Leuk. Biol.* 92 (4), 841–849. doi: 10.1189/jlb.1211601

Passelli, K., Billion, O., and Tacchini-Cottier, F. (2021). The Impact of Neutrophil Recruitment to the Skin on the Pathology Induced by Leishmania Infection. *Front. Immunol.* 12, 649348. doi: 10.3389/fimmu.2021.649348

Pilsczek, F. H., Salina, D., Poon, K. K., Fahey, C., Yipp, B. G., Sibley, C. D., et al. (2010). A Novel Mechanism of Rapid Nuclear Neutrophil Extracellular Trap Formation in Response to Staphylococcus Aureus. *J. Immunol.* 185 (12), 7413–7425. doi: 10.4049/jimmunol.1000675

Regli, I. B., Fernandez, O. L., Martinez-Salazar, B., Gomez, M. A., Saravia, N. G., and Tacchini-Cottier, F. (2018). Resistance of Leishmania (Viannia) Panamensis to Meglumine Antimoniate or Miltefosine Modulates Neutrophil Effector Functions. *Front. Immunol.* 9, 3040. doi: 10.3389/fimmu.2018.03040

Regli, I. B., Passelli, K., Hurrell, B. P., and Tacchini-Cottier, F. (2017). Survival Mechanisms Used by Some Leishmania Species to Escape Neutrophil Killing. *Front. Immunol.* 8, 1558. doi: 10.3389/fimmu.2017.01558

Rochael, N. C., Guimaraes-Costa, A. B., Nascimento, M. T., DeSouza-Vieira, T. S., Oliveira, M. P., Garcia e Souza, L. F., et al. (2015). Classical ROS-Dependent and Early/Rapid ROS-Independent Release of Neutrophil Extracellular Traps Triggered by Leishmania Parasites. *Sci. Rep.* 5, 18302. doi: 10.1038/srep18302

Rojas, R., Valderrama, L., Valderrama, M., Varona, M. X., Ouellette, M., and Saravia, N. G. (2006). Resistance to Antimony and Treatment Failure in Human Leishmania (Viannia) Infection. *J. Infect. Dis.* 193 (10), 1375–1383. doi: 10.1086/503371

Rubiano, L. C., Miranda, M. C., Muvdi Arenas, S., Montero, L. M., Rodriguez-Barraquer, I., Garcerant, D., et al. (2012). Noninferiority of Miltefosine *Versus* Meglumine Antimoniate for Cutaneous Leishmaniasis in Children. *J. Infect. Dis.* 205 (4), 684–692. doi: 10.1093/infdis/jir816

Saravia, N. G., Segura, I., Holguin, A. F., Santrich, C., Valderrama, L., and Ocampo, C. (1998). Epidemiologic, Genetic, and Clinical Associations Among Phenotypically Distinct Populations of Leishmania (Viannia) in Colombia. *Am. J. Trop. Med. Hyg.* 59 (1), 86–94. doi: 10.4269/ajtmh.1998.59.86

Seifert, K., Escobar, P., and Croft, S. L. (2010). *In Vitro* Activity of Anti-Leishmanial Drugs Against Leishmania Donovani is Host Cell Dependent. *J. Antimicrob. Chemother.* 65 (3), 508–511. doi: 10.1093/jac/dkp500

Soto, J., Rea, J., Balderrama, M., Toledo, J., Soto, P., Valda, L., et al. (2008). Efficacy of Miltefosine for Bolivian Cutaneous Leishmaniasis. *Am. J. Trop. Med. Hyg.* 78 (2), 210–211. doi: 10.4269/ajtmh.2008.78.210

Souza, A. S., Giudice, A., Pereira, J. M., Guimaraes, L. H., de Jesus, A. R., de Moura, T. R., et al. (2010). Resistance of Leishmania (Viannia) Braziliensis to Nitric Oxide: Correlation With Antimony Therapy and TNF-Alpha Production. *BMC Infect. Dis.* 10, 209. doi: 10.1186/1471-2334-10-209

Thacker, S. G., McWilliams, I. L., Bonnet, B., Halie, L., Beaucage, S., Rachuri, S., et al. (2020). CpG ODN D35 Improves the Response to Abbreviated Low-Dose Pentavalent Antimonial Treatment in non-Human Primate Model of Cutaneous Leishmaniasis. *PLoS Negl. Trop. Dis.* 14 (2), e0008050. doi: 10.1371/journal.pntd.0008050

van Zandbergen, G., Klinger, M., Mueller, A., Dannenberg, S., Gebert, A., Solbach, W., et al. (2004). Cutting Edge: Neutrophil Granulocyte Serves as a Vector for Leishmania Entry Into Macrophages. *J. Immunol.* 173 (11), 6521–6525. doi: 10.4049/jimmunol.173.11.6521

Velez, I., Lopez, L., Sanchez, X., Mestra, L., Rojas, C., and Rodriguez, E. (2010). Efficacy of Miltefosine for the Treatment of American Cutaneous Leishmaniasis. *Am. J. Trop. Med. Hyg.* 83 (2), 351–356. doi: 10.4269/ajtmh.2010.10-0060

Vermeersch, M., da Luz, R. I., Tote, K., Timmermans, J. P., Cos, P., and Maes, L. (2009). *In Vitro* Susceptibilities of Leishmania Donovani Promastigote and Amastigote Stages to Antileishmanial Reference Drugs: Practical Relevance of Stage-Specific Differences. *Antimicrob. Agents Chemother.* 53 (9), 3855–3859. doi: 10.1128/AAC.00548-09

Zahid, M. S. H., Johnson, M. M., Tokarski, R. J. 2nd, Satoskar, A. R., Fuchs, J. R., Bachelder, E. M., et al. (2019). Evaluation of Synergy Between Host and Pathogen-Directed Therapies Against Intracellular Leishmania Donovani. *Int. J. Parasitol. Drugs Drug Resist.* 10, 125–132. doi: 10.1016/j.ijpddr.2019.08.004

Conflict of Interest: The authors declare that the research was conducted in the absence of any commercial or financial relationships that could be construed as a potential conflict of interest.

Publisher's Note: All claims expressed in this article are solely those of the authors and do not necessarily represent those of their affiliated organizations, or those of the publisher, the editors and the reviewers. Any product that may be evaluated in this article, or claim that may be made by its manufacturer, is not guaranteed or endorsed by the publisher.

frontiers in Cellular and Infection Microbiology

ORIGINAL RESEARCH
published: 01 October 2021
doi: 10.3389/fcimb.2021.687633

Murine Susceptibility to *Leishmania amazonensis* Infection Is Influenced by Arginase-1 and Macrophages at the Lesion Site

Fernanda Tomiotto-Pellissier[1,2], Milena Menegazzo Miranda-Sapla[2], Taylon Felipe Silva[2], Bruna Taciane da Silva Bortoleti[1,2], Manoela Daiele Gonçalves[3], Virginia Márcia Concato[2], Ana Carolina Jacob Rodrigues[1,2], Mariana Barbosa Detoni[2], Idessania Nazareth Costa[2], Carolina Panis[4], Ivete Conchon-Costa[2], Juliano Bordignon[1,5]* and Wander Rogério Pavanelli[1,2]**

[1] Biosciences and Biotechnology Graduate Program, Carlos Chagas Institute (ICC), Fiocruz, Curitiba, Brazil, [2] Laboratory of Immunoparasitology of Neglected Diseases and Cancer (LIDNC), Department of Pathological Sciences, State University of Londrina, Londrina, Brazil, [3] Laboratory of Biotransformation and Phytochemistry, Department of Chemistry, State University of Londrina, Universitary Hospital, Londrina, Brazil, [4] Laboratory of Tumor Biology, State University of Western Paraná (UNIOESTE), Francisco Beltrão, Brazil, [5] Laboratory of Molecular Virology, Carlos Chagas Institute (ICC), Fiocruz, Curitiba, Brazil

OPEN ACCESS

Edited by:
Rossana C.N. Melo,
Federal University of Juiz de Fora, Brazil

Reviewed by:
Kátia Da Silva Calabrese,
Oswaldo Cruz Foundation, Brazil
Guillermo Arango Duque,
Université de Montréal, Canada

***Correspondence:**
Fernanda Tomiotto-Pellissier
fernandatomiotto@gmail.com
Wander Rogério Pavanelli
wanderpavanelli@yahoo.com.br
Juliano Bordignon
bordignonjuliano@gmail.com

Specialty section:
This article was submitted to Parasite and Host, a section of the journal Frontiers in Cellular and Infection Microbiology

Received: 29 March 2021
Accepted: 13 September 2021
Published: 01 October 2021

Citation:
Tomiotto-Pellissier F, Miranda-Sapla MM, Silva TF, Bortoleti BTdS, Gonçalves MD, Concato VM, Rodrigues ACJ, Detoni MB, Costa IN, Panis C, Conchon-Costa I, Bordignon J and Pavanelli WR (2021) Murine Susceptibility to Leishmania amazonensis Infection Is Influenced by Arginase-1 and Macrophages at the Lesion Site. Front. Cell. Infect. Microbiol. 11:687633. doi: 10.3389/fcimb.2021.687633

Cutaneous leishmaniasis is a zoonotic infectious disease broadly distributed worldwide, causing a range of diseases with clinical outcomes ranging from self-healing infections to chronic disfiguring disease. The effective immune response to this infection is yet to be more comprehensively understood and is fundamental for developing drugs and vaccines. Thus, we used experimental models of susceptibility (BALB/c) and partial resistance (C57BL/6) to *Leishmania amazonensis* infection to investigate the local profile of mediators involved in the development of cutaneous leishmaniasis. We found worse disease outcome in BALB/c mice than in C57BL/6 mice, with almost 15 times higher parasitic load, ulcerated lesion formation, and higher levels of IL-6 in infected paws. In contrast, C57BL/6 presented higher levels of IFN-γ and superoxide anion ($^{\bullet}O_2^-$) after 11 weeks of infection and no lesion ulcerations. A peak of local macrophages appeared after 24 h of infection in both of the studied mice strains, followed by another increase after 240 h, detected only in C57BL/6 mice. Regarding M1 and M2 macrophage phenotype markers [iNOS, MHC-II, CD206, and arginase-1 (Arg-1)], we found a pronounced increase in Arg-1 levels in BALB/c after 11 weeks of infection, whereas C57BL/6 showed an initial predomination of markers from both profiles, followed by an M2 predominance, coinciding with the second peak of macrophage infiltration, 240 h after the infection. Greater deposition of type III collagen and lesion resolution was also observed in C57BL/6 mice. The adoptive transfer of macrophages from C57BL/6 to infected BALB/c at the 11th week showed a reduction in both edema and the number of parasites at the lesion site, in addition to lower levels of Arg-1. Thus, C57BL/6 mice have a more effective response against *L. amazonensis*, based on a balance between inflammation and tissue repair, while BALB/c mice have an excessive Arg-1 production at

late infection. The worst evolution seems to be influenced by recruitment of Arg-1 related macrophages, since the adoptive transfer of macrophages from C57BL/6 mice to BALB/c resulted in better outcomes, with lower levels of Arg-1.

Keywords: Leishmaniasis, M1, M2, IFN-γ, wound healing, collagen, iNOS

INTRODUCTION

Leishmaniases are a group of infectious diseases caused by species of protozoan parasites of the *Leishmania* genus, transmitted to animals and humans through the bite of female infected phlebotomine sand flies. The disease main clinical forms are cutaneous leishmaniasis (CL), visceral leishmaniasis, and mucocutaneous leishmaniasis. CL is the most common form, with estimates of 1 million new annual cases worldwide (WHO, 2020).

Classified as a neglected tropical disease by the World Health Organization, leishmaniasis represents a great challenge in the pharmacological field due to the lack of experimental vaccine candidates with satisfactory progression in human trials until now (Lage et al., 2020). Additionally, the available CL treatment is highly toxic and not fully effective (Caridha et al., 2019). A range of factors could explain the lack of vaccines and therapeutic options against CL, like the diversity among *Leishmania* species and the complexity of host's immune responses (Müller et al., 2018; Kaye et al., 2020). Thus, understanding the effective immune response to *Leishmania* infection is fundamental to benefit the processes of drug discovery and vaccine development.

Since the discovery of T $CD4^+$ helper 1 (Th1) and Th2 cells, experimental studies on CL have answered basic immunological questions related to the lesion development (Scott and Novais, 2016). Experimental studies using *L. major* have postulated that C57BL/6 mice present a predominant Th1 response associated with infection control, while BALB/c mice developed a Th2 response, favoring the disease progression (Sacks and Noben-Trauth, 2002; Scott and Novais, 2016). However, it is currently known that the Th1/Th2 paradigm is not valid for all *Leishmania* species.

In *L. amazonensis* infections, BALB/c mice also develop a lesion and a predominant Th2 response; however, C57BL/6 mice manifest a mixed immune response with mediators from both Th1 and Th2 patterns, being considered partially resistant to the infection (Soong, 2012; Pratti et al., 2016; Scott and Novais, 2016). This mixed response is similar to those observed in human infections, validating the biological relevance of these mice models for studying cutaneous leishmaniasis (Soong, 2012).

Leishmania parasites are known to actively manipulate their hosts and subvert the microbicide mechanisms by modifying/delaying the development of a type 1 response (Gregory and Olivier, 2005; Rossi and Fasel, 2018; Aoki et al., 2019). These escape mechanisms have been extensively characterized and vary according to the parasite species and host genetic background (Alexander et al., 1980; Lira et al., 2000; Rosas et al., 2005; Velasquez et al., 2016; Muxel et al., 2017).

Furthermore, the clinical course of *Leishmania* spp. infections does not only depend on T cells response but also involves a complex range of cells, including macrophages, the main host cells for parasite replication. Macrophages have a dual role during infection, providing a safe place for parasites' survival inside the parasitophore vacuole, but also triggering an inflammatory response (cytokine production and oxidative stress response) that can control parasite replication. Therefore, macrophages are the key cell to disease progression, and their interaction with the parasites can dictate the success or failure of the infection (Liu and Uzonna, 2012).

There are two main macrophage types described, M1 or "classically activated" and M2 or "alternatively activated" (Mills et al., 2000). M1 macrophages are activated by the Th1 lymphocyte subpopulation, in addition to producing interferon gamma (IFN-γ) and tumor necrosis factor-alpha (TNF-α), triggering the microbicide machinery and inducing the production of reactive species, especially superoxide anion ($^{\bullet}O_2^-$) by NADPH oxidase enzyme and nitric oxide (NO) by inducible nitric oxide synthase (iNOS), which eliminates *Leishmania* sp. parasites (Rossi and Fasel, 2018). However, an intense activation of M1 macrophages in the attempt to control the infection can trigger inflammation with tissue damage and exacerbation of the lesion (Laskin et al., 2011).

Conversely, M2 macrophages are activated mainly by IL-13 and IL-4 produced by Th2 cells, which, in turn, activate the enzyme arginase-1 (Arg-1), culminating in the synthesis of polyamines, allowing *Leishmania* intramacrophagic replication and favoring parasite survival and disease progression (Tomiotto-Pellissier et al., 2018). Meanwhile, despite the characteristics of permissiveness to infection, the macrophages activated by IL-4/IL-13 are also responsible for recruiting fibroblasts, keratinocytes, endothelial, and stem cells to wounds, which are fundamental to tissue repair and wound healing (Laskin et al., 2011; Krzyszczyk et al., 2018; Li et al., 2021). In CL, the resolution of skin infection is characterized by inflammation control, with lower INF-γ and TNF-α levels and higher deposition of ordered collagen fibers (Baldwin et al., 2007; Miranda et al., 2015). As iNOS and Arg-1 share L-arginine as substrate, these enzymes represent two possible pathways of immune response against *Leishmania* (Mills et al., 2000; Pessenda and Santana da Silva, 2020).

In this context, a balance between a potent microbicide response, combined with a resolutive and healing process, seems to be the key to provide the utmost benefit for the host (Tomiotto-Pellissier et al., 2018). Nonetheless, little is known about such balance and the role of M1 and M2 related molecules in leishmaniasis, whose understanding is important for developing drugs and vaccines. Based on this, our goal was to

demonstrate the differential response established by mice susceptible (BALB/c) and partially resistant (C57BL/6) to *Leishmania amazonensis* infection.

MATERIALS AND METHODS

Culture of *Leishmania (L.) amazonensis*

Promastigote forms of *Leishmania (L.) amazonensis* (MHOM/BR/1989/166MJO) and *Leishmania (L.) amazonensis* expressing an enhanced green fluorescent protein (eGFP) addressed to glycosomes (MHOM/BR/1973/M2269) were maintained in culture medium 199 (GIBCO, Invitrogen, USA) supplemented with 10% fetal bovine serum (FBS, GIBCO Invitrogen), 1 M HEPES, 0.1% human urine, 0.1% L-glutamine, 10 µg/ml penicillin and streptomycin (GIBCO Invitrogen), and 10% sodium bicarbonate (CAQ, Brazil). The eGFP strain was additionally cultured with 10 µM of geneticin G418 (Sigma Aldrich, USA) for parasite selection maintenance. The cell cultures were maintained in an incubator-type B.O.D. at 25°C in 25-cm^2 flasks. In all experiments, promastigote forms were used in the stationary growth phase.

Animals and Infection

BALB/c and C57BL/6 mice weighing approximately 25–30 g and aged 6–12 weeks were kept under sterile conditions and used according to protocols approved by the Institutional Animal Care and Committee. This study was approved by the Ethics Committee for Animal Experimentation of the State University of Londrina, number 8286.2016.60.

Mice were infected on the footpad of both hind paws, subcutaneously, with 10^5 promastigote forms of *L. amazonensis*/paw. The animals were divided into groups and evaluated at 6, 24, 72, 144, and 240 h, and 11 weeks post infection (p.i.). Five to six animals were evaluated in each group/time point.

Paw edema was measured weekly using a digital caliper (Starrett 799). At each time point, both paws were measured, and the data were plotted as the mean between the right and left paws of each animal. Final data are expressed as the mean edema of animals in the group.

After the end of each time point, the animals ($n \geq 5$) were euthanized by intraperitoneal inoculation of 100 mg/kg ketamine (Ceva, Brazil) and 10 mg/kg xylazine (JA, Brazil) followed by cervical dislocation, and the footpads of infected paws were collected, weighed, and processed for the next assays.

Parasite Burden Analysis

Real-time quantitative PCR (RT-qPCR) was performed to determine the tissue parasite load in each group. Briefly, hind paw samples were mechanically homogenized (Tissue-tearor, BioSpec) in TELT buffer (50 mM de Tris-HCl pH 8, EDTA 62,5 mM, Triton-X 4% e $LiCl_2$ 2.5 M), and DNA extraction was performed with the Easy-DNA kit (Invitrogen, USA, K1800-01) according to the manufacturer's instructions. Afterward, a solution of phenol:chloroform:isoamyl alcohol (25:24:1) was added, two volumes of cold ethanol (Merck, Germany) were added to the aqueous phase, and samples were stored at -20°C for 12 h. Samples were then centrifuged for 30 min at 10,000 *g*, washed with 70% ethanol, dried at room temperature, and resuspended in 10 mM Tris-HCl (pH 8.5). Real-time PCR was performed by using GoTaq qPCR Master Mix (Promega, USA) with 100 ng total genomic DNA (gDNA). Parasite quantification was performed using AAP3 gene primer 5'-GGCGGCGGTATTATCTCGAT-3' (Forward) 5'-ACCACGAGGTAGATGACAGACA-3' (Reverse) *Leishmania*-specific primers at 10 pM (Tellevik et al., 2014) in a 10-µl final volume reaction. The samples were amplified with a StepOnePlus Real-Time PCR System (Applied Biosystems, USA) under the following PCR conditions steps: 2 min at 50°C, 2 min at 95°C, 40 cycles of 15 s at 95°C, 1 min at 55°C, followed by a dissociation step of 55–99°C (heating of 0.5°C/s). The results were based on a standard curve constructed with DNA from culture samples of *L. amazonensis* promastigote forms.

Cytokines Determination

Th1, Th2, and Th17 cytokines were evaluated in the supernatant of the paw homogenates of non-infected and 11 weeks infected mice (n=5). The paws fragments were weighted, mechanically homogenized (Tissue-tearor, BioSpec) in PBS (100 mg/ml), and centrifuged (21293 *x* g, 2 min, 4°C). The supernatants were stored at -80°C, and the analyses were performed using Cytometric Beads Array (CBA) assays using a commercial kit (BD Bioscience, USA) following the manufacturer's recommendations. The concentration of each cytokine was determined with reference to the standard curve generated from reading the different dilutions of the recombinant cytokine. The limit of detection for each cytokine was 0.1, 0.03, 1.4, 0.5, 0.9, 0.8, and 16.8 pg/ml, respectively, for IL-2, IL-4, IL-6, IFN-γ, TNF-α, IL-17, and IL-10. The data were obtained in a BD Accuri C6 flow cytometer and analyzed using the FCAP Array v. 3.0.1 software.

Superoxide Anion Measurement

The superoxide anion ($^{\bullet}O_2^-$) production in the paw homogenates was evaluated by testing with nitroblue tetrazolium (NBT, Sigma-Aldrich, USA). For the assay, one of the hind paw fragments was weighted and mechanically homogenized (Tissue-tearor, BioSpec) in KCl 1.15% and centrifuged (21293 *x* g, 2 min, 4°C). Then, 10 µl of supernatants (100 mg/ml) was plated, and 100 µl of the solution containing NBT (1 mg/ml) was added. After 15 min of reaction at room temperature, the samples were fixed with 10 µl of methanol, and the formazan, product of the reaction between NBT and $^{\bullet}O_2^-$, was solubilized by the addition of 120 µl of 2M KOH (Merck). The readings were performed on a spectrophotometer (GloMax Explorer instrument, Promega) at 660 nm, and the results normalized per milligram of tissue. Six animals were evaluated in each group/time point, and uninfected BALB/c and C57BL/6 mice were used as controls (0h).

Determination of N-Acetylglucosaminidase Activity

For the indirect quantification of the presence of macrophages at the infection site, the activity of the enzyme N-acetylglucosaminidase

(NAG) was measured. The evaluation of the cellular infiltrate in the animals' footpad samples was performed by a colorimetric method described by Bradley et al. (1982). Briefly, the paw samples were weighed and added to 50 mM potassium phosphate buffer (pH 6.0) containing 13.72 mM HTAB (hexadecyl trimethyl ammonium bromide) and stored at -20°C. The samples (100 mg/ml) were then homogenized and centrifuged (21,293 *x* g, 2 min, 4°C). The supernatant was used for colorimetric reaction in a 96-well plate. Each aliquot of 15 µl of the sample was added to 200 µl of the reaction solution containing 52.64 mM of N-acetylglucosaminidase. The readings were performed on a spectrophotometer (GloMax Explorer instrument, Promega) at 450 nm, and the number of macrophages per milligram of tissue was determined using a standard curve.

Histological Processing

For the immunohistochemistry, collagen quantification, and immunofluorescence, one of the paws of each animal was fixed in 10% formalin solution and after 24 h they were decalcified for 21 days in 5% nitric acid (Anidrol, Brazil) and then processed for inclusion in paraffin. The cuts (5 µm thick) were adhered to slides treated with poly-L-lysine (Sigma-Aldrich) and deparaffinized xylene (FMAIA, Brazil) and subsequently hydrated with ethanol gradients to water.

Immunohistochemistry of Lesions for iNOS, MHC-II, Arg1, and CD206 Labeling

Typical markers of the M1 (MHC-II, iNOS) and M2 (CD206 and Arg-1) phenotypes were investigated in the histological sections of the infected mice paws. The hydrated histological sections were submitted to antigenic recovery in citrate and acetate buffer solution (pH 6) for 10 min in a microwave (40 W, 90°C). Endogenous peroxidase was blocked in a solution of 3% H_2O_2 (Anidrol), 10% methanol (Merck), and 0.1% Tween-80 (Sigma-Aldrich) for 30 min and, subsequently, the nonspecific sites blocked with PBS containing 1% FBS (GIBCO Invitrogen) for 30 min at room temperature. Then, the primary antibodies were added to the labeling of iNOS (NOS2, dilution 1:500, Santa Cruz Biotechnology, USA, Cat. SC7271), MHC-II (1:500, Santa Cruz, SC59318), arginase-1 (Arg-1, 1:600, Santa Cruz, SC18351), and CD206 (1:400, Santa Cruz, SC34577) for 2 h at 37°C. Subsequently, the universal solution of secondary antibodies with biotinylated antirabbit, antimouse, and antigoat IgG (LSAB + System-HRP, DAKO, Japan) was added for 1 h at room temperature. After three washes with PBS, the slides containing the samples were incubated with the avidin-peroxidase (LSAB + System-HRP, DAKO, K069011-2) complex for 40 min at room temperature. Finally, 3,3'-diaminobenzidine diaminobenzidine (DAB, DAKO, K3468) was added, and the counterstaining was performed with hematoxylin (Merck).

For determining a quantitative scoring, images were evaluated by using the color deconvolution tool from the Image J software (NIH, USA). Data are expressed in pixels (% of labeling in the image area). Five images of two sections of each animal were considered for analysis. Five to six animals were evaluated in each group/time point.

Collagen Quantification

The quantification of collagen in the paws lesion was performed by the Sirius-red staining method, assessed under polarized light through a photomicroscope (CARL ZEISS- Axio Imager A1) with a camera (HBO 100) coupled to a computer using the AxioVision software, with a 200x magnification. Five images of two sections of each animal were considered for analysis using the Image Pro Plus software (version 4.5). The results were expressed as a percentage of area with the presence of total collagen and type III collagen in measured area (Miranda et al., 2015).

In Vitro Infection of Peritoneal Macrophages

Peritoneal macrophages (1×10^5 cells/ml) were recovered from the peritoneal cavity of non-infected BALB/c and C57BL/6 mice with cold PBS supplemented with 3% of FBS (GIBCO Invitrogen) and then cultured in 24-well plates with 200 µl of RPMI 1640 medium (10% FBS) for 2 h (37°C, 5% CO_2). The adherent cells were infected with *L. amazonensis* eGFP promastigotes (2×10^6 cells/ml) for 4 h for the phagocytosis of the parasites. Afterward, the non-internalized parasites were washed with PBS, and the infected cells were cultivated for additional 24 h with RPMI 1640 in the presence or absence of the arginase inhibitor N(omega)-Nitro-L-arginine methyl ester (L-NAME, Sigma) at 70 µM.

After this, the cells were stained with antibody F4/80-PE (dilution 1:100, Santa Cruz Biotech, SC377009), and the antibody staining profile and eGFP fluorescence were analyzed by flow cytometry (BD Accuri C6 flow cytometer) using the FCAP Array v3.0.1 software. A total of 30.000 events were recorded. Infection analyzes were performed considering the percentage of eGFP-positive cells, and the infection intensity was determined based on the eGFP fluorescence intensity. Three independent experiments were performed in duplicate.

Adoptive Transfer of Macrophages

BALB/c and C57BL/6 mice were kept under the same conditions described in the section *Animals and Infection*.

Macrophages were recovered from the peritoneal cavity of non-infected C57BL/6 with cold PBS supplemented with 3% of FBS (GIBCO Invitrogen) and stained with antibodies F4/80-PE (dilution 1:100, Santa Cruz Biotech, SC377009) and CD11b-FITC (dilution 1:100, Santa Cruz Biotech, SC23937). The antibody staining profile was analyzed by flow cytometry (BD Accuri C6 flow cytometer) using the FCAP Array v3.0.1 software.

BALB/c mice were infected on both hind paws, subcutaneously, with 10^5 promastigote forms of *L. amazonensis*/paw, and randomly divided into three groups: BALB/c adoptive transfer of macrophages (ATM) IP—animals that received the ATM with macrophages from C57BL/6 *via* intraperitoneal injection; BALB/c ATM IV—animals that received the ATM with macrophages from C57BL/6 *via* intravenous injection; and BALB/c—animals that did not receive ATM (n = 5/group).

At the ninth week of infection, the BALB/c ATM groups received the transference of $5x10^5$ peritoneal macrophages from

C57BL/6 mice *via* intraperitoneal (BALB/c ATM IP) or by retro-orbital injection (BALB/c ATM IV; under anesthesia with 100 mg/kg ketamine (Ceva) and 10 mg/kg xylazine (JA) (**Figure 6A**). At the end of the 11th week, the animals were euthanized as described in the section *Animals and Infection*. The edema was measured weekly as described in the section *Animals and Infection*, the parasite burden analysis was performed as described in the section *Parasite Burden* Analysis, and the cytokines measurement was performed in the section *Cytokines Determination*.

Enzyme-Linked Immunosorbent Assay for iNOS and Arg-1 in Paws Homogenate

Paws fragments of animal groups (n=5/group) described in the section *In vitro Infection of Peritoneal Macrophages* were processed as follows: RIPA lysis buffer (140 mM sodium chloride, 1% Triton X-100, 0.1% sodium deoxycholate, 0.5% sodium dodecyl sulfate, 1 mM EDTA, 10 mM Tris, pH 8.0, and 1 mM phenylmethanesulfonyl fluoride (PMSF)) was added (1 ml) to the samples, mechanically homogenized (Tissue-tearor, BioSpec), and incubated for 2 h, 4°C. The lysates were collected and centrifuged at 13,000 x *g* for 20 min at 4°C, the supernatants were transferred to a new tube, and the total protein concentration was quantified in NanoVue Plus GE Healthcare (Biochrom, USA). The protein concentration of all samples was normalized to 10 µg/ml, and a 50-µl aliquot was added in a 96-well ELISA plate for adsorption of proteins overnight at 4°C, followed by incubation for 1 h with blocking buffer (ELISA/ELISPOT, eBioscience, USA). The wells were washed three times with wash buffer (PBS + 0.5% Tween 20 (Sigma-Aldrich)) and incubated with primary antibody antimouse iNOS (Santa Cruz Biotech, SC7271) and Arg-1 (Santa Cruz Biotech, SC18351) at 1:500 dilutions for 1 h at room temperature. The wells were washed to remove unbound antibodies, followed by the addition of universal biotinylated secondary antibody (LSAB2 System-HRP, Dako), 1-h incubation, washing, and addition of streptavidin-HRP (LSAB2 System-HRP, Dako) for 1 h. After the incubation time, the wells were washed five times, and 100 µl of TMB Substrate Solution (eBioscience, 00-4201-56) was added, followed by incubation for 30 min, and 100 µl of stop solution (1N sulfuric acid) was added. The plate reading was performed in a microplate reader at 450 nm (GloMax, Promega), and the results are expressed as arbitrary units.

Arginase-1 Immunofluorescence Study

The tissue sections were heated into citrate buffer 1 mM, pH 6.0, for 15 min at 100°C for antigen retrieval. Then, a working solution of bovine fetal serum 5% and Triton X 0.3% was added and incubated at 37°C in a humidified box for 15 min to block nonspecific antigens. Sections were then incubated overnight at 4°C with primary Arg-1 IgG antibody (1:500, Santa Cruz, SC18351). Afterward, they were rinsed five times in saline 0.9% for 5 min protected from light. Then, they were incubated at 37°C for 60 min with a secondary antibody (1:1,000, Alexa Fluor 488 goat anti-mouse IgG, Thermo Fischer Scientific). Subsequently, sections were rinsed two times in saline 0.9% for 5 min each. Afterward, the sections were incubated with 4,6 diamidinofenilindol (DAPI, Sigma Aldrich), 5 mg/ml solution, for 30 min. Slides were mounted with glycerol and stored protected from light for later observation under a fluorescence microscope. Representative images of five animals per group are shown.

Statistical Analysis

Data were expressed as a mean ± SEM. Data were analyzed using the GraphPad Prism statistical software (GraphPad Software, Inc., USA, 500.288). Differences between the two groups were evaluated using the Student's t-test. Comparisons between multiple groups were done using ANOVA followed by Tukey's test. Differences were considered as statistically significant upon $p < 0.05$. At least five animals per group were evaluated.

RESULTS

BALB/c Mice Show Worse Evolution of *L. amazonensis* Infection Comparing With C57BL/6 Mice

We analyzed the evolution of *L. amazonensis* infection through the paw lesion edema, measured weekly until the 11th week after infection. The edema was similar on both BALB/c and C57BL/6 mice until the eighth week of infection; however, from the ninth week on, the BALB/c mice showed significantly higher edema than C57BL/6 (**Figure 1A**). Also, all BALB/c mice showed ulcerated lesions after 11 weeks of infection, while none of the C57BL/6 strain had ulcerations (**Figure 1B**).

Regarding the parasitic load, we found significantly more parasites in the infected paws of BALB/c mice than in the C57BL/6 mice after 11 weeks of infection (**Figure 1C**).

Cytokines Are Differentially Produced by *L. amazonensis*-Infected BALB/c and C57BL/6 Mice Paw

Considering that *L. amazonensis* infection leads to a differential inflammatory response in BALB/c and C57BL/6 mice, we measured the production of inflammatory cytokines in paws homogenates of infected mice after 11 weeks. C57BL/6 mice presented higher levels of IFN-γ (**Figure 2A**), while BALB/c exhibited higher levels of IL-6 (**Figure 2C**). Eleven weeks after infection, BALB/c and C57BL/6 infected mice did not show different TNF-α levels (**Figure 2B**). For having remained below the technique detection limit, we did not interpret the following values: uninfected mice, IL-2, IL-4, IL-10, and IL-17 values of infected mice, as well as IFN-γ, TNF-α, and IL-6 levels at the infection times from 6 to 240 h.

C57BL/6 Mice Produce Higher Levels of $^{\bullet}O_2^-$ in the Infection Site Than BALB/c Mice

Aiming to understand the mechanisms involved at the early- and late-stage pathogenesis of *L. amazonensis* infection in C57BL/6 and BALB/c mice strains, we measured the $^{\bullet}O_2^-$ production (NBT assay) in paws homogenates. C57BL/6 mice had a higher basal production of $^{\bullet}O_2^-$ (0 h) than BALB/c mice. After infection, these radical levels were drastically reduced in both strains of mice (6h) but increased at later times in the C57BL/6 mice (72 h to 11 weeks). In BALB/c mice, we found that $^{\bullet}O_2^-$ levels remained low

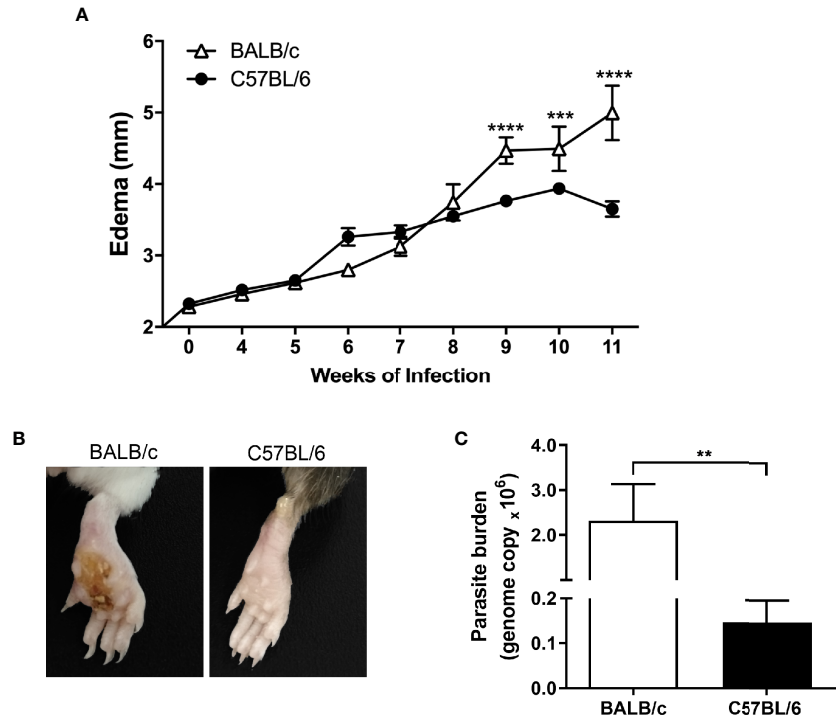

FIGURE 1 | Evolution of *L. amazonensis* infection in BALB/c and C57BL/6 mice. **(A)** BALB/c and C57BL/6 mice were infected on the hind paws with 10^5 promastigote forms of *L. amazonensis*/paw, and the edema was analyzed for 11 weeks. **(B)** Representative images of BALB/c and C57BL/6 mice paws 11 weeks after the infection with *L. amazonensis*. **(C)** Parasitic load (number of *Leishmania amazonensis* kDNA copies) determined in the mouse paw homogenate by quantitative real-time PCR after 11 weeks of infection. Data represent the mean ± SEM of six mice groups. **Significant difference in relation to the opposite strain infected by *L. amazonensis*, $p \leq 0.01$, ***$p \leq 0.001$, ****$p \leq 0.0001$.

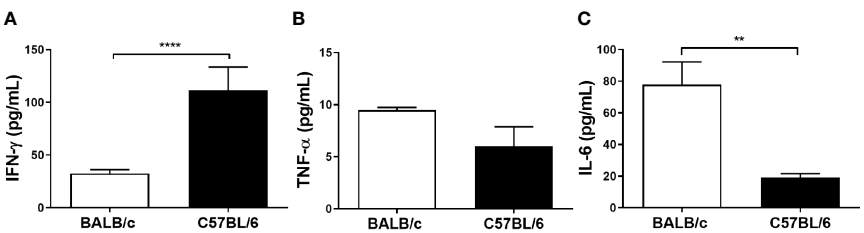

FIGURE 2 | Cytokine levels of BALB/c and C57BL/6 mice infected with *L. amazonensis*. Homogenates of *L. amazonensis*-infected BALB/c and C57BL/6 paws for 11 weeks were submitted to the CBA assay. **(A)** Measurement of IFN-γ, **(B)** TNF-α, and **(C)** IL-6 levels after 11 weeks of infection. Data represent the mean ± SEM of five mice groups. ** Significant difference in relation to the opposite strain infected by *L. amazonensis*, $p \leq 0.01$; ****$p \leq 0.0001$.

for the assessed periods (no statistical difference between 6 h and the later time points) and also presented significantly lower values than C57BL/6 (72 to 240 h) (**Figure 3**).

BALB/c and C57BL/6 Have Different Macrophage Infiltration and M1 and M2 Markers During *L. amazonensis* Infection

To understand the dynamics of macrophage infiltration at the lesion site, we analyzed the quantity of these cells in the paws throughout the infection. BALB/c mice showed a single peak of macrophage infiltration occurring 24 h post *L. amazonensis* infection; in addition, the amount of local macrophages decreases in sequence (144 h to 11 weeks). In contrast, C57BL/6 showed two peaks of macrophage infiltration, one more initial 24 h after infection, and the later one at 240h p.i. (**Figure 4A**).

To identify the profile of macrophages at the infection site, we performed the immunohistochemistry assay to identify the presence of MHC-II and iNOS labeling related to the M1 profile, as well as CD206 and Arg-1 markers, related to the M2 phenotype. We observed that at early infection (6 h), the C57BL/6 mice show markers from both macrophage subpopulations in relation to BALB/c mice. After 24 h, the time point related to the

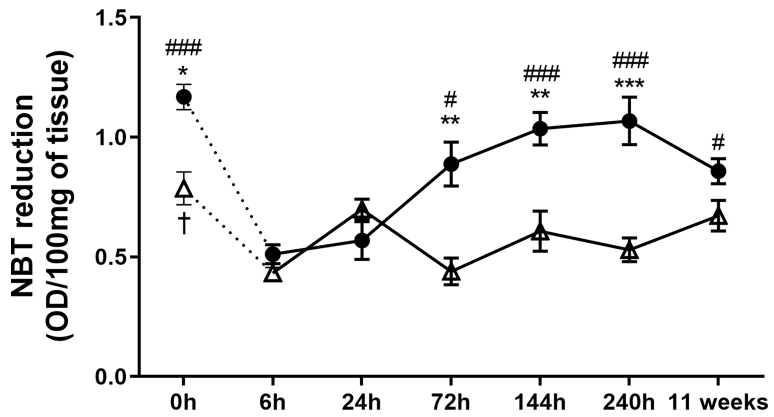

FIGURE 3 | Superoxide anion measured at the paws of BALB/c and C57BL/6 mice infected with *L. amazonensis*. Homogenates of BALB/c and C57BL/6 paws infected with *L. amazonensis* from 6 h to 11 weeks submitted to the NBT assay. Uninfected mice were used as controls (0 h). * Significant difference between mice strains infected by *L. amazonensis*, $p \leq 0.05$; **$p \leq 0.01$, ***$p \leq 0.001$. #Difference in the time points vs. 6 h within C57BL/6 mice, $p \leq 0.05$, ##$p \leq 0.01$, ###$p \leq 0.001$. †Difference in the time points *vs.* 6 *h* within BALB/c mice, $p = 0.016$. Data represent the mean ± SEM of six mice groups.

first macrophage infiltration (**Figure 4A**), C57BL/6 showed high CD206 marking. At 72 h p.i., Arg-1 was higher on C57BL/6 mice paws. After 144 h, C57BL/6 showed higher labeling iNOS, Arg-1, and CD206 than BALB/c mice. At the time point coinciding with the second peak of infiltration, 240 h, C57BL/6 mice presented higher marking for both Arg-1 and CD206 at the infection site. After 11 weeks of infection, this profile was altered, with C57BL/6 presenting more M1 markers, while BALB/c showed significantly higher levels of Arg-1 marking in relation to C57BL/6 (**Figures 4B**–**E**, **G**).

We also found a higher Arg-1/iNOS ratio in C57BL/6 mice than in BALB/c after 240 h of infection. However, after 11 weeks of infection, such balance was reversed, with a substantially higher proportion of marking for Arg-1 in the BALB/c paws compared with C57BL/6 mice (**Figure 4F**).

Furthermore, immunohistochemical images revealed that the intense labeling Arg-1 after 11 weeks of infection coincides with areas with vacuolated macrophages filled with parasites (**Figure 4G**, **Figure S1**). This pattern also appeared in the heatmap (**Figure 4H**), showing a prominent Arg-1 labeling in BALB/c, while the levels found in C57BL/6 were more evenly distributed among the analyzed markers and times.

C57BL/6 Mice Have More Type III Collagen Deposition at the Infection Site at Late Infection Stages

Since tissue repair is closely related to the clinical course of leishmaniasis, we identified total collagen and newly deposited collagen (type III) in the paws of infected mice as a readout of tissue repair (Frahs et al., 2018). The results revealed that at 240 h and 11 weeks p.i., C57BL/6 mice had significantly more total and type III collagen than BALB/c (**Figures 5A, B**). In addition, in C57BL/6, the amount of total collagen increased from 240 h to 11 weeks of infection (**Figure 5A**).

Figure 5C and **Figure S1** show the presence of vacuolated macrophages containing amastigotes (parasitophorous vacuoles) in BALB/c mice 11 weeks after infection, coinciding with areas of low labeling for type I and type III collagen. In C57BL/6 mice, after 240 h, there were no visible vacuoles in the macrophages and consequently lesser parasites at the infection site. In addition, collagen deposition appeared in the C57BL/6 sections, characterizing a tissue repair process.

The Macrophages Recruited to the Lesion Site Are Important for the Evolution of Edema and in the Arginase-1 Presence

Considering the differences in the lesion evolution in the studied mouse strains, we investigated the behavior of the respective macrophages against *L. amazonensis* infection *in vitro*. For this purpose, we infected peritoneal macrophages from mice of both strains with eGFP-promastigote forms (1:10) and assessed their ability to eliminate the parasites. We found that macrophages from BALB/c mice had significantly more parasites per macrophage (indicated by eGPF MFI of F4/80$^+$ eGFP$^+$ cells, **Figure 6A**) and higher percentage of infected macrophages (indicated as percentage of F40/80$^+$ and eGFP$^+$ cells, **Figure 6B**) after 24 h of infection than C57BL/6. Furthermore, the addition of arginase blocker L-NAME led to an important reduction in infection levels in BALB/c macrophages, while the parasite levels in C57BL/6 mice remained without statistical differences (**Figure 6**).

Interestingly, by adding a blocker, BALB/c macrophage infection levels became similar to C57BL/6 macrophage infection levels in the absence of an inhibitor (17.88 ± 1.87 *vs.* 18.22 ± 2.23, respectively) (**Figure 6B**).

Therefore, for an *in vivo* analysis of the role of recruited macrophages on *L. amazonensis* lesion evolution, we performed the adoptive transfer of macrophages (ATM) from partially resistant mice (C57BL/6) to susceptible ones (BALB/c) after 9 weeks of infection, the time point at which the paw edema starts to significantly differ between the mice strains (**Figures 1A**, **7A**). Firstly, peritoneal cells from C57BL/6 were characterized as

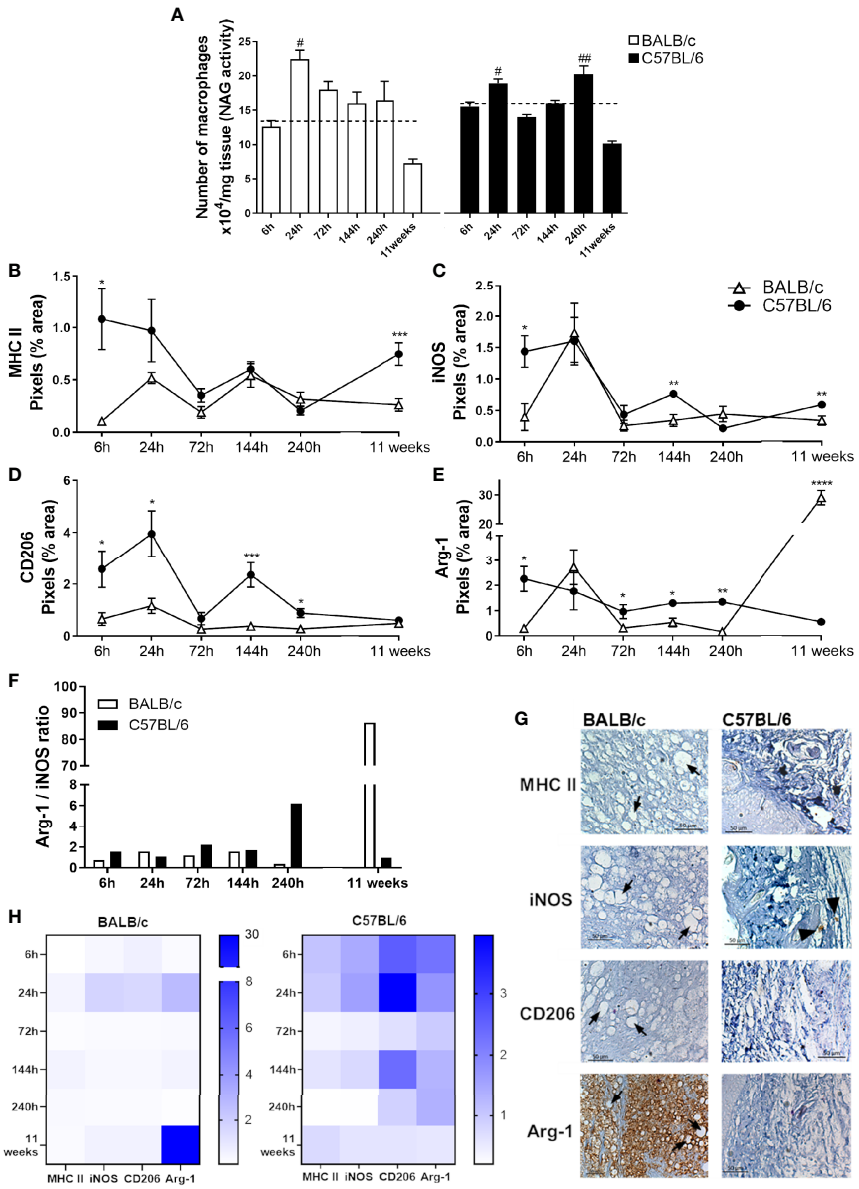

FIGURE 4 | Characterization of local macrophages in infected mice paws. **(A)** Indirect measurement of the macrophage number by NAG activity. **(B)** Immunohistochemical quantification of MHC-II, **(C)** iNOS, **(D)** Arg-1, and **(E)** CD206 staining in the paw of infected mice. #Significant difference in relation to the non-infected mice (dashed lines), $p \leq 0.05$; ##$p \leq 0.01$. *Significant difference between BALB/c and C57BL/6 mice infected with *L. amazonensis*, $p \leq 0.05$; **$p \leq 0.01$, ***$p \leq 0.001$, ****$p \leq 0.0001$. **(F)** Arg-1/iNOS ratio. **(G)** Representative figures of immunohistochemical labeling. The positive marking on immunohistochemistry sections corresponds to the brown areas (arrowhead). Arrows indicate vacuolated macrophages filled with parasites. **(H)** Heatmap of MHC-II, iNOS, Arg-1, and CD206 in all evaluated time points. Data from **(A–E)** represent the mean ± SEM ($n \geq 5$).

predominantly macrophages ($F4/80^+/CD11b^+$) (**Figure 7B**, gate strategy **Figure S2**). Then, we found that mice that received ATM intraperitoneal (ATM IP) presented lower paw edema and more than 250 times less parasite burden (**Figures 7C, D**). Additionally, most ATM animals did not show any ulceration at the infection site, while BALB/c mice presented typical ulcerated lesions (**Figure 7E**).

Analysis of the local cytokines at the 11th week showed ATM mice with higher IFN-γ levels, while mice that did not receive ATM presented higher IL-6 levels (**Figures 8A, B**). We also verified lower Arg-1 levels in ATM IP mice without significant variation in iNOS compared with BALB/c that did not receive ATM (**Figures 8C, D**). Such reduced Arg-1 levels in ATM animals was further confirmed through immunofluorescence (**Figure 8E**). Similar results emerged by performing ATM *via* the intravenous route (ATM IV), with edema and Arg-1 reduction in the ATM IV group, without significantly different iNOS levels (**Figure S3**).

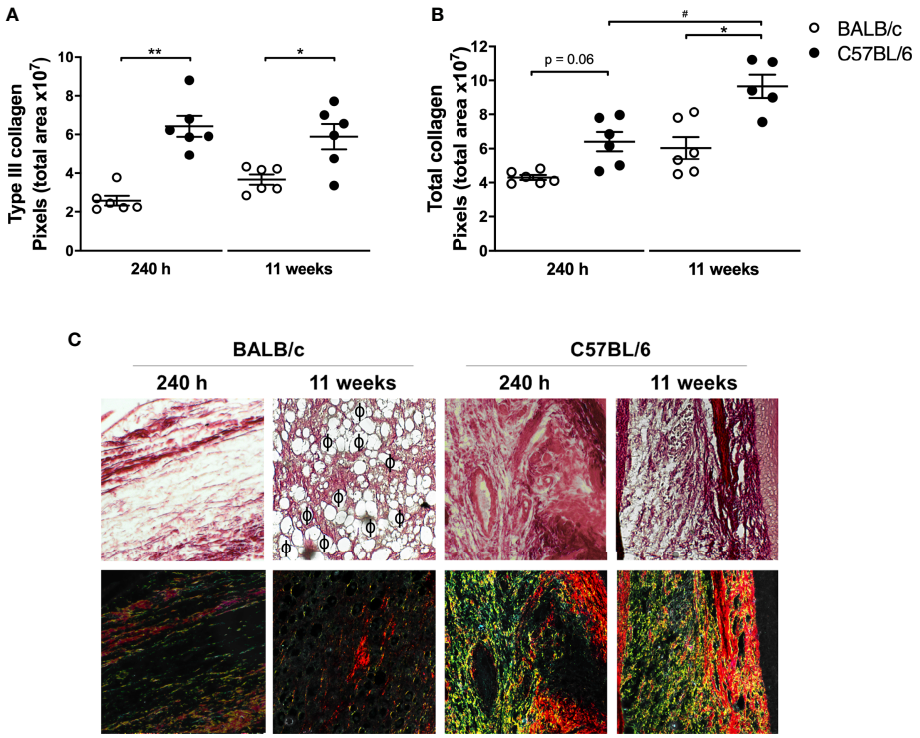

FIGURE 5 | Analysis of collagen in mice paws infected with *L. amazonensis*. Histological sections of the paws of *L. amazonensis*-infected BALB/c and C57BL/6 mice for 240 h or 11 weeks p.i. were stained with Sirius Red to measure **(A)** total collagen and **(B)** type III collagen using the Image-Pro Plus. * Significant difference between the mice strains infected by *L. amazonensis*, $p \leq 0.05$; **$p \leq 0.01$. #Significant difference of time points in C57BL/6 mice, $p \leq 0.05$. **(C)** Representative figures of histological sections of the paws of BALB/c and C57BL/6 mice infected by *L. amazonensis* for 240 h and 11 weeks. ϕ—Indication of some parasitophorous vacuoles. The fibers stained in red correspond to type I collagen and those in yellow/green correspond to deposited type III collagen. Data from **(A, B)** represent the mean ± SEM ($n \geq 5$).

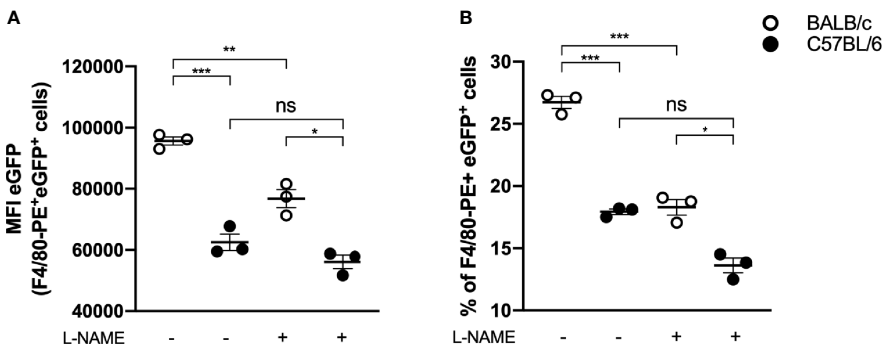

FIGURE 6 | *In vitro* infection of BALB/c and C57BL/6 peritoneal macrophages. Peritoneal macrophages (10^5) of BALB/c and C57BL/6 mice were infected with 10^6 e-GPF parasites and evaluated about **(A)** e-GFP median fluorescence intensity (MFI) of macrophages (F4/80$^+$ cells) and **(B)** percentage of infected macrophages (% of F4/80$^+$ and e-GFP$^+$ cells). Data represent the mean ± SEM of three independent experiments performed in duplicate. * Significant difference $p \leq 0.05$, **$p \leq 0.01$, ***$p \leq 0.001$. L-NAME, N(omega)-Nitro-L-arginine methyl ester; NS, nonsignificative.

DISCUSSION

The pathological mechanisms that lead to cutaneous lesion caused by *L. amazonensis* infection are not yet fully understood. This work aimed to elucidate the role of different molecules and cells by comparing the evolution of *L. amazonensis* infection in mice strains partially resistant and susceptible to infection.

The most studied experimental model of cutaneous leishmaniasis is the *L. major* infection, in which the

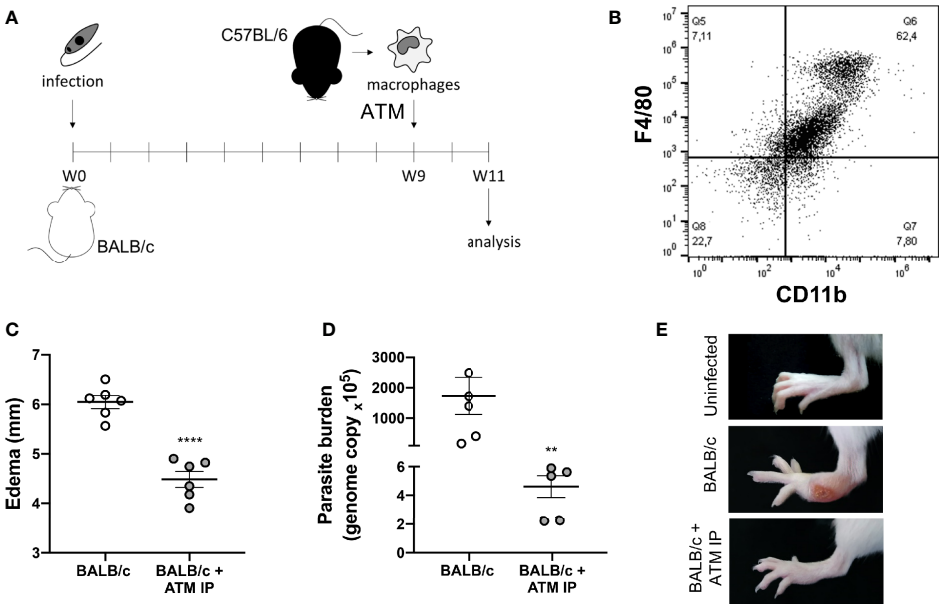

FIGURE 7 | Adoptive transfer of macrophages (ATM). **(A)** Representative scheme of the experimental design: BALB/c mice were infected with *L. amazonensis* and, after 9 weeks, they received peritoneal macrophages isolated from C57BL/6 mice intraperitoneally. **(B)** Dot plot showing the macrophage markers (F4/80$^+$/CD11b$^+$) in the peritoneal cells from non-infected C57BL/6 mice. **(C)** Paw edema of mice that did not receive adoptive transfer of macrophages (BALB/c) and mice that received intraperitoneal ATM (BALB/c + ATM IP) after 11 weeks of infection. **(D)** Parasite burden and **(E)** representative photographs of mice paws after 11 weeks of infection. Data from **(C, D)** represent the mean ± SEM of five mice groups. ** Significant difference in relation to the group that did not receive ATM, $p \leq 0.01$, ****$p \leq 0.0001$.

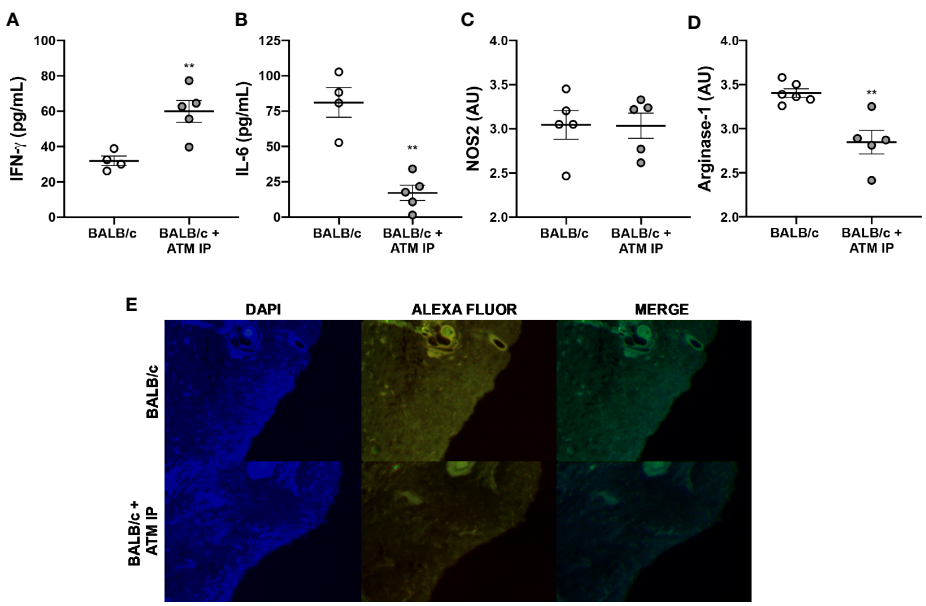

FIGURE 8 | Immunomodulation of ATM mice. Homogenates of *L. amazonensis*-infected BALB/c and BALB/c that received ATM *via* intraperitoneal paws were submitted to **(A)** IFN-γ and **(B)** IL-6 measurement by CBA assay; and **(C)** Arg-1 and **(D)** iNOS measurement by ELISA. Data represent the mean ± SEM of five mice groups. ** Significant difference with the opposite strain infected by *L. amazonensis*, $p \leq 0.01$. **(E)** Arginase-1 immunofluorescence study. Cell nucleus was stained with DAPI and arg-1 was stained with Alexa Fluor. ATM, adoptive transfer of macrophages; AU, arbitrary units; IP, intraperitoneal.

susceptibility of BALB/c mice has been correlated to the predominance of Th2 immune response, while C57BL/6 mice are resistant to infection, with a predominance of Th1 type response (Sacks and Noben-Trauth, 2002; Scott and Novais, 2016). However, such dichotomy is not identified in the disease induced by other *Leishmania* species, as *L. amazonensis* (Soong, 2012; Scott and Novais, 2016). Our study showed that BALB/c mice had progressive edema from 0 to 11 weeks after *L. amazonensis* infection, with ulceration of the lesion and high local parasitic load 11 weeks p.i. In contrast, C57BL/6 mice presented initial edema that was steadied at the later times analyzed, without ulcerated lesions, in addition to lower parasitic load than BALB/c.

We also found higher production of IL-6 in BALB/c mice in ATM IP mice, which play an important role in the leishmaniasis pathogenesis, triggering the down modulation of the microbicide molecules, and the polarization of macrophages to an M2 phenotype, which are more permissive to *Leishmania* proliferation (Hatzigeorgiou et al., 1993; Hu et al., 2018). Conversely, C57BL/6 mice had a significant increase in IFN-γ levels after 11 weeks of infection, a key cytokine in the activation of inflammatory macrophages (M1), associated with protection in several experimental models of infection (Laskin et al., 2011), including *Leishmania* sp. (Wang et al., 1994; Sacks and Noben-Trauth, 2002).

Moreover, IFN-γ triggers the synthesis of reactive oxygen species (ROS), such as $^{\bullet}O_2^-$. ROS are produced by M1 macrophages, causing oxidation of lipids, proteins, and nucleic acids, consequently eliminating intracellular parasites (Murray and Wynn, 2011; Jafari et al., 2014). C57BL/6 mice showed higher levels of $^{\bullet}O_2^-$ over the infection, with lower parasitic load, thus explaining a better lesion evolution in this mice strain.

However, an exacerbated pro-oxidant response can be harmful to the host during *Leishmania* sp. infection since the action of ROS is nonspecific and causes damage to the surrounding host cells, consequently leading to inflammation and tissue injury (Morgado et al., 2018; Herb and Schramm, 2021). Therefore, in the presence of pro-oxidant molecules, such as $^{\bullet}O_2^-$, adaptive homeostasis mechanisms must be activated as a way to protect against tissue damage (Pomatto et al., 2019). Despite producing $^{\bullet}O_2^-$ in a more pronounced manner, mice of the C57BL/6 strain showed higher collagen deposition, suggesting an ability to balance pro- and antioxidant properties, thus explaining the concomitant elimination of the parasite combined with the tissue protection capacity found in C57BL/6 mice (Morgado et al., 2018).

Regarding macrophages, we verified a peak of infiltration in the mice paws of both C57BL/6 and BALB/c mice after 24 h of infection, corroborating the expected kinetics of migration of these cells (Minutti et al., 2017). However, at early infection, there was no clear polarization of macrophages for M1 or M2 phenotype in either mice strain. These data are in accordance with the mixed Th1/Th2 profile induced by *L. amazonensis* infection (Scott and Novais, 2016), as well as with the findings of Ontoria et al. (2018), who found an inconstant distribution of M1 markers throughout the infection by *L. infantum* between 1 and 8 weeks.

The results also showed a second peak of macrophage infiltration in the C57BL/6 mice after 240 h of infection, with higher Arg-1 and CD206 marking than BALB/c. This indicates that macrophages recruited at this point have M2 characteristics, important for tissue remodeling and wound healing (Laskin et al., 2011). The wound healing process is executed and regulated through a signaling network involving numerous growth factors, cytokines, and chemokines. Interestingly, pro- and anti-inflammatory cytokines are important in this process, since the former induces the migration of monocytes to the wound, while the latter is important in the collagen deposition process. Thus, the wound healing is a complex orchestra governed by fine control between responses (Krzyszczyk et al., 2018).

Krzyszczyk et al. (2018) showed that as the tissue begins to recover, the general population of M2 macrophages induces the migration and proliferation of fibroblasts, keratinocytes, and endothelial cells to restore the dermis, epidermis, and vasculature, respectively, by remodeling the injured tissue. In CL wound, such remodeling is marked by the control of inflammation and a higher amount of collagen at the sites from which the parasites have been eliminated (Baldwin et al., 2007; Miranda et al., 2015). Type III collagen is the first deposited in early healing wounds, progressively replaced by type I as scar formation progresses and the tissue remodels (Rangaraj and Harding, 2011). Our data are in agreement with these studies and show that both collagen type levels were higher in C57BL/6 mice than in BALB/c mice, confirming the better lesion evolution in this mice strain. Additionally, collagen deposition was higher in areas with low parasitic load and tissue reorganization in the C57BL/6 mice. We also found a reduction in $^{\bullet}O_2^-$ in C57BL/6 after 11 weeks of infection, which is in accordance with the higher levels of collagen, since a new tissue formation stage is characterized by lower ROS levels (Xu et al., 2017).

Despite an infiltration of M2 macrophages in 240 h in C57BL/6 mice, in the later period studied, 11 weeks, a shift for M1 macrophages occurred, coinciding with higher levels of IFN-γ, with less parasitic load and no apparent lesion. In contrast, BALB/c mice had worse lesion evolution and a marked increase in Arg-1 (a M2 macrophage marker) in the later period analyzed (Muraille et al., 2014). Arginase-1 plays a fundamental role in the survival and multiplication of intracellular amastigotes of *Leishmania* sp., bypassing the amino acid L-arginine for the preferential synthesis of polyamines, fundamental for the parasite's nutrition (Muxel et al., 2017).

In vitro studies showed that *L. amazonensis*-infected BALB/c macrophages present increased L-arginine uptake and expression of arginase and arginase-related genes (Muxel et al., 2017; Aoki et al., 2019). Our data agree with these studies and show that *in vitro* BALB/c macrophages have a lower parasite clearance capacity than C57BL/6 macrophages; however, when arginase was blocked, parasite clearance by BALB/c macrophages increases substantially, reaching levels similar to those of C57BL/6.

It has been reported that arginase activity is inhibited by arginine analog L-NAME, both *in vitro* and *in vivo*; however, its function as an iNOS inhibitor has also been proved (Reisser et al., 2008). Since NO is important for eliminating *L. amazonensis*, reducing its levels would generate a larger number of intracellular parasites (Scott and Novais, 2016); therefore, we believe that in our experiments, L-NAME acted mainly by inhibiting arginase and not iNOS.

The role of Arg-1 from macrophages on CL lesions was further demonstrated through the adoptive transfer of macrophages from C57BL/6 to BALB/c mice, which revealed that mice receiving the cells presented better disease outcome, with similar features to those found in partially resistant mice. The recruited macrophages have been described as important weapons in *Leishmania* control, since the tissue resident macrophages present oxidative deficiency in relation to the recruited ones (Pessenda and Santana da Silva, 2020).

An important role for arginase in the susceptibility of mice to *L. major* infection had been described (Kropf et al., 2005), as well its action in *L. amazonensis* infection *in vitro*. Interestingly, skin biopsies and plasma from CL patients also present high levels of Arg-1 [reviewed in (Muxel et al., 2017)]. However, until now, little was known about Arg-1 in *L. amazonensis* infection *in vivo*. We showed that the participation of this enzyme in the susceptibility of animals is particularly important at later infection.

Peritoneal macrophages are a heterogeneous population of M0, M1, and M2 cells, with the capacity to differentiate or redifferentiate into both in M1 and M2 phenotypes (Zhao et al., 2017). Furthermore, these cells are recruited to other tissue under infection or inflammation conditions (Cassado et al., 2015). In this context, we performed the adoptive transfer of macrophages from C57BL/6 to BALB/c mice, whose results suggest a great importance of the recruited macrophages in controlling susceptibility to *L. amazonensis*. The transfer of macrophages from partially resistant mice (C57BL/6) to a susceptible mouse (BALB/c) modulates the pro-*Leishmania* environment to an anti-leishmania state, with high IFN-γ and low Arg-1 levels, less parasite burden and edema, and better disease outcome.

CONCLUSION

Taking together, the results suggest that a balance between a pro-inflammatory and microbicide M1-related and a tissue restorative M2-related response seems to provide the utmost benefit for the host. We also demonstrated that higher levels of Arg-1 at late infection periods modulate the disease outcome in susceptible mice, but the transference of macrophages from partially resistant mice (C57BL/6) restores the host protection and disease control. These results expand our understanding on the protective immunity against *L. amazonensis*, providing new insights on potential interventions to treat or prevent the disease.

DATA AVAILABILITY STATEMENT

The raw data supporting the conclusions of this article will be made available by the authors, without undue reservation.

ETHICS STATEMENT

The animal study was reviewed and approved by the Ethics Committee for Animal Experimentation of the State University of Londrina.

AUTHOR CONTRIBUTIONS

FT-P: Conceptualization, data curation, formal analysis, investigation, writing—original draft, and project administration. MM-S: Methodology, data curation, formal analysis, investigation, writing—original draft, and supervision. TS, BB, MG, and VC: Methodology, data curation, formal analysis, investigation, and writing—review and editing. VC, AR, and MD: Methodology, data curation, and formal analysis. IC and IC-C: Project administration, supervision, writing—review and editing, and resources. CP: Methodology, data curation, formal analysis, and writing—review and editing. JB: Conceptualization, supervision, validation, writing—review and editing, and resources. WP: Conceptualization, project administration, supervision, writing—review and editing, and resources. All authors contributed to the article and approved the submitted version.

FUNDING

This study was partly financed by the Coordenação de Aperfeiçoamento de Pessoal de Nível Superior—Brazil (CAPES) [Finance Code 001]. WP [301594/2018-0], IC-C [303233/2017-0], and JB [312671/2020-2] are CNPq fellows.

ACKNOWLEDGMENTS

We would like to gratefully acknowledge Dr. Letusa Albrecht and Dr. Guilherme Ferreira Silveira (ICC/FIOCRUZ), who contributed with the critical reviews, suggestions, and discussions during the execution of this work. We also thank Ivy Gobetti for the language edition.

SUPPLEMENTARY MATERIAL

The Supplementary Material for this article can be found online at: https://www.frontiersin.org/articles/10.3389/fcimb.2021.687633/full#supplementary-material

REFERENCES

Alexander, J., Brombacher, F., Peters, N., and Malchiodi, E. L. (1980). T Helper1/T Helper2 Cells and Resistance/Susceptibility to Leishmania Infection: Is This Paradigm Still Relevant? *Front. Immunol.* 3:80. doi: 10.3389/fimmu.2012.00080

Aoki, J. I., Laranjeira-Silva, M. F., Muxel, S. M., and Floeter-Winter, L. M. (2019). The Impact of Arginase Activity on Virulence Factors of Leishmania Amazonensis. *Curr. Opin. Microbiol.* 52, 110–115. doi: 10.1016/j.mib.2019.06.003

Baldwin, T., Sakthianandeswaren, A., Curtis, J. M., Kumar, B., Smyth, G. K., Foote, S. J., et al (2007). Wound Healing Response is a Major Contributor to the Severity of Cutaneous Leishmaniasis in the Ear Model of Infection. *Parasite Immunol.* 29, 501–513. doi: 10.1111/j.1365-3024.2007.00969.x

Bradley, P. P., Priebat, D. A., Christensen, R. D., and Rothstein, G. (1982). Measurement of Cutaneous Inflammation: Estimation of Neutrophil Content With an Enzyme Marker. *J. Invest. Dermatol.* 78, 206–209. doi: 10.1111/1523-1747.ep12506462

Caridha, D., Vesely, B., van Bocxlaer, K., Arana, B., Mowbray, C. E., Rafati, S., et al (2019). Route Map for the Discovery and Pre-Clinical Development of New Drugs and Treatments for Cutaneous Leishmaniasis. *Int. J. Parasitol. Drugs Drug Resist.* 11, 106–117. doi: 10.1016/j.ijpddr.2019.06.003

Cassado, A. A., D'Império Lima, M. R., and Bortoluci, K. R. (2015). Revisiting Mouse Peritoneal Macrophages: Heterogeneity, Development, and Function. *Front. Immunol.* 6:225. doi: 10.3389/fimmu.2015.00225

Frahs, S. M., Oxford, J. T., Neumann, E. E., Brown, R. J., Keller-Peck, C. R., Pu, X., et al (2018). Extracellular Matrix Expression and Production in Fibroblast-Collagen Gels: Towards an In Vitro Model for Ligament Wound Healing. *Ann. Biomed. Eng.* 46 (11), 1882–1895. doi: 10.1007/s10439-018-2064-0

Gregory, D. J., and Olivier, M. (2005). Subversion of Host Cell Signalling by the Protozoan Parasite Leishmania. *Parasitology* 130 (S1), S27–S35. doi: 10.1017/S0031182005008139

Hatzigeorgiou, D. E., He, S., Sobel, J., Grabstein, K. H., Hafner, A., and Ho, J. L. (1993). IL-6 Down-Modulates the Cytokine-Enhanced Antileishmanial Activity in Human Macrophages. *J. Immunol.* 151, 3682–3692.

Herb, M., and Schramm, M. (2021). Functions of ROS in Macrophages and Antimicrobial Immunity. *Antioxidants* 10:313. doi: 10.3390/antiox10020313

Hu, S., Marshall, C., Darby, J., Wei, W., Lyons, A. B., and Körner, H. (2018). Absence of Tumor Necrosis Factor Supports Alternative Activation of Macrophages in the Liver After Infection With Leishmania Major. *Front. Immunol.* 9:1. doi: 10.3389/fimmu.2018.00001

Jafari, M., Shirbazou, S., and Norozi, M. (2014). Induction of Oxidative Stress in Skin and Lung of Infected BALB/C Mice With Iranian Strain of Leishmania Major (MRHO/IR/75/ER). *Iran. J. Parasitol.* 9, 60–69.

Kaye, P. M., Cruz, I., Picado, A., Van Bocxlaer, K., and Croft, S. L. (2020). Leishmaniasis Immunopathology—Impact on Design and Use of Vaccines, Diagnostics and Drugs. *Semin. Immunopathol.* 42, 247–264. doi: 10.1007/s00281-020-00788-y

Kropf, P., Fuentes, J. M., Fähnrich, E., Arpa, L., Herath, S., Weber, V., et al (2005). Arginase and Polyamine Synthesis are Key Factors in the Regulation of Experimental Leishmaniasis In Vivo. *FASEB J.* 19, 1000–1002. doi: 10.1096/fj.04-3416fje

Krzyszczyk, P., Schloss, R., Palmer, A., and Berthiaume, F. (2018). The Role of Macrophages in Acute and Chronic Wound Healing and Interventions to Promote Pro-Wound Healing Phenotypes. *Front. Physiol.* 9:419. doi: 10.3389/fphys.2018.00419

Lage, D. P., Ribeiro, P. A. F., Dias, D. S., Mendonça, D. V. C., Ramos, F. F., Carvalho, L. M., et al (2020). A Candidate Vaccine for Human Visceral Leishmaniasis Based on a Specific T Cell Epitope-Containing Chimeric Protein Protects Mice Against Leishmania Infantum Infection. *NPJ Vaccines* 5, 1–13. doi: 10.1038/s41541-020-00224-0

Laskin, D. L., Sunil, V. R., Gardner, C. R., and Laskin, J. D. (2011). Macrophages and Tissue Injury: Agents of Defense or Destruction? *Annu. Rev. Pharmacol. Toxicol.* 51, 267–288. doi: 10.1146/annurev.pharmtox.010909.105812

Li, M., Hou, Q., Zhong, L., Zhao, Y., and Fu, X. (2021). Macrophage Related Chronic Inflammation in Non-Healing Wounds. *Front. Immunol.* 12:2289. doi: 10.3389/FIMMU.2021.681710

Lira, R., Doherty, M., Modi, G., and Sacks, D. (2000). Evolution of Lesion Formation, Parasitic Load, Immune Response, and Reservoir Potential in C57BL/6 Mice Following High- and Low-Dose Challenge With Leishmania Major. *Infect. Immun.* 68, 5176–5182. doi: 10.1128/IAI.68.9.5176-5182.2000

Liu, D., and Uzonna, J. E. (2012). The Early Interaction of Leishmania With Macrophages and Dendritic Cells and its Influence on the Host Immune Response. *Front. Cell. Infect. Microbiol.* 2:83. doi: 10.3389/fcimb.2012.00083

Mills, C. D., Kincaid, K., Alt, J. M., Heilman, M. J., and Hill, A. M. (2000). M-1/M-2 Macrophages and the Th1/Th2 Paradigm. *J. Immunol.* 164, 6166–6173. doi: 10.4049/jimmunol.164.12.6166

Minutti, C. M., Knipper, J. A., Allen, J. E., and Zaiss, D. M. W. (2017). Tissue-Specific Contribution of Macrophages to Wound Healing. *Semin. Cell Dev. Biol.* 61, 3–11. doi: 10.1016/J.SEMCDB.2016.08.006

Miranda, M. M., Panis, C., Cataneo, A. H. D., da Silva, S. S., Kawakami, N. Y., Lopes, L. G., et al (2015). Nitric Oxide and Brazilian Propolis Combined Accelerates Tissue Repair by Modulating Cell Migration, Cytokine Production and Collagen Deposition in Experimental Leishmaniasis. *PloS One* 10, e0125101. doi: 10.1371/journal.pone.0125101

Morgado, F. N., de Carvalho, L. M. V., Leite-Silva, J., Seba, A. J., Pimentel, M. I. F., Fagundes, A., et al (2018). Unbalanced Inflammatory Reaction Could Increase Tissue Destruction and Worsen Skin Infectious Diseases – a Comparative Study of Leishmaniasis and Sporotrichosis. *Sci. Rep.* 8, 2898. doi: 10.1038/s41598-018-21277-1

Müller, K. E., Solberg, C. T., Aoki, J. I., Floeter-Winter, L. M., and Nerland, A. H. (2018). Developing a Vaccine for Leishmaniasis: How Biology Shapes Policy. *Tidsskr. Nor. Laegeforen.* 138, 1–5. doi: 10.4045/tidsskr.17.0620

Muraille, E., Leo, O., and Moser, M. (2014). TH1/TH2 Paradigm Extended: Macrophage Polarization as an Unappreciated Pathogen-Driven Escape Mechanism? *Front. Immunol.* 5:603. doi: 10.3389/fimmu.2014.00603

Murray, P. J., and Wynn, T. A. (2011). Protective and Pathogenic Functions of Macrophage Subsets. *Nat. Rev. Immunol.* 11, 723–737. doi: 10.1038/nri3073

Muxel, S. M., Aoki, J. I., Fernandes, J. C. R., Laranjeira-Silva, M. F., Zampieri, R. A., Acuña, S. M., et al (2017). Arginine and Polyamines Fate in Leishmania Infection. *Front. Microbiol.* 8:2682. doi: 10.3389/fmicb.2017.02682

Ontoria, E., Hernández-Santana, Y. E., González-García, A. C., López, M. C., Valladares, B., and Carmelo, E. (2018). Transcriptional Profiling of Immune-Related Genes in Leishmania Infantum-Infected Mice: Identification of Potential Biomarkers of Infection and Progression of Disease. *Front. Cell. Infect. Microbiol.* 8:197. doi: 10.3389/fcimb.2018.00197

Pessenda, G., and Santana da Silva, J. (2020). Arginase and its Mechanisms in Leishmania Persistence. *Parasite Immunol.* 42, e12722. doi: 10.1111/pim.12722

Pomatto, L. C. D., Sun, P. Y., Yu, K., Gullapalli, S., Bwiza, C. P., Sisliyan, C., et al (2019). Limitations to Adaptive Homeostasis in an Hyperoxia-Induced Model of Accelerated Ageing. *Redox Biol.* 24:101194. doi: 10.1016/J.REDOX.2019.101194

Pratti, J. E. S., Ramos, T. D., Pereira, J. C., Da Fonseca-Martins, A. M., Maciel-Oliveira, D., Oliveira-Silva, G., et al (2016). Efficacy of Intranasal LaAg Vaccine Against Leishmania Amazonensis Infection in Partially Resistant C57Bl/6 Mice. *Parasit. Vectors* 9, 1–11. doi: 10.1186/s13071-016-1822-9

Rangaraj, A. G., and Harding, K. G. (2011) *Role of Collagen in Wound Management Modelling Diabetic Wound Healing View Project*. Available at: https://www.researchgate.net/publication/265155351 (Accessed August 17, 2021).

Reisser, D., Onier-Cherix, N., and Jeannin, J.-F. (2008). Arginase Activity is Inhibited by L -NAME, Both In Vitro and In Vivo. *J. Enzyme Inhib. Med. Chem.* 17, 267–270. doi: 10.1080/1475636021000006252

Rosas, L. E., Keiser, T., Barbi, J., Satoskar, A. A., Septer, A., Kaczmarek, J., et al (2005). Genetic Background Influences Immune Responses and Disease Outcome of Cutaneous L. Mexicana Infection in Mice. *Int. Immunol.* 17, 1347–1357. doi: 10.1093/intimm/dxh313

Rossi, M., and Fasel, N. (2018). How to Master the Host Immune System? Leishmania Parasites Have the Solutions! *Int. Immunol.* 30, 103–111. doi: 10.1093/intimm/dxx075

Sacks, D., and Noben-Trauth, N. (2002). The Immunology of Susceptibility and Resistance to Leishmania Major in Mice. *Nat. Rev. Immunol.* 2, 845–858. doi: 10.1038/nri933

Scott, P., and Novais, F. O. (2016). Cutaneous Leishmaniasis: Immune Responses in Protection and Pathogenesis. *Nat. Rev. Immunol.* 16, 581–592. doi: 10.1038/nri.2016.72

Soong, L. (2012). Subversion and Utilization of Host Innate Defense by Leishmania Amazonensis. *Front. Immunol.* 3:58. doi: 10.3389/fimmu.2012.00058

Tellevik, M. G., Muller, K. E., Løkken, K. R., and Nerland, A. H. (2014). Detection of a Broad Range of Leishmania Species and Determination of Parasite Load of Infected Mouse by Real-Time PCR Targeting the Arginine Permease Gene AAP3. *Acta Trop.* 137, 99–104. doi: 10.1016/j.actatropica.2014.05.008

Tomiotto-Pellissier, F., Bortoleti, B. T., da, S., Assolini, J. P., Gonçalves, M. D., Carloto, A. C. M., et al (2018). Macrophage Polarization in Leishmaniasis: Broadening Horizons. *Front. Immunol.* 9:2529. doi: 10.3389/fimmu.2018.02529

Velasquez, L. G., Galuppo, M. K., De Rezende, E., Brandão, W. N., Peron, J. P., Uliana, S. R. B., et al (2016). Distinct Courses of Infection With Leishmania (L.) Amazonensis are Observed in BALB/c, BALB/c Nude and C57BL/6 Mice. *Parasitology* 143, 692–703. doi: 10.1017/S003118201600024X

Wang, Z. E., Reiner, S. L., Zheng, S., Dalton, D. K., and Locksley, R. M. (1994). CD4+ Effector Cells Default to the Th2 Pathway in Interferon Gamma-Deficient Mice Infected With Leishmania Major. *J. Exp. Med.* 179, 1367–1371. doi: 10.1084/jem.179.4.1367

WHO - World Health Organization (2020). Available on: www.who.int/news-room/fact-sheets/detail/leishmaniasis.

Xu, H., Zheng, Y.-W., Liu, Q., Liu, L.-P., Luo, F.-L., Hu-Chen, Z., et al (2017). "Reactive Oxygen Species in Skin Repair, Regeneration, Aging, and Inflammation," in *React. Oxyg. Species Living Cells*. IntechOpen. doi: 10.5772/INTECHOPEN.72747

Zhao, Y. L., Tian, P., Han, F., Zheng, J., Xia, X., Xue, W., et al (2017). Comparison of the Characteristics of Macrophages Derived From Murine Spleen, Peritoneal Cavity, and Bone Marrow. *J. Zhejiang Univ. Sci. B* 18, 1055–1063. doi: 10.1631/jzus.B1700003

Conflict of Interest: The authors declare that the research was conducted in the absence of any commercial or financial relationships that could be construed as a potential conflict of interest.

Publisher's Note: All claims expressed in this article are solely those of the authors and do not necessarily represent those of their affiliated organizations, or those of the publisher, the editors and the reviewers. Any product that may be evaluated in this article, or claim that may be made by its manufacturer, is not guaranteed or endorsed by the publisher.

Advantages of publishing in Frontiers

OPEN ACCESS
Articles are free to read for greatest visibility and readership

FAST PUBLICATION
Around 90 days from submission to decision

HIGH QUALITY PEER-REVIEW
Rigorous, collaborative, and constructive peer-review

TRANSPARENT PEER-REVIEW
Editors and reviewers acknowledged by name on published articles

Frontiers
Avenue du Tribunal-Fédéral 34
1005 Lausanne | Switzerland

Visit us: www.frontiersin.org
Contact us: frontiersin.org/about/contact

REPRODUCIBILITY OF RESEARCH
Support open data and methods to enhance research reproducibility

DIGITAL PUBLISHING
Articles designed for optimal readership across devices

FOLLOW US
@frontiersin

IMPACT METRICS
Advanced article metrics track visibility across digital media

EXTENSIVE PROMOTION
Marketing and promotion of impactful research

LOOP RESEARCH NETWORK
Our network increases your article's readership